Catalytic Hydrosilylation in Reductive Ether Synthesis and Reductive Beckmann Rearrangements

James Wilson (MChem)

Thesis submitted to the University of Nottingham for the degree of Doctor of Philosophy

March 2022

Acknowledgements

Over the past 4 years of study, I have had the privilege of working with exceptional supervisors, co-workers, and friends. While this thesis certainly could not have been written without their support, their contribution goes far beyond the work summarised in these pages. These interactions have shaped my education, professional development, and have given me lasting memories and enduring friendships. There is no doubt that my PhD would have been poorer and a lot more difficult without them.

Firstly to Ross, I would like to express my gratitude for all of your support during my time in your group. You have given me advice and encouragement as well as the opportunity and independence to explore my own ideas. I hope to be a much better chemist because of the training which your group has provided.

I also cannot continue without acknowledging the members of the Denton group who have made this experience so vibrant and enjoyable. They are a hub of practical knowledge, a source of innovation and an excellent sounding board. Although I have enjoyed working with every member, I would like to pay a special thanks to the outstanding contributions of Val, Rhydian and of course Ben. My time at Nottingham would also have been incomplete without the close friendships with Dara, Aaron and Meg which have supported me through the challenges of the past 4 years.

I would also like to thank the organisations which made and funded this PhD. The CDT in Sustainable chemistry has provided training and collaboration for which I am grateful to the senior management team and fellow students. My industrial supervisor, Helen Sneddon, has given thoughtful discussion throughout my studentship, and I would like to thank all the support staff in the Chemistry department who have made this research possible.

Finally, I would like to thank my parents, who give unconditional support in whatever I do — even if they don't quite understand it. Studying for this PhD has been a tough and frustrating process, but as this experience comes to an end it is the friendships and countless moments of joy which will make my time at Nottingham unforgettable.

Abstract

This thesis explores some of the applications of hydrosilanes as reducing agents for the introduction of carbon-heteroatom bonds in contemporary organic synthesis. Two approaches are considered in detail: the synthesis of ethers through ester reduction and a reductive variation of the Beckmann rearrangement for the installation of a secondary amine.

Chapter 1 introduces the chemistry of organosilicon compounds and their role in synthesis. This chapter gives a theory-based overview of bonding at silicon which is used to explain the unique properties of organosilanes. This is supplemented by selected examples of practical synthesis methods where silicon plays an essential role in mediating reactivity. The chapter finishes on the main strategies to activate hydrosilanes and describes how this enables their widespread use as versatile reducing agents.

Chapter 2 explores methods for the formation of a carbon-oxygen bond, focussing on catalytic hydrosilylation as an emerging technique to synthesise ethers from esters. It describes the novel application of iron trichloride as an abundant and inexpensive catalyst for this transformation. Efforts to optimise this reaction are presented along with its implementation in a telescoped one-pot reductive etherification, using carboxylic acids as abundant electrophiles.

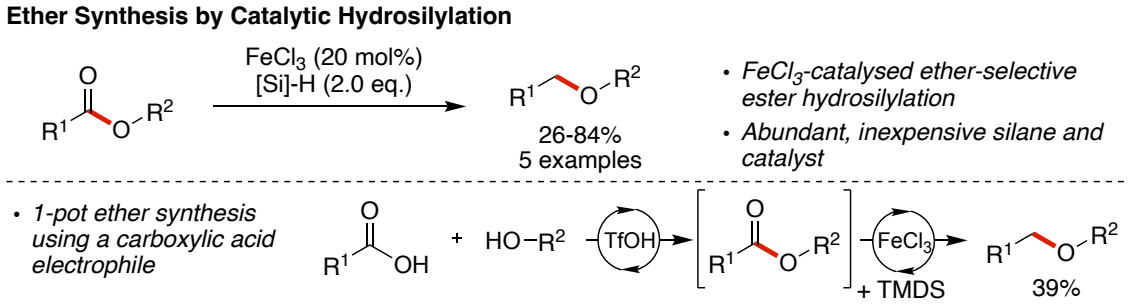

Figure 1. *The developed $FeCl_3$-catalysed reduction of an ester to an ether and its implementation in a 1-pot ether synthesis from a carboxylic acid and an alcohol.*

Chapter 3 broadly focusses on the merger of the hydrosilylation with the Beckmann rearrangement to reductively insert a nitrogen atom into a carbon-carbon bond. Two methods are described. The first uses triflic anhydride to facilitate an

interrupted Beckmann rearrangement wherein the rich chemistry of nitrilium ions can be exploited (Figure 2A and 2B). The scope of this activation has been explored through the development of a mild, catalytic hydrosilylation to access structurally diverse amines, however further diversifications have also been demonstrated. The second-generation procedure (Figure 2C) initiates a Beckmann rearrangement using substoichiometric mesic anhydride, with the resulting sulfonic acid by-products being used to activate phenylsilane towards a zinc-catalysed amide reduction. Finally, the reductive Beckmann reaction has been utilised in the first enantioselective synthesis of (-)-meptazinol, in which the active pharmaceutical ingredient is constructed over 6 steps in an 11% yield with an enantiomeric excess of 92%.

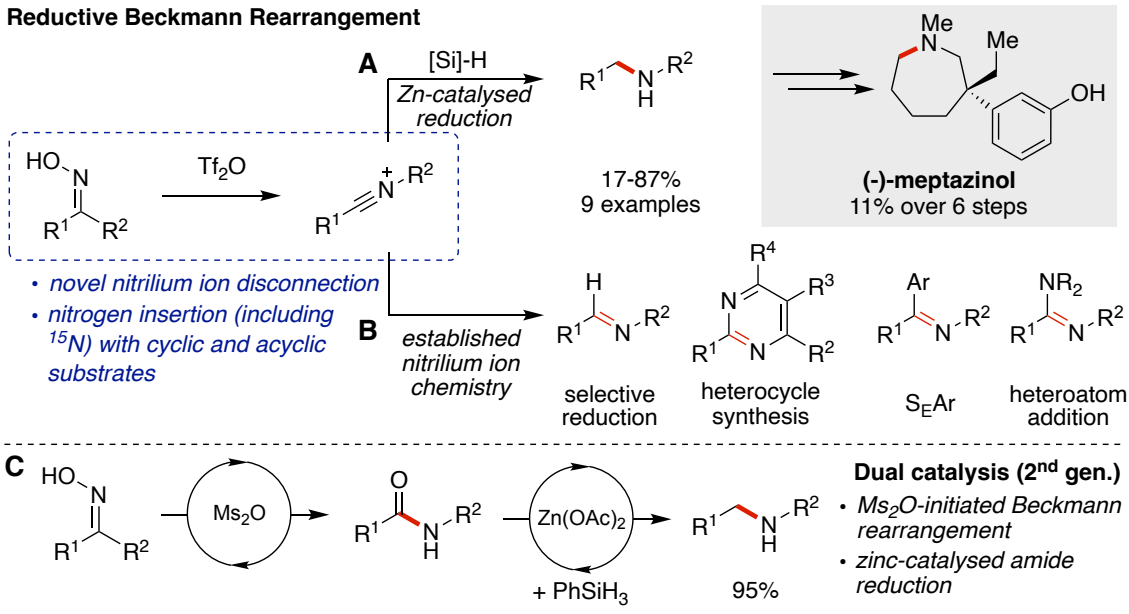

Figure 2. *An interrupted Beckmann rearrangement to generate a nitrilium ion which enables* ***A****) zinc-catalysed hydrosilylation,* ***B****) previously established nitrilium-specific derivatisations. A second-generation reductive Beckmann rearrangement (****C****) proceeds via an amide intermediate using sub-stoichiometric mesic anhydride and zinc acetate.*

Abbrieviations

Å	angstrom
$[\alpha]_D$	specific rotation
Ac	acetyl
acac	acetylacetone
atm.	atmospheres
Boc	tert-butoxycarbonyl
Bs	*para*-bromophenylsulfonyl
cat.	catalyst
COD	1,5-cyclooctadiene
Cp	cyclopentadienyl
d	doublet (NMR spectroscopy)
d.r.	diastereomeric ratio
D4	octamethylcyclotetrasiloxane
DCE	1,2-dichloroethane
DCM	dichloromethane
DEAD	diethylazodicarboxylate
DIBAL-H	diisobutylaluminium hydride
DIC	N,N'-diisopropylcarbodiimide
DMAP	4-dimethylamino pyridine
DMEAD	di-2-methoxyazodicarboxylate
DMF	*N,N*-dimethylformamide
DTBAD	di-tert-butylazodicarboxylate
e.e.	enantiomeric excess
EI	electron ionisation
eq.	equivalents
ESI	electrospray ionisation
Et	ethyl
g	gram
GC	gas chromatography
h	hour
HPLC	high performance liquid chromatography
HRMS	high resolution mass spectrometry
^{i}Pr	isopropyl
IR	infrared
J	coupling constant (NMR spectroscopy)
LC-MS	liquid chromatography-mass spectroscopy
m	multiplet (NMR spectroscopy)

m/z	mass-to-charge ratio
mCBA	*meta*-chlorobenzoic acid
mCPBA	*meta*-chloroperbenzoic acid
Me	methyl
mol%	mole percent
Ms	methanesulfonyl
MS	molecular sieves
NMR	nuclear magnetic resonance
NOESY	Nuclear Overhauser Effect Spectroscopy
Nu	nucleophile
pc	phthalocyanine
Ph	phenyl
PMHS	polymethylhydrosiloxane
ppm	parts per million
q	quartet (NMR spectroscopy)
R	unspecified group
r.t.	room temperature
r.t.	room temperature
R_f	retardation factor
RME	reaction mass efficiency
s	singlet (NMR spectroscopy)
S_EAr	electrophilic aromatic substitution
S_N2	bimolecular nucleophilic substitution
t	triplet (NMR spectroscopy)
t-BuPyOx	4-(tert-butyl)-2-(pyridin-2-yl)-4,5-dihydrooxazole
Tf	trifluoromethylsulfonyl
TFA	trifluoroacetic acid
TFAA	trifluoroacetic anhydride
THF	tetrahydrofuran
TLC	thin layer chromatography
TMDS	tetramethydisiloxane
TMS	trimethylsilyl
Ts	*para*-toluenesulfonyl
UHP	urea - hydrogen peroxide
δ	chemical shift
ν_{max}	adsorption maximum (IR spectroscopy)

Contents

Chapter 1: An Introduction to the Organic Chemistry of Silicon

1.1 An Introduction to Silicon 2
1.2 The Influence of Bond Strengths on Reactivity at Silicon 2
1.2.1 The Silicon-Silicon Bond 2
1.2.2 The Silicon-Carbon Bond 3
1.2.3 The Silicon-Oxygen Bond 4
1.2.3.1 The Brook Rearrangement 6
1.2.4 The Silicon-Fluorine Bond 7
1.3 Hyperconjugation at Silicon 8
1.3.1 Stabilisation of α-anions 8
1.3.1.1 The Peterson Olefination 9
1.3.2 Stabilisation of β-cations 12
1.3.2.1 The Hosomi-Sakurai Allylation 14
1.3.2.2 The Mukaiyama Aldol Reaction 17
1.4 Hypercoordination at Silicon 20
1.4.1 Bonding at 5- and 6- Coordinate Silicon 20
1.4.2 Reactivity of 5- and 6- Coordinate Silicon 22
1.4.2.1 Hiyama Coupling 24
1.5 Hydrosilanes as Reducing Agents 27
1.5.1 The Silicon-Hydrogen Bond 27
1.5.2 Base-Mediated Reductions 28
1.5.3 Acid-Mediated Reductions 29
1.5.4 Radical Reductions 31
1.5.5 Transition Metal-Catalysed Reductions 33
1.5.5.1 The Fukuyama Reduction 34
1.5.5.2 The Mukaiyama Hydration 35
1.6 References 38

Chapter 2: Catalytic Methods for the Synthesis of Ethers from Esters and Carboxylic Acids

2.1 Introduction 45
2.1.1 Significance of Ethers 45
2.1.2 Ether Synthesis by Stoichiometric Alcohol Activation 45
2.1.3 Ether Synthesis by Catalytic Substitution 48
2.1.4 Reduction of Esters to Ethers 51
2.1.5 Reductive *O*-Alkylation of Alcohols using Carboxylic Acids 59
2.2 Project Aims 64
2.3 Results and Discussion 66
2.3.1 Development of a Model Reaction 66
2.3.2 Ester Reduction Screening 68

2.3.3 Optimisation of $FeCl_3$-catalysed Ester Reduction 71
2.3.4 Scope of $FeCl_3$-catalysed Ester Reduction 78
2.3.4 Reductive *O*-Alkylation using $FeCl_3$-catalysis 80
2.3.5 Investigations Towards a Reductive Baeyer-Villiger Reaction 82
2.4 Conclusions 85
2.5 References 87
2.6 Experimental 90
2.6.1 General Reaction Information 90
2.6.2 General Analysis and Characterisation Information 90
2.6.3 Synthesis of Standards 91
2.6.4 General Procedure for Catalyst Screening 95
2.6.5 Ester Synthesis 96
2.6.6 Substrate Scope 100
2.6.7 References 104

Chapter 3: Reductive Rearrangements of Oximes

3.1 Introduction 106
3.1.1 Nitrilium and Keteniminium ions 106
3.1.2 The Beckmann Rearrangement 110
3.1.2 Reductive Beckmann Rearrangements 114
3.2 Project Aims 117
3.3 Results and Discussion 119
3.3.1 Tf_2O-mediated Reductive Beckmann Rearrangement 119
3.3.1.1 An Interrupted Beckmann Rearrangement 119
3.3.1.2 Reduction of Nitrilium ions 120
3.3.1.3 Substrate Synthesis and Scope 127
3.3.2 Nitrilium Ion Chemistry through an Interrupted Beckmann Rearrangement 134
3.3.3 Discovery of a "Dual Catalytic" Reductive Beckmann Reaction 136
3.3.4 A Reductive Beckmann approach to the Synthesis of (-)-Meptazinol 138
3.4 Conclusions 148
3.5 References 150
3.6 Experimental 153
3.6.1 General Reaction Information 153
3.6.2 General Analysis and Characterisation 153
3.6.3 The Synthesis of Oximes 153
3.6.4 The Reductive Beckmann Substrate Scope 164
3.6.5 Nitrilium Ion Chemistry 173
3.6.6 Meptazinol Experimental 178
3.6.7 References 194

Chapter 1

An Introduction to the Organic Chemistry of Silicon

1.1 An Introduction to Silicon

First discovered in 1823, silicon is a metalloid group 14 element. It is an extremely abundant, contributing 27% w/w of the Earth's crust, largely in the form of silicate minerals such as quartz. This is present in easily accessible feedstocks such as sand, stone, and clay, which historically have been used as bulk building materials. However, silicon is also the basis of two of the most important materials in human development. Reliable production of high quality glass has facilitated many modern technologies; from Swan's lightbulbs to fibre optic cables.[1] More recently the element's semi-conducting properties have played an essential role in the computing industry, giving rise to what some have dubbed the 'silicon age'.[2]

The chemistry of silicon is often compared to carbon due to its position in group 14 of the periodic table and usual valence of 4. Naturally, the true relationship is more complex. Although silicon cannot match the plethora of organic chemistry that which has made carbon the building block for life,[3] it has its own unique properties which – coupled with its natural abundance – make it a valuable element in organic synthesis.[4]

1.2 The Influence of Bond Strengths on Reactivity at Silicon

1.2.1 The Silicon-Silicon Bond

From a thermodynamic perspective, the chemistry of each element is defined by the stability of the bonds it makes with surrounding atoms. For silicon, the main differentiator between itself and carbon is its larger and more diffuse orbitals. This results in weaker element-element bonds and as a result, catenation rarely seen. For example, the only silane of the formula Si_nH_{n+2} which is indefinitely stable at room temperature is SiH_4. Disilane (Si_2H_6), which contains one Si-Si bond, slowly decomposes at room temperature (2.8% over 8 months) and higher silanes become increasingly reactive. Furthermore, all silanes of the formula Si_nH_{n+2} are pyrophoric and are rarely encountered.[1] In comparison, alkanes of varying chain length have a high degree of thermal stability, with almost all alkanes up to C12 having autoignition temperatures of over 200 °C.[5]

	C	Si	H	F	Cl	Br	I	O	N
C-X	368	360	435	453	351	293	216	360	305
Si-X	360	340	393	565	381	310	234	452	322

Table 1. *A comparison of the strength of common bonds for carbon and silicon. All values are in kJ·mol^{-1}* [6,7]

1.2.2 The Silicon-Carbon Bond

Organosilanes, combine the useful properties of silicon with the stability of organic compounds, and are therefore much more practical as reagents in organic chemistry. Another advantage of organosilanes is the ability to moderate reactivity by functionalisation. However, whilst bespoke silanes are certainly obtainable, their commercial viability depends on the efficiency of their synthesis. There are 3 main routes to commercial organosilanes (Scheme 1).

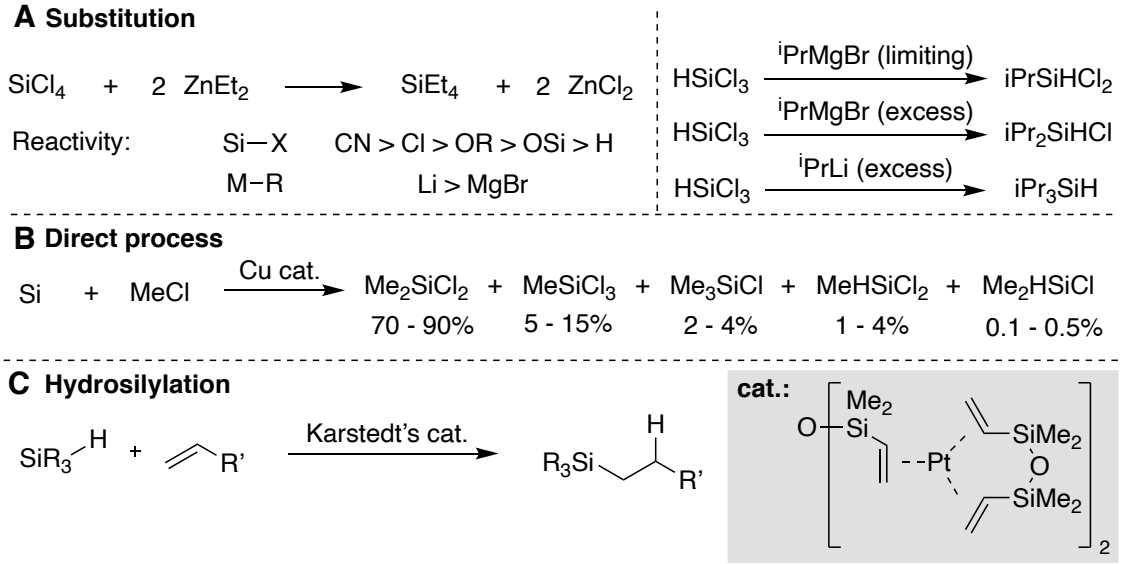

Scheme 1. *Common preparative methods for the formation of a C-Si bond;* ***(A)*** *The original substitution reported by Friedel and Crafts, order of reactivity, and sequential chloride substitution at trichlorosilane;* ***(B)*** *The direct process and the distribution of products isolated on scale;* ***(C)*** *General scheme for hydrosilylation with Karstedt's catalyst which is the modern industrial benchmark.*

The first reaction designed to create a Si-C bond was reported by Friedel and Crafts in 1863 and involved substitution of tetrachlorosilane with diethylzinc to give tetraethylsilane (Scheme 1A).[8,9] Extensive research by Kipping[10] found this approach to be general for many combinations of organometallics and halo- or *pseudo*halosilanes. Substitution is possibly the most practical laboratory method for the synthesis of bespoke organosilanes, particularly as – under controlled conditions – the substitution of $SiCl_4$ can progress sequentially. The degree of

substitution can be further moderated by carefully matching the reactivity of reagents.[11] Despite this lab-scale utility, after 50 years and 50 publications entitled "Organic Derivatives of Silicon", in 1936 Kipping remarked that "the prospect of any immediate and important advance in this section of organic chemistry does not seem very hopeful."[12]

Despite these downcast remarks, just 5 years later Rochow and Müller simultaneously discovered what became known as the 'direct process' which is now a mainstay of the silicone industry (Scheme 1B).[13] The reaction involves reacting crushed silicon with an alkyl, alkenyl or aryl chloride at high temperatures and pressures in the presence of a copper catalyst. Whilst this is possible for many substrates such as vinyl chloride and chlorobenzene, by far the most used important substrate is chloromethane which is operated on a megatonne scale. The resultant dimethyldichlorosilane is purified by distillation and forms the feedstock for silicone polymers, which have numerous applications from surfactants and personal care products to industrial lubricants and coatings.[14,15] As a result of this process, methyl and particularly dimethyl substituted silanes are often inexpensive.

Organosilanes can also be made by the addition of Si-H across a double bond (Scheme 1C). Alkene hydrosilylation is accomplished using noble metal catalysis and will be discussed further in section 1.5.5.1.

1.2.3 The Silicon-Oxygen Bond

By far the most important bond in the chemistry of silicon is the Si-O bond. At 452 $kJ \cdot mol^{-1}$, it is considerably stronger than a C-O single bond (360 $kJ \cdot mol^{-1}$) and at 1.63 Å it is around 0.2 Å shorter than predicted from the sum of covalent radii.[16] The origin of its strength has in the past been a subject of contention, however the currently accepted model involves synergistic back-bonding in which the lone pairs on oxygen are stabilised by particularly good overlap with a low-energy Si-X σ^* orbital. This overlap is maximised when donor lone pairs occupy colinear orbitals of higher p character (Figure 1).[17]

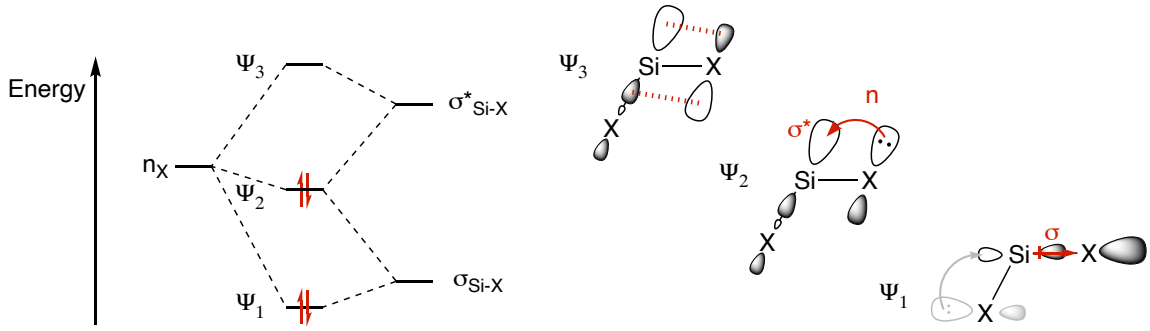

Figure 1. *Molecular orbital diagram describing the hyperconjugation from the heteroatom lone pair (n_O) into the Si-X σ and σ* bond. Orbital overlaps are shown with the key interactions.*[18]

Empirically, this reduction in hybridisation can be observed by the comparison of disiloxane and dimethyl ether. Dimethyl ether has a COC bond angle of 111.2° from which the lone pairs are calculated to have 78.3% p character; close to the 75% of an idealised sp^3 hybrid orbital.[17] In contrast, the siloxane oxygen lone pairs retain 95.2% p character to maximise the n→σ* overlap, and consequently, the central oxygen is predominantly sp hybridised. As a result, the SiOSi has a measured bonding angle of 151.2°.[19]

	bond angle ∠XOX	O-charge Q_O	H-bond strength ΔE_{HB}
$H_3C{-}O{-}CH_3$	111.2°	-0.6 *e*	27.0 kJ·mol^{-1}
$H_3Si{-}O{-}SiH_3$	151.2°	-1.3 *e*	15.4 kJ·mol^{-1}

Table 2. *Comparison of physical properties of dimethyl ether and disiloxane*

As silicon is more electropositive than carbon (Pauling electronegativity; C 2.50, Si 1.90),[20] the Si-O bond has significant ionic contributions giving an overall charge at oxygen of -1.3 electrons (*e*) for disilylether compared to -0.6 *e* in dimethyl ether. Counterintuitively however, dimethyl ether is more basic, and can form hydrogen bonds which are 8-13 kJ·mol^{-1} stronger than disilyl ether. This is rationalised by considering the synergistic nature of the bond. Despite the higher overall charge, hyperconjugation from oxygen's lone pairs into a neighbouring σ* orbital reduces availability and occupancy of the lone pair orbitals from ~1.97 *e* in dimethyl ether to ~1.93 *e* in disilyl ether. This movement of electrons from oxygen to silicon is complementary to the σ bonding which is strongly polarised in the opposite direction (Figure 1). Furthermore, for species with more than one electronegative

heteroatom, *X*, polarisation is further strengthened by partial occupancy of the σ* orbital. The overall effect of this phenomenon is an increase in the oxygen-silicon bond strength by 96 kJ·mol^{-1} or 28%. With such an affinity for oxygen, one of the most common roles for silanes are as alcohol protecting groups. In this function the tunability of silanes offers benefits in moderating reactivity with respect to protection and deprotection (Table 3).[21–23]

	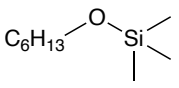 -OTMS	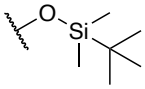 -OTBS	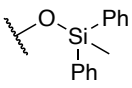 -ODPMS	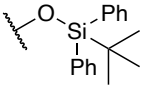 -OTBDPS	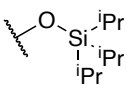 -OTIPS
1% HCl in MeOH	≤ 1 min	≤ 1 min	14 mins	225 mins	55 mins
5% NaOH in MeOH	≤ 1 min	> 24 h	≤ 1 min	> 24 h	> 24 h

Table 3. *Rates of deprotection of hexyl silyl ethers under acidic and basic conditions.*

1.2.3.1 The Brook Rearrangement

In addition, the formation of the Si-O bond often plays a role as a thermodynamic sink in organosilicon chemistry which, in some instances, can open new modes of reactivity. In 1973 Brook summarised a series of molecular rearrangements of α-silyl alcohols under basic conditions to give silyl ethers.[24] Through a detailed kinetic investigation, he showed these rearrangements had a large negative entropy of activation and a strongly positive Hammett reaction constant (substitution on alcohols). In combination with the observed retention of stereochemistry at silicon, Brook characterised these rearrangements as proceeding through an anionic 3-membered transition state (Scheme 2). This Brook rearrangement is driven by formation of the silicon oxygen bond, and whilst similar reactions are known for other oxyphilic atoms, for example the α-hydroxyphosphonate-phosphate rearrangement,[25] a carbon analogue is thus far unknown.

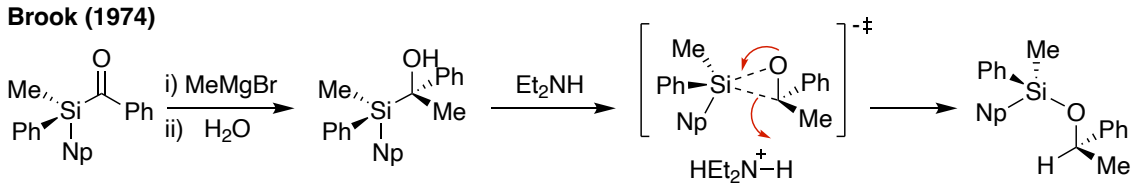

Scheme 2. *Synthesis and Brook rearrangement of an α-silyl alcohol showing retention of stereochemistry at silicon and the anionic 3-membered transition state.*

1.2.4 The Silicon-Fluorine Bond

Fluorine forms the strongest bonds with silicon, and similarly to oxygen, hyperconjugation is the stabilising force. At 540 kJ·mol^{-1} these are the second strongest single bonds in chemistry, just behind HF at 569 kJ·mol^{-1}.[6] It is therefore not surprising that addition of fluoride ions can be employed as a mild, neutral method for the deprotection of silyl ethers or indeed silyl enol ethers. This is demonstrated in the selective deprotection of a TES group in Holton's taxol synthesis[26] which occurred in a quantitative yield despite an array of other functional groups including an OTBS group (Scheme 3A).

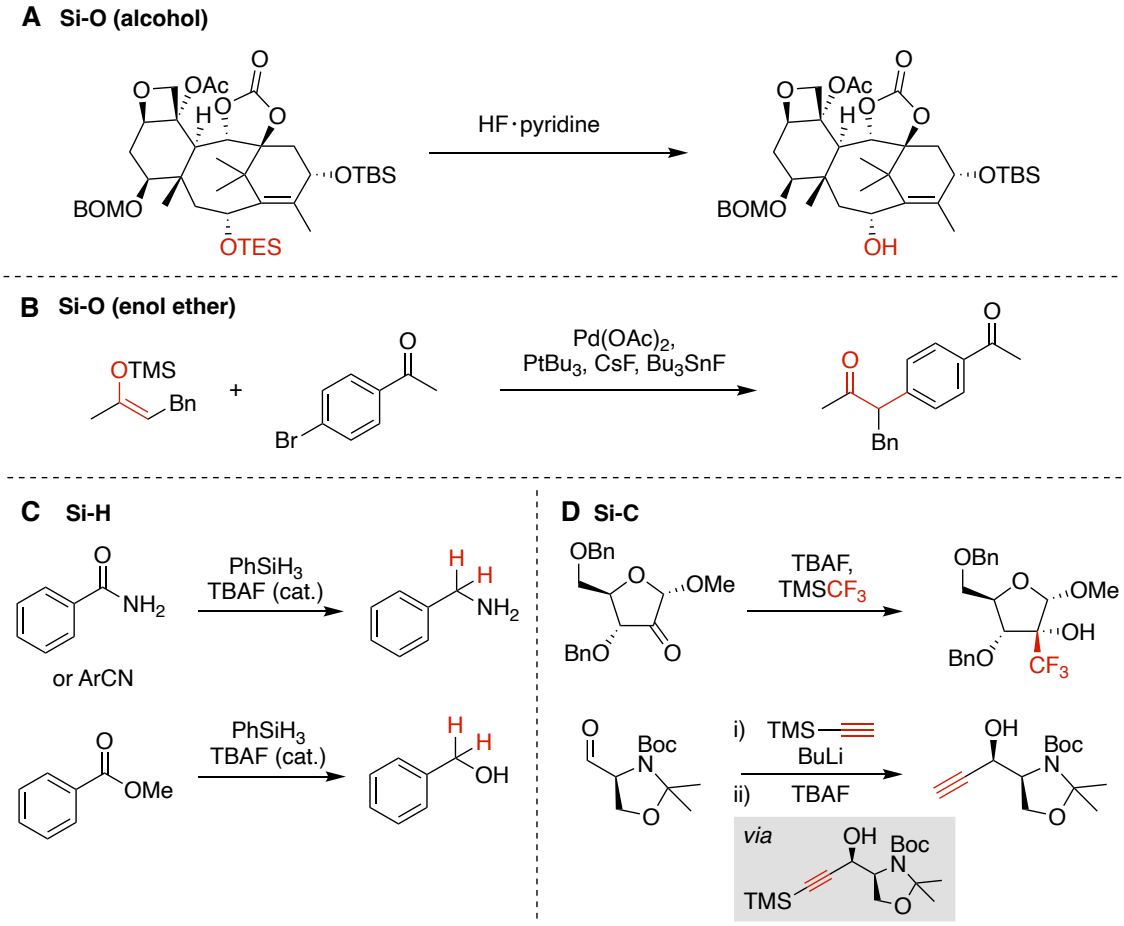

Scheme 3. *Activation of Si-X bonds;* ***(A)*** *Mild, selective deprotection of silyl ethers;* ***(B)*** *Activation of a silyl enol ether for cross-coupling;* ***(C)*** *Silane activation for reduction;* ***(D)*** *Application of the Ruppert-Prakesh reagent and deprotection of a TMS-alkyne.*

The mildness is further exemplified by Hartwig's use of fluoride-activated silyl enol ethers in a palladium-catalysed cross coupling with aryl halides[27] which is regiospecific, non-basic and largely avoids diarylation (Scheme 3B). Even poor leaving groups such as hydrides and carbanions can liberated with fluoride.

Phenylsilane, for example, can be activated for the reduction of aryl amides, nitriles and esters (Scheme 3C).[28–32] Similarly, using catalytic TBAF, the Ruppert-Prakash reagent[33,34] can cleave a Si-C bond to formally add a TMS-CF_3 to a carbonyl group (Scheme 3D). Other somewhat stabilised anions such as alkynes are also viable leaving groups and importantly, this allows TMS groups to be used as convenient protecting groups for terminal alkynes (Scheme 3D).[35,36]

1.3 Hyperconjugation at Silicon

1.3.1 Stabilisation of α-anions

The larger and more diffuse orbitals around silicon have implications beyond the atom's immediate coordination sphere. Hyperconjugation plays a large part in the utility of organosilanes and contributes to the stabilisation of α anions and β cations.

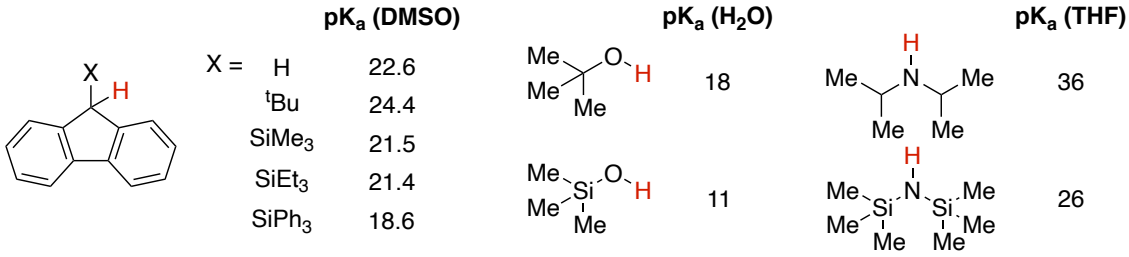

Figure 2. *pK_a of selected C-H, O-H and N-H bonds in silyl-substituted compounds compared to unsubstituted equivalents.*

In the case of α anions, large similarities can be drawn with the stabilisation of lone pairs in silicon-oxygen and silicon-fluorine bonds. Once again charge delocalisation into a low energy σ* orbital provides the stabilisation and counteracts electron donating effects from the relatively electropositive silicon. Additionally, the large and diffuse orbitals on silicon are more easily polarised and the creation of an induced dipole helps to spread the charge which is calculated to reduce the energy of carbanions by 59-84 kJ·mol^{-1}.[37] This α-anion effect is evident in the increased acidity of silicon substituted compounds (Figure 2)[38–40] with extends across a range of solvents with different heteroatoms.

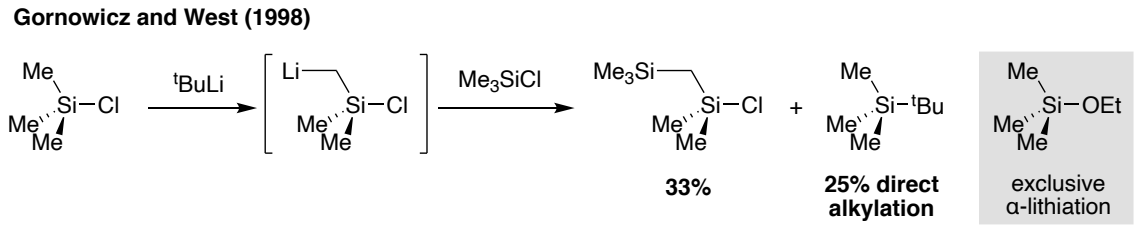

Scheme 4. *Formation of a disilylated species from α-metallation of trimethylsilyl chloride.*

In an interesting example, Gornowicz and West showed that whilst trimethylsilyl chloride (TMSCl) is usually alkylated by reactions with organometallics, with ^{t}BuLi a competing deprotonation occurs which reacts further to form a disilylated species. This selectivity is only possible due a combination of steric hindrance and the greater acidity of the α protons which increase the relative rate of deprotonation over substitution. Additionally, while the lithiation of TMSCl occurs in under a minute at room temperature, $SiMe_4$ was found to be significantly less kinetically acidic, taking 4 days to deprotonate. This exemplifies the importance of suitable low energy σ* acceptor orbital to facilitate the α-anion effect.[41] The ability to direct a deprotonation in this way, particularly at carbon, is a powerful tool and a gateway to practical methodologies for strategic bond construction in organic synthesis.

1.3.1.1 The Peterson olefination

A practical application of the silicon α-anion is the Peterson olefination, which describes i) addition of an α-silyl anion into a carbonyl group to form an α-silyl alcohol, ii) elimination of a silanol to give an alkene (Scheme 5).[42] Whether these two steps are discrete or not depends on the stability of the reactive intermediate. In cases when a lithium, magnesium, or cerium salt of an unstabilised α-silyl anion ($R^1/R^2 \neq$ EWG) is used, the resulting alkoxide is less susceptible to elimination and can be purified and isolated. This is potentially useful because – whilst addition of the silyl anion can be influenced by sterics and oxygen-silicon interactions – the diastereoselectivity is generally poor.[43,44] This can result in a mixture of α-silyl alcohols which, in turn eliminate to give a mixture of E/Z alkene diastereomers. Isolation of the α-silyl alcohol is beneficial where these alkene E/Z isomers are difficult to separate and has the potential to converge both intermediates to a single product by controlled application of different elimination conditions.

Perhaps the most interesting feature of the Peterson reaction is that the elimination of the silyl alcohol is stereospecific and can used to give *either syn-* or *anti-*elimination depending on the reaction conditions. Under basic conditions (NaH, KH, KO^{t}Bu), coordination of the alkoxide to silicon enforces elimination of the silanol from a *syn*-periplanar conformation.[45] In contrast, in acidic media (AcOH, H_2SO_4, $BF_3{\cdot}OEt_2$) an *anti*-periplanar conformation is sterically favoured as in the standard E2 reaction mechanism.[46]

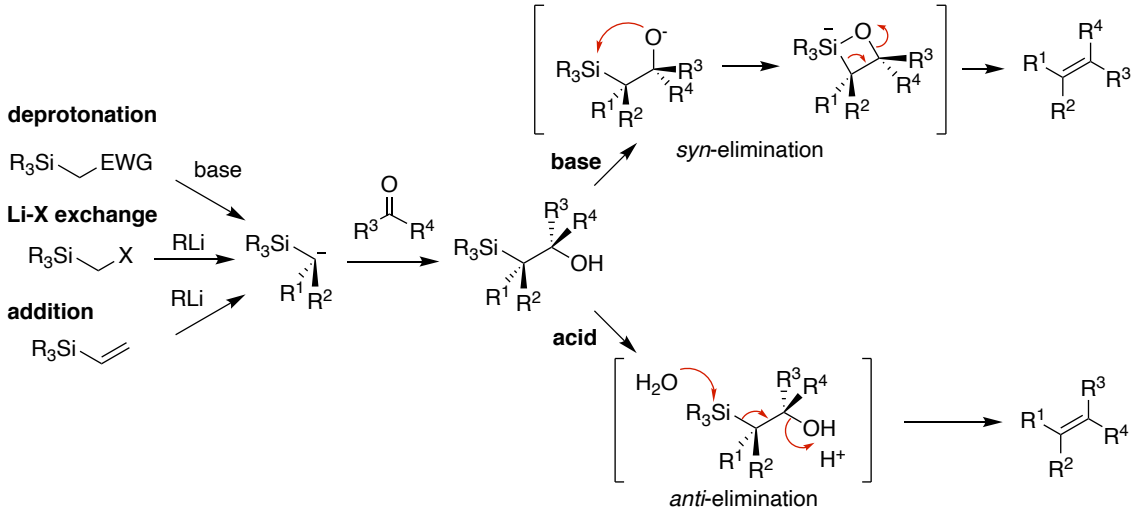

Scheme 5. *The Peterson elimination featuring 3 strategies to form the α-silyl anion and both acid and base mediated elimination pathways.*

Although useful, this reaction is often disfavoured over other olefinations (Wittig, Horner-Wadsworth-Emmons, Julia-Kocienski). The first reason is that, whilst partially stabilised by the α-anion effect, α-silyl anions are still far more basic than phosphorus ylides or sulfones.[47] They typically require either an additional electron withdrawing group to stabilise the negative charge, or harsher deprotonation conditions such as BuLi·TMEDA.[41,48] Additionally, as the anions are very reactive, they exhibit less functional group tolerance and require transmetallation with $CeCl_3$ with base-sensitive substrates.[49] Whilst alternative methods of generating anions such as lithium halogen exchange or addition across a vinyl silane are possible, this approach is generally less versatile.[50] The second disadvantage is that the poor selectivity in the addition of the α-anion into the carbonyl group necessitates chromatographic purification; either to separate the diastereomeric α-silyl alcohols

or E/Z alkenes. Consequently, recent developments have focussed on accessing α-silyl alcohols from α-silyl ketones or epoxides.[50]

Although less mild, the higher reactivity of the Peterson olefination can be valuable for the reaction of sterically hindered ketones, as exemplified by Monti's synthesis of lacifolol (Scheme 6A).[51] A key step in this synthesis was a (*Z*)-selective ketone olefination however use of a Wittig reagent gave no olefination and only epimerisation of the α-methyl ketone. Addition-rearrangement strategies such as the Meyer-Schuster reaction also failed, however use of the Peterson reaction gave the desired product in 82% yield as a 93:7 *Z*:*E* diastereomeric mixture. As well as greater rates of addition, the elimination of silicon reagents is also faster than comparative methods. This is illustrated by reactions of doubly stabilised anions which give exclusively Peterson olefination over Horner-Wadsworth Emmons or Julia-Kocienski products (Scheme 6B and C).[52,53] This in turn can be used to synthesise of vinyl triflones or vinyl phosphonates.

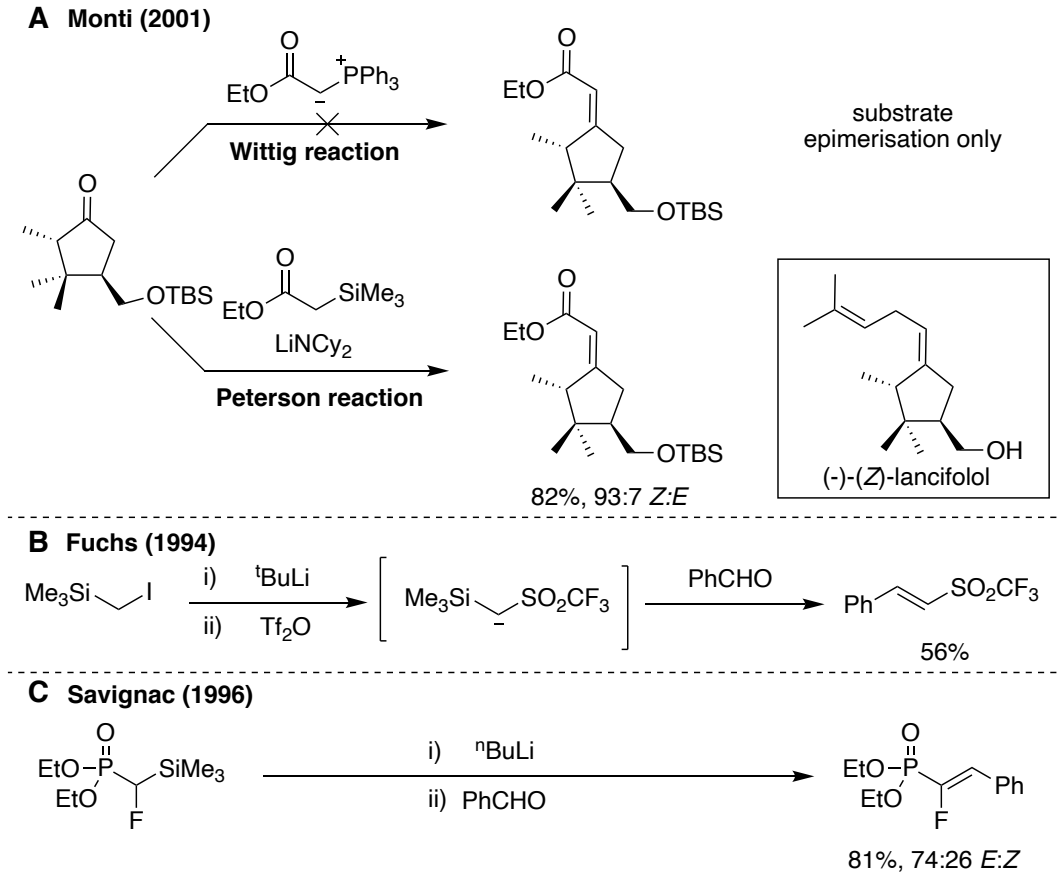

Scheme 6. *Applications of the Peterson reaction;* ***(A)*** *Step in (-)-(Z)-lancifolol synthesis employing the Peterson reaction as a more reactive Wittig alternative;* ***(B)*** *Selective Peterson to a vinyltriflone;* ***(C)*** *Selective Peterson reaction to an α-fluorovinylphosphonate.*

1.3.2 Stabilisation of β-cations

Complementary to α-anions, silicon also stabilises β-cations by hyperconjugation from a Si-C σ bond into a vacant p orbital (Figure 3A). Whilst similar effects are present in alkylated carbocations, the larger and more diffuse orbitals on silicon are particularly efficient electron donors due to their high energy and large orbital overlap.[54,55] This is evident in the calculated stability of simple cations; in comparison to a methyl cation, ethyl and *n*-propyl cations which benefit from C-H and C-C hyperconjugation are 142 and 194 kJ·mol^{-1} more stable (Figure 3B).[56] However, donation from a C-Si bond is roughly twice as powerful making the corresponding ion 301 kJ·mol^{-1} lower in energy. This can be largely deconvoluted from hyperconjugation by calculating the energy of $SiH_3CH_2CH_2^+$ in which the σ donor orbital lies orthogonal to the p acceptor orbital. This conformer, which is only inductively stabilised, has a relative stability of -177 kJ·mol^{-1}. Such a large energy difference is unexpected for torsional strain[57] and suggests hyperconjugation mostly accounts for the remaining 124 kJ·mol^{-1} in the silicon β-cation effect. These *in silico* predictions are supported work from Zhang and co-workers[58] who used quantitative mass spectrometry to calculate stability of ions relative to an ethyl cation. They found that for a secondary alkyl cation, β-trimethylsilyl substitution gave stabilisation in the order of 146 kJ·mol^{-1} which is similar to the 159 kJ·mol^{-1} increase in stability going from the ethyl to the β-silyl ethyl cation.

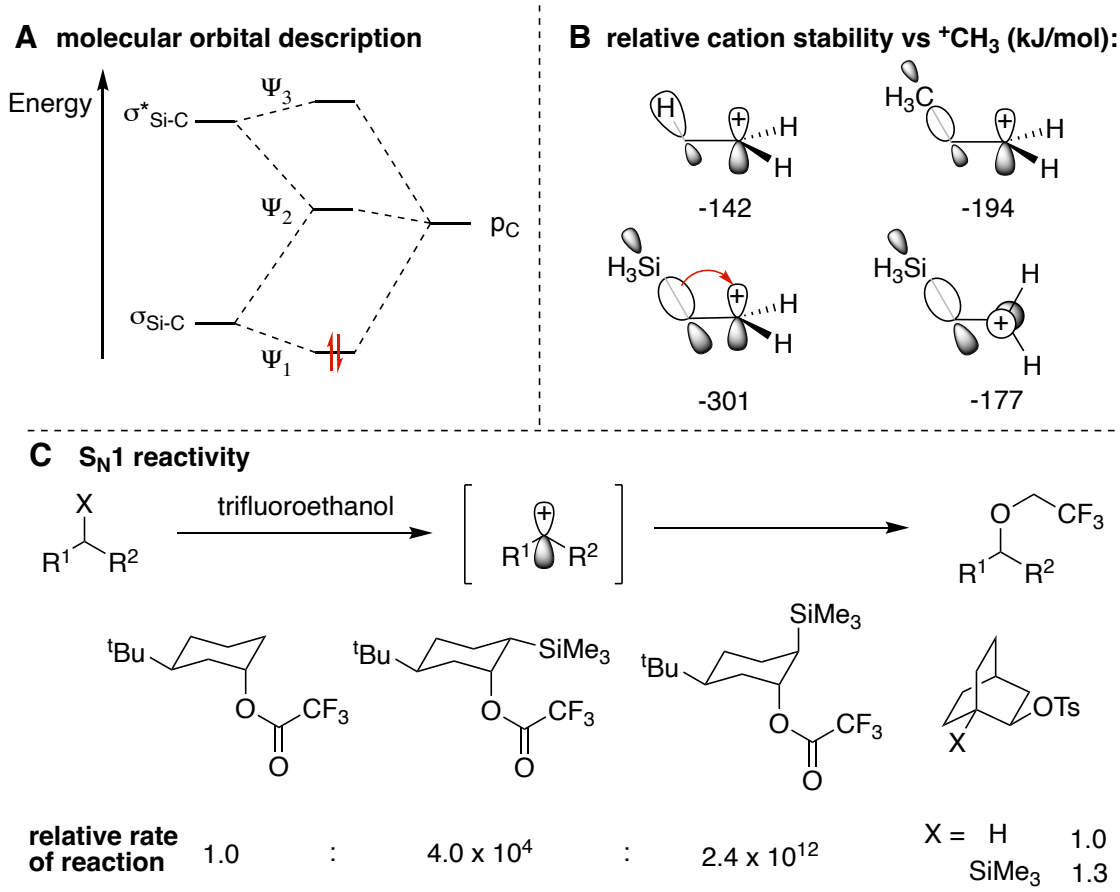

Figure 3. *The β-silicon effect;* ***(A)*** *Interaction of molecular orbitals;*[18] ***(B)*** *Cation energies relative to the methyl cation with the stabilising orbital interaction highlighted;*[56] ***(C)*** *The relative rate of S_N1 substitution at conformationally locked β silyl electrophiles.*[55]

The empirical consequences of the β-cation effect are clearly illustrated in the substitution of conformationally locked β-silyl TFA esters (Figure 3C).[54–56] Under S_N1 conditions, the rate of reaction is markedly increased with a β-silicon because of the stabilisation of the cationic intermediate. However, the degree of stabilisation strongly dependent on conformation, and reflects the spatial orbital overlap between the donor and acceptor orbitals. In an antiperiplanar conformation the dihedral angle between the largest lobes of the Si-C donor and C-O σ* acceptor orbital is 180°, which provided optimal overlap in the transition state and an increase in rate by a factor of 10^{12}. However, in the conformationally locked gauche isomer, the 60° dihedral angle gives less efficient interactions which results in higher energy transition states and a rate increase of only 10^4 over the unsubstituted analogue.[55] In the extreme case where the two groups are locked into a 90° dihedral angle, the orbitals are orthogonal and the interaction is minimal.[59,60] This is shown

in bicyclo[2.2.2]octane where the rates of S_N1 substitution is much more similar for the unsubstituted and trimethylsilyl bicyclo[2.2.2]octyl tosylates. Nevertheless, for some substrates, stabilisation of a β-cations can be enough to open new reaction pathways.

1.3.2.1 The Hosomi-Sakurai Allylation

The Hosomi-Sakurai allylation of aldehydes and ketones in enabled by β-cation stabilisation from silicon. Original reports of this reaction used oxyphilic metal Lewis acids ($TiCl_4$, $AlCl_3$, $BF_3{\cdot}OEt_2$, $SnCl_4$) to activate a carbonyl group or acetal, towards attack from a mildly nucleophilic allylsilane (Mayr nucleophilicity N = 1.6 for trimethylallylsilane).[61–63]

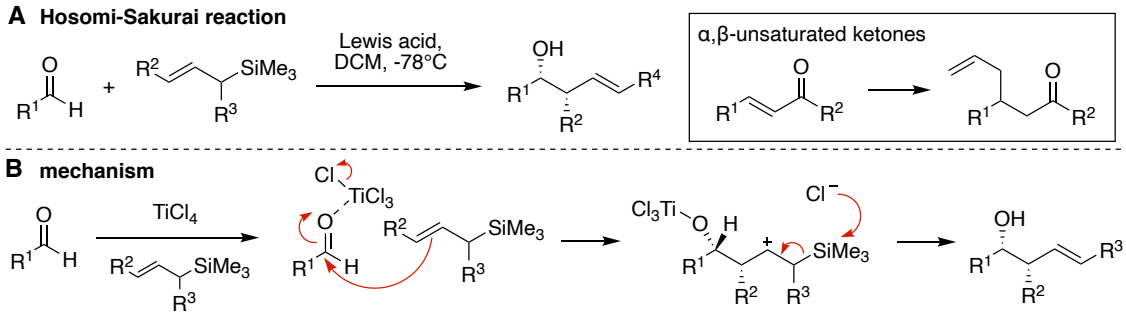

Scheme 7. *The Hosomi-Sakurai allylation;* ***(A)*** *General scheme and conditions for aldehydes with 1,4 addition highlighted for α,β-unsaturated ketones;* ***(B)*** *Mechanism for $TiCl_4$-mediated allylation.*

This leads to a β-silyl cation intermediate in which the silyl group is cleaved using a halide from the Lewis acid. The TMS halide and metal alkoxide and are quenched on work-up to give a homoallylic alcohol. In the case of α,β-unsaturated electrophiles, aldehydes give the expected homoallylic alcohols, however ketones which have a less electrophilic carbonyl tend to undergo conjugate addition.[64,65]The addition and elimination is not diastereoselective, meaning both (*R*)- and (*S*)-C1 substituted allylsilanes both predominantly give (*E*)-alkenes which are the thermodynamic and kinetic products.[66]

However, when the allyl silane has C3 substitution, *syn*- and *anti*- diastereomers are both possible products. Distribution of these depend on the reaction conditions, however in most cases *syn* addition predominates. Initially the reason for this was

presumed to be an open, antiperiplanar transition state which minimises destabilising steric clashes (Scheme 8A and 8B).[67]

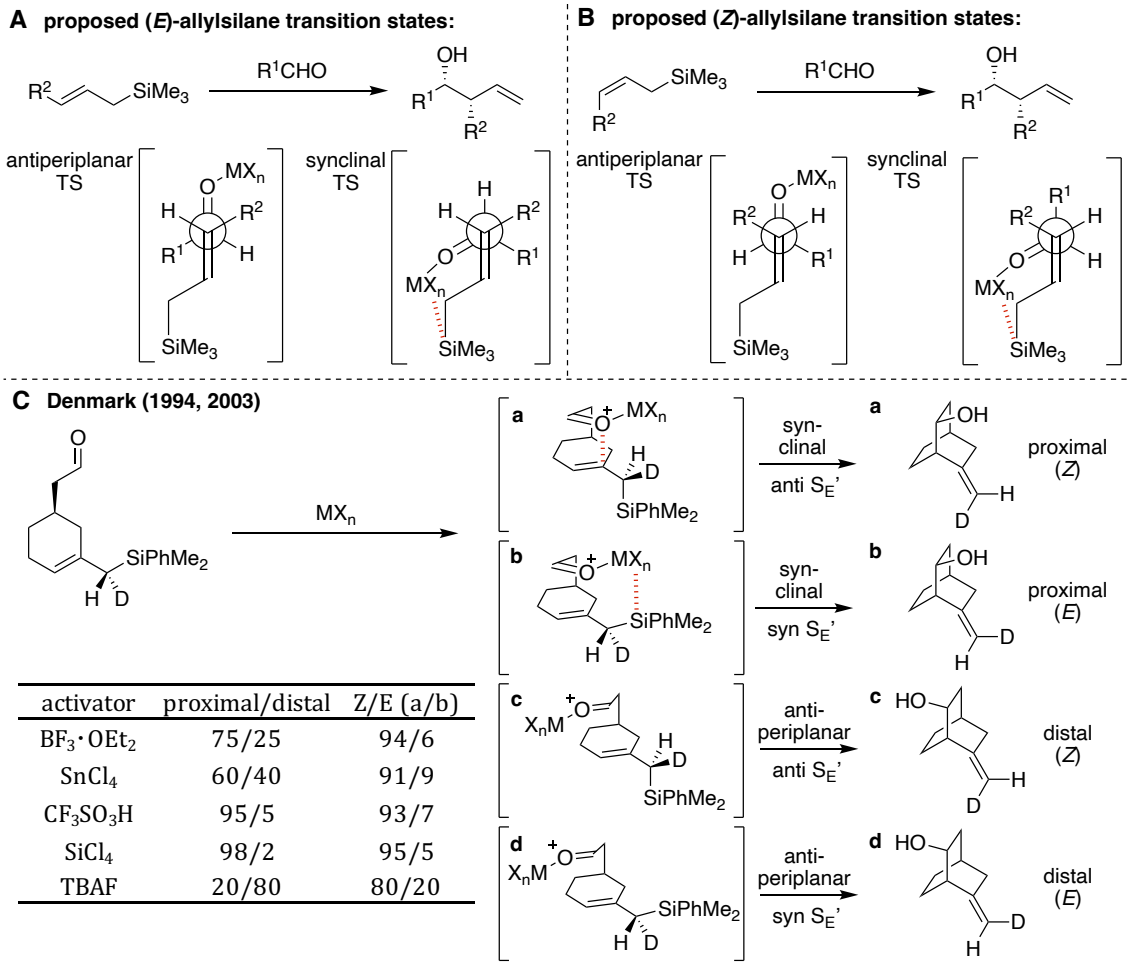

activator	proximal/distal	Z/E (a/b)
$BF_3 \cdot OEt_2$	75/25	94/6
$SnCl_4$	60/40	91/9
CF_3SO_3H	95/5	93/7
$SiCl_4$	98/2	95/5
TBAF	20/80	80/20

Scheme 8. *Diastereoselectivity in the Hosomi-Sakurai allylation;* ***(A)*** *syn-selective addition of (E)-allylsilanes rationalised by either an antiperiplanar or synclinal transition state;* ***(B)*** *syn-selective addition of (Z)-allylsilanes rationalised by either an antiperiplanar or synclinal transition state;* ***(C)*** *Intramolecular mechanistic studies by Denmark with possible reaction pathways with experimental selectivity tabulated for several acids and TBAF.*

However, using a rigid intramolecular model reaction, Denmark and co-workers[68] have shown that the transition state generally favours a synclinal arrangement of the carbonyl group relative to the allyl silane (Scheme 8C, transition states a and b) leading to proximal homoallylic alcohols.

Furthermore, this preference is dependent on the Lewis acid used. Computational modelling by Bottoni and co-workers[69] suggested a concerted mechanism proceeding through an 8-membered transition state with a key interaction between the Lewis acid halide ligands and the silicon (Scheme 8, synclinal transition states in (A) and (B), transition state b in (C), highlighted in red). This would require the

silyl group to be on the same face of the alkene as the electrophile (*syn* S_E'). However, using a deuterated and enantiomerically enriched substrate, Denmark[70] observed strong (*Z*) alkene diastereoselectivity resulting from an *anti* S_E' pathway for all Lewis acids. This led to the conclusion that: i) the preference for the carbonyl and alkene to be *syn*-periplanar driven by a secondary orbital interaction between the oxygen and the transient carbocation (Scheme 8C, transition state a), ii) the *anti* S_E' silyl conformation is favoured for all Lewis acids and arises from both steric repulsion and more stabilising orbital interaction from an *anti* C-Si σ orbital with the π^* orbital.[71,72]

The Hosomi-Sakurai allylation can also be catalytic in Lewis acid. In these examples, trimethyl silyl iodides,[73] triflates,[74] mesylates[75] and chlorides (with additional $InCl_3$)[76] are used. $Ti(Cp)_2OTf_2$[77] and Ph_3COTf[78] can also be used substoichiometrically, however Hollis and Bosnich[79] found that in these instances their role changed to an initiator of a self-propagating reaction in which the $SiMe_3X$ by-product is the catalytically active species (Scheme 9A). This partially explains why enantioselective variations using enantioenriched Lewis acids can be difficult to achieve. Nevertheless, catalytic asymmetric Sakurai reactions are known and operate through 3 main mechanisms (Scheme 9). Lewis acids without labile ligands can be used such as Yamamoto's tartatic acid derived boronic esters.[80,81] BINOL and silver[82]/titanium[83] fluorides are also viable catalysts although generally allylstannanes[72] which are more active and more toxic give higher enantiomeric excesses. Lewis bases[84–88] can also be used in conjunction with allyltrichlorosilane which enables an intramolecular allylation proceeding through 6-coordinate silicon cations. Finally, chiral superacids[89–91] have been used as enantiomerically enriched TMS-transfer agents which work as part of the TMS-X catalytic cycle.

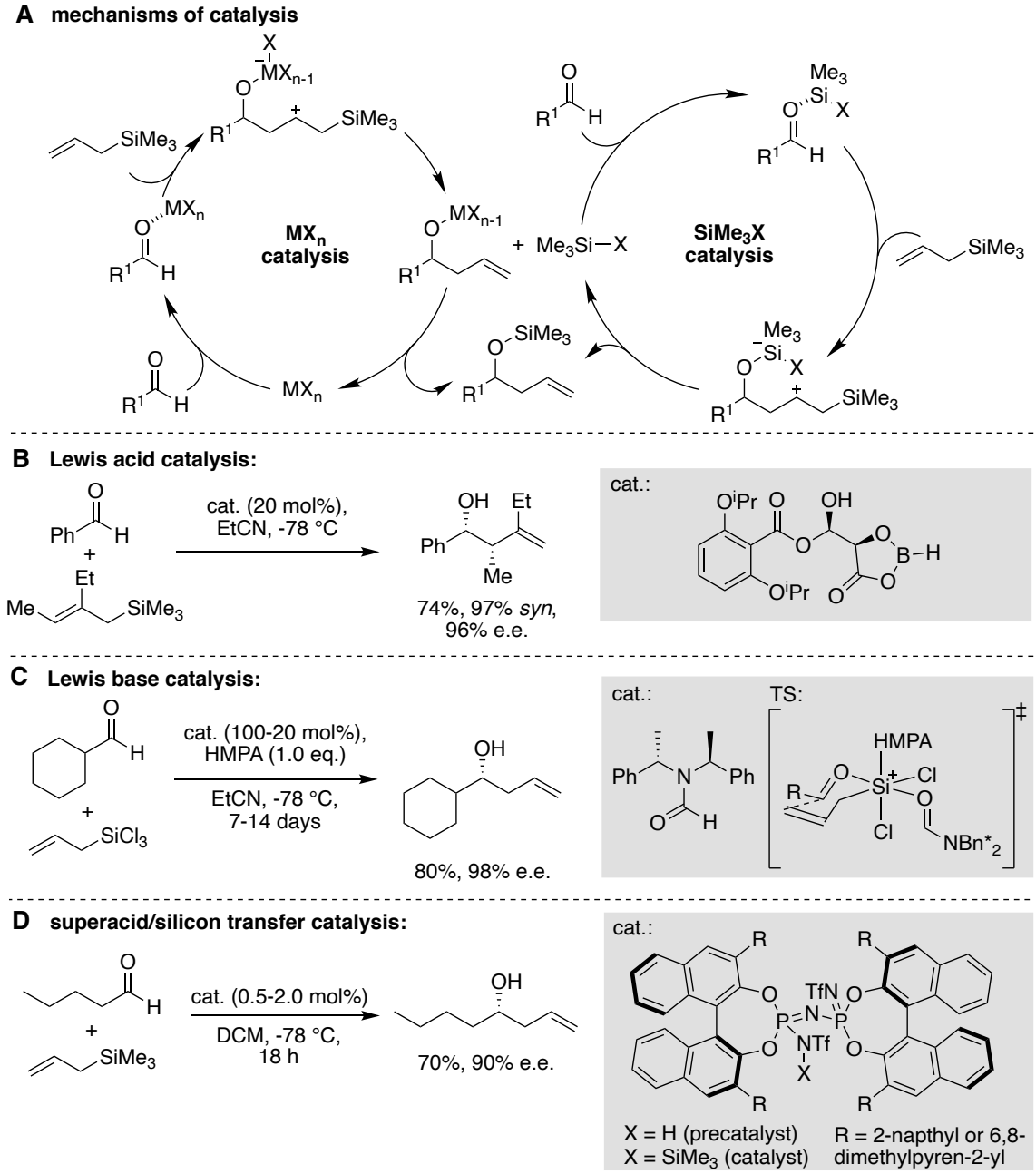

Scheme 9. *The catalytic Hosomi-Sakurai allylation;* ***(A)*** *Mechanisms of Lewis acid and silicon transfer catalysis;* ***(B)*** *Enantioselective Lewis acid catalyst;* ***(C)*** *Enantioselective Lewis base catalysis;* ***(D)*** *Enantioselective superacid catalysis*

1.3.2.2 The Mukaiyama Aldol Reaction

The Mukaiyama aldol addition[92,93] is another reaction which can be considered to transition through a β-silyl cation. Unlike the Hosomi-Sakurai allylation, in this case the carbocation receives only inductive stabilisation from the silicon, as the oxygen lone pair is a better donor than hyperconjugation from the Si-C σ bond. This increases the nucleophilicity of the silyl enol ether (Mayr nucleophilicity N = 5.4 for

2-(trimethylsiloxy)propene vs 1.6 for trimethylallylsilane)[63,94] and as a result, many more Lewis acid are known to catalyse the reaction. These include but are not limited to Sn(IV), Sn(II), Sc (III), Mg(II), Zn(II), Li(I), Bi(III), Ln(III), Pd(II), Ti(IV), Zr(IV), Ru(II), Rh(II), Fe(II), Fe(III), Al(III), Cu(II), Ce (III) Au(I), R_3SiX, Ar_3C^+, superacids as well as calcinated clay.[95–101] Asymmetric catalysis is also possible and has been reviewed regularly.[95,98,99,102–104]

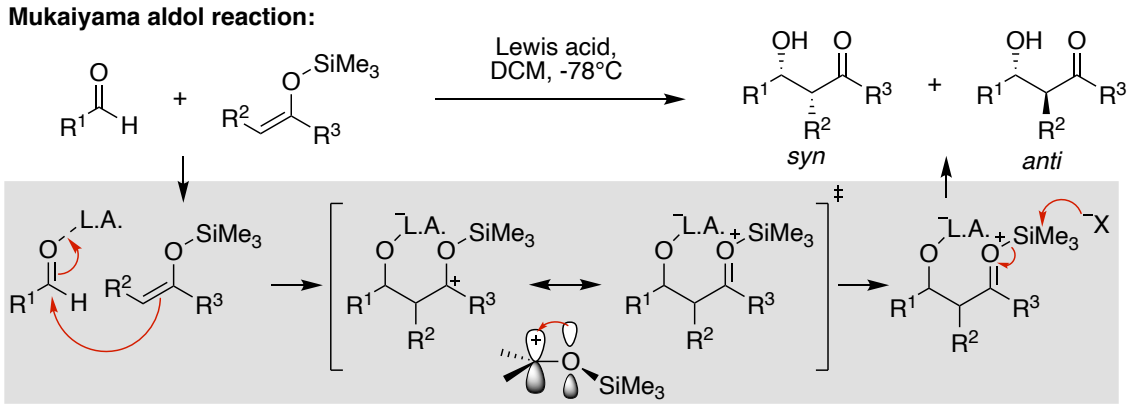

Scheme 10. *Overview and mechanism of the Mukaiyama aldol reaction with general Lewis acid L.A.*

Due to the variety of conditions used in these reactions, several distinct mechanisms can be invoked, however the relative diastereoselectivity is mainly rationalised using 4 key transition states.[105] In contrast to the cyclic transition states Zimmerman and Traxler[106] proposed for the anionic aldol, the Mukaiyama aldol predominantly proceeds through an open transition state with the carbonyl antiperiplanar to the silyl enol ether (Scheme 11).[107] This is favourable by minimisation of the induced dipole; however due to the congested transition state it is generally the steric rather than electronic component which has the greatest influence on stability. This is particularly important for large Lewis acids which coordinate to the aldehyde in a trans geometry.

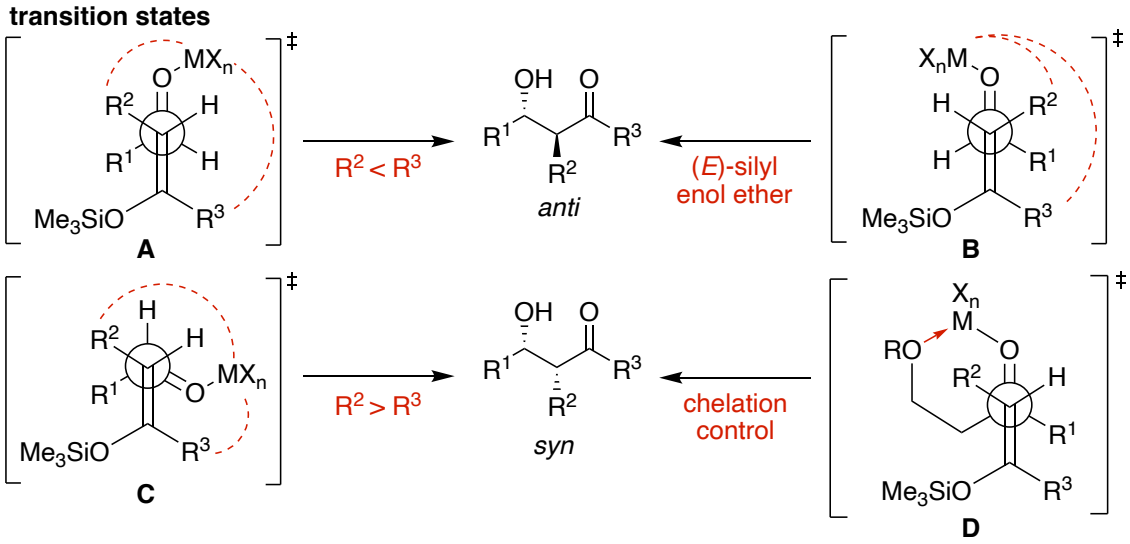

Scheme 11. *Transition states leading to anti- and syn- aldol products with red dotted lines showing key steric repulsions and dative bond showing chelation control.*

Reactions with *anti* diastereoselectivity often proceed through transition states A and B (Scheme 11) as these conformations provide sufficient spacing between the Lewis acid and R groups where R^3 is large or an (*E*)-silyl enol ether is used.[105] Where R^2 is large, syn selectivity predominates. While an antiperiplanar transition state has been used to rationalise the observed *syn* selectivity,[105] computational modelling by Wiest *et al.*[108] showed a synclinal type transition state is more probable due to better minimisation of sterics resulting in lower energy transition structures. Chelation control can also be used to generate *syn* diastereoisomers.[97,109]

In comparison to the anionic aldol reaction, the Mukaiyama aldol has numerous advantages. Firstly, preparation of the active nucleophile in a separate step enables conditions to be selected to preferentially form either the kinetic or thermodynamic silyl enol ether. Unlike metal enolates, silyl enol ethers are usually stable so can be isolated, purified (distillation or column chromatography) and stored without cleavage of the strong Si-O bond.[110] The use of stereochemically pure starting materials allows the Mukaiyama aldol to proceed with full regiospecificity.[96] Additionally, silyl enol ethers are also neither basic nor acidic and are unreactive on their own. However, they are easily activated – even by mild Lewis acids at low temperatures – which conveys a high degree of functional group tolerance as well as avoiding self-condensation. Furthermore, due to chelation to Lewis acids,

formation of tertiary alcohols is possible without subsequent elimination to α,β-unsaturated carbonyls (Scheme 12).[93,111,112]

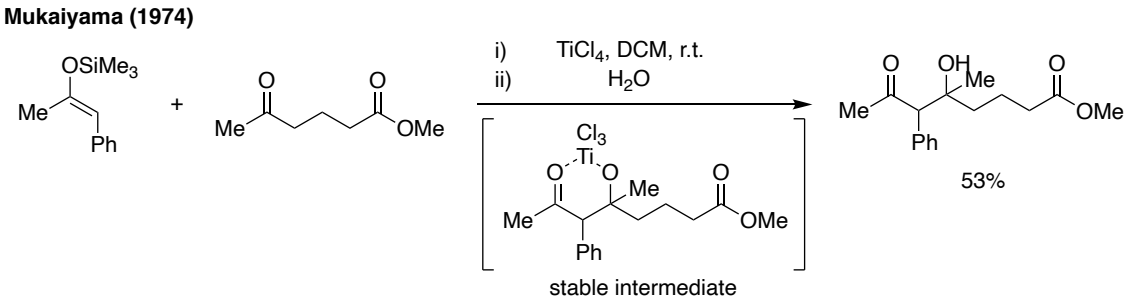

Scheme 12. *The Mukaiyama aldol reaction for the synthesis of labile β-hydroxyketones without elimination.*

1.4 Hypercoordination at Silicon

1.4.1 Bonding at 5- and 6- Coordinate Silicon

One aspect of silicon chemistry which is completely unlike carbon is hypercoordination. This is where a central atom can form any type of bonding interaction with a greater number of groups than can be rationalised using the octet rule.[113–115] In the case of silicon this involves forming penta- and hexacoordinate species. In this respect silicon can be compared to phosphorus, sulfur and chlorine, which commonly adopt coordination numbers beyond their traditional octet. For these elements a wide range of hypercoordinated species are stable (phosphine oxides, phosphoranes, sulfoxides, sulfoniums, sulfones, sulfoxoniums, chlorate, perchlorate etc.). However, unlike phosphorus, sulfur and chlorine, silicon cannot reach higher oxidation states and instead relies on its Lewis acidity to expand its coordination sphere.[116] Consequently, hypercoordination at silicon is either achieved by weak dative bonds or the formation of anionic species which generally reduces the stability of the complexes. As such, the number and diversity of stable and isolable hypercoordinated silanes is limited, generally requiring small, chelating ligands to give thermodynamic stability. Electronegative donor atoms are also beneficial in accepting the increase in electron density in the silicon complex.[117,118]

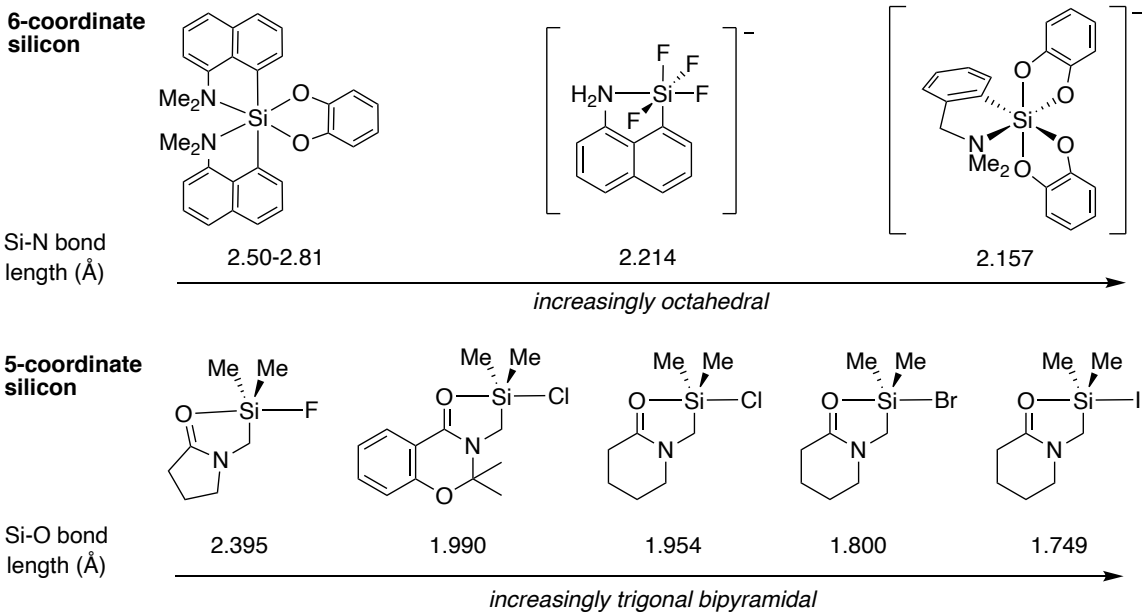

Figure 4. *Isolated 6- and 5-coordinate silicon species with bond lengths indicating the strength of the key dative bonds. Typical Si-O bond length is 1.65 Å and Si-N is 1.75 Å.*[17,119]

As these hypercoordinated species are only possible for elements in the third row and beyond, a seemingly reasonable and popular early explanation was that d orbitals facilitated the additional bonding similarly to transition metal complexes.[120] However, from the beginning of the 1990s Magnusson and others[121] showed that, as is shown for the alpha anion effect, the σ* orbitals are lowest in energy and are the first to accept electron density, leading to a 3 centre 4 electron bond. This can also be imagined using a linear combination of atomic orbital approach, as Rundle[122,123] described for PH_5 which is isoelectronic with SiH_5^-.

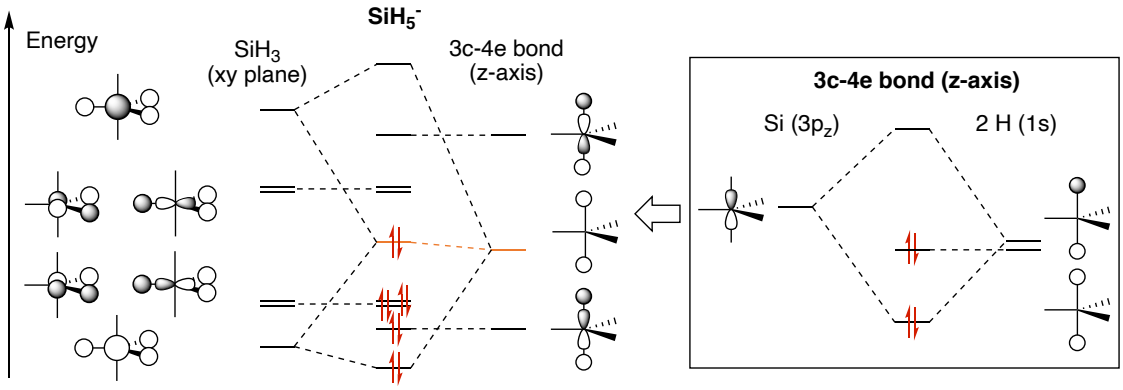

Figure 5. *Rundle's LCAO approach to the molecular orbital diagram for pentacoordinate third row elements (designed for phosphorus). The ligand-associated HOMO is highlighted in orange.*

As the molecular orbital diagram (Figure 5) shows, the HOMO in SiH_5^- is a non-bonding orbital of the axial 3-centre 4-electron bond. This orbital results from an in-

phase interaction of the two ligands only and has no net interaction with silicon's p orbitals. As a result, upon complexation the additional charge and electron density is entirely localised around the axial hydrogens which become more negative and more nucleophilic.[118] The silicon, on the other hand, now possesses an additional (relatively) electronegative ligand. Therefore, despite the complex having an overall anionic charge, the silicon becomes more electrophilic.[118] Expanding coordination from 5 to 6 has a similar effect in increasing ligand nucleophilicity but silicon ceases to be electrophilic due to its coordinative saturation.

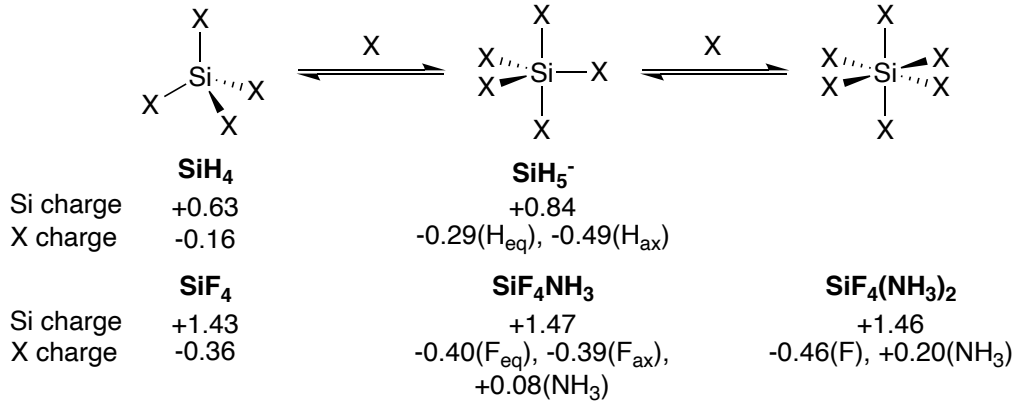

Figure 6. *Hypercoordinated silanes with calculated Mulliken charges showing the increasing charge separation between the electropositive silicon and its ligands.*[118]

1.4.2 Reactivity at 5- and 6- Coordinate Silicon

The increased reactivity of hypercoordinated complexes has a number of consequences for organosilicon chemistry.[124] The first fundamental point of difference is that unlike second row elements, nucleophilic substitution at silicon (S_N2@Si) can proceed through an associative mechanism with an intermediate transition complex.[117]

Many research groups have used chloride exchange to model substitution at silicon.[125] One of the clearest descriptions came from Bento and Bickelhaupt[126,127] who calculated the potential energy surface of the reaction, clearly showing deviation from a 'normal' S_N2 pathway. As shown in figure 7, the major difference is the greater stability of hypercoordinated silicon the transition complex in comparison to the transition state at carbon. This generally lowers the activation barrier for the reaction, but the extent of stabilisation is largely defined by the sterics of the R groups. Large groups disfavour additional coordination and follow a

higher energy pathway similarly to substitution at carbon. At the other extreme, small methyl groups make the substitution barrierless and for chlorosilane (R = H) the pentacoordinate intermediate complex becomes an energy minimum.

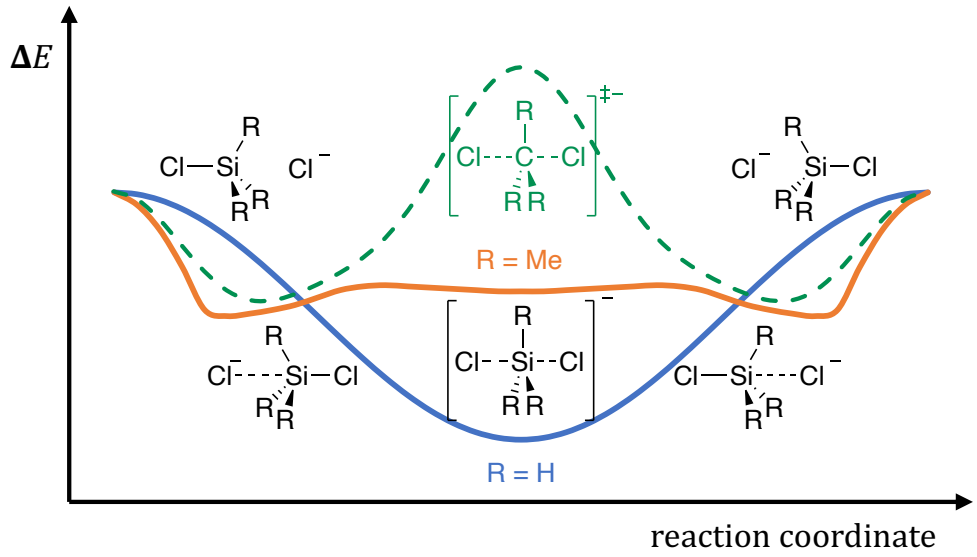

Figure 7. *Representation of the computed potential energy surface along the reaction coordinate for chloride substitution at SiH_3Cl (blue), $SiMe_3Cl$ (orange) and R_3CCl (green dashed).*

As well as being low-energy intermediates, hypercoordinated species show greater reactivity than 4-coordiante silanes. Charge separation between the silicon and the ligand as described above makes the silicon more electrophilic and the ligands more nucleophilic and better leaving groups. This principle was exemplified by Corriù and co-workers[31] with a kinetic study of nucleophilic substitution at silicon. Tetravalent $PhMe_2SiF$ and preformed $[K(18\text{-crown-6})][PhMe_2SiF_2]$ were each reacted with MeMgBr under identical conditions. The former reaction reached completion in 5 hours whilst the pentacoordinate species quantitatively formed $PhSiMe_3$ in under 3 minutes.

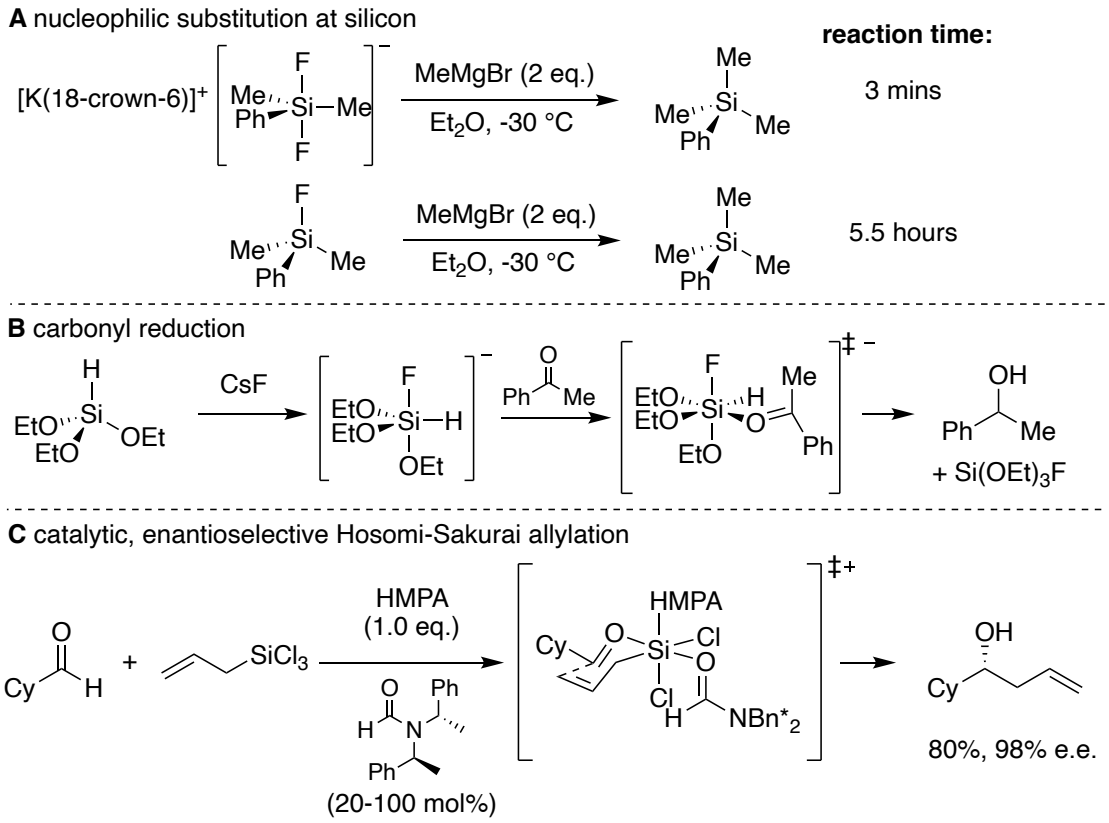

Scheme 13. *Applications of increased reactivity at hypercoordinated silicon;* ***(A)*** *Increased rate of nucleophilic substitution;* ***(B)*** *Fluoride activation of silanes for carbonyl reduction;* ***(C)*** *Enantioselective Lewis base catalysis in the Hosomi-Sakurai allylation.*

Similarly, fluoride activation can enable the departure of poor leaving groups. In Corriù's carbonyl reduction the addition of a fluoride salt to $(EtO)_3SiH$ a pentacoordinate complex which is vastly more reducing than its parent compound. It is likely that the intermediate is a hexacoordinate complex in which hypercoordination increased both the nucleophilicity of the hydride and the electrophilicity of the carbonyl.[28,32,128,129] In more contemporary work, a hexacoordinate complex is the proposed transition state for a base-catalysed Hosomi-Sakurai allylation.[130–132] In this example, the aldehyde, the additive and the enantioenriched catalyst are all neutral donors to the cationic intermediate.[87]

1.4.2.1 Hiyama Coupling

The principles of hypercoordination also extend into cross coupling chemistry. In 1978 Kumada and coworkers showed that potassium organoperfluorosilicates $K_2[RSiF_5]$ could be used in palladium-catalysed cross coupling reactions with aryl and allyl halides.[133,134] This idea was then simplified by Hiyama and Hatanaka,[135,136]

who used fluoride sources such as TBAF and TASF to form the reactive pentacoordinate species *in situ*. This methodology is now referred to as the Hiyama cross-coupling (Scheme 14). The use of a silicon-based nucleophilic coupling partner is attractive for several reasons including the abundance of silicon, its low cost, and the diversity of silane syntheses. Furthermore, in comparison to zinc or magnesium salts, silanes gave increased functional group tolerance and stability to acids, bases, and water. Organosilicon compounds are also far less toxic than organotin species and are more stable than boronates: 2-pyridyl/furfuryl silanes, for example, do not readily protodesilylate when used in Hiyama cross couplings with copper or silver activation (Scheme 15B).[137–139] However, under standard conditions the major problem from a sustainability perspective was requirement for stoichiometric and soluble fluoride source such as TBAF. Additionally, although tetraalkylsilanes are desirable starting materials, the lack of Lewis acidity at silicon restricts hypercoordination meaning only more reactive substrates undergo transmetallation with palladium or nickel.[140]

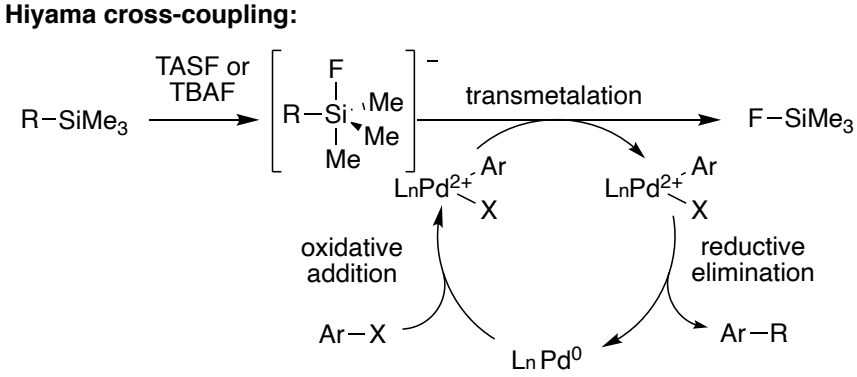

Scheme 14. *Overview and simplified mechanism for the Hiyama cross coupling.*

Generally the scope of Hiyama-type reactions is much greater for halo- and alkoxy-silanes which are more electrophilic and readily form the pentacoordinate intermediates.[141–145] Their greater Lewis acidity also enables activation by hydroxide, to give tolerance of silyl protecting groups and less costly, more sustainable processes.[146,147] However, the increased reactivity must necessarily be balanced against decreasing stability; the reagents are no longer stable with respect to acid or base (Scheme 15A).

A further improvement came independently from Hiyama and Denmark[148–150] who demonstrated that deprotonated silanols were able to transmetallate with palladium (Scheme 15C). The so called Hiyama-Denmark cross coupling benefits from extremely broad functional group tolerance including esters, ketones, and silyl protecting groups and used mild bases such as $KOSiMe_3$ and Cs_2CO_3.[151–153] The silanols can also be deprotonated and isolated as their silanolate salts prior to reaction which was found to eliminate the need for activation and suppressed protodesilylation.[154–158] Although the initial mechanistic proposals[150,159] for this system involved a hypercoordinate intermediate, Denmark and Sweis[160] reported reaction kinetics which suggested direct transmetallation from the 4 coordinate silanoate.

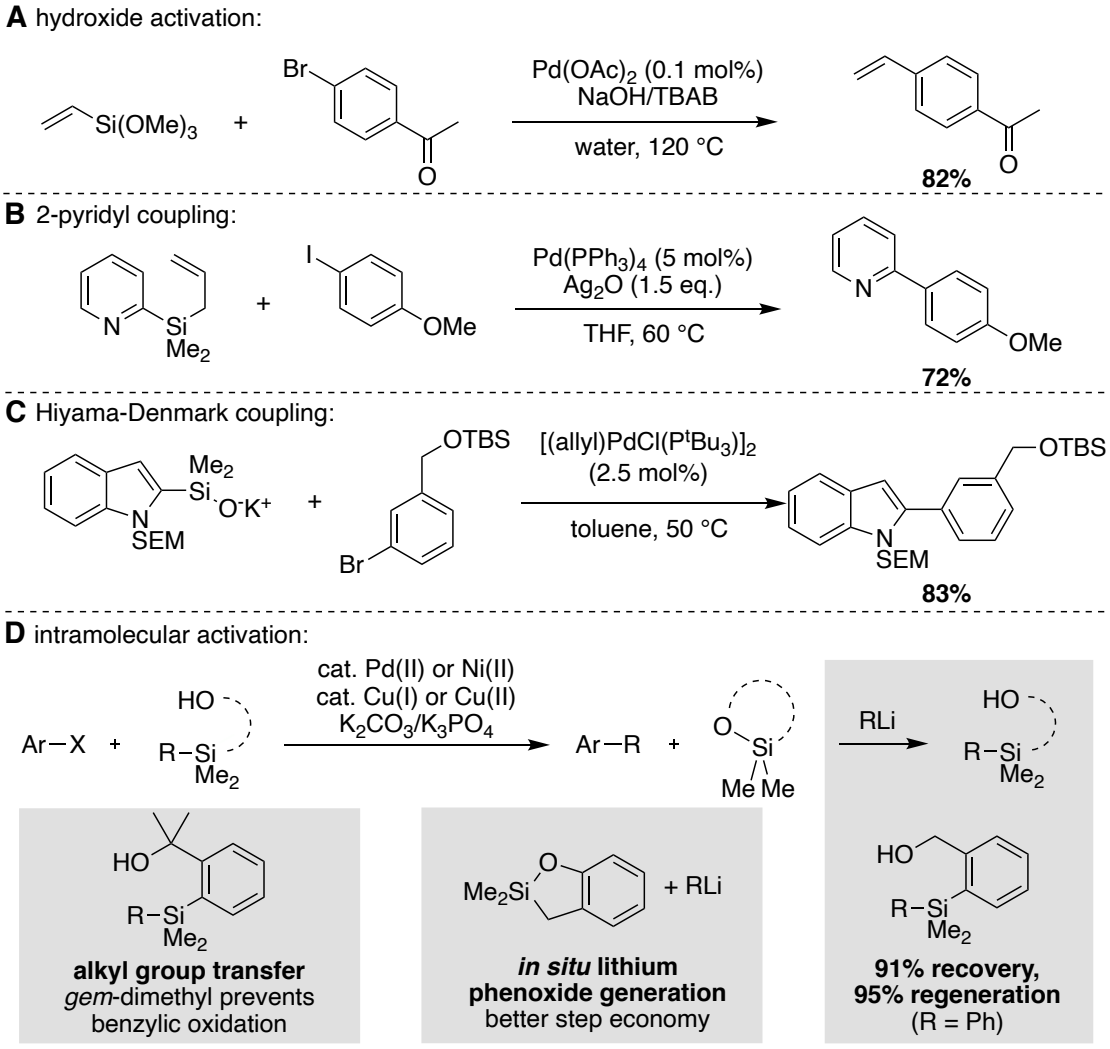

Scheme 15. *Variations on the Hiyama cross-coupling;* ***(A)*** *Hydroxide activation of trimethoxyvinylsilane;* ***(B)*** *Cross coupling of 2-pyridyl silanes;* ***(C)*** *The Hiyama-Denmark cross-coupling proceeding without activation;* ***(D)*** *Hiyama cross-coupling with alcohol-tethered silanes enabling a mild base-mediated reaction. This type of reagent can transfer alkyl groups, be generated in situ, and be recovered after reaction.*

Finally, Hiyama and Nakao[161] have designed bespoke silanes with a tethered hydroxyl group positioned to enable silane activation *via* an intramolecular interaction (Scheme 15D). Due to their preorganisation, transmetallation to a copper co-catalyst occurs under mild conditions and gives exceptional functional group tolerance. Additionally, the silyl ether by-product can be recovered and realkylated for further reactions which somewhat compensates for the expense of making a bespoke reagent.[162,163] Further scaffold modifications allow transmetalation of alkyl groups[164] and a one pot procedure which combined the silane functionalisation and coupling steps.[165]

1.5 Hydrosilanes as Reducing Agents

1.5.1 The Silicon-Hydrogen Bond

One of the most comprehensively studied roles for hydrosilanes is as mild, inexpensive, air- and often water-stable hydride sources. This feature is not defined by weak bond strengths; the Si-H bond dissociation energy is generally only slightly smaller for silanes compared to hydrocarbons (378 $kJ \cdot mol^{-1}$ for TMS-H compared to ~385 $kJ \cdot mol^{-1}$ for $(CH_3)_3C$-H).[166] The predominant reasoning is the inversion of bond polarisation. Whereas hydrocarbons are slightly polarised toward the more electronegative carbon, the electropositive nature of silicon results in greater electron density on the hydrogens which become partially hydridic (Pauling electronegativity; C 2.50, H 2.20, Si 1.90).[20] This couples with the multiple methods in which silanes can be activated to result in hydride transfer under various reaction manifolds. These include basic, acidic, radical and transition-metal catalysed reductions (Scheme 16).

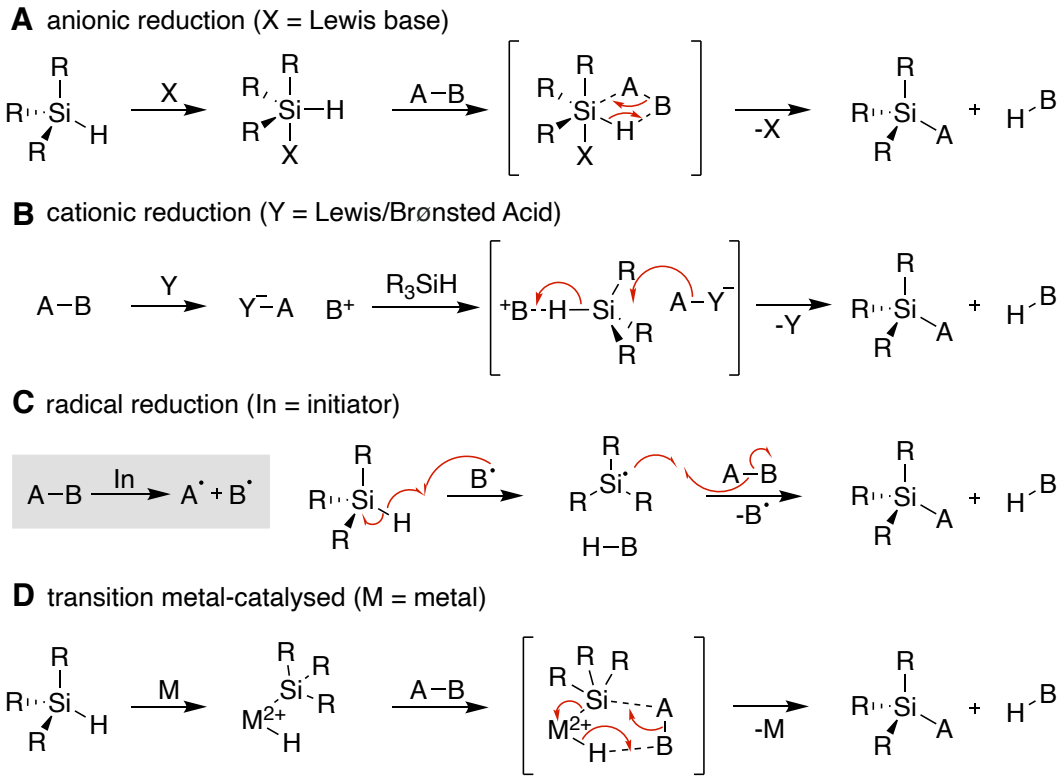

Scheme 16. *General mechanisms for silane reductions under different conditions;* ***(A)*** *Anionic;* ***(B)*** *Cationic;* ***(C)*** *Radical;* ***(D)*** *Transition metal catalysed reductions.*

1.5.2 Base Mediated Reductions

Lewis base mediated reductions involve a donor atom coordinating to the hydrosilane to form an initial pentacoordinate intermediate. Due to the 3-centre 4-electron bond the central silicon atom becomes more electrophilic and the ligands become increasingly nucleophilic which together activate the parent silane for reduction. This is described in more detail in section 1.4. Factors which favour hypercoordination therefore also favour reduction, and silanes, bases and solvent can be selected on this principle. The most active silanes are Lewis acidic with electronegative groups which support the increasing electron density in the hypercoordinated intermediate. As such, out of the commercially available reagents hydroalkoxysilanes perform well whereas those with electron rich alkyl group give poorer reactivity.[167] Similarly, strongly Lewis-basic and electronegative activating agents such as fluoride give the greatest reactivity and can be further enhanced by reducing interactions with the counter cation. Solvent can also have a large impact on reaction efficiency with coordinating and Lewis-basic solvents such as HPMA and DMF giving the greatest rate enhancement.[30,168]

Due to the charge separation of the transition state, the reaction is selective for polar functional groups, in particular carbonyls. Aldehydes react faster than ketones which are both much more reactive than ester and selectivity can be achieved by reagent selection. Other functional groups such as alkenes, bromo, nitro and amide groups remain untouched.[30] Additionally, α,β unsaturated carbonyl compounds are reduced selectively at the carbonyl carbon[169] and the stereoselective reduction of α-chiral carbonyls is consistent with the Felkin-Anh model of asymmetric induction.[170,171]

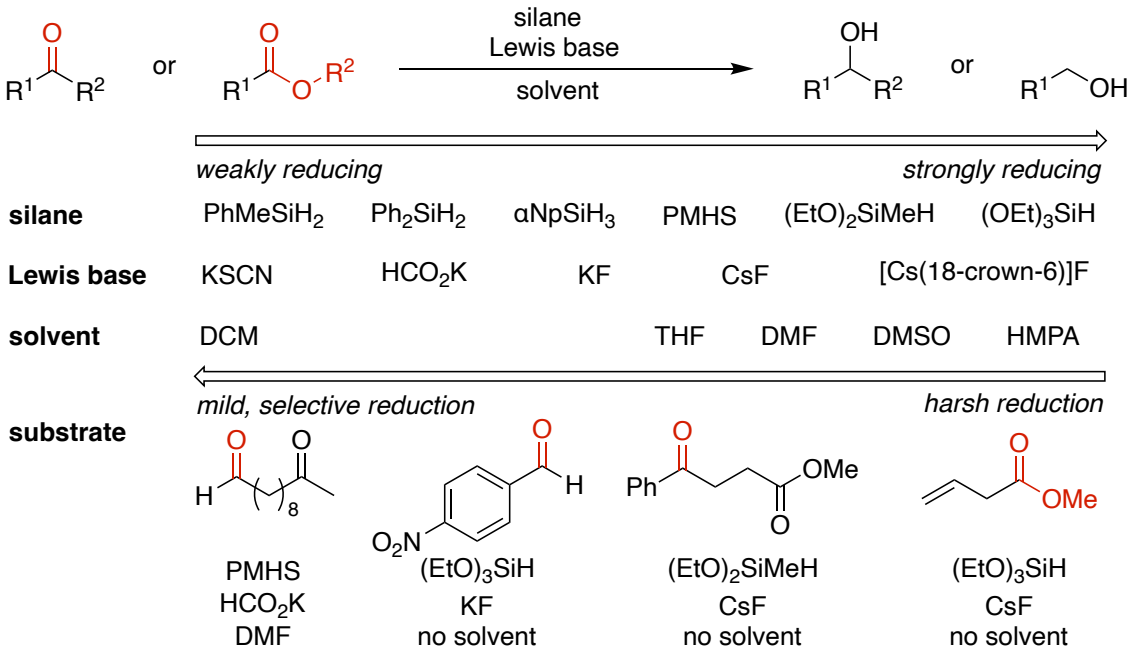

Figure 8. *Summary of reductions with silanes and Lewis bases including trends in reactivity and examples of selective reduction.*

1.5.3 Acid-Mediated Reductions

Without activation, silanes are poor hydride donors and are only able to reduce groups of significant cationic character. Appropriate substrates are limited under neutral conditions but can be accessed by treatment of alcohols, haloalkanes, alkenes and aldehydes, ketones and imines with Brønsted and Lewis acids.

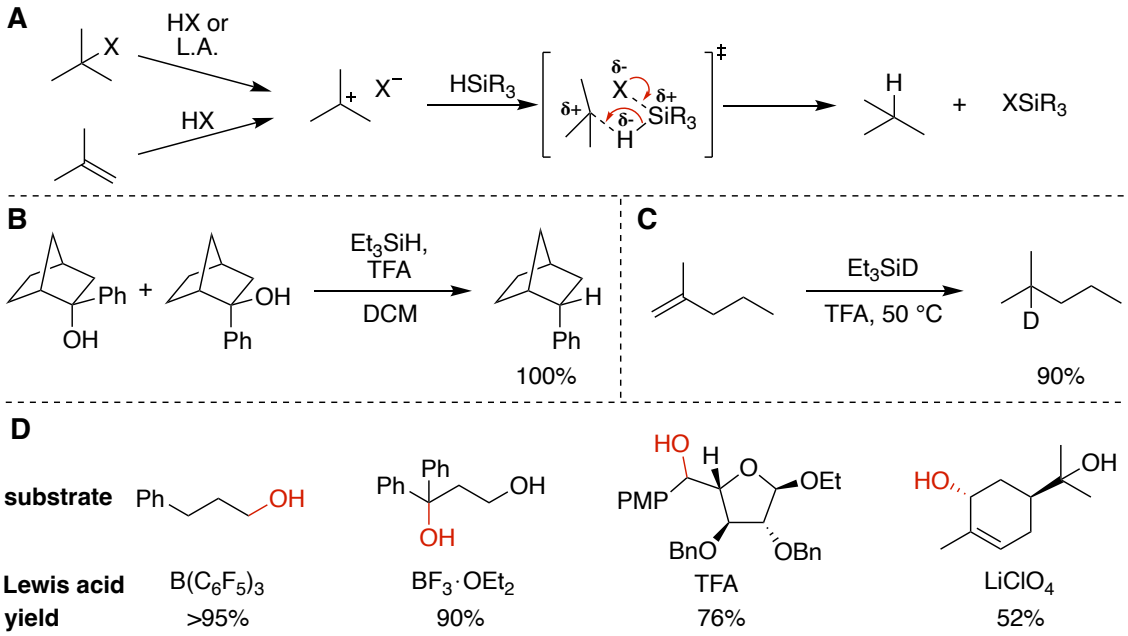

Scheme 17. *Acid-mediated silane reductions;* ***(A)*** *General reaction scheme for cation generation and reduction;* ***(B)*** *Stereoconvergent reduction of norbornanol;* ***(C)*** *Markovnikov selectivity in the deuteration of a gem-disubstituted alkene;* ***(D)*** *Alcohol reductions and the acids needed to accomplish them (selectively).*

The mechanism for these reactions proceeds through ionisation of the substrate to give carbocation.[172] Gas phase ionisation studies suggest that transfer of a hydride from a silane to a carbocation is favourable by around 33 kJ·mol^{-1},[173] however due to their extreme electrophilicity, trivalent silylium ions are doubtful in solution.[174] More likely is that either solvent or a counteranion coordinates to and stabilises the silane. This is supported by the observed rate enhancement of reduction in polar solvents. Even in cases where the use of a nonpolar solvent suppresses both ionisation and coordination, a 4-centred transition state is advocated based on both retention of stereochemistry at silicon and first order kinetics in both substrate and silane (Scheme 17A).[175,176] In solvents with higher dielectric constants such as DCM, full ionic dissociation to a carbocation is possible. The effect of this is shown in the reduction of norbornanol in which both isomers converge to the *endo*-product (Scheme 17B) based on the kinetically favoured *exo*-approach of the silane to the planar carbocation.[172] Consistent with this model, hydride (or deuteride) transfer to alkenes proceeds with Markovnikov selectivity, which is aligned with carbocation formation rather than a concerted and sterically driven mechanism (Scheme 17C).[177,178]

The acidity required to initiate the reaction is determined by the rate of carbocation formation. Primary alcohols are slow to reduce and require strong acids such as $B(C_6F_5)_3$ whereas the reduction of tertiary and benzylic alcohols proceeds under milder conditions. Where there is a clear difference in reactivity, selective reductions are possible, and for very stabilised cations use of mild acids gives tolerance for tertiary alcohols, acetals, and benzyl ethers (Scheme 17D).[179,180]

Using a similar mechanism, the Lewis acid-catalysed reduction of carbonyl groups was also proposed to occur via a an oxocarbenium ion. In the first reports,[181,182] stoichiometric $BF_3{\cdot}OEt_2$ was used to reduce aromatic aldehydes and ketones to alcohols with the BF_3 presumed to coordinate to the carbonyl. However, in a similar protocol using catalytic $B(C_6F_5)_3$, Piers and co-workers[183,184] unexpectedly found that more electrophilic substrates were reduced fastest. Furthermore, the rate of hydrosilylation is inhibited by increasing substrate concentrations suggesting carbonyl coordination to the Lewis acid is not a productive part of the catalytic cycle. Instead, KIEs and deuterium exchange suggested the incomplete and rapidly reversible transfer of a hydride from the silane to the catalyst to give $[SiR_3]^+[HC(C_6F_5)_3]^-$. In the proposed mechanism it is the silylium cation which activates the carbonyl group towards hydride transfer from the resulting borohydride (Scheme 18).

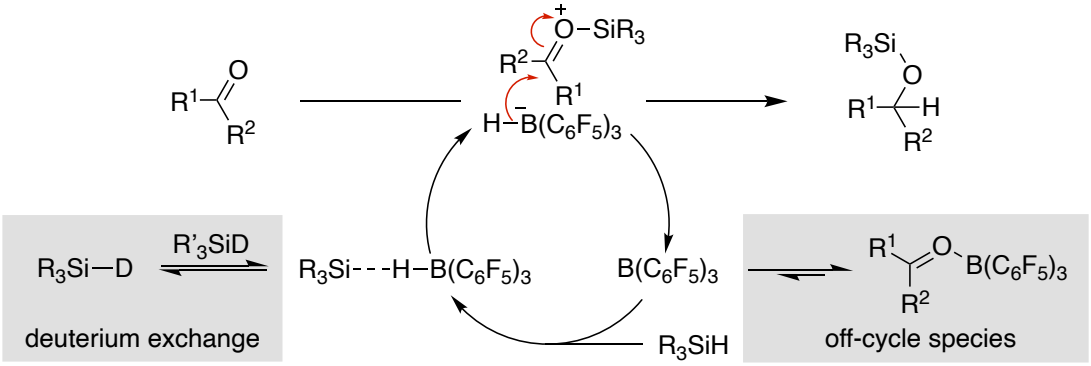

Scheme 18. *Catalytic cycle proposed by Piers for the reduction of ketones catalysed by $B(C_6F_5)_3$.*

1.5.4 Radical Reductions

For radical reductions the typical Si-H bond strength of a trialkylsilane is 398 $kJ{\cdot}mol^{-1}$ which is too high to allow efficient homolysis.[185,186] However, successive replacement of an alkyl group for a trimethylsilyl substituent decreases bond

strength by ~17 kJ·mol^{-1} per substitution. For $(TMS)_3SiH$ the Si-H bond dissociation enthalpy falls to 351 kJ·mol^{-1}; approaching that of the established chain transfer agent and radical reductant, Bu_3SnH (329 kJ·mol^{-1}). Therefore $(TMS)_3SiH$ offers a less toxic and environmentally damaging alternative as pioneered by the Chatgilialoglu group.[187] Additionally, Roberts and coworkers[188] have substantially accelerated the reaction by pairing the reductant with a polarity reversing catalyst (Scheme 19A). In this way an electrophilic hydrogen atom transfer agent such as a thiol can lower the kinetic barrier of the reduction of an alkyl radical to form a silyl radical – both of which are nucleophilic. In such systems the rate of reduction for primary radicals surpasses that of Bu_3SnH, minimising side reactions and increasing the scope of the reduction. Other advantages of $(TMS)_3SiH$ are: i) less reactive C-Cl bonds can be reduced due to the relative strength of the Si-Cl bond, ii) the steric bulk of the reagent enables diastereoselectivity in free radical reductions and, iii) the reagent is stable to both water and oxygen despite weak Si-Si bonds.[186,189] In contemporary organic chemistry this finds substantial application in photoredox[190] and radical nickel catalysis (Scheme 19B).[191,192]

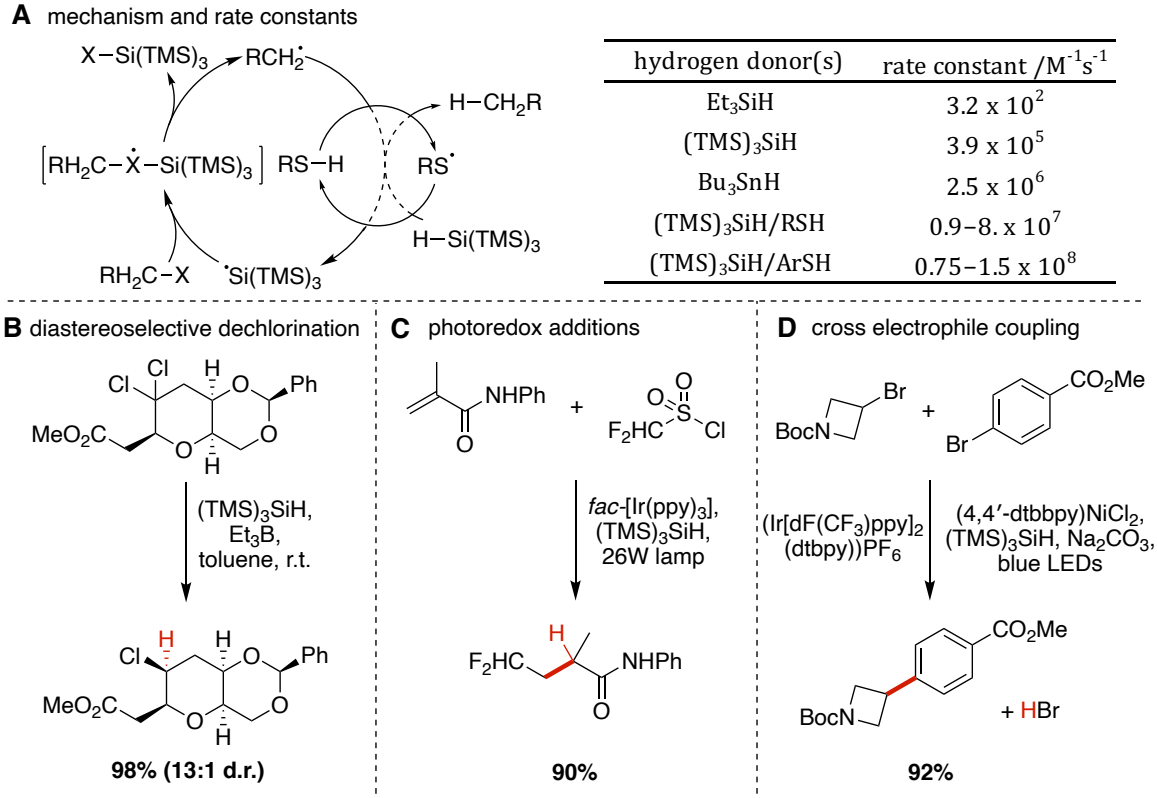

Scheme 19. *Radical reductions with $(TMS)_3SiH$;* ***(A)*** *General mechanism for reduction and table showing rate enhancement with weaker bonds and polarity reversing thiol catalysts;* ***(B)*** *Diastereoselective C-Cl reduction;* ***(C)*** *Photoredox desulfination-addition;* ***(D)*** *Photoredox radical cross electrophile coupling.*

1.5.5 Transition Metal-Catalysed Reductions

The final method of silane activation is through transition metal catalysis. Alkene hydrosilylation is one of the most established methods to form a C-Si bond and is of vital importance in producing lubricating oils and coatings in the silicone industry. Crucially, this relies on oxidative addition into a strong Si-H bond so was historically limited to noble metals and in particular platinum. Speier's complex (H_2PtCl_6)[193–195] was the first example and provided turnover numbers of up to 1 million on an industrial scale. By modification of the cations, Lukevic improved solubility ($(NBu_4)_2PtCl_6$), however it is Karstedt's complex which is the modern industrial benchmark due to its activity, selectivity, solubility and simplicity of activation.[194,196] These precatalysts have practical similarities; they all have an incubation time and from colloidal nanoparticles which eventually aggregate to platinum black. These observations suggest Pt(0) catalysis, however, whether the nanoparticles or mononuclear complexes are active is less well understood.[197,198]

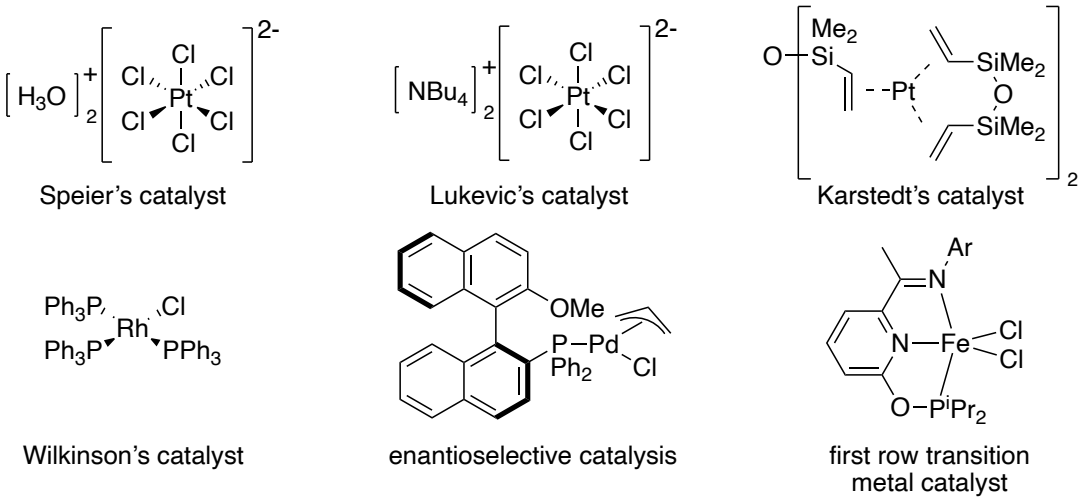

Figure 9. *Selected complexes which catalyse alkene hydrosilylation by oxidative addition into the Si-H bond.*

On large scales the process benefits from very high catalyst efficiency and high atom economy, however the platinum cannot be recovered from the organosilicon products. This contaminates the product streams, consumes rare metals (5.6 tonnes of platinum in 2007, ~3% of worldwide production)[199] and adds economic burden to organosilicon production (Pt consumption accounts for up to 30% of silicone costs).[200,201] Additionally, the process is often accompanied by side reactions including alkene hydrogenation, isomerisation and dehydrogenative silylation

which typically reduces yields by 20%.[202] As a result, a variety of molecular complexes (Pt, Pd, Ir, Rh, Ru)[200,203] have been developed including enantioselective variants (Pd, Fe, Co)[204–206] and catalysts without rare metals (Fe, Ni, Co, Mo, Ti, Ca).[201,202,207,208]

Catalytic alkene hydrosilylation reactions which occur via oxidative addition into the Si-H bond are described by the Chalk-Harrod mechanism (Scheme 20).[209] In this pathway, after addition into the Si-H bond, the metal coordinates to the alkene which subsequently undergoes a 1,2 migratory insertion. For most metals including platinum, this is rate determining and insertion into the metal hydride bond is kinetically favoured over the metal silicon bond. Reductive elimination of the alkyl silane then closes the catalytic cycle.[210,211] However, for some complexes such as Wilkinson's catalyst, the migratory insertion has a much lower energy barrier than the final reductive elimination which puts both hydrometallation isomers in dynamic equilibrium. Regioselectivity is determined by the rate of reductive elimination which is faster for the Rh-H bond over the Rh-Si bond, resulting in overall Markovnikov hydrosilylation. This is known as the modified Chalk-Harrod mechanism.[212]

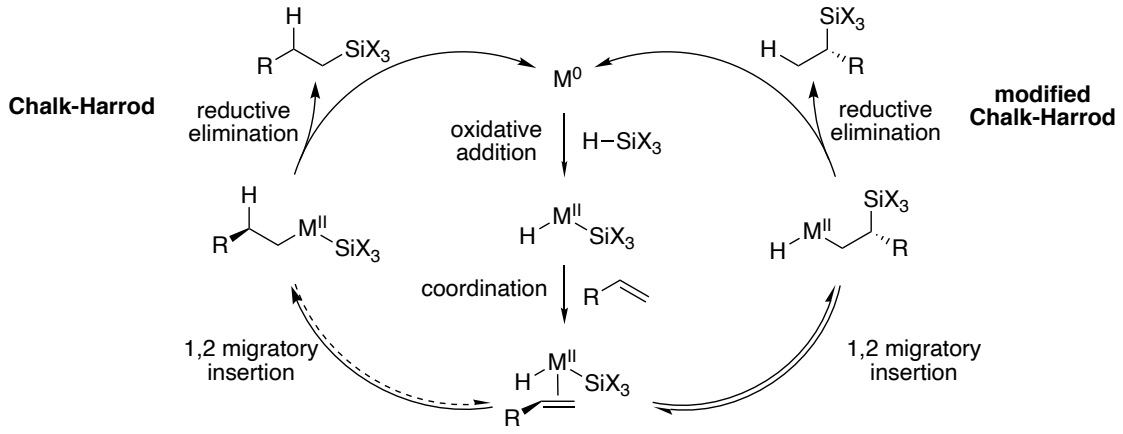

Scheme 20. *Catalytic cycle showing the mechanism for alkene hydrosilylation by (left) the Chalk-Harrod mechanism and (right) the modified Chalk-Harrod mechanism.*

1.5.5.1 The Fukuyama Reduction

Silanes can also be applied in catalytic reductions without the challenging oxidative addition into the Si-H bond. The Fukuyama reduction[213,214] is an especially mild method for the reduction of thiol esters to aldehydes without overreduction to

alcohols (Scheme 21). In this mechanism, the reaction is initiated by oxidative addition into the C-S bond by palladium (0) – typically palladium on carbon. Here, the thiol transmetallates with the silane, delivering a hydride to the metal and the thiol to the silicon. Reductive elimination furnishes the desired aldehyde as well as a silyl thioether as the by-product.[215]

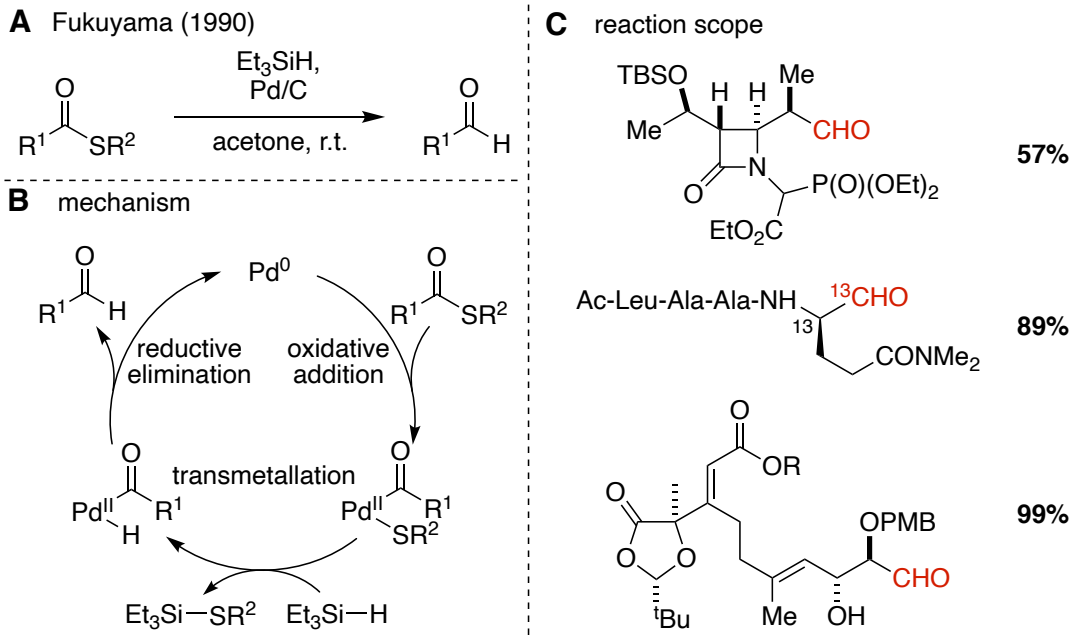

Scheme 21. *The Fukuyama reduction;* ***(A)*** *Reaction overview;* ***(B)*** *Mechanism;* ***(C)*** *Reaction scope including functional groups intolerant to strong acid, base and reducing agents.*

As one of a select few methods to reductively form aldehydes, the main benefit of the Fukuyama reduction is its tolerance towards functional groups. The neutral, room-temperature reaction tolerates acetals, ketone, sulfone, β-lactams[216,217] and alkenes (using Lindlar's catalyst)[218] as well as common protecting groups such as Boc, Cbz, Fmoc and Phth groups.[219] As a result, the Fukuyama reduction frequently play a part in natural product synthesis, particularly with oligopeptides with labile stereocentres.[219–221] The reaction also lends itself to the coupling of thioesters with aryl and alkyl zinc reagents to give ketones.[222]

1.5.5.2 The Mukaiyama Hydration

In a further reaction mode, silanes can be used to generate (and regenerate) metal hydrides such as those used in the Mukaiyama hydration of alkenes (Scheme 22).[223–225] In this catalytic reaction, a reductant and molecular oxygen is required to activate $Co(acac)_2$ to a Co(III) hydride. This complex then hydrometallates across the

substrate followed by insertion of molecular oxygen into the C-Co bond. Additional reducing agent is required to release the organic peroxide and regenerate a cobalt hydride. Generally, the reaction has strong Markovnikov selectivity based on the increased stability of substituted radicals and wide functional group tolerance which includes ketones, amides, alcohols, and acetals.

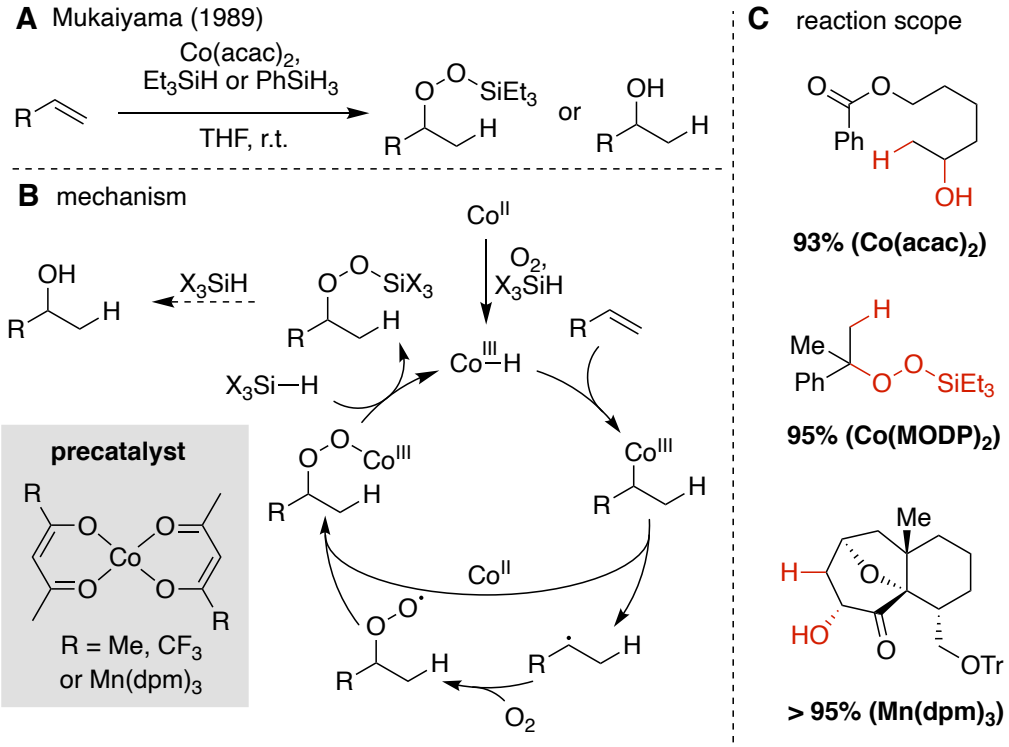

Scheme 22. *The Mukaiyama hydration;* ***(A)*** *Reaction overview;* ***(B)*** *Mechanism;* ***(C)*** *Scope of the reaction including synthesis of alcohols, silyl peroxides and tolerance of reducible functional groups.*

In early reports of the reaction,[226] secondary alcohols were used as the reducing agents. Whilst this enabled catalytic hydration, yields were eroded by oxidation of the alcohol product, with simultaneous over-reduction to the alkane. Additionally, despite optimisation of the solvent and ligand, higher temperatures (75 °C) and high catalyst loadings were required (20 mol%) for full conversion.[227,228] Similar results were obtained with triethylsilane in 1-propanol[229] however upon moving to aprotic solvents the silyl peroxide could be obtained in excellent yield.[230,231] This unprecedented transformation was also accomplished at room temperature with just 5 mol% catalyst. Furthermore, by changing to phenylsilane the peroxide could subsequently be reduced in the same pot, yielding an alcohol directly.[232] A similar manganese-based system has since been developed by Mukaiyama[233] and later by

Magnus and coworkers,[234,235] which has been shown to increase the substrate scope to include less reactive electron deficient alkenes.

In many ways the favourable qualities of the Mukaiyama hydration are reflective of silanes overall. Silanes can be used as mild and selective reducing agents, with unique reactivity which can be refined through modification their organic groups. More generally, their multiple modes of activation point to a richness and diversity in the chemistry of silicon which continues to be relevant in the exploration of new and sustainable methodology.

1.6 References

1 N. N. Greenwood and A. Earnshaw, *Chemistry of the Elements (2nd Edition)*, John Wiley & Sons, Ltd, 1997.
2 I. M. Ross, *Phys. Today*, 1997, **50**, 34–39.
3 J. J. Petkowski, W. Bains and S. Seager, *Life*, 2020, **10**, 1–47.
4 L. A. Paquette, *Science*, 1982, **217**, 793–800.
5 Hydrocarbons - Autoignition Temperatures and Flash Points, https://www.engineeringtoolbox.com/flash-point-autoignition-temperature-kindling-hydrocarbons-alkane-alkene-d_1941.html, (accessed 14 February 2022).
6 T. L. Cottrell, *The strengths of chemical bonds*, Butterworths Scientific Publications, London, 1958.
7 E. Blokker, X. Sun, J. Poater, J. M. van der Schuur, T. A. Hamlin and F. M. Bickelhaupt, *Chem. Eur. J.*, 2021, **27**, 15616–15622.
8 C. Friedel and J. M. Crafts, *Compt. Rendus*, 1863, **56**, 590–593.
9 J. Wisniak, *Educ. Química*, 2009, **20**, 447–455.
10 F. S. Kipping and N. W. Cusa, *J. Chem. Soc.*, 1935, 1088.
11 H. Sakurai, in *Encyclopedia of Inorganic Chemistry*, John Wiley & Sons, Ltd, 2006, pp. 1–27.
12 F. S. Kipping, *Proc. R. Soc. London. Ser. A - Math. Phys. Sci.*, 1937, **159**, 139–148.
13 L. Rösch, P. John and R. Reitmeier, in *Ullmann's Encyclopedia of Industrial Chemistry*, Wiley-VCH Verlag GmbH & Co. KGaA, Weinheim, Germany, 2000, p. 1.
14 R. D. Palacio, P. J. Negret, J. Velásquez-Tibatá, A. P. Jacobson, E. G. Rochow and W. S. Tatlock, *Inorg. Synth.*, 1950, **1**, 56–58.
15 D. Seyferth, *Organometallics*, 2001, **20**, 4978–4992.
16 L. Pauling, *Am. Mineral.*, 1980, **65**, 321–323.
17 F. Weinhold and R. West, *Organometallics*, 2011, **30**, 5815–5824.
18 I. Fleming, in *Molecular Orbitals and Organic Chemical Reactions*, John Wiley & Sons, Ltd, Chichester, UK, 2010, pp. 69–125.
19 J. R. Durig, M. J. Flanagan and V. F. Kalasinsky, *J. Chem. Phys.*, 1976, **66**, 2775–2785.
20 S. Gronert, R. Glaser and A. Streitwieser, *J. Am. Chem. Soc.*, 1989, **111**, 3111–3117.
21 J. S. Davies, C. L. Higginbotham, E. J. Tremeer, C. Brown and R. C. Treadgold, *Perkin Trans. 1*, 1992, 3043–3048.
22 C. Prakash, S. Saleh and I. A. Blair, *Tetrahedron Lett.*, 1989, **30**, 19–22.
23 A. S. Pilcher and P. DeShong, *J. Org. Chem.*, 1993, **58**, 5130–5134.
24 A. G. Brook, *Acc. Chem. Res.*, 1974, **7**, 77–84.
25 S. Prechelmacher, K. Mereiter and F. Hammerschmidt, *Org. Biomol. Chem.*, 2018, **16**, 3672–3680.
26 R. A. Holton, H. B. Kim, C. Somoza, F. Liang, R. J. Biediger, P. D. Boatman, M. Shindo, C. C. Smith, S. Kim, H. Nadizadeh, Y. Suzuki, C. Tao, P. Vu, S. Tang, P. Zhang, K. K. Murthi, L. N. Gentile and J. H. Liu, *J. Am. Chem. Soc.*, 1994, **116**, 1599–1600.
27 W. Su, S. Raders, J. G. Verkade, X. Liao and J. F. Hartwig, *Angew. Chem. Int. Ed.*, 2006, **45**, 5852–5855.
28 J. Boyer, R. J. P. Corriu, R. Perz and C. Reye, *Tetrahedron*, 1981, **37**, 2165–2171.
29 J. Boyer, R. J. P. Corriu, R. Perz and C. Réyé, *J. Chem. Soc. Chem. Commun.*, 1981, 121–122.
30 C. Chuit, R. Corriu, R. Perz and C. Reyé, *Synth.*, 1982, **1982**, 981–984.
31 R. J. P. Corriu, C. Guerin, B. J. L. Henner and W. W. C. Wong Chi Man, *Organometallics*, 1988, **7**, 237–238.
32 R. Corriu, C. Guérin, B. Henner and Q. Wang, *J. Organomet. Chem.*, 1989, **365**, 7–10.
33 G. K. S. Prakash and A. K. Yudin, *Chem. Rev.*, 1997, **97**, 757–786.
34 C. P. Johnston, T. H. West, R. E. Dooley, M. Reid, A. B. Jones, E. J. King, A. G. Leach and G. C. Lloyd-Jones, *J. Am. Chem. Soc.*, 2018, **140**, 11112–11124.
35 S. Lnuki, Y. Yoshimitsu, S. Oishi, N. Fujii and H. Ohno, *Org. Lett.*, 2009, **11**, 4478–4481.
36 G. L. Larson, *Synth.*, 2018, **50**, 2433–2462.
37 E. A. Brinkman, S. Berger and J. I. Brauman, *J. Am. Chem. Soc.*, 1994, **116**, 8304–8310.
38 S. Zhang, X.-M. Zhang and F. G. Bordwell, *J. Am. Chem. Soc.*, 1995, **117**, 602–606.
39 M. F. Lappert, M. J. Slade, A. Singh, J. L. Atwood, R. D. Rogers and R. Shakir, *J. Am. Chem. Soc.*, 1983, **105**, 302–304.
40 T. Kagiya, Y. Sumida and T. Tachi, *Bull. Chem. Soc. Jpn.*, 1970, **43**, 3716–3722.
41 G. A. Gornowicz and R. West, *J. Am. Chem. Soc.*, 1968, **90**, 4478–4479.

42 D. J. Peterson, *J. Org. Chem.*, 1968, **33**, 780–784.
43 A. R. Bassindale, R. J. Ellis, P. G. Taylor, J. Ellis and P. G. Taylor, *Tetrahedron Lett.*, 1984, **25**, 2705–2708.
44 A. R. Bassindale, R. J. Ellis and P. G. Taylor, *J. Chem. Synop.*, 1996, **1**, 34–35.
45 P. F. Hudrlik, E. L. O. Agwaramgbo and A. M. Hudrlik, *J. Org. Chem.*, 1989, **54**, 5613–5618.
46 P. F. Hudrlik and D. Peterson, *J. Am. Chem. Soc.*, 1975, **1464**, 154–155.
47 A. Streitwieser, L. Xie, P. Wang and S. M. Bachrach, *J. Org. Chem.*, 1993, **58**, 1778–1784.
48 D. J. Peterson, *J. Org. Chem.*, 1968, **33**, 780–784.
49 C. R. Johnson and B. D. Tait, *J. Org. Chem.*, 1987, **52**, 281–283.
50 D. J. Ager, *Synth.*, 1984, **1984**, 384–398.
51 J. M. Galano, G. Audran and H. Monti, *Tetrahedron Lett.*, 2001, **42**, 6125–6128.
52 R. Waschbüsch, J. Carran and P. Savignac, *Tetrahedron*, 1996, **52**, 14199–14216.
53 A. Mahadevan and P. L. Fuchs, *Tetrahedron Lett.*, 1994, **35**, 6025–6028.
54 J. B. Lambert and E. C. Chelius, *J. Am. Chem. Soc.*, 1990, **112**, 8120–8126.
55 J. B. Lambert, Y. Zhao, R. W. Emblidge, L. A. Salvador, X. Liu, J. H. So and E. C. Chelius, *Acc. Chem. Res.*, 1999, **32**, 183–190.
56 S. G. Wierschke, J. Chandrasekhar and W. L. Jorgensen, *J. Am. Chem. Soc.*, 1985, **107**, 1496–1500.
57 B. K. Rai, V. Sresht, Q. Yang, R. Unwalla, M. Tu, A. M. Mathiowetz and G. A. Bakken, *J. Chem. Inf. Model.*, 2019, **59**, 4195–4208.
58 W. Zhang, J. A. Stone, M. A. Brook and G. A. McGibbon, *J. Am. Chem. Soc.*, 1996, **118**, 5764–5771.
59 M. Karplus, *J. Chem. Phys.*, 1959, **30**, 11–15.
60 M. Karplus, *J. Am. Chem. Soc.*, 1963, **85**, 2870–2871.
61 A. Hosomi and H. Sakurai, *Tetrahedron Lett.*, 1976, **17**, 1295–1298.
62 A. Hosomi, M. Endo and H. Sakurai, *Chem. Lett.*, 1976, 941–942.
63 J. Ammer, C. Nolte and H. Mayr, *J. Am. Chem. Soc.*, 2012, **134**, 13902–13911.
64 A. Hosomi and H. Sakurai, *J. Am. Chem. Soc.*, 1977, **99**, 1673–1675.
65 H. Sakurai, A. Hosomi and J. Hayashi, *Org. Synth.*, 1984, **62**, 86.
66 T. Hayashi, M. Konishi, H. Ito and M. Kumada, *J. Am. Chem. Soc.*, 1982, **104**, 4962–4963.
67 T. Hayashi, K. Kabeta, I. Hamachi and M. Kumada, *Tetrahedron Lett.*, 1983, **24**, 2865–2868.
68 S. E. Denmark, B. R. Henke and E. Weber, *J. Am. Chem. Soc.*, 1987, **109**, 2512–2514.
69 A. Bottoni, A. L. Costa, D. Di Tommaso, I. Rossi and E. Tagliavini, *J. Am. Chem. Soc.*, 1997, **119**, 12131–12135.
70 S. E. Denmark and N. G. Almstead, *J. Org. Chem.*, 1994, **59**, 5130–5132.
71 S. E. Denmark and S. Hosoi, *J. Org. Chem.*, 1994, **59**, 5133–5135.
72 S. E. Denmark and J. Fu, *Chem. Rev.*, 2003, **103**, 2763–2794.
73 H. Sakurai, K. Sasaki and A. Hosomi, *Tetrahedron Lett.*, 1981, **22**, 745–748.
74 T. Tsunoda, M. Suzuki and R. Noyori, *Tetrahedron Lett.*, 1980, **21**, 71–74.
75 M. W. Wang, Y. J. Chen and D. Wang, *Synlett*, 2000, 385–387.
76 P. H. Lee, K. Lee, S. Sung and S. Chang, *J. Org. Chem.*, 2001, **66**, 8646–8649.
77 T. K. Hollis, N. P. Robinson, J. Whelan and B. Bosnich, *Tetrahedron Lett.*, 1993, **34**, 4309–4312.
78 T. Mukaiyama, H. Nagaoka, M. Murakami and M. Ohshima, *Chem. Lett.*, 1985, **14**, 977–980.
79 T. K. Hollis and B. Bosnich, *J. Am. Chem. Soc.*, 1995, **117**, 4570–4581.
80 K. Furuta, M. Mouri and H. Yamamoto, *Synlett*, 1991, **1991**, 561–562.
81 K. Ishihara, M. Mouri, Q. Gao, T. Maruyama, K. Furuta and H. Yamamoto, *J. Am. Chem. Soc.*, 1993, **115**, 11490–11495.
82 A. Yanagisawa, H. Kageyama, Y. Nakatsuka, K. Asakawa, Y. Matsumoto and H. Yamamoto, *Angew. Chem. Int. Ed.*, 1999, **38**, 3701–3703.
83 D. R. Gauthier and E. M. Carreira, *Angew. Chem., Int. Ed.* , 1996, **35**, 2363–2365.
84 K. Iseki, Y. Kuroki, M. Takahashi, S. Kishimoto and Y. Kobayashi, *Tetrahedron*, 1997, **53**, 3513–3526.
85 K. Iseki, Y. Kuroki, M. Takahashi and Y. Kobayashi, *Tetrahedron Lett.*, 1996, **37**, 5149–5150.
86 K. Iseki, S. Mizuno, Y. Kuroki and Y. Kobayashi, *Tetrahedron Lett.*, 1998, **39**, 2767–2770.
87 K. Iseki, S. Mizuno, Y. Kuroki and Y. Kobayashi, *Tetrahedron*, 1999, **55**, 977–988.
88 T. Shimada, A. Kina, S. Ikeda and T. Hayashi, *Org. Lett.*, 2002, **4**, 2799–2801.
89 M. Mahlau, P. García-García and B. List, *Chem. Eur. J.*, 2012, **18**, 16283–16287.
90 P. S. J. Kaib, L. Schreyer, S. Lee, R. Properzi and B. List, *Angew. Chem. Int. Ed.*, 2016, **55**,

13200–13203.
91 M. Sai and H. Yamamoto, *J. Am. Chem. Soc.*, 2015, **137**, 7091–7094.
92 T. Mukaiyama, K. Narasaka and K. Banno, *Chem. Lett.*, 1973, **2**, 1011–1014.
93 T. Mukaiyama, K. Banno and K. Narasaka, *J. Am. Chem. Soc.*, 1974, **96**, 7503–7509.
94 H. Mayr, T. Bug, M. F. Gotta, N. Hering, B. Irrgang, B. Janker, B. Kempf, R. Loos, A. R. Ofial, G. Remennikov and H. Schimmel, *J. Am. Chem. Soc.*, 2001, **123**, 9500–9512.
95 H. Gröger, E. M. Vogl and M. Shibasaki, *Chem. Eur. J.*, 1998, **4**, 1137–1141.
96 T. Mukaiyama and J. Matsuo, in *Modern Aldol Reactions*, Wiley-VCH Verlag GmbH, Weinheim, Germany, 2005, vol. 36, pp. 127–160.
97 R. Mahrwald, *Chem. Rev.*, 1999, **99**, 1095–1120.
98 T. D. Machajewski and C.-H. Wong, *Angew. Chem. Int. Ed.*, 2000, **39**, 1352–1375.
99 T. Kitanosono and S. Kobayashi, *Adv. Synth. Catal.*, 2013, **355**, 3095–3118.
100 A. Rodríguez-Gimeno, A. B. Cuenca, J. Gil-Tomás, M. Medio-Simón, A. Olmos and G. Asensio, *J. Org. Chem.*, 2014, **79**, 8263–8270.
101 T. P. Loh and X. R. Li, *Tetrahedron*, 1999, **55**, 10789–10802.
102 C. Palomo, M. Oiarbide and J. M. García, *Chem. Soc. Rev.*, 2004, **33**, 65–75.
103 J. I. Matsuo and M. Murakami, *Angew. Chem. Int. Ed.*, 2013, **52**, 9109–9118.
104 Y. Yamashita, T. Yasukawa, W. J. Yoo, T. Kitanosono and S. Kobayashi, *Chem. Soc. Rev.*, 2018, **47**, 4388–4480.
105 C. H. Heathcock, S. K. Davidsen, K. T. Hug and L. A. Flippin, *J. Org. Chem.*, 1986, **51**, 3027–3037.
106 H. E. Zimmerman and M. D. Traxler, *J. Am. Chem. Soc.*, 1957, **79**, 1920–1923.
107 S. E. Denmark and W. Lee, *J. Org. Chem.*, 1994, **59**, 707–709.
108 J. M. Lee, P. Helquist and O. Wiest, *J. Am. Chem. Soc.*, 2012, **134**, 14973–14981.
109 M. T. Reetz, *Acc. Chem. Res.*, 1993, **26**, 462–468.
110 J. K. RASMUSSEN, *Synth.*, 1977, **1977**, 91–110.
111 K. Banno and T. Mukaiyama, *Chem. Lett.*, 1975, **4**, 741–744.
112 K. Banno, *Bull. Chem. Soc. Jpn.*, 1976, **49**, 2284–2291.
113 J. I. Musher, *Angew. Chem., Int. Ed.* , 1969, **8**, 54–68.
114 W. B. Jensen, *J. Chem. Educ.*, 2006, **83**, 1751.
115 D. W. Smith, *J. Chem. Educ.*, 2005, **82**, 1202.
116 R. R. Holmes, *Chem. Rev.*, 1996, **96**, 927–950.
117 A. A. Macharashvili, V. E. Shklover, Y. T. Struchkov, G. I. Oleneva, E. P. Kramarova, A. G. Shipov and Y. I. Baukov, *J. Chem. Soc. Chem. Commun.*, 1988, 683.
118 S. N. Tandura, M. G. Voronkov and N. V. Alekseev, 1986, pp. 99–189.
119 M. S. El-Shall, *Chem. Phys. Lett.*, 1989, **159**, 21–26.
120 A. Rauk, L. C. Allen and K. Mislow, *J. Am. Chem. Soc.*, 1972, **94**, 3035–3040.
121 E. Magnusson, *J. Am. Chem. Soc.*, 1990, **112**, 7940–7951.
122 R. Hoffmann, J. M. Howell and E. L. Muetterties, *J. Am. Chem. Soc.*, 1972, **94**, 3047–3058.
123 R. E. Rundle, in *Survey of Progress in Chemistry*, ed. A. F. SCOTT, Elsevier, 1963, vol. 1, pp. 81–131.
124 C. Chuit, R. J. P. Corriu, C. Reye and J. C. Young, *Chem. Rev.*, 1993, **93**, 1371–1448.
125 J. C. Sheldon, R. N. Hayes and J. H. Bowie, *J. Am. Chem. Soc.*, 1984, **106**, 7711–7715.
126 T. A. Hamlin, M. Swart and F. M. Bickelhaupt, *ChemPhysChem*, 2018, **19**, 1315–1330.
127 A. P. Bento and F. M. Bickelhaupt, *J. Org. Chem.*, 2007, **72**, 2201–2207.
128 R. Corriu, C. Guérin, B. Henner and Q. Wang, *Inorganica Chim. Acta*, 1992, **198–200**, 705–713.
129 R. J. P. Corriu, C. Guérin, K. A. Scheidt, R. B. Lettan, G. Nikonov and L. Yunnikova, in *Encyclopedia of Reagents for Organic Synthesis*, John Wiley & Sons, Ltd, Chichester, UK, 2014, vol. 1, pp. 1–10.
130 A. Hosomi, S. Kohra, K. Ogata, T. Yanagi and Y. Tominaga, *J. Org. Chem.*, 1990, **55**, 2415–2420.
131 T. Hayashi, Y. Matsumoto, T. Kiyoi, Y. Ito, S. Kohra, Y. Tominaga and A. Hosomi, *Tetrahedron Lett.*, 1988, **29**, 5667–5670.
132 A. Hosomi, S. Kohra and Y. Tominaga, *J. Chem. Soc. Chem. Commun.*, 1987, **35**, 1517.
133 J. Yoshida, K. Tamao, M. Takahashi and M. Kumada, *Tetrahedron Lett.*, 1978, **19**, 2161–2164.
134 J. Yoshida, K. Tamao, H. Yamamoto, T. Kakui, T. Uchida and M. Kumada, *Organometallics*, 1982, **1**, 542–549.
135 Y. Hatanaka and T. Hiyama, *J. Org. Chem.*, 1989, **54**, 268–270.

136 Y. Hatanaka, S. Fukushima and T. Hiyama, *Chem. Lett.*, 1989, 18, 1711–1714.
137 E. Tyrrell and P. Brookes, *Synth.*, 2003, **2003**, 0469–0483.
138 P. Pierrat, P. Gros and Y. Fort, *Org. Lett.*, 2005, **7**, 697–700.
139 T. Nokami, Y. Tomida, T. Kamei, K. Itami and J. I. Yoshida, *Org. Lett.*, 2006, **8**, 729–731.
140 Y. Hatanaka and T. Hiyama, *J. Org. Chem.*, 1988, **53**, 918–920.
141 N. A. Strotman, S. Sommer and G. C. Fu, *Angew. Chem. Int. Ed.*, 2007, **46**, 3556–3558.
142 H. Matsuhashi, M. Kuroboshi, Y. Hatanaka and T. Hiyama, *Tetrahedron Lett.*, 1994, **35**, 6507–6510.
143 K. Tamao, K. Kobayashi and Y. Ito, *Tetrahedron Lett.*, 1989, **30**, 6051–6054.
144 C. J. Handy, A. S. Manoso, W. T. McElroy, W. M. Seganish and P. DeShong, *Tetrahedron*, 2005, **61**, 12201–12225.
145 K. Shibata, K. Miyazawa and Y. Goto, *Chem. Commun.*, 1997, 1309–1310.
146 E. Hagiwara, K. I. Gouda, Y. Hatanaka and T. Hiyama, *Tetrahedron Lett.*, 1997, **38**, 439–442.
147 E. Alacid and C. Nájera, *J. Org. Chem.*, 2008, **73**, 2315–2322.
148 K. Hirabayashi, J. Kawashima, Y. Nishihara, A. Mori and T. Hiyama, *Org. Lett.*, 1999, **1**, 299–301.
149 S. E. Denmark and D. Wehrli, *Org. Lett.*, 2000, **2**, 565–568.
150 S. E. Denmark and R. F. Sweis, *J. Am. Chem. Soc.*, 2001, **123**, 6439–6440.
151 S. E. Denmark and R. F. Sweis, *Acc. Chem. Res.*, 2002, **35**, 835–846.
152 Y. Nakao and T. Hiyama, *Chem. Soc. Rev.*, 2011, **40**, 4893.
153 F. Foubelo, C. Nájera and M. Yus, *Chem. Rec.*, 2016, **16**, 2521–2533.
154 S. E. Denmark and J. D. Baird, *Chem. Eur. J.*, 2006, **12**, 4954–4963.
155 S. E. Denmark and J. M. Kallemeyn, *J. Am. Chem. Soc.*, 2006, **128**, 15958–15959.
156 S. E. Denmark and C. R. Butler, *J. Am. Chem. Soc.*, 2008, **130**, 3690–3704.
157 S. E. Denmark, R. C. Smith, W. T. T. Chang and J. M. Muhuhi, *J. Am. Chem. Soc.*, 2009, **131**, 3104–3118.
158 S. E. Denmark, J. D. Baird and C. S. Regens, *J. Org. Chem.*, 2008, **73**, 1440–1455.
159 S. E. Denmark and R. C. Smith, *J. Am. Chem. Soc.*, 2010, **132**, 1243–1245.
160 S. E. Denmark and R. F. Sweis, *J. Am. Chem. Soc.*, 2004, **126**, 4876–4882.
161 J. Chen, M. Tanaka, A. K. Sahoo, M. Takeda, A. Yada, Y. Nakao and T. Hiyama, *Bull. Chem. Soc. Jpn.*, 2010, **83**, 554–569.
162 Y. Nakao, H. Imanaka, A. K. Sahoo, A. Yada and T. Hiyama, *J. Am. Chem. Soc.*, 2005, **127**, 6952–6953.
163 Y. Nakao, H. Imanaka, J. Chen, A. Yada and T. Hiyama, *J. Organomet. Chem.*, 2007, **692**, 585–603.
164 Y. Nakao, M. Takeda, T. Matsumoto and T. Hiyama, *Angew. Chem. Int. Ed.*, 2010, **49**, 4447–4450.
165 E. C. Son, H. Tsuji, T. Saeki and K. Tamao, *Bull. Chem. Soc. Jpn.*, 2006, **79**, 492–494.
166 R. Walsh, *Acc. Chem. Res.*, 1981, **14**, 246–252.
167 L. Horner and J. Mathias, *J. Organomet. Chem.*, 1985, **282**, 155–174.
168 Y. Goldberg, E. AbAbele, M. Shymanska and e. Lukevics, *J. Organomet. Chem.*, 1989, **372**, 8–10.
169 M. Deneux, I. C. Akhrem, D. V. Avetissian, E. I. Myssoff and M. E. Vol'pin, *Bull. Soc. Chim. Fr.*, 1973, 2638.
170 M. Chérest, H. Felkin and N. Prudent, *Tetrahedron Lett.*, 1968, **9**, 2199–2204.
171 O. Eisenstein and N. T. Anh, *Nouv. J. Chim.*, 1977, 61–70.
172 F. A. Carey and H. S. Tremper, *J. Am. Chem. Soc.*, 1968, **90**, 2578–2583.
173 G. G. Hess, F. W. Lampe and L. H. Sommer, *J. Am. Chem. Soc.*, 1965, **87**, 5327–5333.
174 G. Bertrand, *Science*, 2004, **305**, 783–785.
175 J. Y. Corey and R. West, *J. Am. Chem. Soc.*, 1963, **85**, 2430–2433.
176 J. D. Austin and C. Eaborn, *J. Chem. Soc.*, 1964, 2279–2280.
177 Z. N. Parnes, G. A. Khotimskaya, Y. I. Lyakhovetskii and P. V. Petrovskii, *Bull. Acad. Sci. USSR, Div. Chem. Sci. (Engl. Transl.)*, 1971, **20**, 1463.
178 W. Markownikoff, *Ann. der Chemie und Pharm.*, 1870, **153**, 228–259.
179 H. H. Baer and M. Zamkanei, *J. Org. Chem.*, 1988, **53**, 4786–4789.
180 D. J. Wustrow, W. J. Smith and L. D. Wise, *Tetrahedron Lett.*, 1994, **35**, 61–64.
181 J. L. Fry, M. Orfanopoulos, M. G. Adlington, W. P. Dittman and S. B. Silverman, *J. Org. Chem.*, 1978, **43**, 374–375.
182 M. P. Doyle, C. T. West, S. J. Donnelly and C. C. McOsker, *J. Organomet. Chem.*, 1976, **117**, 129–

140.
183 D. J. Parks and W. E. Piers, *J. Am. Chem. Soc.*, 1996, **118**, 9440–9441.
184 D. J. Parks, J. M. Blackwell and W. E. Piers, *J. Org. Chem.*, 2000, **65**, 3090–3098.
185 C. Chatgilialoglu, *Chem. Rev.*, 1995, **95**, 1229–1251.
186 C. Chatgilialoglu and M. Newcomb, in *Advances in Organometallic Chemistry*, 1999, vol. 44, pp. 67–112.
187 C. Chatgilialoglu, *Acc. Chem. Res.*, 1992, **25**, 188–194.
188 B. P. Roberts, *Chem. Soc. Rev.*, 1999, **28**, 25–35.
189 C. Chatgilialoglu, *Chem. Eur. J.*, 2008, **14**, 2310–2320.
190 X. J. Tang, Z. Zhang and W. R. Dolbier, *Chem. Eur. J.*, 2015, **21**, 18961–18965.
191 P. Zhang, C. C. Le and D. W. C. MacMillan, *J. Am. Chem. Soc.*, 2016, **138**, 8084–8087.
192 C. Chatgilialoglu, C. Ferreri, Y. Landais and V. I. Timokhin, *Chem. Rev.*, 2018, **118**, 6516–6572.
193 J. L. Speier, J. A. Webster and G. H. Barnes, *J. Am. Chem. Soc.*, 1957, **79**, 974–979.
194 P. W. N. M. van Leeuwen, Ed., in *Homogeneous Catalysis: Understanding the Art*, Springer Netherlands, Dordrecht, 2004, pp. 371–385.
195 J. L. Speier, in *Advances in Organometallic Chemistry*, 1979, vol. 17, pp. 407–447.
196 I. G. Iovel, Y. S. Goldberg, M. V. Shymanska and E. Lukevics, *Organometallics*, 1987, **6**, 1410–1413.
197 L. N. Lewis and N. Lewis, *J. Am. Chem. Soc.*, 1986, **108**, 7228–7231.
198 J. Stein, L. N. Lewis, Y. Gao and R. A. Scott, *J. Am. Chem. Soc.*, 1999, **121**, 3693–3703.
199 A. J. Holwell, *Platin. Met. Rev.*, 2008, **52**, 243–246.
200 D. Troegel and J. Stohrer, *Coord. Chem. Rev.*, 2011, **255**, 1440–1459.
201 L. D. Almeida, H. Wang, K. Junge, X. Cui and M. Beller, *Angew. Chemie*, 2021, **133**, 558–573.
202 Y. Nakajima and S. Shimada, *RSC Adv.*, 2015, **5**, 20603–20616.
203 S. Shamna, J. Fairoosa, C. M. A. Afsina and G. Anilkumar, *J. Organomet. Chem.*, 2022, **960**, 122236.
204 Y. Uozumi and T. Hayashi, *J. Am. Chem. Soc.*, 1991, **113**, 9887–9888.
205 B. Cheng, W. Liu and Z. Lu, *J. Am. Chem. Soc.*, 2018, **140**, 5014–5017.
206 B. Cheng, P. Lu, H. Zhang, X. Cheng and Z. Lu, *J. Am. Chem. Soc.*, 2017, **139**, 9439–9442.
207 Y. Nakajima, K. Sato and S. Shimada, *Chem. Rec.*, 2016, **16**, 2379–2387.
208 R. Hofmann, M. Vlatković and F. Wiesbrock, *Polymers*, 2017, **9**, 534.
209 A. J. Chalk and J. F. Harrod, *J. Am. Chem. Soc.*, 1965, **87**, 16–21.
210 G. Giorgi, F. De Angelis, N. Re and A. Sgamellotti, *Futur. Gener. Comput. Syst.*, 2004, **20**, 781–791.
211 S. Sakaki, N. Mizoe and M. Sugimoto, *Organometallics*, 1998, **17**, 2510–2523.
212 S. Sakaki, M. Sumimoto, M. Fukuhara, M. Sugimoto, H. Fujimoto and S. Matsuzaki, *Organometallics*, 2002, **21**, 3788–3802.
213 T. Fukuyama, S. C. Lin and L. Li, *J. Am. Chem. Soc.*, 1990, **112**, 7050–7051.
214 T. Hidetoshi and T. Fukuyama, *Aldrichimica Acta*, 2004, **37**, 87–96.
215 M. Kimura and M. Seki, *Tetrahedron Lett.*, 2004, **45**, 3219–3223.
216 H. Takayama, R. Fujiwara, Y. Kasai, M. Kitajima and N. Aimi, *Org. Lett.*, 2003, **5**, 2967–2970.
217 O. Sakurai and H. Horikawa, *Tetrahedron Lett.*, 1996, **37**, 7811–7814.
218 D. A. Evans and J. S. Johnson, *J. Org. Chem.*, 1997, **62**, 786–787.
219 H. Tokuyama, S. Yokoshima, S.-C. Lin, L. Li and T. Fukuyama, *Synth.*, 2002, **2002**, 1121–1123.
220 B. A. Malcolm, C. Lowe, S. Shechosky, R. T. McKay, C. C. Yang, V. J. Shah, R. J. Simon, J. C. Vederas and D. V. Smith, *Biochemistry*, 1995, **34**, 8172–8179.
221 M. K. Eberle, A. M. Jutzi-Eme and F. Nuninger, *J. Org. Chem.*, 1994, **59**, 7249–7258.
222 Y. Mori and M. Seki, *J. Org. Chem.*, 2003, **68**, 1571–1574.
223 T. Mukaiyama and T. Yamada, *Bull. Chem. Soc. Jpn.*, 1995, **68**, 17–35.
224 T. Okamoto and S. Oka, *J. Org. Chem.*, 1984, **49**, 1589–1594.
225 S. W. M. Crossley, C. Obradors, R. M. Martinez and R. A. Shenvi, *Chem. Rev.*, 2016, **116**, 8912–9000.
226 T. Mukaiyama, S. Isayama, S. Inoki, K. Kato, T. Yamada and T. Takai, *Chem. Lett.*, 1989, **18**, 449–452.
227 S. Inoki, K. Kato, T. Takai, S. Isayama, T. Yamada and T. Mukaiyama, *Chem. Lett.*, 1989, **18**, 515–518.
228 K. Kato, T. Yamada, T. Takai, S. Inoki and S. Isayama, *Bull. Chem. Soc. Jpn.*, 1990, **63**, 179–186.
229 S. Isayama and T. Mukaiyama, *Chem. Lett.*, 1989, **18**, 569–572.

230 S. Isayama and T. Mukaiyama, *Chem. Lett.*, 1989, **18**, 573–576.
231 S. Isayama, *Bull. Chem. Soc. Jpn.*, 1990, **63**, 1305–1310.
232 S. Isayama and T. Mukaiyama, *Chem. Lett.*, 1989, **18**, 1071–1074.
233 S. Inoki, K. Kato, S. Isayama and T. Mukaiyama, *Chem. Lett.*, 1990, **19**, 1869–1872.
234 P. Magnus, A. H. Payne, M. J. Waring, D. A. Scott and V. Lynch, *Tetrahedron Lett.*, 2000, **41**, 9725–9730.
235 P. Magnus, D. A. Scott and M. R. Fielding, *Tetrahedron Lett.*, 2001, **42**, 4127–4129.

Chapter 2

Catalytic Methods for the Synthesis of Ethers from Esters and Carboxylic Acids

2.1 Introduction

2.1.1 Significance of Ethers

The ether linkage is a common functional group in organic chemistry, occurring in natural products as well as in solvents, polymers and fine chemicals.[1] Aryl ethers in particular are important motifs for agrochemicals and pharmaceuticals with around 35% of recently-published library compounds consisting of at least one alkyl aryl ether[2] (Figure 1).[3–5] Despite this, an inexpensive, versatile, sustainable and high-yielding ether synthesis has not yet been realised. Currently the most robust methods for ether synthesis are oxygen-centred nucleophilic substitution reactions, which account for around 5% of all reactions in medicinal chemistry.[2,6] A further 2% of reactions involve the activation of alcohols for nucleophilic substitution. However, strategies to avoid this wasteful step have been highlighted as a key green research area by the pharmaceutical roundtable.[7]

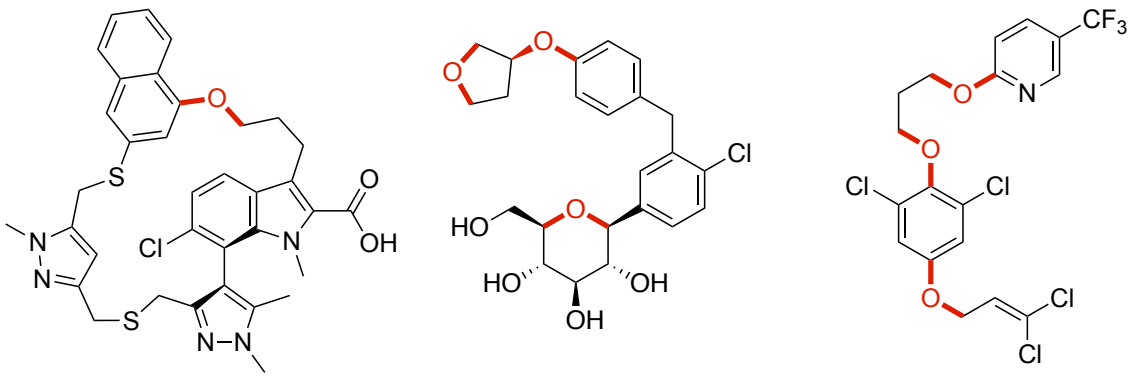

Figure 1. *Three ether-containing fine chemicals which are produced in kilogram to multi-tonne quantities.[3–5]*

2.1.2 Ether Synthesis by Stoichiometric Alcohol Activation

The ideal ether synthesis would involve the dehydrative coupling of two different alcohols to generate water as the sole by-product. In practice, this reaction is unfeasibly slow due to the poor leaving group ability of hydroxide ions and the low electrophilicity at the carbon undergoing substitution. Additionally, this simplistic approach cannot selectively produce unsymmetrical ethers.

Known since 1850, the Williamson ether synthesis[8] overcomes the slow kinetics of alcohol condensation by using a strong electrophile such as a halide or sulfonate ester and activating the nucleophilic alcohol with a strong base (Scheme 1). This reaction remains one of the most widely used methods for making ethers[9] and has prevailed over time because it is simple, robust, and non-commercial electrophiles can be easily prepared from an alcohol in one step.

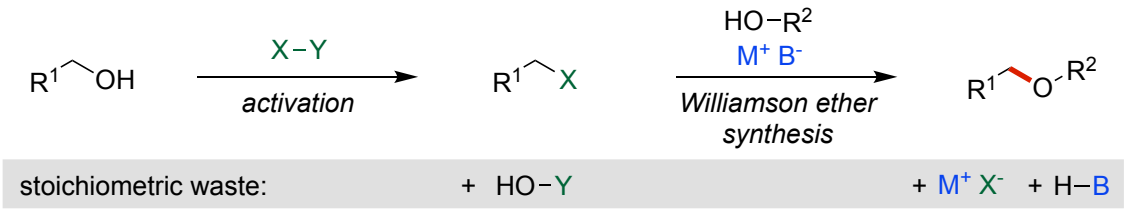

Scheme 1. *The Williamson ether synthesis using X-Y to halogenate an alcohol.*

Whilst reliable, the Williamson ether synthesis is inefficient, adding a stoichiometric activation step and, therefore, generating stoichiometric waste. Furthermore, secondary, tertiary, and benzylic electrophiles are prone to elimination, which limits the scope of this method. To minimise this competing side reaction, polar, aprotic solvents such as DMF can be used which stabilise the S_N2 transition state (polar protic solvents reduce reactivity by stabilising the nucleophilic alkoxide with hydrogen bonding). Whilst this can improve yield, there are a limited number of polar aprotic solvents which are recognised as practical, safe and sustainable by industry;[10] DMF for example is reprotoxic, persists in the environment and can be difficult to remove from the reaction.

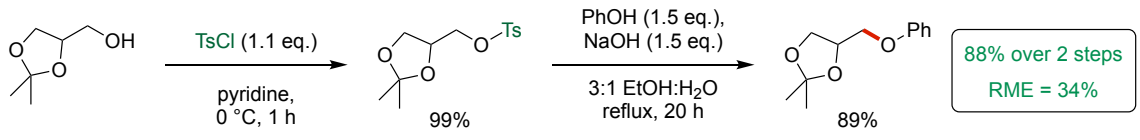

Scheme 2. *Preparation of a precursor to Tafluprost using the Williamson ether synthesis.*

A recent application of the Williamson ether synthesis was reported in a synthesis of Tafluprost; a prodrug for the treatment of glaucoma (Scheme 2).[11] Although both steps are high-yielding, the reaction mass efficiency (RME)[12] is only 34%, which is largely due to use of *p*-toluenesulfonyl chloride (TsCl) as a high molecular weight activating group that is not incorporated into the product.

The Mitsunobu reaction offers an alternative, one-step method to activate alcohols with respect to nucleophilic substitution (Scheme 3).[13,14] In this reaction a Morrison-Brunn-Huisgen betaine forms from the addition of a phosphine to a diazodicarboxylate. This both deprotonates the pronucleophile and acts as an electrophilic phosphonium salt which can be attacked by the alcohol to make it better leaving group. Due to the exclusively S_N2 nature of the final substitution, the reaction proceeds with complete inversion of stereochemistry around secondary and, in selected examples, tertiary alcohols.[15]

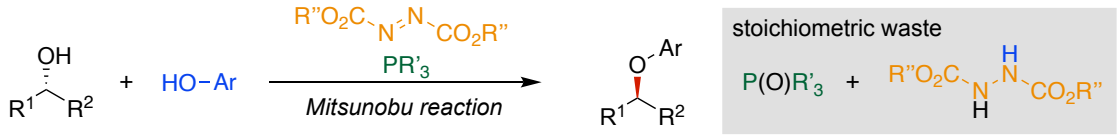

Scheme 3. *The Mitsunobu reaction with a phenol to make an aryl ether.*

A diverse range of pronucleophiles can be used in this reaction, but in the context of ether formation, phenolic alcohols are most common.[16] This is because the pronucleophile must be deprotonated by the betaine ($pK_{aH} \simeq 13$ for DEAD (diethyl azodicarboxylate) in water), so only acidic alcohols with an aqueous of pK_a 11 or less react cleanly with standard reagents.[17,18] This limits the scope of the reaction to the formation of alkyl aryl ethers.

The key feature of the Mitsunobu reaction is formation of a P=O bond, which provides a large thermodynamic driving force for alcohol displacement. Mild reaction conditions can also be used, tolerating a range of functional groups and solvents under neutral conditions, either at ambient temperature or with cooling to 0 °C. However, the use of phosphines is also arguably one of the biggest drawbacks, as significant waste is produced which is often difficult to separate from the product. Additionally, the use of heavy, stoichiometric reagents has a large impact on atom economy.

Since its inception in 1967 and particularly over the last two decades, significant progress has been made to overcome these difficulties. The two main research areas have been modification of both reagents to facilitate simple purification strategies and making the reaction catalytic. More progress has been made with reagent modification, with a host of new reagents being commercialised (Figure 2A).

DMEAD for example contains hydrophilic ethers for aqueous separation whereas the ^{t}butoxycarbonyl moiety of DTBAD renders it labile to acid-catalysed decomposition. PPh_2Py and Tris-DAP both contain can be easily extracted by an acidic wash. More recently Beddoe and co-workers[19] have demonstrated a catalytic Mitsunobu reaction which can form C-O, C-N and C-S bonds with strongly acidic pronucleophiles (pK_a < 1 in water). Using a simple P(V) organocatalyst, good to excellent levels of stereoinversion was observed at secondary alcohols and - as the reaction is redox neutral - phosphine sensitive functional group were also tolerated (Figure 2B). However, the limitations of this methodology are its narrow pronucleophile scope, and reliance on high temperatures with efficient water removal for catalyst turnover.

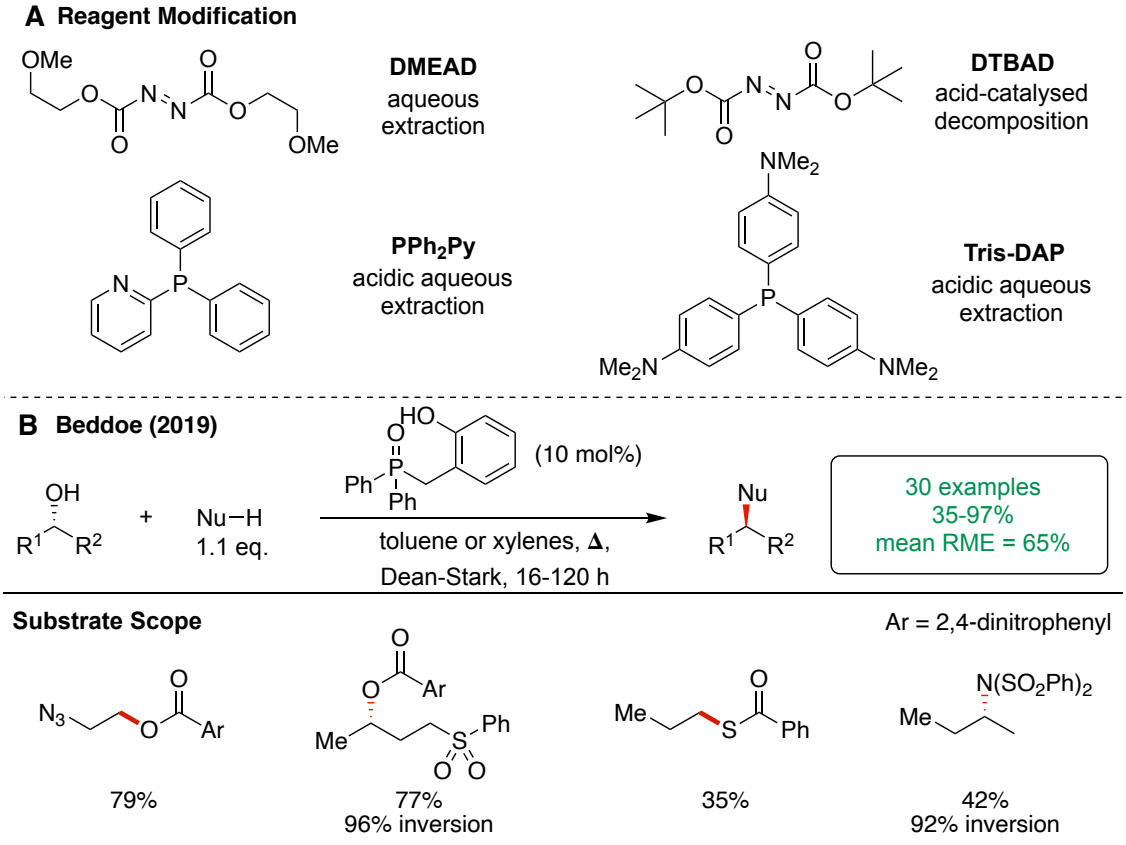

Figure 2. *State-of the art Mitsunobu reaction;* ***(A)*** *Modified Mitsunobu reagents which facilitate facile purification;* ***(B)*** *Beddoe's catalytic Mitsunobu reaction.*

2.1.3 Ether Synthesis by Catalytic Substitution

In comparison to the formation of C-N bonds, transition-metal-catalysed routes to ethers are far less prevalent. Organometallic approaches are inherently limited by slow reductive elimination steps which are often outcompeted by β-hydride

elimination in sp^3-centred alcohols. Nevertheless, by choosing sterically demanding ligands or electron-rich metals, certain couplings can be achieved.

The first reaction in this class was the Ullmann condensation of phenols and aryl halides using a powdered copper metal catalyst and stoichiometric base.[20] The original procedure is of limited synthetic value due to low yields, extended reaction times and temperatures of 100 – 300 °C. However, significant progress was made in the late 90s and early 2000s as the Buchwald and Venkataraman groups reported a general and practical Ullmann coupling using a copper (I) phenanthroline complex (Scheme 4).[21–23]

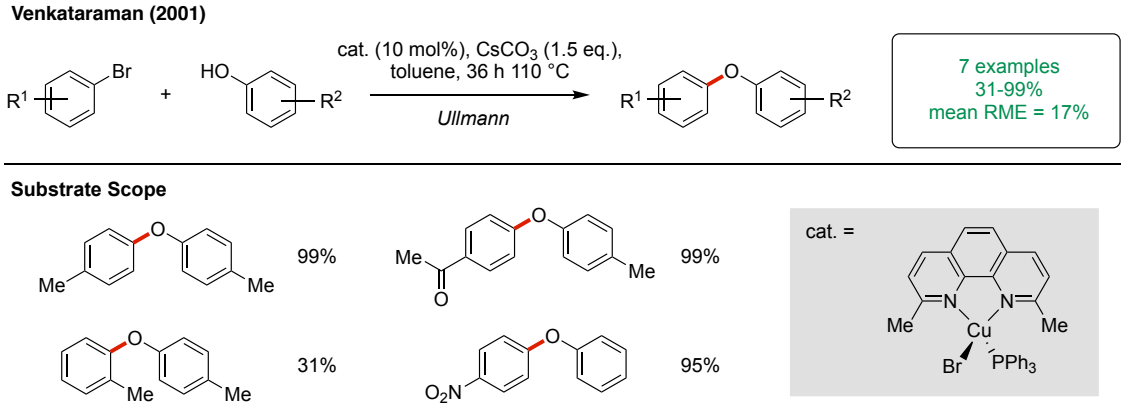

Scheme 4. *General conditions and substrate scope for the Ullmann condensation.*[22]

Following these advances, a plethora of copper-catalysed reactions were developed, mostly using polydentate ligands to access alkyl, vinyl and cyclic ethers.[24,25] Each variant has its own merits, but as a whole the reaction is still reliant on high temperatures, high catalyst loadings, strong bases and yield is very substrate dependent.

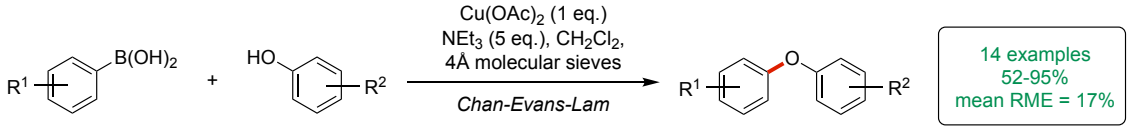

Scheme 5. *General conditions for the Chan-Evans-Lam coupling.*

Significant progress in copper-mediated biaryl ether synthesis has been made using alternative coupling partners to aryl halides. Potassium trifluoroborates, siloxanes, iodonium salts, stannanes, leads and bismuths can all be employed,[26] but perhaps the most useful iteration was the use of aryl boronic acids and esters[27] which was

simultaneously developed by Chan, Evans and Lam (Scheme 5).[28–33] Contrary to the Ullmann condensation, the Chan-Evans-Lam reaction couples two nucleophilic fragments using copper (II) acetate as an oxidant.[34] Although the best yields are obtained using stoichiometric copper, the loading can be minimised to as low as 10% using *in situ* oxidation from an oxygen atmosphere.[32] The major advantages over the Ullmann condensation are the expanded substrate scope, lower temperatures and the use of mild bases.

Whilst both the Ullman and the Chan-Evans-Lam couplings have found applications in chemical synthesis, they are two of the ten worst yielding reactions in medicinal chemistry with average conversions of just 50% and 46% respectively (Table 1).[9]

Top Ten Lowest Yielding Reactions	Median Yield /%
Carboxylic acid + sulfonamide reaction	43
Fluorination	44
Chan-Lam arylamine coupling	45
Chloro Buchwald-Hartwig amination	45
Chan-Lam ether coupling	**46**
Iodo *N*-arylation	46
Quinazolinone synthesis	47
Ullmann condensation	**50**
Bromo *N*-arylation	50
Bromo Buchwald-Hartwig amination	52

Table 1. *The top ten worst reactions in medicinal chemistry by median yield.*[9]

Palladium-catalysed etherification reactions have also been documented. One of the most useful of these is the Tsuji-Trost reaction[35–41] (Scheme 6) in which the substrate contains a leaving group adjacent to an alkene. Oxidative addition of the metal into this bond gives rise to an electrophillic allyl palladium species with inversion of stereochemistry. Under typical reaction conditions, alcohols or other nucleophiles may then add to the least hindered end of the allyl ligand *via* an invertive, outer-sphere reductive elimination to give overall retention of stereochemistry.[42,43] However, Trost[44,45] has extensively studied modifications to induce stereochemistry using chiral ligands which provides moderate to good enantiomeric excess.

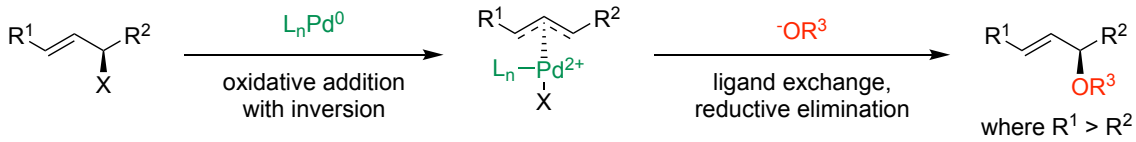

Scheme 6. *General steps in the Tsuji-Trost reaction with overall retention of stereochemistry.*

Palladium catalysts have also been used in the etherification of alcohols with alkyl halides. A great deal of this work has been done by Buchwald who has attempted to elaborate the hugely successful Buchwald-Hartwig amination of aryl halides. Bulky, electron-rich ligands that favour reductive elimination have been be used to synthesise a range of diaryl ethers,[46] fused aryl heterocycles,[47,48] aryl vinyl ethers[49] and alkyl aryl ethers[50–52] in good yields (Scheme 7). However, the method is not very general. Consequently numerous structurally and electronically challenging systems often require ligand screening or use of bespoke dialkylbiaryl phosphine "Buchwald" ligands.[53,54]

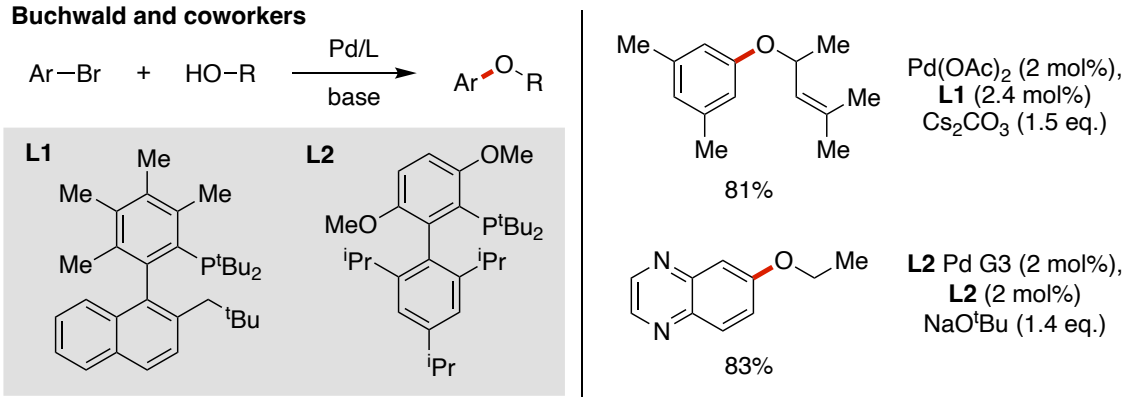

Scheme 7. *Palladium mediated cross-coupling to form aryl ethers using a bespoke Buchwald-type ligand (**L1**) and commercial ᵗBuBrettPhos (**L2**).*

Despite requiring only 1-5 mol% of palladium, the disadvantages of these catalysts in comparison to copper are obvious: higher price, increased toxicity, lower abundance, and the need for more bespoke ligands. Combined with low yields, this has restricted the application of these advances to synthesis.

2.1.4 Reduction of Esters to Ethers

Another approach to the formation of ethers is to reduce esters, which already contain the desired carbon-oxygen-carbon bonds. Whilst this strategy requires an additional step, esters are easily accessible through many reactions with readily available starting materials (*cf.* Fischer esterification). The main challenge in this

procedure is that most conventional reducing agents such as lithium aluminium hydride reduce esters to alcohols exclusively. To overcome this, the carbonyl oxygen must be made into a better leaving group so that it is lost in the reduction rather than the alkoxide. One strategy to achieve this is to use silanes. In this case, selectivity for ethers is possible when the α-anion stabilisation of the siloxide-type leaving group **4** (Scheme 8) is greater than the *inductive* β-cation stabilisation in the silyl-oxocarbenium ion **1** – hyperconjugation from the Si-O bond is not possible with simultaneous stabilisation from the oxygen lone pairs (*cf.* the Mukaiyama aldol reaction).

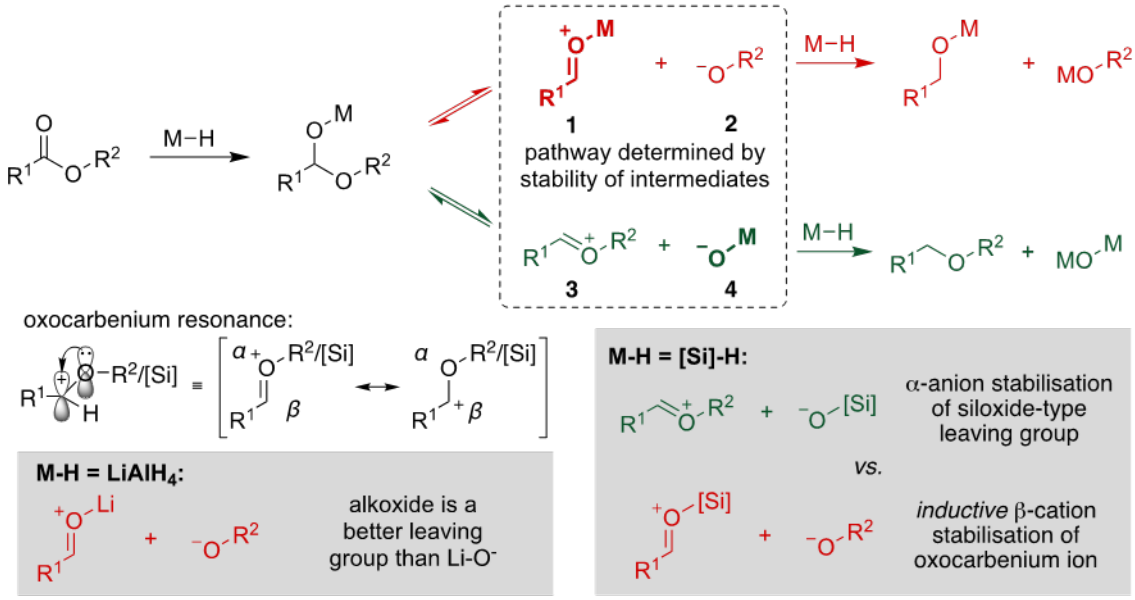

Scheme 8. *Simplified pathways for the reduction of esters to alkoxides (red) and an ether (green).*

In 1995 Cutler and co-workers first reported that silanes could reduce esters to ethers using manganese acetyl precatalysts (Scheme 9).[55] The procedure was similar to previous work by the Buchwald group;[56,57] however, unlike earlier titanium based catalysts, Cutler's manganese catalyst had selectivity for ethers rather than silyl ethers. Good yields were achieved for the reduction of straight-chain aliphatic esters, but the main limitation was substrate scope. Any structural deviation in the ester including branched, cyclic, and phenolic analogues gave significant silyl ether and silyl acetal by-products a result of simultaneous over and under-reduction. Nevertheless, for amenable esters this reductive strategy is relatively mild, requiring only stoichiometric silane and 3 mol% catalyst loading to react fully at ambient temperature in 1 hour.

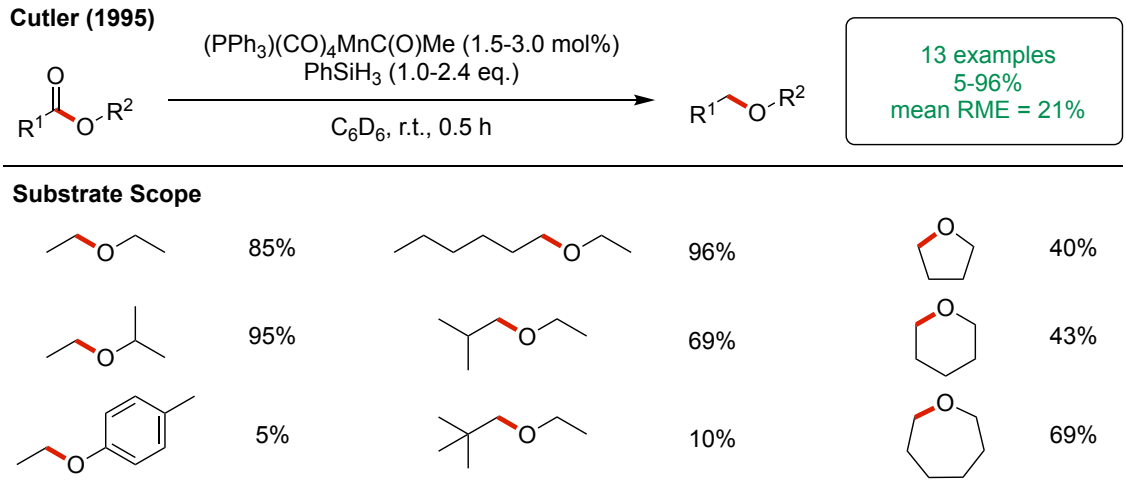

Scheme 9. *General conditions and substrate scope for Cutler's ester reduction.*

In the proposed mechanism, the precatalyst forms a coordinatively unsaturated manganese silyl complex **5** *in situ* which is thought to be the catalytically active species (Scheme 10). This coordinates the ester and adds across the carbonyl bond to give a manganese-silyl acetal **6**. Through an oxidative addition-reductive elimination sequence, **6** is reduced by a silane to form the silyl acetal intermediate and the regenerated catalyst. Finally, a second intermolecular hydrosilylation reduces the silyl acetal **7** to the desired ether **8**, with formation of the siloxane by-product. The key to the success of this reaction was the use of silane, which reduces the ester, makes the carbonyl oxygen a better leaving group, and provides the thermodynamic sink due to the formation of strong silicon oxygen bonds.

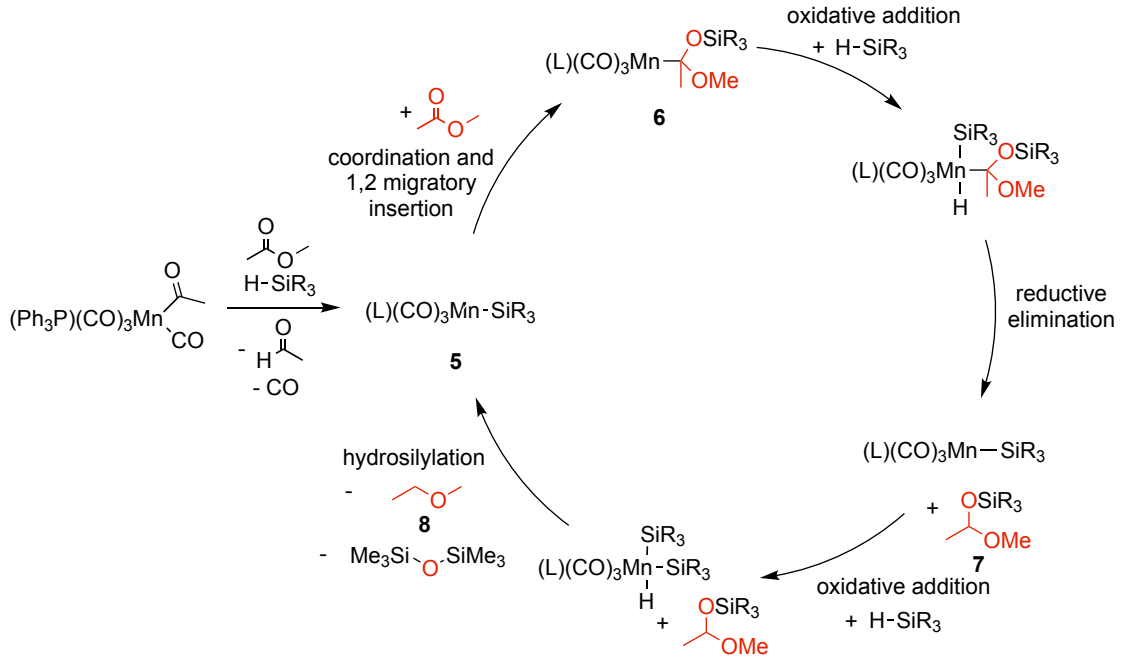

Scheme 10. *Proposed catalytic cycle for Cutler's ester reduction.*

In the 20 years since the inception of this methodology, new catalysts for this reduction have been scarce. The first example reported by Yato *et al.*[58] uses a combination of $TiCl_4$ and TMSOTf (Scheme 11). Although mechanistic studies were not reported, previous experiments had shown that this mixture forms ($TiCl_2(OTf)_2$) *in situ*, which was believed to be the active catalyst. However, it was noted that if the reaction was performed using silver triflate rather than TMSOTf, yields for the reduction of methyl 4-phenylbutylate dropped from 73% to 63%. This led the authors to suggest that TMSCl, which is generated through precatalyst activation, may also play a role in the reaction.

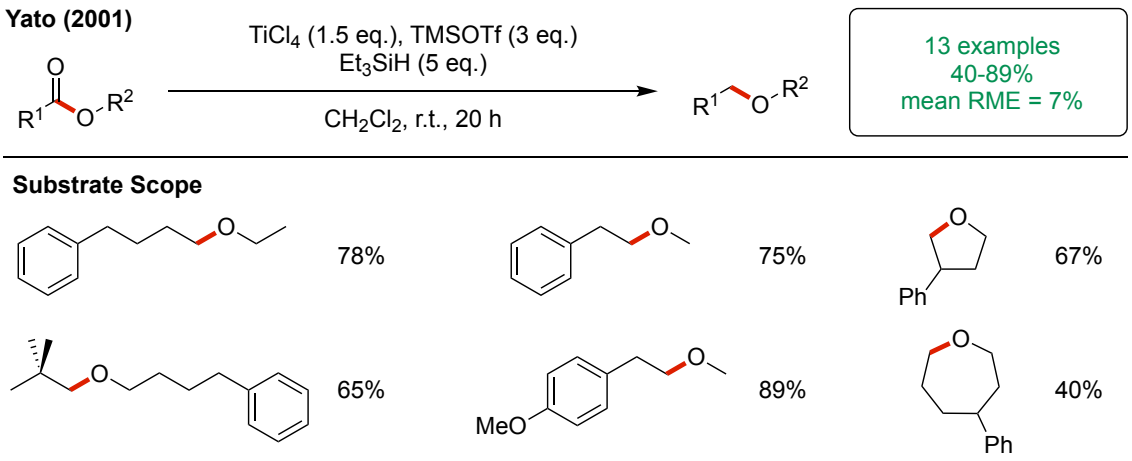

Scheme 11. *General conditions and substrate scope for Yato's ester reduction.*

The advantage of this procedure is a modest increase in structural tolerance of the reduction. Using this process, lactones and esters derived from bulky carboxylic acids can be reduced in moderate yields, though phenolic and sterically demanding alcohols remained challenging. However, the increase in versatility comes at a significant cost to sustainability. Optimised conditions require 5 equivalents of triethylsilane, 3 equivalents of TMSOTf and 1.5 equivalents of $TiCl_4$, which gives less than half the reaction mass efficiency of Cutler's process.

The most versatile and sustainable transition metal catalysed reduction to date was developed by the Beller group in 2012 (Scheme 12).[59] Its design was based around the simple iron carbonyl complexes which Nagashima had previously used to reduce amides.[60] The active catalyst in the reaction is believed to be the coordinatively unsaturated iron tricarbonyl $Fe(CO)_3$ which was most easily accessed through thermolytic decomposition of triiron dodecacarbonyl ($Fe_3(CO)_{12}$). Subsequently, 10 mol% of this precatalyst and tetramethyldisiloxane (TMDS) was used to selectively reduce linear, moderately bulky and cyclic ethers in moderate to good yields, although some of the more challenging phenolic and bulky substrates were not reported.

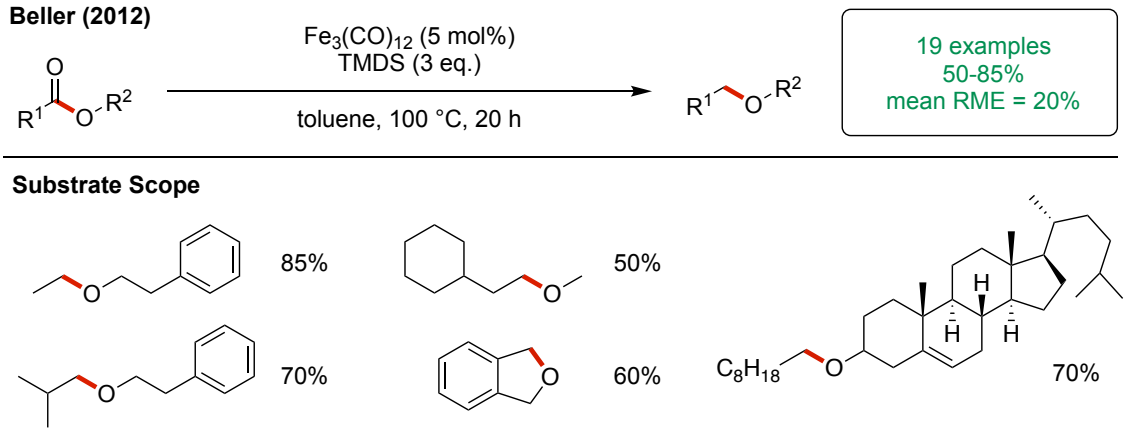

Scheme 12. *General conditions and substrate scope for the Beller group's iron catalysed ester reduction.*

The proposed mechanism (Scheme 13) is believed to involve a double oxidative addition of the iron into the two Si-H bonds to form a disilaferricyclic intermediate **9**. A double hydrosilylation of the carbonyl then forms the desired ether and a siloxane *via* a silyl acetal **10**.

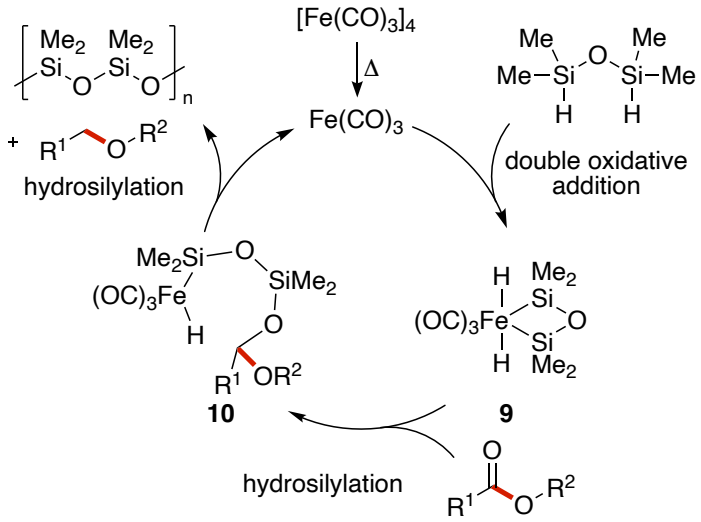

Scheme 13. *Proposed mechanism for Beller's ester reduction.*

With an increased reaction scope and a return to sub-stoichiometric quantities of first-row transition metal catalysts, this synthetic procedure is currently the most sustainable. The required reagents are all abundant, inexpensive and relatively green, for instance TMDS is a by-product of the silicon industry[61] and iron carbonyls are mass produced.[62] However, despite the innocuous nature of most iron compounds, iron carbonyls are volatile, acutely toxic[63] and in this reaction relatively high loadings of 10 mol% (of the trimeric complex) are required. This poses safety concerns which somewhat detracts from the green credentials of the reaction.

The first general and high yielding reduction of esters to ethers emerged in 2007 as the Sakai group discovered that, contrary to previous reports,[64] indium tribromide could mediate ester reduction with Et_3SiH (Scheme 14).[65,66] Furthermore it gave conversions of up to 99% and excellent selectivity for the formation of alkyl ethers.

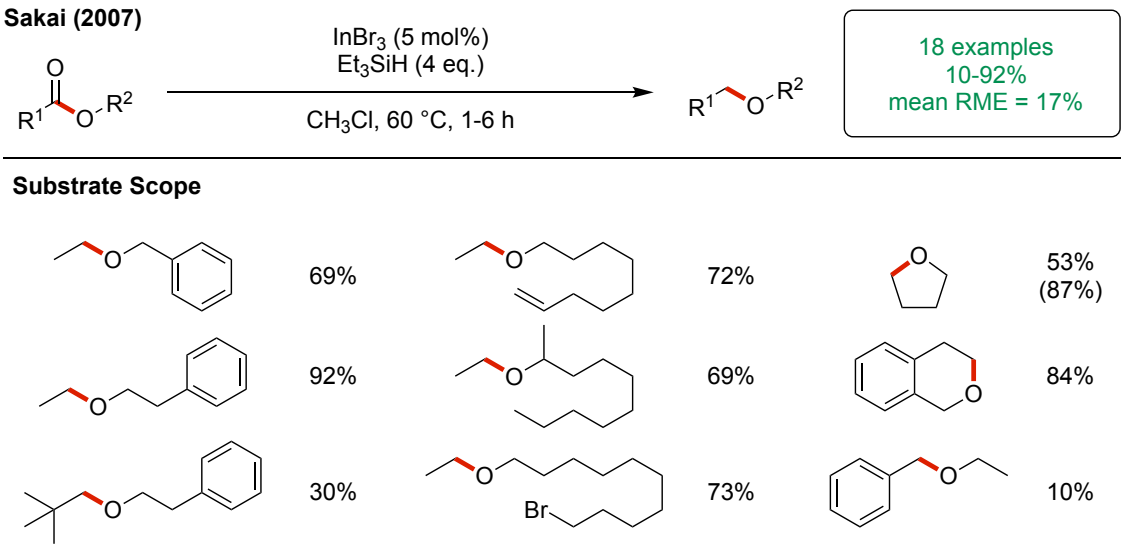

Scheme 14. *General conditions and substrate scope for Sakai's ester reduction.*

The structural tolerance of this reaction was very good. Linear esters gave almost quantitative conversions by GC although the recovered yields were somewhat lower. Branched, brominated, unsaturated and cyclic esters were also tolerated, however the reduction of ethyl benzoate was very slow and gave lower yields. The only substrates for which this procedure did not work were esters derived from benzylic alcohols such as methyl diphenyl acetate **11**. In these cases, the parent alcohols were reduced to hydrocarbons (Scheme 15).

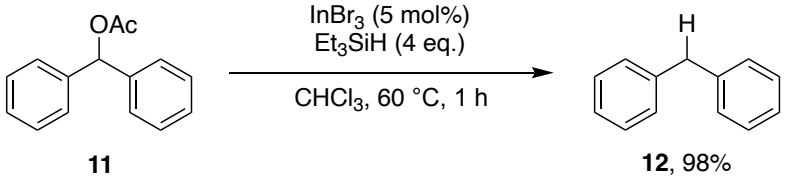

Scheme 15. *Reduction of methyl diphenyl acetate in Sakai's ester reduction reaction.*

A radical-based mechanism was initially proposed based on the complete suppression of the reaction when radical scavenger 2,2,6,6-tetramethyl-1-piperidinyloxy radical (TEMPO) was added. However, later work by Sakai and co-workers[67] showed that aryl iodides were not reduced under the reaction conditions despite the low bond strength. The updated mechanistic proposal suggests that indium bromide simply acts as a Lewis acid to activate the carbonyl oxygen towards reduction.

This protocol has many advantages, primarily its versatility and high yields. However, in terms of sustainability there are also several weaknesses. Firstly, the use of heavy metals is a significant disadvantage when cost, sustainability, and waste treatment is considered, especially as a 5 mol% loading is required. Also, despite Et_3SiH being one of the less expensive silanes, a two-fold excess significantly reduces the reaction mass efficiency. One of the largest drawbacks is the use of chloroform as a toxic and carcinogenic solvent, although it was possible to use toluene for the reduction of ethyl hydrocinnamate with just a 9% reduction in yield.

With this in mind, Biermann and Metzger investigated a more sustainable reduction of fatty acid esters (Scheme 16).[63] The process optimisation started by screening alternative metal halides which showed that gallium bromide was a more effective precatalyst. After further reaction development, it became possible to reduce the neat fatty acid ester in good yields using just 1.1 equivalents of TMDS and 1 mol% of the catalyst. Additionally, the ether products could be distilled from the polysiloxane by-products without the need for a work-up.

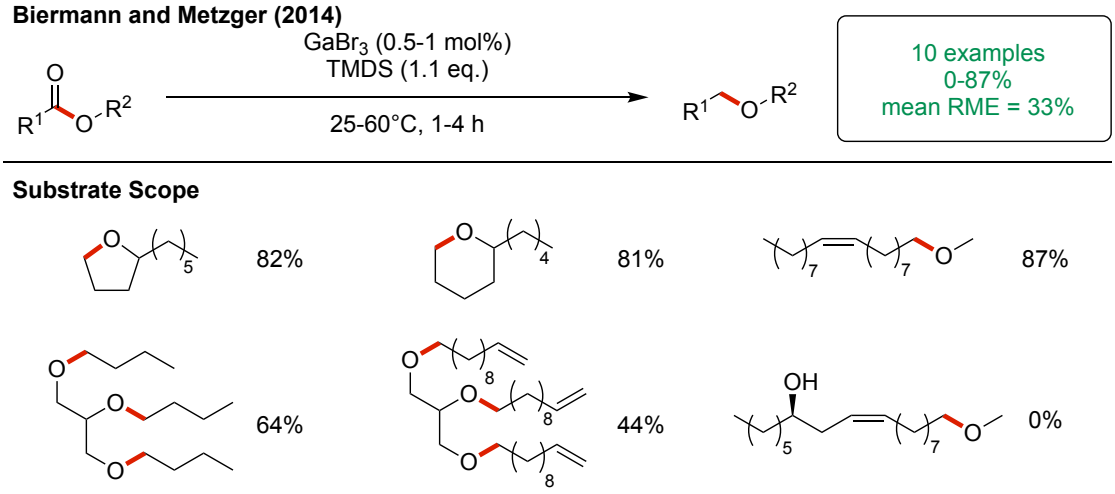

Scheme 16. *General conditions and substrate scope for Biermann's ester reduction.*

This reaction gave moderate to good yields for most esters, although the scope of the report was limited to fatty acid derivatives which were predominantly linear or cyclic. The only ester which was not compatible was methyl ricinoleate which contains a free alcohol that was presumed to deactivate the catalyst.

Reduction of esters using with this method has substantial advantages over its predecessor. For example, whilst it may not be suitable for all substrates, solvent-

free conditions and purification by distillation significantly reduces the mass intensity of the reaction. Furthermore, use of stoichiometric silanes and just 1 mol% of a simple precatalyst increases the average reaction mass efficiency to 33%. Additionally, as this transformation can be carried out near ambient temperatures with inexpensive and non-toxic reagents, the process is more attractive from operational, economic, and environmental perspectives.

2.1.5 Reductive *O*-Alkylation of Alcohols using Carboxylic Acids

The reductive coupling of carboxylic acids and alcohols is a promising new strategy for the formation of ethers. Unlike the Williamson ether synthesis, this methodology allows a two-component ether synthesis to be done in a single reaction, thus reducing step count for a given route. Additionally, carboxylic acids are much more accessible starting materials in comparison to alcohols, with database searches returning 1.8 times as many commercial products and 2.3 times as many carboxylic acid syntheses.[68] Therefore, following the advancement in ester reduction there has been significant research into this concept over the past decade.

Since Lewis acids are already known as to catalyse both esterifications and ester reductions, a one pot procedure for the reductive coupling of carboxylic acids and alcohols is a credible concept. In 2015, Beller and co-workers published an effective example of this strategy using a combination of aluminium triflate and a ruthenium triphos hydrogenation catalyst (Scheme 17).[1] Three reductive couplings were reported using this method, of which the reaction of benzoic acid and methanol was the fastest, giving a yield of 84% after 24 hours. Primary alkyl ethers reacted more slowly and, although not explicitly shown, secondary alcohols reportedly gave yields of less than 20%.

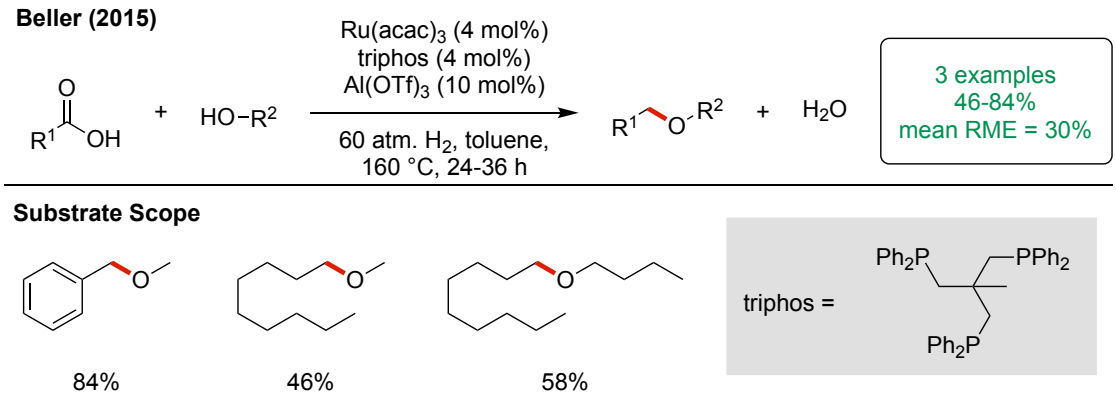

Scheme 17. *General conditions and scope for Beller's reductive O-alkylation.*

From this extremely limited substrate scope, an average reaction mass efficiency of 30% can calculated which, whilst still not very high, is better than most of the ester reduction reactions. A major factor in this improvement is the use of molecular hydrogen which is the ideal reducing agent in terms of mass efficiency. However, to generate a high-pressure hydrogen atmosphere, this process is likely to have used hydrogen in substantial excess which metrics cannot account for without specific volumetric parameters. Furthermore, the use of a flammable gas at high pressures and temperatures is a considerable safety and engineering concern. This process also uses two equivalents of alcohol which, depending on the value of the alcohol may be financially prohibitive.

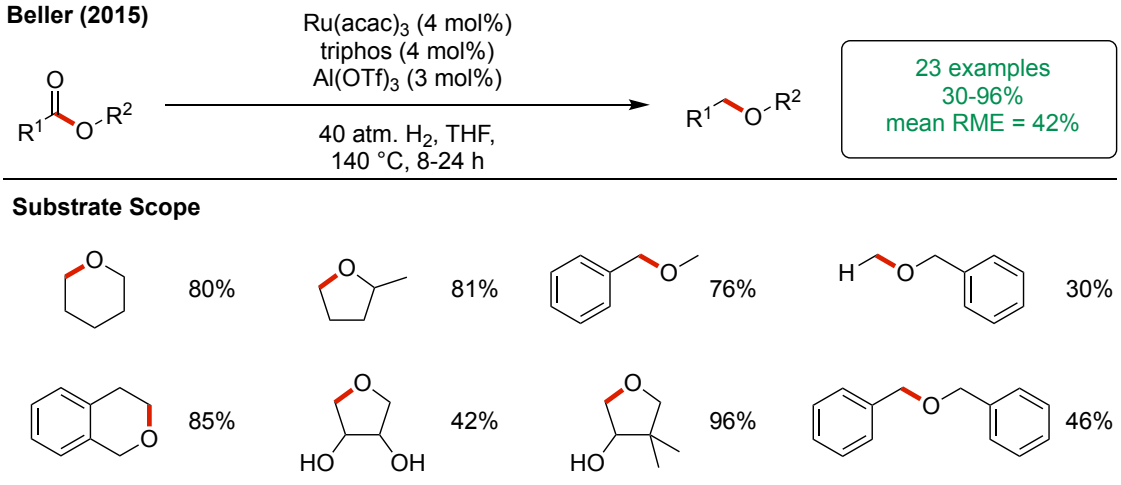

Scheme 18. *General conditions and substrate scope for Beller's ruthenium catalysed ester reduction.*

Despite this being the first reaction of its kind, most of the investigation into the scope and mechanism of this procedure was performed by reducing pre-existing esters (Scheme 18). 23 predominantly cyclic and benzylic esters were hydrogenated

using this method with an average yield of 66% and an average reaction mass efficiency of 42%. However, in contrast to the telescoped procedure, lactones were also reduced smoothly indicating a degree of disparity between the two processes.

Sakai and co-workers also sought to elaborate their $InBr_3$-catalysed ester reduction, to reductive transformations of carboxylic acids (Scheme 19).[69–72] Without modification of the reaction conditions, carboxylic acids could be dehydrogenatively coupled with silanes, giving silyl esters **13** which were reduced to silyl ethers **14**. Furthermore, under the reaction conditions the remaining carbon-oxygen bond became labile, allowing substitution by chloride,[69] bromide, iodide,[70] or thiols.[71] This was further elaborated to include oxygen-centred nucleophiles[72] using a second equivalent of carboxylic acid with sulfuric acid catalysis. In this substitution, the resultant ester **15** was then subsequently reduced to an ether **16** in accordance with the original procedure.

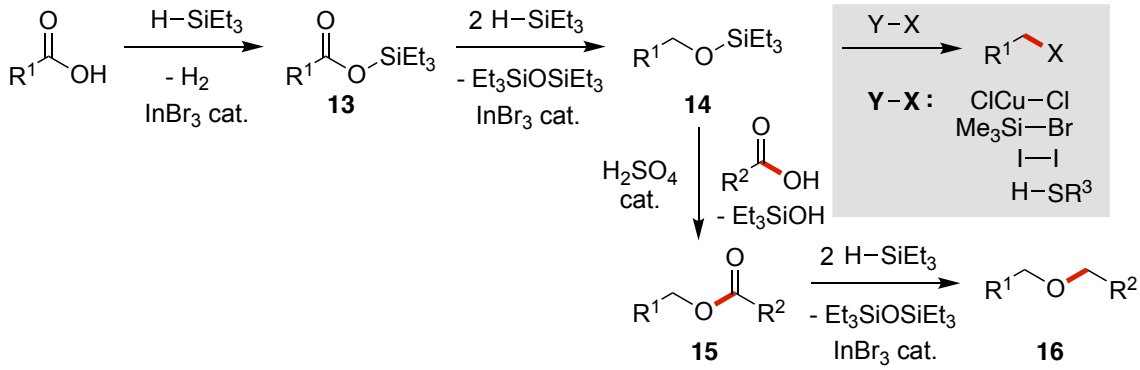

Scheme 19. *Proposed mechanism for Sakai's reductive functionalisation of carboxylic acids.*

Using this manifold, Sakai reported a one-pot synthesis of symmetrical ethers from their carboxylic acids (Scheme 20).[72] Good yields were achieved for linear aliphatic ethers; however, apart from aryl halides, no other functional groups were attempted. Crossed etherifications using two different carboxylates were not reported which suggests the reaction was not thought to possess any selectivity for unsymmetrical ethers. Additionally, sterically hindered carboxylic acids were omitted from the substrate scope because earlier work showed they were partially reduced to alcohols through a competing side reaction. Consequently, the only high yielding products from this reaction are symmetrical, linear, aliphatic ethers.

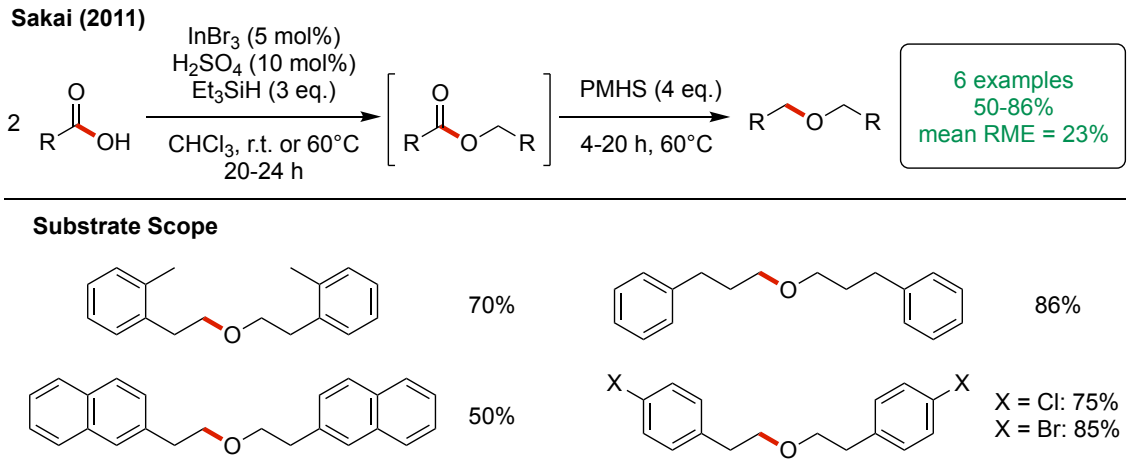

Scheme 20. *General conditions and substrate scope for Sakai's reductive O-alkylation.*

However, just one year later, the Sakai group found that indium tribromide could also catalyse a Fischer esterification, furnishing unsymmetrical esters which could in turn be reduced to ethers in a one pot process (Scheme 21).[67] This strategy again gave good yields for simple unfunctionalized substrates. However, activated alkenes, sterically bulky substrates or strongly coordinating groups such as nitros of thioethers inhibited the reduction.

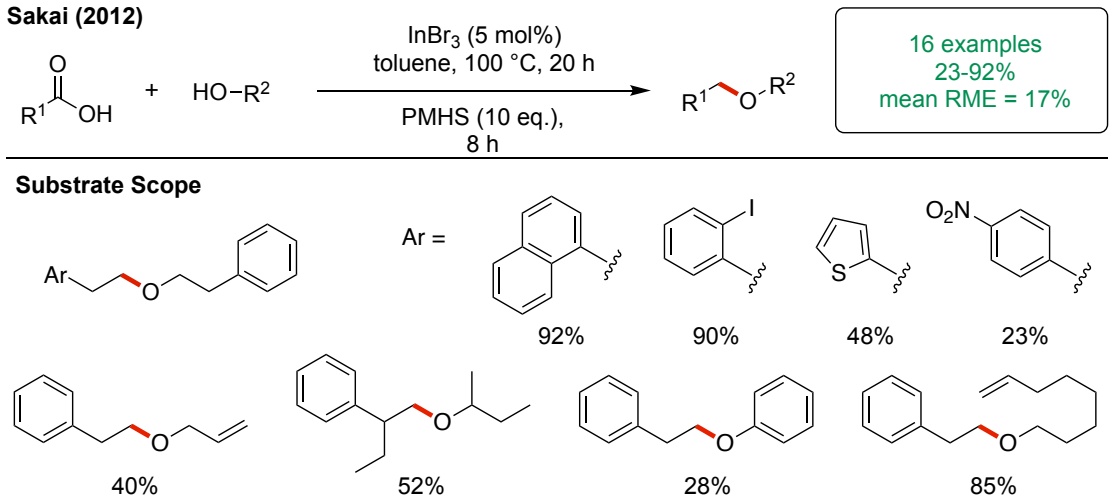

Scheme 21. *General conditions and substrate scope for Sakai's reductive O-alkylation for unsymmetrical ethers.*

The use of a large excess of polymethylhydrosiloxane is a drawback. However, the reduced mass efficiencies are compensated by the silane's availability as an inexpensive industrial by-product. The main limitation of PMHS is that the oxidised by-product crosslinks to form a solid gel in the reaction mixture. This makes industrial implementation of this procedure unpracticable and the use of other silanes resulted in diminished yields.

Since Cutler's seminal publication in 1995,[55] several iterations of ester hydrosilylation have made progress towards a sustainable and widely applicable ether synthesis. Some of the most valuable contributions have come from the Sakai group,[65] employing $InBr_3$ as a simple catalyst to enable ester reduction with inexpensive silanes. Beller and co-workers[59] have since demonstrated selective ester reduction using $Fe_3(CO)_{12}$ as an earth abundant metal catalyst. A major advancement in operational simplicity also came with Sakai's esterification-reduction[67] which exploited indium tribromide's Lewis acidity to facilitate a one-pot bond-forming ether synthesis. Despite these advances, current methodology is still limited by moderate to poor yields for all but simple substrates and is consequently overlooked as a general approach to ether synthesis. To establish a synthetically useful reductive etherification would require re-developed processes with increased functional group tolerance whilst avoiding the use of rare metal catalysis.

2.2 Project Aims

The basis of this project was the Denton group's recent use of carboxylic acids in the reductive alkylation of primary and secondary amines (Scheme 22).[73,74] In this research, a novel one-pot procedure was created using phenylsilane both as a coupling and reducing agent. This provided a facile amine alkylation using safe, abundant, and inexpensive electrophiles without overalkylation.

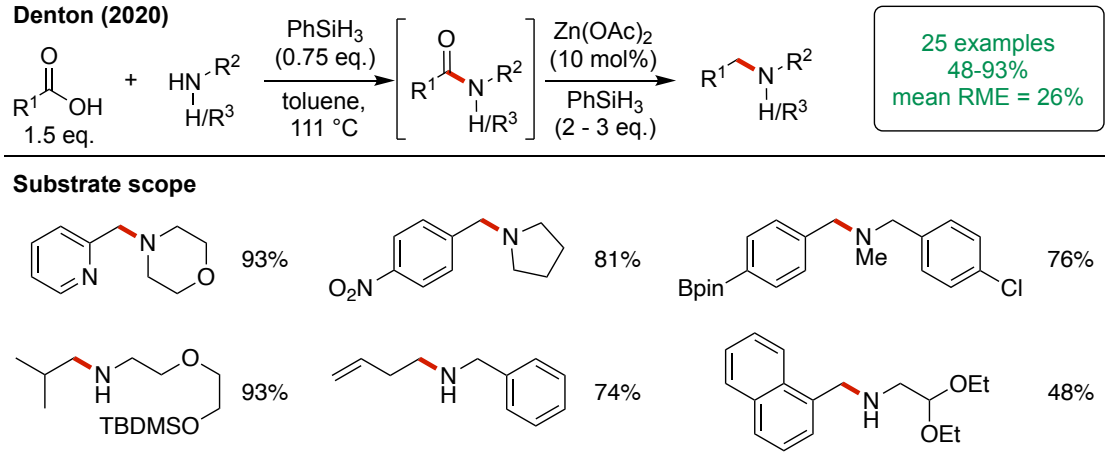

Scheme 22. *General conditions and substrate scope for Denton's reductive N-alkylation.*

It was initially believed that these conditions may be able to reduce esters to ethers, however a preliminary study found this not to be the case.[75] The ester intermediates are much less Lewis basic at oxygen and less prone to hydrosilylation using some of the milder Lewis acids. Nevertheless, the desire for an industrially applicable reductive strategy encouraged continued research into this underdeveloped area.

Current procedures for the catalytic hydrosilylation of esters are limited in terms of substrate scope and sustainability. The greatest opportunity to improve existing methods was to find an easier, more sustainable, and more versatile ester reduction catalyst.

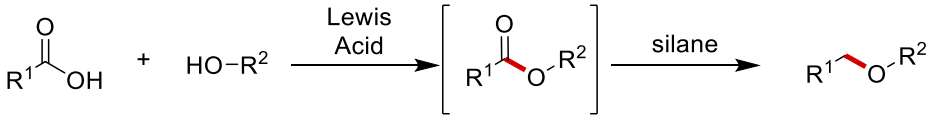

Scheme 23. *General strategy for the reductive O-alkylation of alcohols with carboxylic acids.*

Furthermore, to increase the value of this strategy it was desirable to integrate this transformation with a method for ester synthesis; the simplest being a Fischer

esterification. While these reactions are not usually challenging transformations, their reversibility can often limit conversions, especially using only stoichiometric alcohol. Therefore, as well as finding an efficient ester reduction, catalysts which could be complimentary to both reactions were especially pursued with the aim of developing a versatile one-pot procedure for the reductive *O*-alkylation of alcohols with carboxylic acids.

2.3 Results and Discussion

2.3.1 Development of a Model Reaction

To begin method development, it was desirable to have an efficient way to screen prospective catalysts and reaction conditions. A model reaction was envisaged, requiring substrates which were: i) easily to analyse, ii) known to be reactive, iii) of low toxicity, iv) inexpensive and readily available. Motivated by the power of ^{19}F NMR spectroscopy, aryl fluorides were chosen as 'analytical tags' that could be used to probe the reaction with maximum resolution, minimal time, and without significantly altering the electronic properties (Hammett constant $\sigma_p = 0.06$).[76] The ester moiety was also designed to be in a sterically unhindered alkyl chain as Cutler and co-workers showed that these were the most reactive substrates.[55] Thus, after searching commercial suppliers, 2-(4-fluorophenyl)acetic acid **17** and 2-(2-fluorophenyl)ethan-1-ol **18** were chosen as model reactants based on their low cost and toxicity.

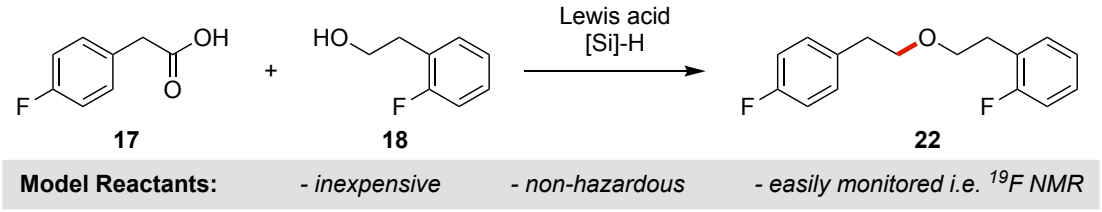

Scheme 24. *Model reaction for facile process development.*

However, although ^{19}F NMR spectroscopy can give a quantitative distribution of species, in the absence of reference signals the spectrum can only give a qualitative comparison of electron density at fluorine. To be able to assign peaks, it was necessary to synthesis a library of potential products which would enable greater reaction understanding.

Synthesis began with the model ester which utilised a DMF-catalysed activation of carboxylic acid **17** to the acyl chloride followed by displacement with alcohol **18**. This sequence facilitated the preparation of 8.2 g of the desired ester, **19**, in a 91% yield which could be used for screening work.

Next, potential reduction products were explored (Scheme 25). Hydrosilylation methodology from the Denton group[74] was used to synthesise alcohol **20.** However,

20 was furnished in only a 43% yield after difficulties in removing the silanol and siloxane by-products. A portion of this was then oxidised using Dess-Martin periodinane[77] to give aldehyde **21** in a disappointing 26% yield.

Ether **22** was synthesised using the Sakai group's ester reduction methodology[67] and was isolated in 60% yield, along with 15% of an inseparable mixture of both triethylsilyl ethers, **23a** and **23b**. This highlighted that, even using amenable substrates under literature conditions, this catalytic reduction is not completely selective. Finally, partially reduced silyl acetal **24** was synthesised using Cheng and Brookhart's iridium-catalysed hydrosilylation methodology.[78] This intermediate could not be isolated by aqueous work-up of column chromatography but was stable enough to give a clean ^{19}F NMR spectrum.

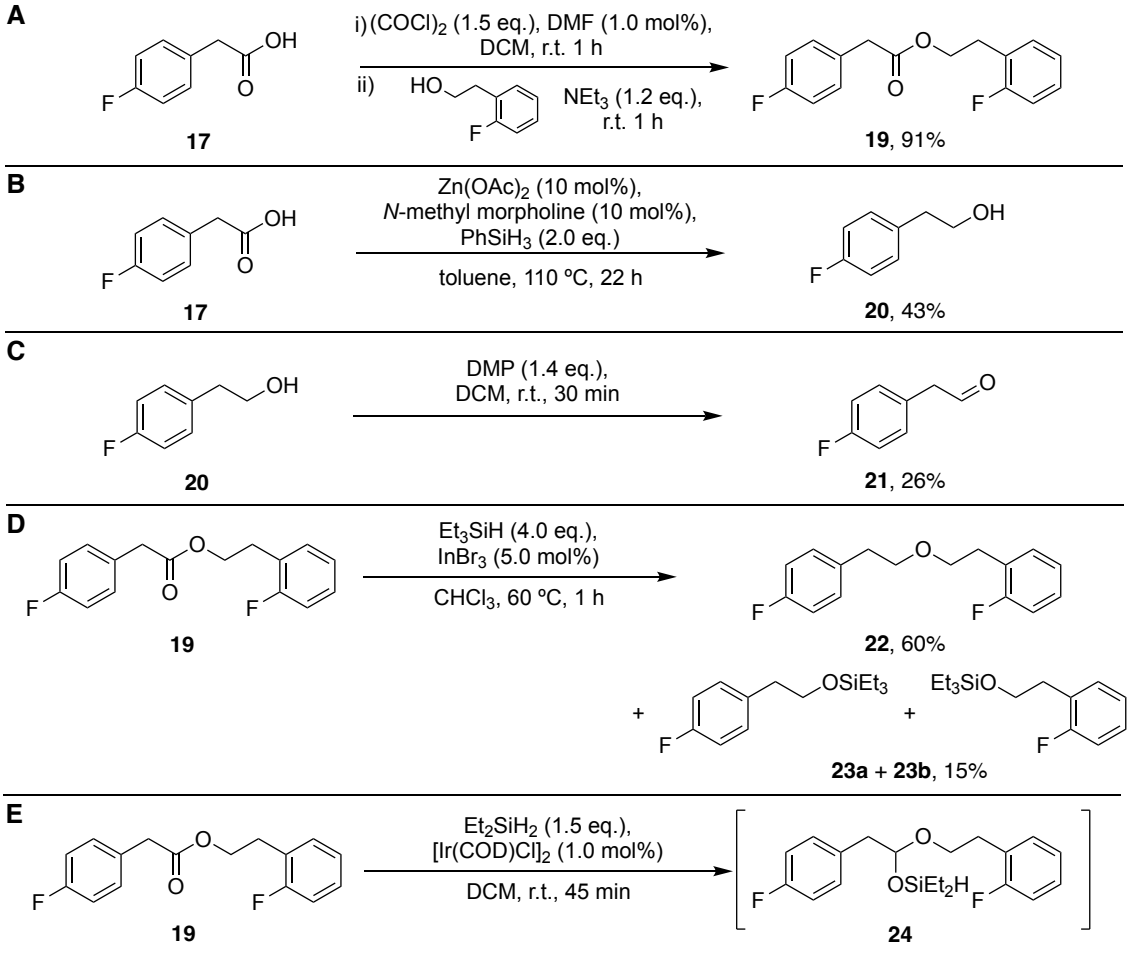

Scheme 25. *Synthesis of ^{19}F reference compounds in preparation for catalyst screening.*

After the synthesis of all analytical standards was completed, the fluorine NMR spectra were compared (Figure 3). Thankfully, almost all species were resolved by at least 0.1 ppm despite having several atoms between the reactive centre and the fluorine marker. Additionally, without proton decoupling the spectra displayed peak splitting characteristic of the substitution pattern on the aryl ring. The spin-lattice relaxation times (T1) for the ^{19}F nuclei in the ester **19**, the ether **22**, and trifluorotoluene (as an internal standard) were also measured, allowing quantitative reaction monitoring (5 x T1 = 18 s).

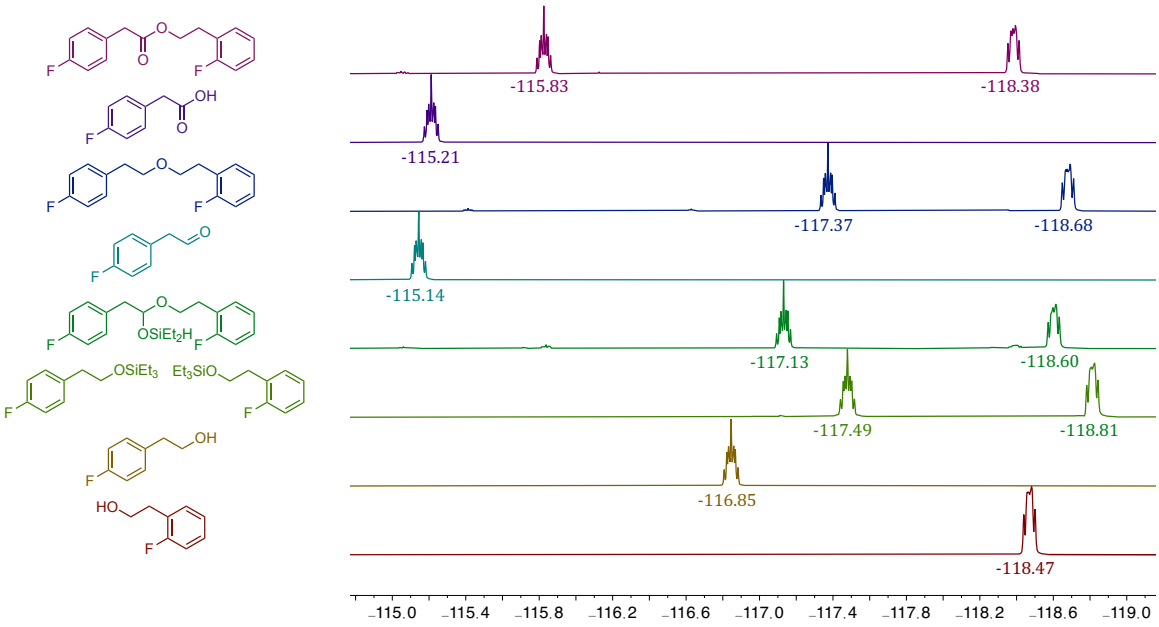

Figure 3. *A comparison of the ^{19}F NMR of prepared analytical standards.*

2.3.2 Ester Reduction Screening

Using the model reaction, two sets of conditions and three different silanes were varied. Toluene and dichloromethane were chosen as solvents as they are both common in literature[58,59,67,79] but are constitutionally very different and allowed a wide temperature range to be examined (boiling points 40 °C and 111 °C respectively). As for the silane, it is well-known that phenylsilane is a powerful reducing agent,[80] however we also wanted to investigate silanes with different steric and electronic qualities. Diethylsilane was chosen as a simple disubstituted silane and tetramethyldisiloxane (TMDS) was selected due to its heteroatom and so-called "dual Si-H" effect. This effect describes the observed but poorly understood increase in activity Nagashima and co-workers found for TMDS over mono-hydridic

analogues.[81–83] To trial these conditions and to set a benchmark, the ester reduction was performed using three known catalysts in their literature loading.[59,63,65]

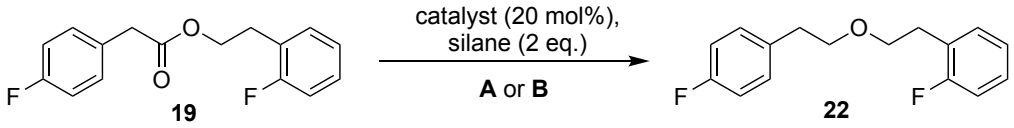

A: dichloromethane, 40 °C, 24 h **B:** toluene, 100 °C, 24 h

Catalyst (loading /%)	A			Catalyst (loading /%)	B		
	$PhSiH_3$	Et_2SiH_2	TMDS		$PhSiH_3$	Et_2SiH_2	TMDS
$InBr_3$ (5%)	**18**	**5**	**44**	**$InBr_3$ (5%)**	**60**	**66**	**98**
$GaBr_3$ (1%)	**3**	**10**	**24**	**$GaBr_3$ (1%)**	**71**	**36**	**59**
$Fe_3(CO)_{12}$ (10%)	**0**	**0**	**0**	**$Fe_3(CO)_{12}$ (10%)**	**9**	**0**	**0**
$Zn(OAc)_2$	0	0	0	$Zn(OAc)_2$	0	0	0
$Zn(OTf)_2$	0	0	0	$Zn(OTf)_2$	0	0	0
$ZnBr_2$	**0**	**0**	**0**	**$ZnBr_2$**	**0**	**0**	**4**
$CeCl_3.7H_2O$	0	0	0	$CeCl_3.7H_2O$	0	0	0
$Sm(OTf)_3$	0	0	0	$Sm(OTf)_3$	0	0	0
$Sc(OTf)_3$	0	0	0	$Sc(OTf)_3$	0	0	0
$TiCl_4$	**0**	**0**	**10**	**$TiCl_4$**	**0**	**0**	**5**
$Ti(O^iPr)_4$	0	0	0	$Ti(O^iPr)_4$	0	0	0
TMS(OTf)	0	0	0	TMS(OTf)	0	0	0
$TiCp_2Cl_2$	0	0	0	$TiCp_2Cl_2$	0	0	0
$ZrCp_2Cl_2$	0	0	0	$ZrCp_2Cl_2$	0	0	0
$ZrCl_4$	0	0	0	$ZrCl_4$	0	0	0
$AlBr_3$	0	0	0	$AlBr_3$	0	0	0
$AlCl_3$	0	0	0	$AlCl_3$	0	0	0
DABAL-Me_3	0	0	0	DABAL-Me_3	0	0	0
$ZnCl_2$	0	0	0	$ZnCl_2$	0	0	0
ZnI_2	0	0	0	ZnI_2	0	0	0
$B(C_6F_5)_3$	**0**	**2**	**3**	**$B(C_6F_5)_3$**	**0**	**0**	**0**
$CuCl_2$	0	0	0	$CuCl_2$	0	0	0
$CuBr_2$	**0**	**0**	**13**	**$CuBr_2$**	**0**	**0**	**0**
CuI	0	0	0	CuI	0	0	0
$CoBr_2$	0	0	0	$CoBr_2$	0	0	0
$FeCl_3$	**3**	**10**	**69**	**$FeCl_3$**	**1**	**0**	**6**
$BiBr_3$	0	0	0	$BiBr_3$	0	0	3
$FeBr_3$	**0**	**0**	**87**	**$FeBr_3$**	**0**	**0**	**8**
$Fe(acac)_3$	0	0	0	$Fe(acac)_3$	0	0	0
$FeCl_2$	0	0	0	$FeCl_2$	0	0	0

Table 2. *Lewis acid screening for the reduction of esters to ethers for reaction conditions **A** and **B**, with ^{19}F NMR yields calculated against an internal standard of α,α,α-trifluorotoluene. Previous literature examples (highlighted in grey) were performed with their reported loading which is given in parenthesis. All other catalyst loadings are 20 mol%.*

As shown from the literature catalysts, the yield is highly dependent on silane, solvent, and temperature. Indium tribromide and TMDS in toluene produced the best results, giving 98% conversion from ester to ether. Despite its lower loading gallium bromide also gave good conversion but also tended to form more impurities. The choice of silane had a large impact on yield and the most effective silane varied for each catalyst. Contrary to literature,[59,60,80] iron dodecacarbonyl gave no conversion with TMDS and only 9 % was reduced using phenylsilane. The exact reason for this is unknown, although the original procedure uses rigorously anhydrous conditions and a recrystallised catalyst.

Other Lewis acids from across the periodic table were also screened. Some, such as zinc halides had literature precedent for the hydrosilylation of amides,[84] whilst others were known to activate carbonyl compounds but were relatively unexplored in this context. Most metal salts were completely ineffective and returned the starting each time, however, seven Lewis acids gave some for the reduction of esters to ethers.

Zinc (II) bromide, copper (II) bromide and bismuth (III) bromide each gave modest conversion with TMDS, demonstrating the significance of the dual hydride effect. However, in each case the activity is low; giving poor NMR yields and mostly returned starting material. This was not ideal given the already long reaction times and high metal loadings.

Harder Lewis acids seemed to be more able to activate the carbonyl oxygen for example $TiCl_4$ gave 10 % NMR yield in a clean reaction under conditions **A**. Using the harsher conditions all the starting material was consumed, however a complex mixture of products was obtained with only 5 % of the desired ether. This closely resembled an existing methodology developed by Yato *(vide infra)*,[58] which required superstoichometric titanium tetrachloride, trimethylsilyl triflate and triethylsilane. Indeed when 2 equivalents of titanium tetrachloride were used under conditions A, a 96 % NMR yield was achieved, however the novelty, sustainability and practicality of this method was not suited to this project.

Tris(pentafluorophenyl)borane, $B(C_6F_5)_3$, is also a powerful Lewis acid which fully consumed starting material but also gave low conversions with numerous side

products under both sets of conditions. Optimisation of this result to give a selective reduction seemed unlikely based on previous reports where ketones were fully reduced to hydrocarbons.[85,86] The best result from this screening was achieved with iron trichloride, which gave a 69 % NMR yield in the first instance. A small exploration of other iron salts showed iron tribromide was also highly active but neither FeF_3, $Fe(acac)_3$, or $FeCl_2$ gave any conversion.

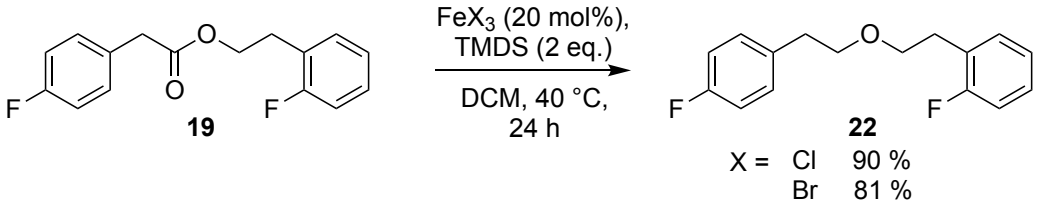

Scheme 26. *Reduction of the model substrate with $FeCl_3$ and $FeBr_3$ and the NMR yields of ether.*

On a larger scale and with greater reagent control, conversions for $FeCl_3$ and $FeBr_3$ were found to be 90% and 81% respectively with no apparent side reactions (Scheme 26). This was a promising lead as iron trichloride is an inexpensive commodity chemical which is used to etch copper and as a flocculant for water treatment.[87] Additionally, $FeCl_3$ was already established as an effective catalyst in the Fischer esterification of simple esters,[88] so was seemingly compatible with a one pot reductive alkylation.

2.3.3 Optimisation of $FeCl_3$-catalysed Ester Reduction

Initial observations

A 90% NMR yield was a good place to begin optimisation. However, there were several undesirable aspects of the reaction which were targets for improvement. Perhaps the main barrier to the development of an industrially relevant process was the use of DCM as a solvent; however, the long reaction times were also undesirable. Additionally, despite the availability of $FeCl_3$, the 20 mol% catalyst loading is high and when this was lowered to 10 mol%, yield dropped to 65%.

Catalyst degradation over the course of the catalyst was visually apparent; the yellow colour of dissolved iron chloride fades with simultaneous formation of a white precipitate. Mass spectrometry of the precipitate confirmed that $FeCl_3^-$ and $FeCl_4^-$ ions were indeed present. ^{19}F NMR of the solid showed no apparent signals,

suggesting the precipitate is unrelated to the substrate, however the presence of the paramagnetic Fe^{3+} nucleus prevented gaining meaningful insight by ^{1}H or ^{13}C NMR spectroscopy.

The Role of Ligands

To keep the iron in solution it was believed that a tightly binding ligand may stop the iron coordinating to the silicon-containing by-product thereby increasing turnover number and allowing reduced loadings. To test this the reaction was repeated with a series of ligands at a 10 mol% iron trichloride loading to observe any positive or negative effects (Scheme 27).

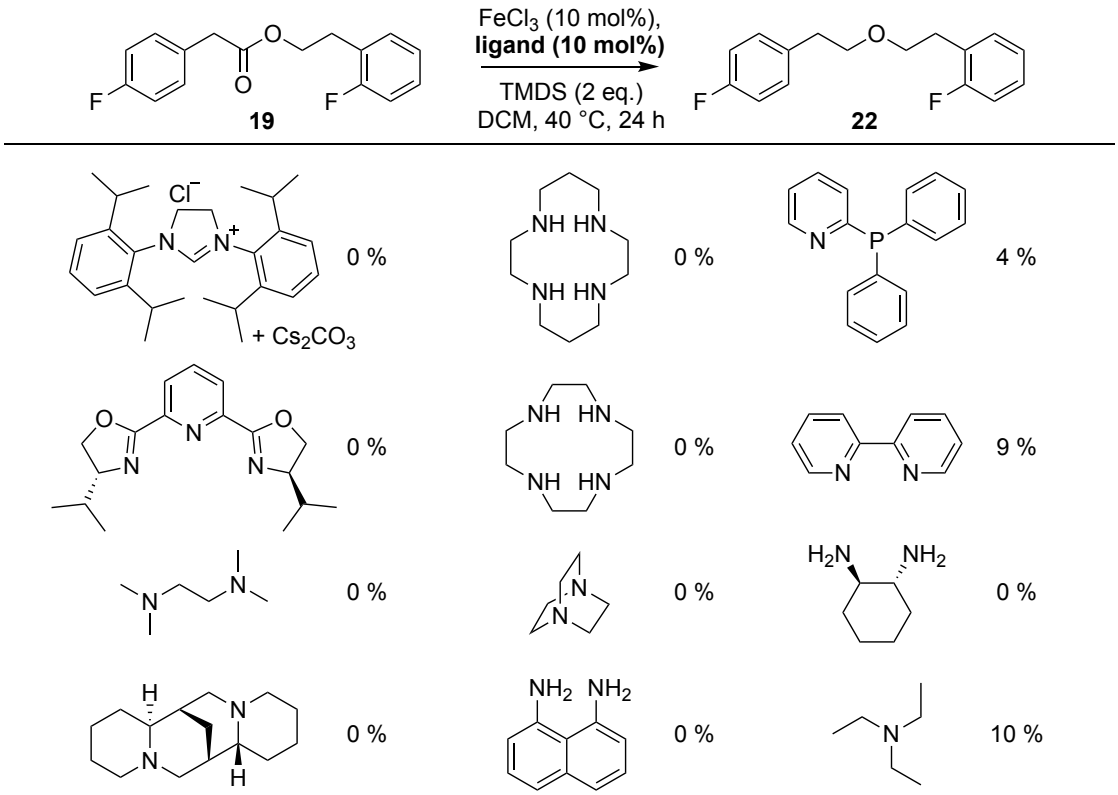

Scheme 27. *Ligand screening for the reduction of esters to ethers with NMR yields given.*

It was found that the addition of any ligand was damaging to the reaction with complete suppression for strongly electron donating groups. Less basic ligands such as 2,2'-bipyridine and diphenyl-2-pyridylphosphine did give 4 and 9 % conversions respectively, presumably because they are poor σ donors and π back-bonding is weak in electron deficient metal centres. The smallest reduction in yield was observed the with triethylamine, which is intrinsically poor at coordinating metals

based on steric repulsion. The fact that the best result was obtained with the worst ligand illustrated that this strategy was fundamentally flawed.

Reaction Additives

Previous reports suggested that the major by-product of TMDS reductions is octamethylcyclotetrasiloxane[89] (also called **D4**) and its was reasoned that this cyclic ether could strongly complex iron due to the macrocyclic effect. If true, then another metal additive of a suitable size could displace the ferric ion and prevent precipitation of the supramolecular complex **25**.

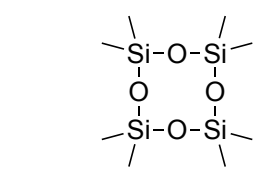

Octamethylcyclotetrasiloxane
D4

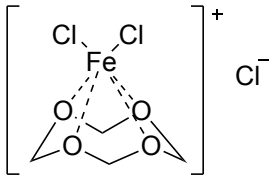

25

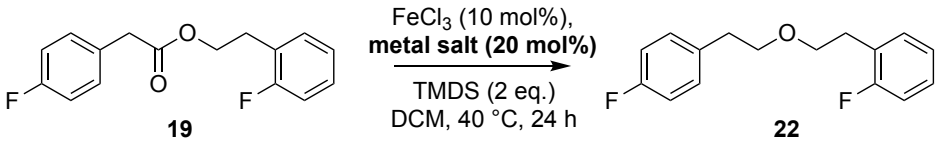

19 **22**

Metal salt additive	Metal ionic radius /pm	NMR Yield /%
LiCl	74	7
NaCl	102	25
KBr	138	5
CsCl	149	55

Scheme 28 and Table 3. *Proposed siloxane by-product octamethylcyclotetrasiloxane and, a potential iron (III) salt which could form by complexation of a macrocyclic ligand. Table shows the changing NMR yield as alkali metal halides of varying cationic radii are added.*

To examine this a series of alkali metal halides were examined as additives in the reduction of the model substrate (Table 3). All salts, however, gave inferior yields to the 64% which was obtained using 10 mol% iron trichloride alone. It is difficult to establish any trends based on only 4 unrepeated results, however, yield roughly increased with increasing cation size. The exception to this was potassium bromide which gave only 5% yield and a dark brown reaction mixture reminiscent of iron tribromide solutions. This suggested the counterion was not innocent and the chlorides on iron are labile.

To investigate whether siloxanes really would inhibit ester reduction, 1 equivalent of a commercial sample of **D4** was spiked into the model reaction. This gave almost identical results to those achieved using initial conditions, suggesting another by-product - but not **D4** - was inhibitive.

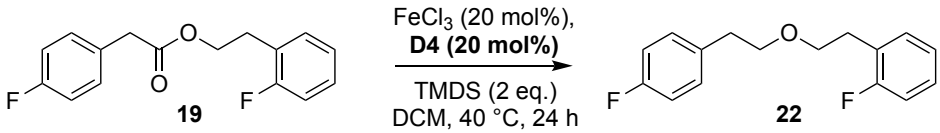

Scheme 29. *NMR yield and conversion for the reduction of the model ester, spiked with an equivalent of D4.*

Silanols were the most plausible species which would poison the iron, and when 1 equivalent of triethylsilanol was added to the reaction, the yield of the ether dropped to just 2% along with the formation of a white precipitate (Table 4). Curiously, adding 0.1 equivalents of the silanol seemed to give a slightly increased yield, either due to an unknown effect or by experimental error.

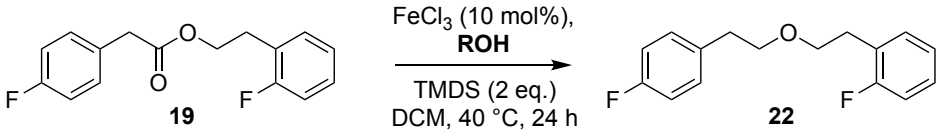

Additive	NMR yield /%	
	0.1 eq.	1.0 eq
-	64	
H_2O	79	13
MeOH	45	0
^{i}PrOH	50	0
CF_3CH_2OH	64	52
Et_3SiOH	73	2
$PhCO_2H$	37	4

Table 4. *The reduction of model ester and its inhibition with various oxygen-based additives. Yield was measured by 19F NMR against an internal standard of α,α,α-trifluorotoluene.*

The nature of catalyst inhibition was further investigated with alcohols, water, and benzoic acid. Water gave a similar effect to triethylsilanol, increasing yield to 79% in substoichiometric quantities, however stoichiometric water was deleterious to yield. Addition of 0.1 eq. of alcohols (methanol, isopropanol and 2,2,2-trifluoroethanol) reduced conversions in a manner broadly in line with their nucleophilicity. Benzoic acid, which is less nucleophilic but strongly coordinating,

had the greatest impact at 0.1 equivalents and in this case, a gas (presumably hydrogen) was also evolved. This investigation suggests that, similarly to Sakai's methodology, strongly coordinating substrates may not be tolerated under the reaction conditions.[67]

The Role of Solvent

To improve the scalability of this reaction attention was turned to the solvent. The hope was that another solvent may i) prevent catalyst degradation, ii) be more sustainable and iii) be able to access higher temperatures to allow Fischer esterification. Solvents containing alcohols, ketones, esters and amides were assumed to be too reactive, however the screening included the more sustainable solvents such as anisole and propylene carbonate (Table 5).[90]

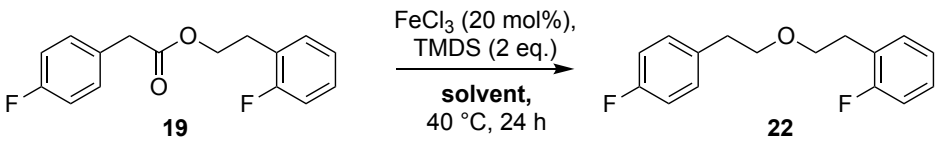

Solvent	NMR Yield /%
DCM	44
DMSO	0
propylene carbonate	0
toluene	2
anisole	0
TBME	0
dioxane	0
THF	0
acetonitrile	0
heptane	0
α,α,α-trifluoroethanol	0
1,2 dichlorobenzene	1
trifluorotoluene	15
chloroform	26
chlorobenzene	30
1,2-dichloroethane	32
fluorobenzene	38

Table 5. *A screen of solvents for the reduction of the model substrate. Yield was measured by 19F NMR against an internal standard of α,α,α-trifluorotoluene, or fluorobenzene.*

Generally, yields were lower than previous reactions, possibly as the catalyst and substrate were added as a stock solution followed by evaporation and redissolution

in a new solvent. This was consistent throughout, so although the yields may not be accurate, the results should be comparable. In terms of yield, a suitable replacement for dichloromethane was not identified, and successful reactions were always accompanied by precipitation of an iron species. Significant reactivity was only observed using halogenated solvents, with fluorobenzene giving the next highest yield. Typically, halogenated solvents tend to be avoided in industry as they often have associated health hazards and are difficult to incinerate, recycle or treat biologically.[90] However, despite having significant aquatic impact, fluorobenzene is not a suspected carcinogen, can be incinerated and has a much more convenient boiling point than DCM (fluorobenzene, 85 °C; DCM, 40 °C), so was used in subsequent work.[91]

Reaction Parameters

Finally, the reaction was optimised with respect to the silane, temperature, and concentration (Table 6). Yield was highly variable and using typically more reactive silanes such as phenylsilane or triethoxysilane, only starting material was returned, whilst limited reduction was found with triethylsilane and polymethylhydrosiloxane. Using just one silane equivalent also gave more modest yields, whereas an 83 % NMR yield was attained using 4 equivalents.

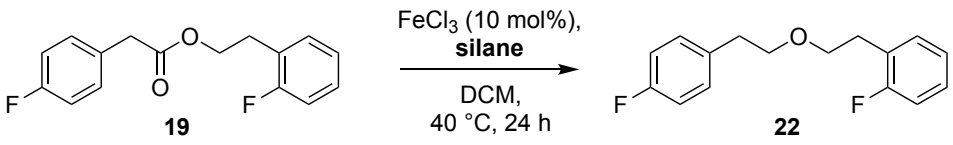

Silane	Equivalents	'Hydride' Equivalents	NMR Yield /%
$PhSiH_3$	2	6	0
Et_2SiH_2	2	4	0
Et_3SiH	4	4	11
$(EtO)_3SiH$	4	4	0
PMHS	4	4	5
TMDS	2	4	64
TMDS	1	2	57
TMDS	4	8	83

Table 6. *Optimisation of ester reduction with respect to silane identity and equivalents. Yield was measured by 19F NMR against an internal standard of α,α,α-trifluorotoluene.*

Although TMDS is relatively cheap industrial by-product, it is around 20 times more expensive than iron trichloride and of a similar molecular weight. Therefore, contrary to most catalysis, the metrics and economics of this reaction are heavily favour increasing yield with higher catalyst loadings (Table 7).

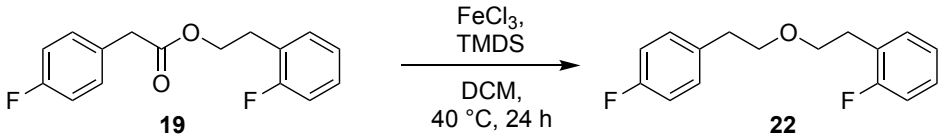

$FeCl_3$ loading /mol%	TMDS equivalents	Yield /%	Reaction Mass Efficiency /%	COG per mole of product /£.mol^{-1}
20	2	90	41	182
10	4	83	26	375

Table 7. *Conditions for similarly yielding ester reductions and comparison of the reactions based on reaction mass efficiencies and cost of goods of the silane and iron trichloride.*

The effects of temperature and concentration were also investigated but the initial set of conditions could not be improved (Table 8). Temperatures beyond 40 °C made the yellow hue from the iron chloride disappear faster, but also reduced yield. At 30 °C the solution remained yellow after 24 hours indicating the reaction was slow. As TMDS has a boiling point of 70-71 °C, the reaction was not investigated beyond this temperature. Increasingly concentrated solutions also gave faster reactions and slightly reduced yields.

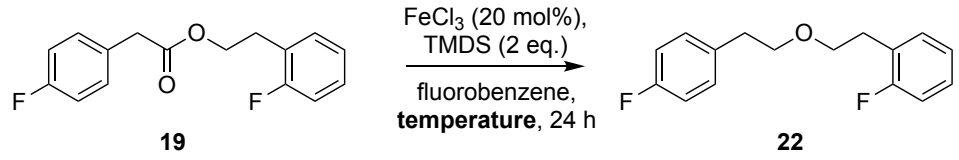

Temperature /°C	NMR Yield /%
30	46
40	50
50	45
60	42
70	38

Concentration /mol.dm^{-3}	NMR Yield /%
0.36	50
0.48	47
0.72	42
1.45	31
neat	6

Table 8. *Optimisation of the ester reduction with respect to temperature and concentration. Yield was measured by 19F NMR against an internal standard of α,α,α-trifluorotoluene.*

2.3.4 Scope of $FeCl_3$-catalysed Ester Reduction

Before continuing with this work further, several small-scale reactions were performed on other substrates to prove the reaction was general. Methyl cinnamate **26e**, furfuryl propionate **26c**, and diethyl diallylmalonate **26i** are commercially available whereas the other esters were synthesised using a Steglich Esterification with *N,N'*-diisopropylcarbodiimide (DIC) and 4-dimethylamino pyridine (DMAP). The dibenzylated lactone **26h** was prepared by alkylation of γ-butyrolactone under basic conditions.[92]

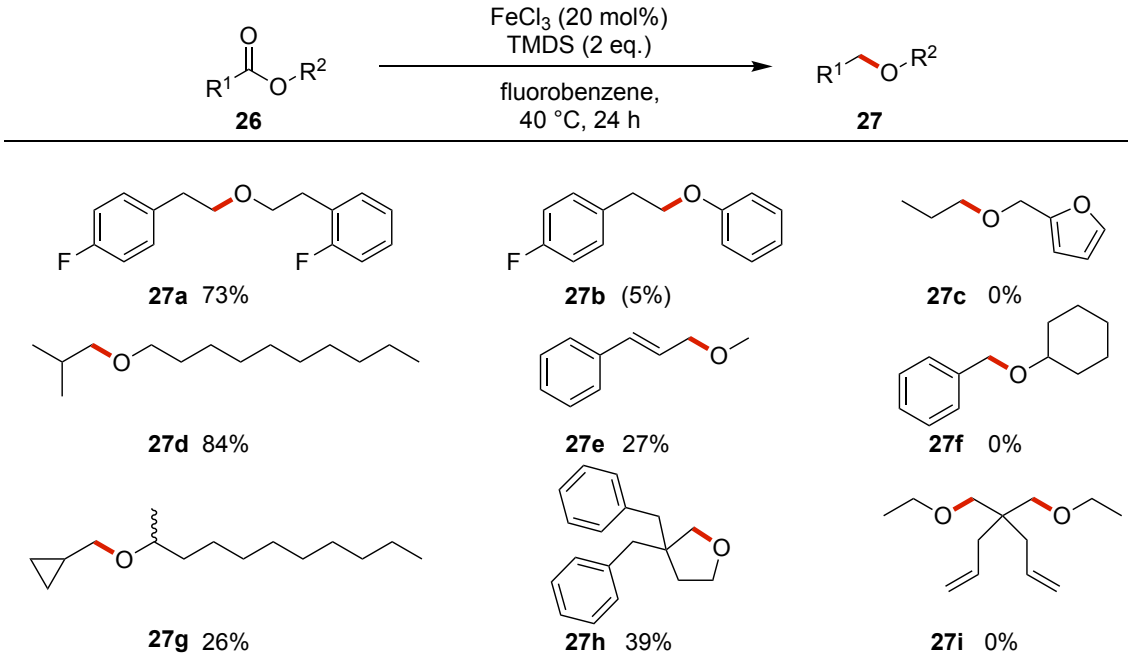

Scheme 30. *General conditions and substrate scope for ester reduction.*

Other esters could indeed be reduced with this method. Furthermore, unfunctionalized ester decyl isobutyrate **27d** gave greater reactivity than the model substrate, forming the unsymmetrical ether **27d** in 84% yield without the formation of any side products. However, although sterically hindered lactone **26h** could also be reduced without the observable formation of by-products, the yield was just 39%. From previous procedures, phenol and benzoic acid derived esters **26b** and **26f** were known to be challenging substrates[59,67] and when these were subjected to the reaction conditions poor yields were observed. The attempted reduction of **26f** resulted in mainly starting material with a few small unidentified impurities. Similarly, phenyl ester **26b**, was largely unreacted however a small number of new species were visible by ^{19}F NMR peaks. The largest of these, accounting for 5% of

the total integral, was found to match the desired product, **27b**, which was independently synthesised using the Olofsson group's alcohol arylation (Scheme 31B).[93]

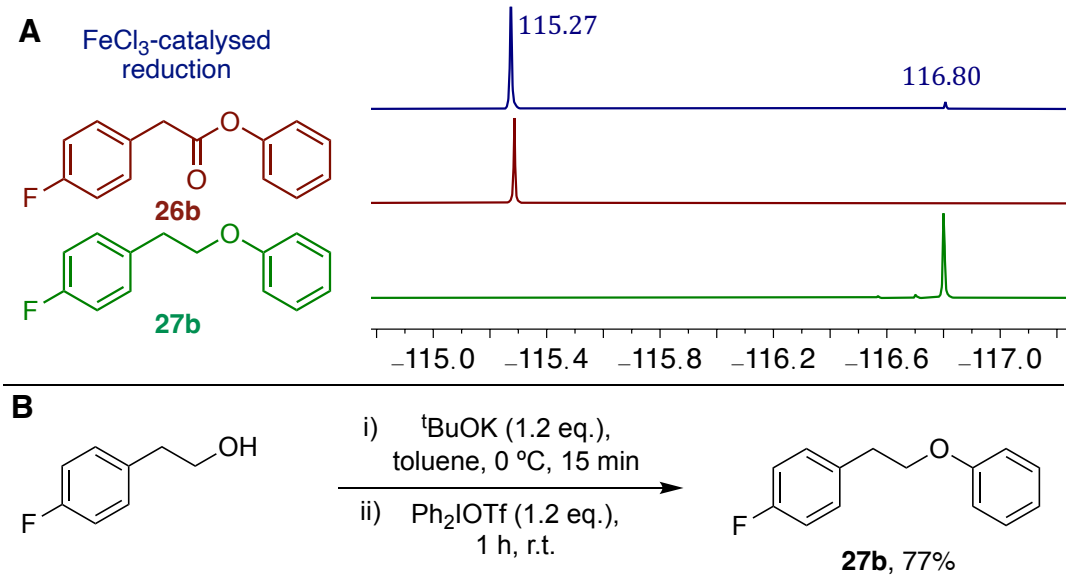

Scheme 31. *Reduction of a phenol ester;* ***(A)*** *Crude reaction* ^{19}F *NMR compared with isolated starting material and product;* ***(B)*** *Synthesis of aryl ether* ***27b****.*

As $FeCl_3$ is a moderately strong Lewis acid, sensitive substrates can undergo side reactions. Furfuryl propionate **26c** for example formed propionic acid in the crude reaction mixtures, presumably from a Lewis acid catalysed elimination (Scheme 32). Several aromatic 2-methyl furfuryl derivatives also seemed to be visible but were not isolated. Additionally, despite the structural similarities of **26d** to **26g**, the more branched substrate gave a much poorer yield. It is believed the reason for this is steric rather than suggestive of a radical process as, by NMR spectroscopy, alkenes were not observed, and the starting material was still the largest component.

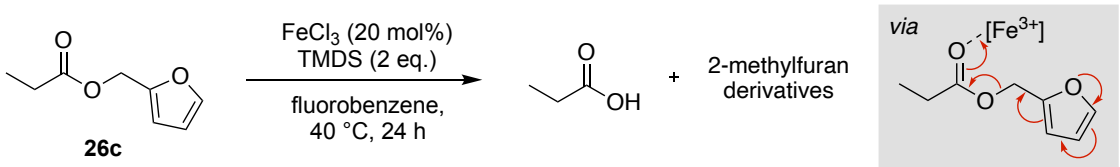

Scheme 32. *The attempted reduction of furfuryl propionate, yielding propionic acid and 2-methyl furan derivatives form a Lewis acid catalysed elimination.*

The selectivity of the reaction for 1,2-reduction over 1,4-reduction was also examined using methyl cinnamate **26e** (Scheme 33). Under the developed conditions two main products were observed: cinnamyl methyl ether **27e** (27 %)

and 1-indanole **28** (28 %). The first comes from the expected 1,2 reduction whereas **28** presumably comes from a 1,4-reduction, followed by a Friedel-Crafts-like intramolecular electrophilic aromatic substitution.

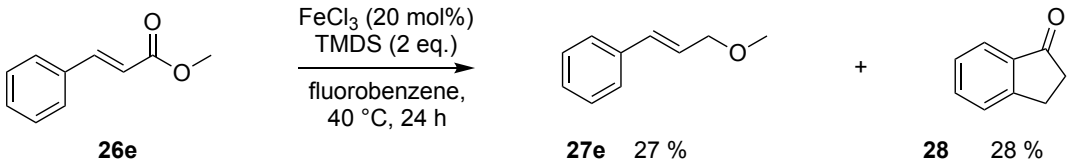

Scheme 33. *The reduction of methyl cinnamate giving cinnamyl methyl ether and 1-indanone with in their respective yields.*

2.3.4 Reductive *O*-Alkylation using $FeCl_3$-catalysis

Although the Fischer esterification is already a well understood reaction the use of catalytic iron trichloride was investigated with the intention of developing a one pot reductive esterification. In a previous report[88] on the esterification of long chain acids with stoichiometric alcohols showed it was found that just 0.5 mol% $FeCl_3 \cdot 6H_2O$ could catalyse the complete conversion to an ester in 24 hours in refluxing *m*-xylene.

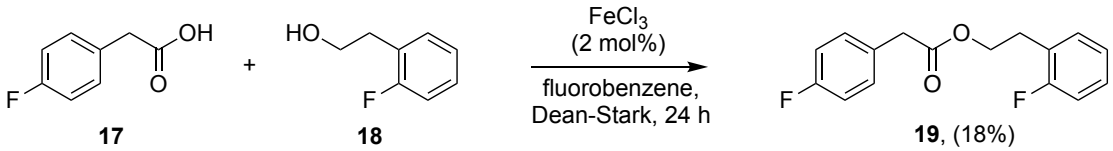

Scheme 34*. The desired Fischer esterification reaction with model reactants.*

Recognising that the same temperatures could not be replicated in fluorobenzene, the catalyst loading was increased to 2 mol% and the reaction was repeated for esterification of the model substrates. Using the same reaction concentrations as for ester reduction, only 18% conversion to the desired ester was obtained after refluxing overnight with a Dean-Stark trap.

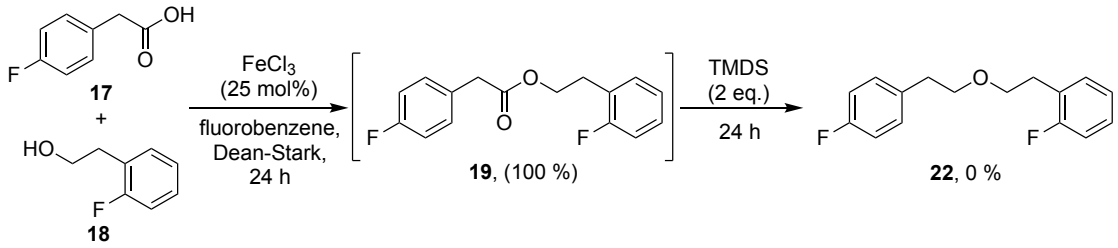

Scheme 35. *An attempted one-pot esterification and reduction, giving clean formation of the intermediate ester but no ether.*

After discovering that large loadings of iron trichloride was essential for an efficient and high yielding reduction, the esterification was repeated at a higher concentration. Using 25 mol% of iron, after leaving for 24 hours the reaction reached completion by ^{19}F NMR. Regrettably, after dilution with fresh fluorobenzene and addition of TMDS, precipitation occurred quickly without formation of any ether. It is likely that the iron trichloride did not survive the esterification, as prior to the addition of silane the reaction mixture was black with a metallic-looking precipitate.

Catalyst	Loading /mol%	Concentration /mol.dm^{-3}	Time /h	NMR yield /%
$FeCl_3$	2	0.40	19.5	18
-	-	0.72	24.0	14
$FeCl_3$	5	0.72	24.0	68
$FeCl_3{\cdot}6H_2O$	5	0.72	24.0	83
H_2SO_4	5	0.72	24.0	19
HCl	5	0.72	24.0	15
p-TsOH	5	0.72	24.0	98
TfOH	5	0.72	24.0	98

Table 9. *Screen of acids for the Fischer esterification of the model substrates, including catalyst loading, concentration, and reaction time.*

Following this, a short screen was performed to compare iron trichloride to Brønsted acid catalysis (Table 9). HCl or H_2SO_4 gave only minor rate increases over the uncatalyzed esterification. Iron trichloride was a much more active, especially the hexahydrate which furnished an 83% NMR yield in 24 hours. However, sulfonic acids proved better still, each giving a 98% NMR yield under the same reaction conditions.

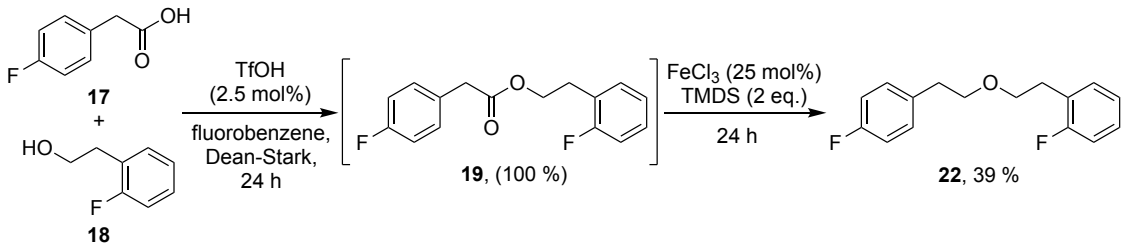

Scheme 36. *A second attempted reductive O-alkylation with triflic acid.*

As the reaction was known to be tolerant of triflic acid, the telescoped esterification-reduction was repeated with a 2.5 mol% loading of the acid. After 24 hours with a Dean-Stark trap the esterification cleanly yielded the ester with < 2% of excess acid, excess alcohol, or any other impurities. Encouragingly, following the addition of $FeCl_3$ the reaction appeared similar in appearance to using the preformed ester, however, after 24 hours the NMR conversion was only 44%, and only 39% of product was isolated (Scheme 36).

2.3.6 Investigations Towards a Reductive Baeyer-Villiger Reaction

To find another application for the reductive etherification, other disconnections for ester syntheses were considered. The Baeyer-Villiger reaction stood out as an interesting example, as it too operates under acidic conditions, but rather than joining two fragments, an oxygen atom is inserted into a carbon-carbon bond during the oxidative rearrangement of a ketone. Coupling this with a reductive etherification would amount to a novel reductive oxygen insertion which may be particularly useful in the synthesis of cyclic ethers. However, it was immediately clear that classical conditions, which use super-stoichiometric mCPBA, would not be tolerated with either the $FeCl_3$ or $InBr_3$ catalysed reduction due to the formation of stoichiometric mCPBA as a by-product (see 3.3.3 additives).

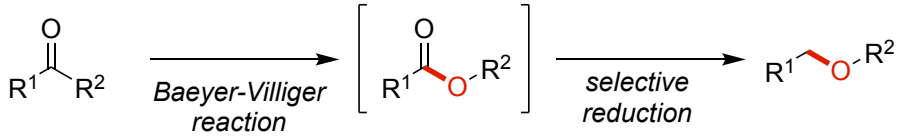

Scheme 37. *Proposed sequence for a reductive Baeyer-Villiger reaction, overall giving a reductive oxygen insertion.*

Optimistically, $FeCl_3$, $InBr_3$, and $BF_3{\cdot}OEt_3$ were screened as Lewis acid catalysts in the Baeyer-Villiger reaction for 4-fluoroacetophenone with an anhydrous source of

hydrogen peroxide (Table 10). Unfortunately, the Lewis acids did not give any conversion and visually seemed to catalyse the decomposition of the hydrogen peroxide into gaseous oxygen. Contrasting that with established procedures, use of stoichiometric TFAA to activate the hydrogen peroxide resulted in a conversion of 86%.

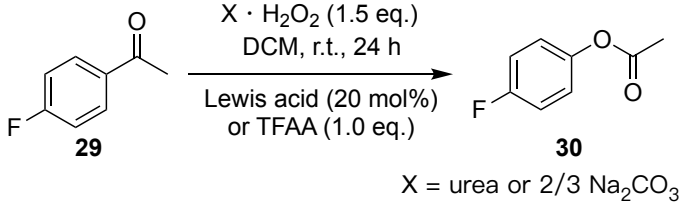

Activating Agent	NMR Yield /%	
	UHP	sodium percarbonate
$InBr_3$	0	0
$FeCl_3$	0	0
$BF_3{\cdot}OEt_2$	0	0
TFAA	86	0

Table 10. Use of ester reduction catalysts to try and catalyse a Baeyer-Villiger reaction compared to activation of hydrogen peroxide with stoichiometric TFAA.

Next, more conventional Baeyer-Villiger reactions were explored to see if the reaction could be done using complementary conditions to ester reduction. In order be tolerated with the silane and Lewis acid, the reaction conditions would need to; i) give very high conversions, ii) used near stoichiometric and anhydrous oxidising agents and iii) give poorly nucleophilic by-products.

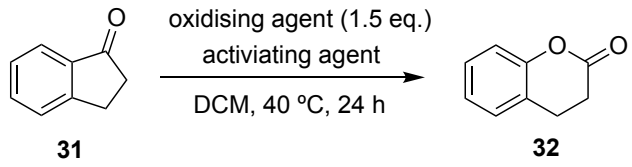

Oxidising Agent	Activating Agent	NMR Yield /%
UHP	Tf_2O	56
	Ms_2O	0
	TFAA	40
sodium percarbonate	Tf_2O	0
	Ms_2O	0
	TFAA	76
oxone®	TfOH	22

***Table 11**. A screen of activating agents and peroxide sources to try and find a high yield and compatible Baeyer-Viliger reaction.*

Three different oxidising agents; urea hydrogen peroxide (UHP), sodium percarbonate and oxone were trialled on the Baeyer-Villiger oxidation of 1-indanone, **31**. Hydrogen peroxide sources were activated with stoichiometric anhydrides whereas oxone was protonated by the addition of triflic acid. However, even with 1.5 equivalents of the peroxide, high yields could not be obtained (Table 11). The greatest yield was obtained using sodium percarbonate and TFAA, which generates 3 equivalents of trifluoroacetic acid and 2 equivalents of sodium

trifluoroacetate as by-products. As well as being inefficient, these have non-negligible nucleophilicity which would likely interfere with the ester reduction. Furthermore, increased quantities of reagent would be needed improve yields. These results cast doubt on whether the development of a telescoped procedure would be prudent, given that high yields can already be obtained for the individual reactions in discrete steps.

2.4 Conclusions

Reducing an ester to an ether remains a hugely difficult reaction. Not many Lewis acids are powerful enough to catalyse this unusual transformation and fewer still can perform this reaction efficiently and selectivity. In this project a novel ester reduction has been discovered using iron trichloride as an earth abundant metal catalyst. The main advantage of this process is that iron trichloride is an inexpensive catalyst; being around 20 times cheaper than the tetramethyldisiloxane, which itself is an industrial by-product. Additionally, although iron trichloride is harmful due to its acidity, iron is much less toxic than heavier metals like indium; making the reaction safer to run and requiring with fewer regulatory controls of metal impurities at scale.

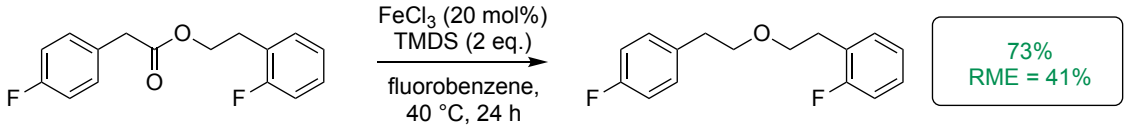

***Scheme 38**. General conditions for the developed ester reduction with the yield for the model substrate and its reaction mass efficiency.*

However, challenges remain. Despite optimisation of the reaction, it remains dependent on halogenated solvents and dilute conditions. Additionally, as the reaction progresses, a precipitate brings the iron out of solution meaning relatively high catalytic loadings (20 mol%) are required for good yields. Whilst this methodology works well for simple linear substrates there does not seem to be any additional substrate scope over existing reactions, giving reduced yields for sterically hindered substrates and side reactions for acid-sensitive substrates.

The application of this methodology into a tandem reductive etherification was also investigated. Initial reactions used iron trichloride as a catalyst for both processes, however although it could catalyse the Fischer esterification, degradation of the catalyst inhibited the subsequent ester reduction. A triflic acid-catalysed esterification was found to be more robust and could be incorporated into a one-pot reaction, albeit with reduced yields compared to the isolated reaction. Overall these lower yields and increased practical difficulties are a significant disadvantage when compared to single step procedures such as the Sakai group's reductive esterification.[72]

To overcome the current limitations, it may be valuable to interrogate the reaction mechanism in more detail. It has been noted that the dependence on a halogenated solvent is reminiscent of the Schindler group's $FeCl_3$-catalysed carbonyl-olefin metathesis for aliphatic ketones (Scheme 39).[94] In this case, reaction kinetics, IR spectroscopy and a DFT study was used to assign catalytic activity to a Fe_2Cl_6 homodimer superelectrophile.[95] A similar study for ester hydrolysation could be used to investigate the species in solution and the catalyst degradation pathway.

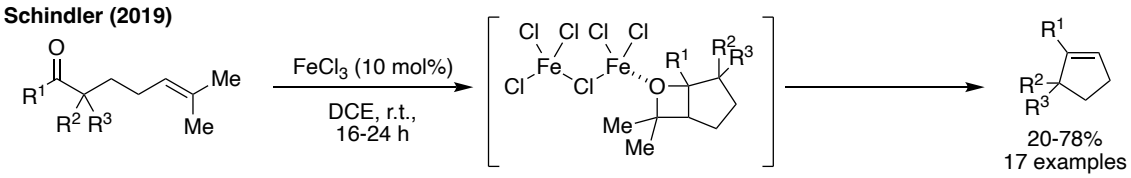

Scheme 39. *$FeCl_3$-catalysed carbonyl-olefin metathesis in which the active complex is a Fe_2Cl_6 homodimer.*

A second study could fully elaborate the substrate scope of the reaction. Thus far only 9 substrates have been exposed to the reaction and highly variable yields have been obtained (5 – 84%). From an investigation of additional substrates and identification of trends, the scope of the methodology could be more accurately defined. This may reveal instances in which the $FeCl_3$-catalysed ester hydrosilylation could be synthetically advantageous.

2.5 References

1 Y. Li, C. Topf, X. Cui, K. Junge and M. Beller, *Angew. Chem. Int. Ed.*, 2015, **54**, 5196–5200.
2 S. D. Roughley and A. M. Jordan, *J. Med. Chem.*, 2011, **54**, 3451–3479.
3 A. E. Tron, M. A. Belmonte, A. Adam, B. M. Aquila, L. H. Boise, E. Chiarparin, J. Cidado, K. J. Embrey, E. Gangl, F. D. Gibbons, G. P. Gregory, D. Hargreaves, J. A. Hendricks, J. W. Johannes, R. W. Johnstone, S. L. Kazmirski, J. G. Kettle, M. L. Lamb, S. M. Matulis, A. K. Nooka, M. J. Packer, B. Peng, P. B. Rawlins, D. W. Robbins, A. G. Schuller, N. Su, W. Yang, Q. Ye, X. Zheng, J. P. Secrist, E. A. Clark, D. M. Wilson, S. E. Fawell and A. W. Hird, *Nat. Commun.*, 2018, **9**, 5341.
4 N. A. McGrath, M. Brichacek and J. T. Njardarson, *J. Chem. Educ.*, 2010, **87**, 1348–1349.
5 A. Liu, W. Yu, M. Liu, J. Bai, W. Liu, X. Liu, H. Pei, L. Hu, M. Huang and X. Wang, *J. Agric. Food Chem.*, 2015, **63**, 7469–7475.
6 J. S. Carey, D. Laffan, C. Thomson and M. T. Williams, *Org. Biomol. Chem.*, 2006, **4**, 2337–2347.
7 D. J. C. Constable, P. J. Dunn, J. D. Hayler, G. R. Humphrey, J. L. Leazer, Jr., R. J. Linderman, K. Lorenz, J. Manley, B. A. Pearlman, A. Wells, A. Zaks and T. Y. Zhang, *Green Chem.*, 2007, **9**, 411–420.
8 A. Williamson, *London, Edinburgh, Dublin Philos. Mag. J. Sci.*, 1850, **37**, 350–356.
9 N. Schneider, D. M. Lowe, R. A. Sayle, M. A. Tarselli and G. A. Landrum, *J. Med. Chem.*, 2016, **59**, 4385–4402.
10 D. Prat, A. Wells, J. Hayler, H. Sneddon, C. R. McElroy, S. Abou-Shehada and P. J. Dunn, *Green Chem.*, 2016, **18**, 288–296.
11 M. Krupa, M. Chodyński, A. Ostaszewska, P. Cmoch and I. Dams, *Molecules*, 2017, **22**, 217.
12 D. J. C. Constable, A. D. Curzons and V. L. Cunningham, *Green Chem.*, 2002, **4**, 521–527.
13 O. Mitsunobu, M. Yamada and T. Mukaiyama, *Bull. Chem. Soc. Jpn.*, 1967, **40**, 935–939.
14 O. Mitsunobu, *Synth.*, 1981, **01**, 1–28.
15 Y. J. Shi, D. L. Hughes and J. M. McNamara, *Tetrahedron Lett.*, 2003, **44**, 3609–3611.
16 T. Shintou and T. Mukaiyama, *J. Am. Chem. Soc.*, 2004, **126**, 7359–7367.
17 S. Fletcher, *Org. Chem. Front.*, 2015, **2**, 739–752.
18 K. C. K. Swamy, N. N. B. Kumar, E. Balaraman and K. V. P. P. Kumar, *Chem. Rev.*, 2009, 2551–2651.
19 R. H. Beddoe, K. G. Andrews, V. Magné, J. D. Cuthbertson, J. Saska, A. L. Shannon-Little, S. E. Shanahan, H. F. Sneddon and R. M. Denton, *Science*, 2019, **365**, 910–914.
20 F. Ullmann and P. Sponagel, *Ber. Dtsch. Chem. Ges.*, 1905, **38**, 2211–2212.
21 J. F. Marcoux, S. Doye and S. L. Buchwald, *J. Am. Chem. Soc.*, 1997, **119**, 10539–10540.
22 R. K. Gujadhur, C. G. Bates and D. Venkataraman, *Org. Lett.*, 2001, **3**, 4315–4317.
23 M. Wolter, G. Nordmann, G. E. Job and S. L. Buchwald, *Org. Lett.*, 2002, **4**, 973–976.
24 C. Lee and R. Matunas, *Compr. Organomet. Chem. III*, 2007, 649–693.
25 K. Keerthi Krishnan, S. M. Ujwaldev, K. S. Sindhu and G. Anilkumar, *Tetrahedron*, 2016, **72**, 7394–7407.
26 S. V. Ley and A. W. Thomas, *Angew. Chem. Int. Ed.*, 2003, **42**, 5400–5449.
27 J. C. Vantourout, R. P. Law, A. Isidro-Llobet, S. J. Atkinson and A. J. B. Watson, *J. Org. Chem.*, 2016, **81**, 3942–3950.
28 D. M. T. Chan, K. L. Monaco, R. P. Wang and M. P. Winters, *Tetrahedron Lett.*, 1998, **39**, 2933–2936.
29 P. Y. S. Lam, C. G. Clark, S. Saubern, J. Adams, M. P. Winters, D. M. T. Chan and A. Combs, *Tetrahedron Lett.*, 1998, **39**, 2941–2944.
30 D. M. T. Chan, K. L. Monaco, R. Li, D. Bonne, C. G. Clark and P. Y. S. Lam, *Tetrahedron Lett.*, 2003, **44**, 3863–3865.
31 D. A. Evans, J. L. Katz and T. R. West, *Tetrahedron Lett.*, 1998, **39**, 2937–2940.
32 P. Y. S. Lam, G. Vincent, C. G. Clark, S. Deudon and P. K. Jadhav, *Tetrahedron Lett.*, 2001, **42**, 3415–3418.
33 P. Y. S. Lam, G. Vincent, D. Bonne and C. G. Clark, *Tetrahedron Lett.*, 2003, **44**, 4927–4931.
34 J. C. Vantourout, H. N. Miras, A. Isidro-Llobet, S. Sproules and A. J. B. Watson, *J. Am. Chem. Soc.*, 2017, **139**, 4769–4779.
35 J. Tsuji and K. Ohno, *Tetrahedron Lett.*, 1965, **6**, 3969–3971.
36 B. M. Trost and T. J. Fullerton, *J. Am. Chem. Soc.*, 1973, **95**, 292–294.
37 K. E. Atkins, W. E. Walker and R. M. Manyik, *Tetrahedron Lett.*, 1970, **11**, 3821–3824.

38 G. Hata, K. Takahashi and A. Miyake, *Chem. Commun.*, 1970, **2**, 1392–1393.
39 T. Satoh, M. Ikeda and M. Miura, *J. Am. Chem. Soc.*, 1997, **62**, 4877.
40 Y. Kayaki, T. Koda and T. Ikariya, *J. Org. Chem.*, 2004, **69**, 2595–2597.
41 C. Frost, J. Howarth and J. Williams, *Tetrahedron: Asymmetry*, 1992, **3**, 1089–1122.
42 R. S. Babu and G. A. O'Doherty, *J. Am. Chem. Soc.*, 2003, **125**, 12406–12407.
43 J. Muzart, *Tetrahedron*, 2005, **61**, 5955–6008.
44 B. M. Trost and M. L. Crawley, *Chem. Rev.*, 2003, **103**, 2921–2943.
45 B. M. Trost, M. R. Machacek and A. Aponick, *Acc. Chem. Res.*, 2006, **39**, 747–760.
46 A. Aranyos, D. W. Old, A. Kiyomori, J. P. Wolfe, J. P. Sadighi and S. L. Buchwald, *J. Am. Chem. Soc.*, 1999, **121**, 4369–4378.
47 S. I. Kuwabe, K. E. Torraca and S. L. Buchwald, *J. Am. Chem. Soc.*, 2001, **123**, 12202–12206.
48 K. E. Torraca, S. I. Kuwabe and S. L. Buchwald, *J. Am. Chem. Soc.*, 2000, **122**, 12907–12908.
49 M. C. Willis, D. Taylor and A. T. Gillmore, *Chem. Commun.* , 2003, 2222–3.
50 K. E. Torraca, X. Huang, C. A. Parrish and S. L. Buchwald, *J. Am. Chem. Soc.*, 2001, **123**, 10770–10771.
51 C. A. Parrish and S. L. Buchwald, *J. Org. Chem.*, 2001, **66**, 2498–2500.
52 C. W. Cheung and S. L. Buchwald, *Org. Lett.*, 2013, **15**, 3998–4001.
53 A. V. Vorogushin, X. Huang and S. L. Buchwald, *J. Am. Chem. Soc.*, 2005, **127**, 8146–8149.
54 C. H. Burgos, T. E. Barder, X. Huang and S. L. Buchwald, *Angew. Chem. Int. Ed.*, 2006, **45**, 4321–4326.
55 Z. Mao, B. T. Gregg and A. R. Cutler, *J. Am. Chem. Soc.*, 1995, **117**, 10139–10140.
56 S. C. Berk and S. L. Buchwald, *J. Org. Chem.*, 1992, **57**, 3751–3753.
57 K. J. Barr, S. C. Berk and S. L. Buchwald, *J. Org. Chem.*, 1994, **59**, 4323–4326.
58 M. Yato, K. Homma and A. Ishida, *Tetrahedron*, 2001, **57**, 5353–5359.
59 S. Das, Y. Li, K. Junge and M. Beller, *Chem. Commun.*, 2012, **48**, 10742–10744.
60 H. Tsutsumi, Y. Sunada and H. Nagashima, *Chem. Commun.* , 2011, **47**, 6581–6583.
61 J. Deng, *Synlett*, 2011, 2102–2103.
62 R. Wildermuth, E., Stark, H., Friedrich, G., Ebenhöch, F. L., Kühborth, B., Silver, J. and Rituper, in *Inorganic Syntheses*, John Wiley & Sons, Inc., 2000, pp. 46–48.
63 U. Biermann and J. O. Metzger, *ChemSusChem*, 2014, **7**, 644–649.
64 M. Yasuda, Y. Onishi, M. Ueba, T. Miyai and A. Baba, *J. Org. Chem.*, 2001, **66**, 7741–7744.
65 N. Sakai, T. Moriya and T. Konakahara, *J. Org. Chem.*, 2007, **72**, 5920–5922.
66 N. Sakai, T. Moriya, K. Fujii and T. Konakahara, *Synth.*, 2008, **2008**, 3533–3536.
67 N. Sakai, Y. Usui, T. Moriya, R. Ikeda and T. Konakahara, *Eur. J. Org. Chem.*, 2012, 4603–4608.
68 Synthesis search done by comparing results for "synthesis of carboxlic acids" to "synthesis of alcohols" on the Reaxys® chemical database, https://new.reaxys.com 30/03/22. 24,511 reactions for carboxylic acids compared to 10,658 for alcohols. Commercial search done by comparing results for "carboxylic acid" to "alcohol" on the Sigma-Aldrich® catalogue search, https://www.sigmaaldrich.com/catalog/AdvancedSearchPage.do 30/03/22. 8,260 matches for carboxylic acids compared to 4,484 for alcohols.
69 N. Sakai, T. Nakajima, S. Yoneda, T. Konakahara and Y. Ogiwara, *J. Org. Chem.*, 2014, **79**, 10619–10623.
70 T. Moriya, S. Yoneda, K. Kawana, R. Ikeda, T. Konakahara and N. Sakai, *J. Org. Chem.*, 2013, **78**, 10642–10650.
71 N. Sakai, T. Miyazaki, T. Sakamoto, T. Yatsuda, T. Moriya, R. Ikeda and T. Konakahara, *Org. Lett.*, 2012, **14**, 4366–4369.
72 N. Sakai, Y. Usui, R. Ikeda and T. Konakahara, *Adv. Synth. Catal.*, 2011, **353**, 3397–3401.
73 K. G. Andrews, D. M. Summers, L. J. Donnelly and R. M. Denton, *Chem. Commun.*, 2016, **52**, 1855–1858.
74 E. L. Stoll, T. Tongue, K. G. Andrews, D. Valette, D. J. Hirst and R. M. Denton, *Chem. Sci.*, 2020, **11**, 9494–9500.
75 L. Sytchenko, 2018.
76 C. Hansch, A. Leo and R. W. Taft, *Chem. Rev.*, 1991, **91**, 165–195.
77 Y. Takeda, K. Narita and T. Katoh, *Eur. J. Org. Chem.*, 2017, **2017**, 901–907.
78 C. Cheng and M. Brookhart, *Angew. Chem. Int. Ed.*, 2012, **51**, 9422–9424.
79 N. A. Morra and B. L. Pagenkopf, *Synth.*, 2008, 511–514.
80 D. Addis, S. Das, K. Junge and M. Beller, *Angew. Chem. Int. Ed.*, 2011, **50**, 6004–6011.
81 S. Hanada, Y. Motoyama and H. Nagashima, *Tetrahedron Lett.*, 2006, **47**, 6173–6177.
82 S. Hanada, T. Ishida, Y. Motoyama and H. Nagashima, *J. Org. Chem.*, 2007, **72**, 7551–7559.

83 S. Hanada, E. Tsutsumi, Y. Motoyama and H. Nagashima, *J. Am. Chem. Soc.*, 2009, **131**, 15032–15040.
84 S. Das, D. Addis, K. Junge and M. Beller, *Chem. Eur. J.*, 2011, **17**, 12186–12192.
85 D. J. Parks and W. E. Piers, *J. Am. Chem. Soc.*, 1996, **118**, 9440–9441.
86 D. J. Parks, J. M. Blackwell and W. E. Piers, *J. Org. Chem.*, 2000, **65**, 3090–3098.
87 N. N. Greenwood and A. Earnshaw, *Chemistry of the Elements*, Pergamon Press, 1st edn., 1986.
88 N. Ieda, K. Mantri, Y. Miyata, A. Ozaki, K. Komura and Y. Sugi, *Ind. Eng. Chem. Res.*, 2008, **47**, 8631–8638.
89 J. Pesti and G. L. Larson, *Org. Process Res. Dev.*, 2016, **20**, 1164–1181.
90 C. M. Alder, J. D. Hayler, R. K. Henderson, A. M. Redman, L. Shukla, L. E. Shuster and H. F. Sneddon, *Green Chem.*, 2016, **18**, 3879–3890.
91 L. J. Diorazio, D. R. J. Hose and N. K. Adlington, *Org. Process Res. Dev.*, 2016, **20**, 760–773.
92 S. Thaisrivongs, D. T. Pals, S. R. Turner and L. T. Kroll, *J. Med. Chem.*, 1988, **31**, 1369–1376.
93 R. Ghosh, E. Lindstedt, N. Jalalian and B. Olofsson, *ChemistryOpen*, 2014, **3**, 54–57.
94 J. R. Ludwig, P. M. Zimmerman, J. B. Gianino and C. S. Schindler, *Nature*, 2016, **533**, 374–379.
95 H. Albright, P. S. Riehl, C. C. McAtee, J. P. Reid, J. R. Ludwig, L. A. Karp, P. M. Zimmerman, M. S. Sigman and C. S. Schindler, *J. Am. Chem. Soc.*, 2019, **141**, 1690–1700.

2.6 Experimental

2.6.1 General Reaction Information

Reagents and technical grade solvents were purchased from commercial suppliers and used without further purification. Petrol refers to 40-60 petroleum ether. Unless otherwise stated, all DCM was dried by either by passing over two columns of activated alumina, or by distillation from calcium hydride onto 4 Å molecular sieves. All toluene was dried by passing over two columns of activated alumina then stored over sodium wire. All fluorobenzene was dried by distillation from calcium hydride onto 4 Å molecular sieves. All water was deionised before use. Cobalt (II) bromide was dried by heating to > 130 °C under vacuum. Unless stated, all reactions were performed under an argon balloon of flow of nitrogen. Unless stated, all reactions were carried out in conventional oven-dried glassware. 'Room temperature' indicates temperatures between 15 °C and 25°C.

2.6.2 General Analysis and Characterisation Information

Thin Layer Chromatography (TLC) was performed on Polgram SIL G/UV254 silica-aluminium plates and visualized either with ultraviolet (UV) irradiation (254 nm) or potassium permanganate staining. Column chromatography was carried out according to Still's method, using Fluorochem silica gel 60 Å (40-63 mesh). All NMR spectra were recorded on either a Bruker AV 400 or 3400 and are internally referenced to residual solvent signals ($CDCl_3$ is referenced at δ 7.26 and 77.0 for ^1H and ^{13}C NMR respectively; DMSO-d_6 is referenced to δ 2.50 and 39.52 for ^1H and ^{13}C NMR respectively). All NMR chemical shifts (δ) were reported in parts per million (ppm) and coupling constants (J) are given in Hertz (Hz). The ^1H NMR spectra are reported as follows: δ (multiplicity, coupling constant J, number of protons, atom assignment). Fourier Transform Infrared Spectrometry (FTIR) was carried out using a Bruker Tensor 27 using an Attenuated Total Reflection (ATR) attachment and peaks are reported in terms of frequency of absorption (cm^{-1}). High Resolution Mass Spectrometry (HRMS) was measured on a Bruker microTOF II with Electron Spray Ionisation (ESI) or a JEOL AccuTOF GCX with Electron Ionisation (EI). Melting

points were measured using a Stuart SMP3. Specific rotations $[\alpha]_D$ were measured using an Anton Paar MCP 100 Modular Circular Polarimeter using a 100 mm cell.

2.6.3 Synthesis of Analytical Standards

2-Fluorophenethyl 2-(4-fluorophenyl)acetate (19)

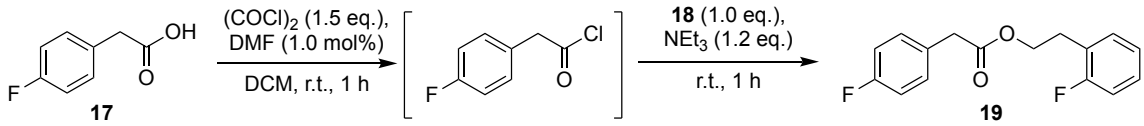

To a solution of 2-(4-fluorophenyl)acetic acid (**17**) (5.01 g, 32.5 mmol) in DCM (40.0 mL) was added DMF (25.0 µL, 325 µmol). Oxalyl chloride (4.12 mL, 49.7 mmol) was then added dropwise over 20 minutes and the exothermic reaction was left for a further hour by which time the vigorous effervescence had ceased. The reaction mixture was then concentrated *in vacuo* to remove excess oxalyl chloride. The crude acyl chloride was redissolved in DCM (40.0 mL) and 2-(2-fluorophenyl)ethan-1-ol (**18**) (4.35 mL, 32.4 mmol) was added. The solution was left to stir for 1 hour, cooled to 0 °C, and neutralised by the dropwise addition of NEt_3 (5.40 mL, 38.9 mmol) over 10 minutes. The organic phase was then washed with water (40 mL), NaOH (40 mL of a 0.50 M aqueous solution) and HCl (40 mL of a 1.0 M aqueous solution), dried over anhydrous $MgSO_4$ and concentrated *in vacuo*. The crude residue was purified using flash column chromatography (15% Et_2O in petrol; 0.46) to give a clear colourless oil (8.17 g, 29.5 mmol, 91%).

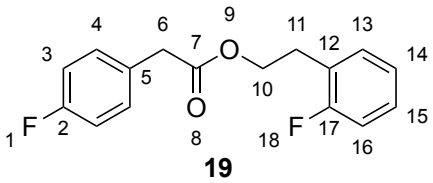

19

^{1}H NMR (400 MHz, $CDCl_3$) δ 7.30 – 7.17 (m, 3H, H-4, H-15), 7.16 – 7.10 (m, 1H, H-13), 7.09 – 6.96 (m, 4H, H-3, H-14, H-16), 4.34 (t, *J* = 6.8 Hz, 2H, H-10), 3.58 (s, 2H, H-6), 2.99 (t, *J* = 6.8 Hz, 2H, H-11); **^{13}C{^{1}H} NMR** (101 MHz, $CDCl_3$) δ 171.3 (C-7), 162.0 (d, *J* = 245.3 Hz, C-2), 161.3 (d, *J* = 245.4 Hz, C-17), 131.2 (d, *J* = 4.7 Hz, C-13), 130.9 (d, *J* = 8.1 Hz, C-4), 129.6 (d, *J* = 3.2 Hz, C-5), 128.4 (d, *J* = 8.1 Hz, C-15), 124.6 (d, *J* = 15.9 Hz, C-12), 124.0 (d, *J* = 3.5 Hz, C-14), 115.4 (d, *J* = 21.4 Hz, C-3), 115.3 (d, *J* = 22.0

Hz, C-16), 64.1 (d, *J* = 1.5 Hz, C-10), 40.5 (C-6), 28.5 (d, *J* = 2.3 Hz, C-11); **^{19}F NMR** (376 MHz, $CDCl_3$) δ -115.83 (tt, *J* = 8.8, 5.3 Hz, F-1), -118.39 (m, F-18). **FTIR** (neat) ν_{max} /cm^{-1} 3046, 2963, 1733, 1606, 1586, 1509, 1493, 1456, 1420; **HRMS** (ESI) *m/z* calc'd for $C_{16}H_{14}O_2F_2Na$ $[M+Na]^+$: 299.0854, found: 299.0846.

2-(4-Fluorophenyl)ethan-1-ol (20)

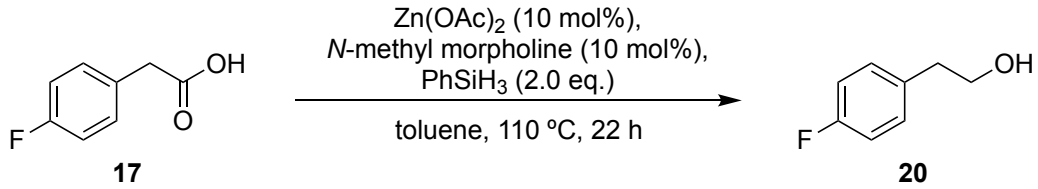

Synthesised using an adapted literature procedure.[1] To a suspension of 2-(4-fluorophenyl)acetic acid (**17**) (600 mg, 3.89 mmol) and $Zn(OAc)_2$ (71.4 mg, 389 μmol) in toluene (4.00 mL), 4-methylmorpholine (43.0 μL, 0.389 mmol) and phenylsilane (960 μL, 7.78 mmol) were added and the mixture was heated to 110 °C. After 22 hours, the black reaction mixture was cooled to room temperature and quenched with NaOH (2.0 mL of a 2.0 M aqueous solution). After stirring for 20 minutes, the solution was neutralised with HCl (1.0 M) and diluted with EtOAc (5.0 mL) and water (10 mL). The phases were separated, extracting the organic with additional water (10 mL) and the aqueous with EtOAc (2 x 10 mL). The combined organic phases were then dried over anhydrous $MgSO_4$ and concentrated *in vacuo*. The crude residue was purified by flash column chromatography (25% EtOAc in petrol; R_f 0.26) to give a colourless oil (237 mg, 1.69 mmol, 43%).

^{1}H NMR (400 MHz, $CDCl_3$) δ 7.25 – 7.13 (m, 2H, Ar*H*), 7.10 – 6.95 (m, 2H, Ar*H*), 3.85 (td, *J* = 6.6, 0.8 Hz, 2H, C*H*$_2$OH), 2.86 (t, *J* = 6.6 Hz, 2H, C*H*$_2$CH$_2$OH), 1.60 (br. s, 1H, O*H*); **^{13}C{^{1}H} NMR** (101 MHz, $CDCl_3$) δ 161.8 (d, *J* = 244.2 Hz, C_q), 134.3 (d, *J* = 3.3 Hz, C_q), 130.5 (d, *J* = 8.0 Hz, CH), 115.5 (d, *J* = 21.2 Hz, CH), 63.7 (CH_2), 38.4 (CH_2); **^{19}F NMR** (376 MHz, $CDCl_3$) δ -116.78 – -116.89 (m); **FTIR** (neat) ν_{max} /cm^{-1} 3336 (br.), 2941, 2877, 1601, 1476, 1435, 1416; **GC-HRMS** (EI) *m/z* calc'd for C_8H_9OF $[M]^+$: 140.0632, found: 140.0638. Data are consistent with literature.[2]

2-(4-Fluorophenyl)acetaldehyde (21)

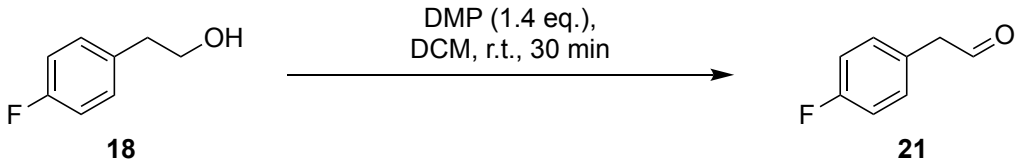

18 **21**

Synthesised using an adapted literature procedure.[3] To a solution of 2-(4-fluorophenyl)ethanol (**18**) (100 mg, 0.71 mmol) in DCM (5.00 mL) was added Dess-Martin periodinane (606 mg, 1.40 mmol) and the cloudy mixture was stirred at room temperature. After 30 minutes, the reaction was quenched with $Na_2S_2O_3$ (5.0 mL of a saturated aqueous solution) and diluted with $CHCl_3$ (10 mL). The organic phase was washed with brine (2 x 10 mL) and the aqueous phase was washed with chloroform (2 x 10 mL). The combined organic phases were then dried over anhydrous $MgSO_4$ and concentrate *in vacuo*. The crude residue was purified by flash column chromatography (10% acetone in petrol; R_f 0.29) to give a colourless oil (26.0 mg, 0.19 mmol, 26%).

^{1}H NMR (400 MHz, $CDCl_3$) δ 9.74 (t, *J* = 2.2 Hz, 1H, C*H*O), 7.23 – 7.12 (m, 2H, Ar*H*), 7.09 – 7.02 (m, 2H, Ar*H*), 3.68 (d, *J* = 2.2 Hz, 2H, CH_2); **^{13}C{^{1}H} NMR** (101 MHz, $CDCl_3$) δ 199.1 (CH), 162.3 (d, *J* = 246.1 Hz, C_q), 131.3 (d, *J* = 8.1 Hz, CH), 127.7 (d, *J* = 3.3 Hz, C_q), 116.0 (d, *J* = 21.5 Hz, CH), 49.8, (CH_2); **^{19}F NMR** (376 MHz, $CDCl_3$) δ -115.1 (tt, *J* = 8.7, 5.3 Hz); **FTIR** (neat) ν_{max} /cm^{-1} 3045, 2930, 2829, 2729, 1723, 1603, 1510, 1417; **HRMS** (ESI) *m/z* calc'd for $C_8H_{11}NOF$ $[M+NH_4]^+$: 156.0819, found: 156.0817. Data are consistent with literature.[4]

1-Fluoro-2-(2-(4-fluorophenethoxy)ethyl)benzene, (22)

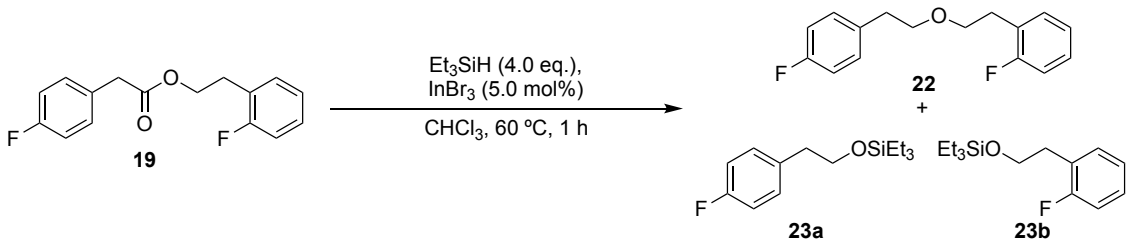

19 **23a** **23b**

Synthesised using an adapted literature procedure.[5] To a solution of 2-fluorophenethyl 2-(4-fluorophenyl)acetate (**19**) (259 mg, 937 μmol) and $InBr_3$ (18.0 mg, 50.8 μmol) in chloroform (1.00 mL) was added Et_3SiH (575 μL, 3.62 mmol)

and the pale yellow solution was heated to 60 °C. After 1 hour the reaction was quenched with water (2.5 mL), forming an orange precipitate. The reaction was stirred until the precipitate redissolved (30 minutes), then the mixture was diluted with DCM (5.0 mL), separated, and the aqueous phase was washed with DCM (2 x 5.0 mL). The combined organic phases were dried over anhydrous $MgSO_4$ and concentrated *in vacuo*. The crude residue was purified using flash column chromatography (2.5% Et_2O in petrol) to give ether **22** as clear colourless oil (R_f 0.11, 147 mg, 560 μmol, 60%), and a 1:1 inseparable mixture of silyl ethers **23a**, and **23b** (R_f 0.24, 71.8 mg, 141 μmol, 15%).

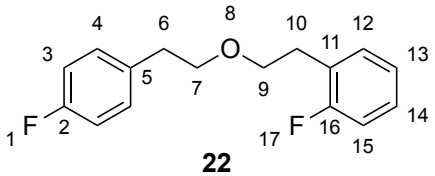

22

^{1}H NMR (400 MHz, $CDCl_3$) δ 7.23 – 7.17 (m, 2H, H-12, H-14), 7.17 – 7.11 (m, 2H, H-4), 7.09 – 6.98 (m, 2H, H-13, H-15), 6.98 – 6.91 (m, 2H, H-3), 3.66 (t, *J* = 7.0 Hz, 2H, H-9), 3.63 (t, *J* = 6.9 Hz, 2H, H-7), 2.92 (td, *J* = 7.0, 1.2 Hz, 2H, H-10), 2.84 (t, *J* = 6.9 Hz, 2H, H-6); **^{13}C{^{1}H} NMR** (101 MHz, $CDCl_3$) δ 161.3 (d, *J* = 243.6 Hz, C-2), 161.1 (d, *J* = 244.8 Hz, C-16), 134.6 (d, *J* = 3.2 Hz, C-5), 131.1 (d, *J* = 4.9 Hz, C-12), 130.1 (d, *J* = 7.8 Hz, C-4), 127.7 (d, *J* = 8.1 Hz, C-14), 125.6 (d, *J* = 15.8 Hz, C-11), 123.7 (d, *J* = 3.6 Hz, C-13), 115.0 (d, *J* = 22.2 Hz, C-15), 114.8 (d, *J* = 21.1 Hz, C-3), 71.5 (C-7), 70.2 (C-9), 35.3 (C-6), 29.3 (d, *J* = 2.2 Hz, C-10); **^{19}F NMR** (376 MHz, $CDCl_3$) δ -117.4 (tt, *J* = 8.8, 5.5 Hz), -118.6 – -118.8 (m). **FTIR** (neat) ν_{max} /cm^{-1} 2936, 2863, 1601, 1585, 1509 1492, 1455; **HRMS** (ESI) *m/z* calc'd for $C_{16}H_{16}OF_2Na$ $[M+Na]^+$: 285.1061, found: 285.1066.

Triethyl(4-fluorophenethoxy)silane (23a) & triethyl(2-fluorophenethoxy) silane, (23b)

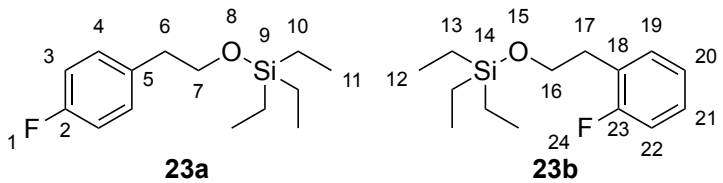

23a **23b**

^{1}H NMR (400 MHz, $CDCl_3$) δ 7.25 – 7.13 (m, 4H, H-4, H-19, H-21), 7.08 – 6.92 (m, 4H, H-3, H-20, H-22), 3.81 (t, *J* = 7.0 Hz, 2H, H-16), 3.78 (t, *J* = 7.0 Hz, 2H, H-7), 2.89 (td, *J* = 7.0, 1.2 Hz, 2H, H-17), 2.80 (t, *J* = 7.0 Hz, 2H, H-6), 0.92 (t, *J* = 7.9 Hz, 18H, H-11, H-12), 0.56 (q, *J* = 7.9 Hz, 12H, H-10, H-13); **^{19}F{^{1}H} NMR** (376 MHz, $CDCl_3$) δ -117.5, -118.8;). **FTIR** (neat) ν_{max} /cm^{-1} 2954, 2912, 2876, 1602, 1586, 1509, 1493, 1458; **GC-HRMS** (EI) *m/z* calc'd for $C_{14}H_{22}OFSi$ $[M-H]^+$: 253.1418, found: 253.0849 (224 ppm error, no ionisation by ESI). Data consistent with literature for **23a**,[6] **23b** unknown.

Diethyl(1-(2-fluorophenethoxy)-2-(4-fluorophenyl)ethoxy)silane (24)

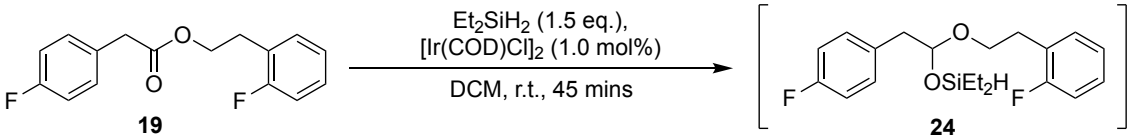

Synthesised using an adapted literature procedure.[7] To a solution of 2-fluorophenethyl 2-(4-fluorophenyl)acetate (**19**) (394 mg, 1.43 mmol) and $[Ir(COD)Cl]_2$ (9.5 mg, 14 μmol) in anhydrous dichloromethane (1.00 mL) was added diethylsilane (218 μL, 2.14 mmol). After 30 minutes, a crude NMR of the reaction mixture was taken. The product was unstable to both silica and alumina TLC, so purification was not attempted.

^{19}F NMR (376 MHz, $CDCl_3$) δ -117.1 (tt, *J* = 8.8, 5.5 Hz), -118.5 – -118.7 (m).

2.6.4 General Procedure for Catalyst Screening

Reactions are performed in oven-dried (120 °C, > 4 h) 20 mL microwave vials with magnetic flea stirrer. After addition of solids, vessels were sealed with a crimped PTFE/silicon cap and an inert atmosphere was accomplished either by displacing the air with argon (2 balloon volumes) or by 3 swing purges with a high vacuum/nitrogen Schlenk line.

In an oven-dried vial, a stock solution of the ester was prepared by dissolving 2-fluorophenethyl 2-(4-fluorophenyl)acetate (**19**) (400 mg, 1.45 mmol) in dry solvent (8.00 mL). To each reaction vial was then added catalyst (29 μmol), stock solution (800 μL, 0.145 mmol), and silane (0.29 mmol). The vessels were then immediately

positioned on a preheated heating block at either 40 °C or 100 °C. After 24 hours the reaction was cooled to room temperature and trifluorotoluene (~ 25 μL) was weighed directly into the vessels, followed by immediate analysis by quantitative ^{19}F NMR (5 x T1 = 18 s).

2.6.5 Ester Synthesis

Phenyl 2-(4-fluorophenyl)acetate (26b)

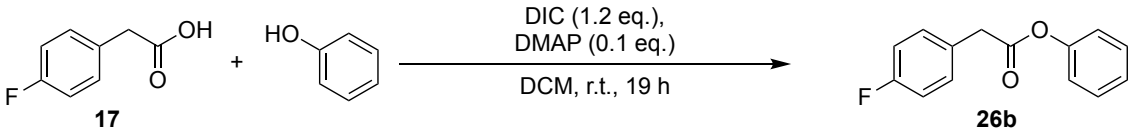

Synthesised using an adapted literature procedure.[8] To a solution of DMAP (31.8 mg, 260 μmol), 4-fluorophenylacetic acid (**17**) (401 mg, 2.60 mmol) and phenol (244 mg, 2.60 mmol) in DCM (10.0 mL) was added N,N'-diisopropylcarbodiimide (483 μL, 3.12 mmol) and the reaction was left stirring at room temperature. After 19 hours the white suspension was filtered through a silica plug, washing with DCM (2 x 25 mL), and concentrated *in vacuo*. The crude residue was purified using flash column chromatography (10% Et_2O in petrol; R_f 0.28) to give a clear, colourless oil (522 mg, 2.27 mmol, 87 %).

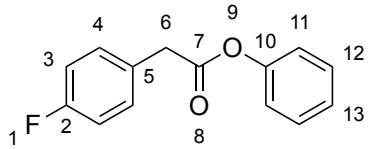

26b

^{1}H NMR (400 MHz, $CDCl_3$) δ 7.42 – 7.32 (m, 4H, H-4, H-12), 7.22 (tt, *J* = 7.4, 1.1 Hz, 1H, H-13), 7.12 – 7.01 (m, 4H, H-3, H-11), 3.84 (s, 2H, H-6); **^{13}C{^{1}H} NMR** (101 MHz, $CDCl_3$) δ 170.0 (C-7), 162.3 (d, *J* = 245.8 Hz, C-2), 150.8 (C-10), 131.1 (d, *J* = 8.1 Hz, C-4), 129.6 (C-12), 129.3 (d, *J* = 3.3 Hz, C-5), 126.1 (C-13), 121.5 (C-11), 115.8 (d, *J* = 21.6 Hz, C-3), 40.7 (C-6); **^{19}F{^{1}H} NMR** (376 MHz, $CDCl_3$) δ -115.3; **FTIR** (neat) ν_{max} /cm^{-1} 3072, 3045, 1750, 1592, 1509, 1492, 1419; **GC-HRMS** (EI) *m/z* calc'd for $C_{14}H_{11}O_2F$ $[M]^+$: 230.0743, found: 230.0197 (237 ppm error, no ionisation by ESI). Data consistent with literature.[9]

Decyl isobutyrate (26d)

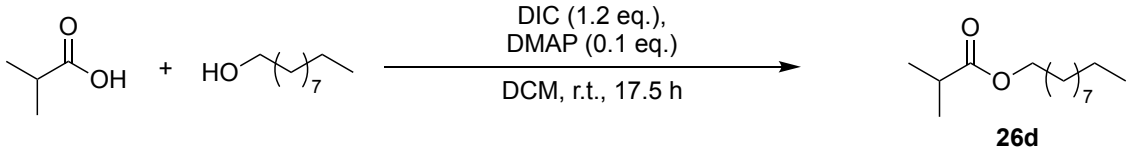

26d

Synthesised using an adapted literature procedure.[8] To a solution of 4-dimethylamino pyridine (31.8 mg, 260 μmol), 1-decanol (496 μL, 2.60 mmol) and isobutyric acid (241 μL, 2.60 mmol) in DCM (10.0 mL) was added N,N'-diisopropylcarbodiimide (483 μL, 3.12 mmol) and the reaction was left stirring at room temperature. After 17.5 hours the white suspension was filtered through a silica plug, washing with DCM (5 x 10 mL), and concentrated *in vacuo*. The crude residue was purified using flash column chromatography (5% EtOAc in hexanes; R_f 0.26) to give a clear, colourless oil (460 mg, 2.02 mmol, 78 %).

^{1}H NMR (500 MHz, $CDCl_3$) δ 4.05 (t, *J* = 6.7 Hz, 2H, CO_2CH_2), 2.53 (hept, *J* = 7.0 Hz, 1H, $CHCO_2$), 1.61 (p, *J* = 6.7 Hz, 2H, $CO_2CH_2CH_2$), 1.38 – 1.20 (m, 14H, CH_2), 1.16 (d, *J* = 7.0 Hz, 6H, $(CH_3)_2CH$), 0.87 (t, *J* = 6.9 Hz, 3H, CH_2CH_3); **^{13}C{^{1}H} NMR** (126 MHz, $CDCl_3$) δ 177.4 (C_q), 64.5 (CH_2), 34.2 (CH), 32.0 (CH_2), 29.7 (2 x CH_2), 29.44 (CH_2), 29.39 (CH_2), 28.8 (CH_2), 26.0 (CH_2), 22.8 (CH_2), 19.2 (2 x CH_3), 14.2 (CH_3); **FTIR** (neat) ν_{max} /cm^{-1} 2956, 2924, 2855, 1735 1469; **HRMS** (ESI) *m/z* calc'd for $C_{15}H_{29}O_2$ $[M+H]^+$: 241.2162, found: 241.2156.

Cyclohexyl benzoate (26f)

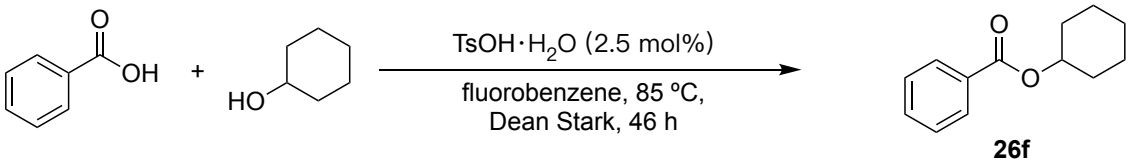

26f

To a solution of benzoic acid (489 mg, 4.00 mmol) and *p*-toluenesulfonic acid monohydrate (19.0 mg, 0.100 mmol) in fluorobenzene (5.00 mL) was added cyclohexanol (423 μL, 4.00 mmol) and the solution was heated until steady distillation was achieved in the Dean Stark trap. After 46 hours at reflux the clear solution was concentrated *in vacuo* and purified by flash column chromatography

(10% EtOAc in petrol; R_f 0.20) to give a clear colourless oil (465 mg, 2.30 mmol, 57%).

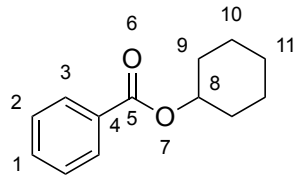

26f

^{1}H NMR (400 MHz, $CDCl_3$) δ 8.08 – 8.01 (m, 2H, H-3), 7.54 (t, *J* = 7.5 Hz, 1H, H-1), 7.48 – 7.38 (m, 2H, H-2), 5.04 (tt, *J* = 8.5, 3.8 Hz, 1H, H-8), 2.01 – 1.89 (m, 2H, H-9), 1.84 – 1.74 (m, 2H, H-10), 1.67 – 1.52 (m, 3H, H-9, H-11), 1.52 – 1.28 (m, 3H, H-10, H-11); **^{13}C{^{1}H} NMR** (101 MHz, $CDCl_3$) δ 166.0 (C-5), 132.7 (C-1), 131.0 (C-4), 129.5 (C-3), 128.3 (C-2), 73.0 (C-8), 31.7 (C-9), 25.5 (C-11), 23.7 (C-10); **FTIR** (neat) ν_{max} /cm^{-1} 2935, 2859, 1712, 1603, 1585, 1450; **HRMS** (ESI) *m/z* calc'd for $C_{13}H_{17}O_2$ $[M+H]^+$: 205.1223, found: 205.1220. Data consistent with literature.[10]

Undecan-2-yl cyclopropanecarboxylate (26g)

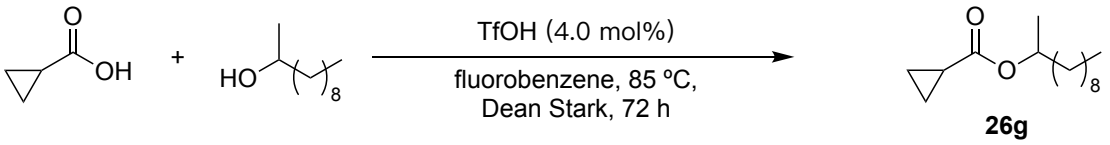

26g

To a solution of cyclopropane carboxylic acid (345 mg, 4.01 mmol) and 2-undecanol (690 mg, 4.00 mmol) in fluorobenzene (8.00 mL) was added triflic acid (3.50 µL, 40.0 µmol) and the solution was heated until steady distillation was achieved in the Dean Stark trap. After 24 and 48 hours, additional portions of TfOH (3.50 µL, 40 µmol and 7.00 µL, 80.0 µmol respectively) were added. After 72 hours the reaction was cooled to room temperature and washed with $NaHCO_3$ (8.0 mL of a saturated aqueous solution), water (8.0 mL) and NaCl (8.0 mL of a saturated aqueous solution). The organic phase was concentrated *in vacuo* and purified by flash column chromatography (1% Et_2O in petrol; R_f 0.20) to give a clear colourless oil (311 mg, 1.37 mmol, 34%).

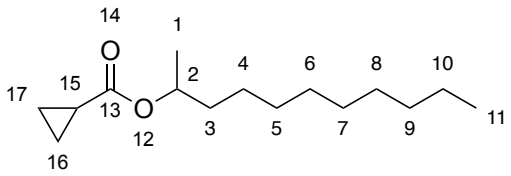

26g

^{1}H NMR (500 MHz, $CDCl_3$) δ 4.89 (h, *J* = 6.4 Hz, 1H, H-2), 1.61 – 1.53 (m, 2H, H-13, H-3), 1.51 – 1.41 (m, 1H, H-3), 1.34 – 1.22 (m, 14H, H-4 – H-9), 1.19 (d, *J* = 6.4 Hz, 3H, H-1), 0.99 – 0.95 (m, 2H, H-16, H-17), 0.88 (t, *J* = 6.9 Hz, 3H, H-11), 0.86 – 0.78 (m, 2H, H-16, H-17); **^{13}C{^{1}H} NMR** (126 MHz, $CDCl_3$) δ 174.7 (C-13), 71.1 (C-2), 36.1 (C-3), 32.0 (C-9), 29.7 (CH_2), 29.6 (CH_2), 29.5 (CH_2), 25.5 (C-4), 22.8 (C-10), 20.1 (C-1), 14.3 (C-11), 13.3 (C-15), 8.3 (C-16, C-17); **FTIR** (neat) ν_{max} /cm^{-1} 2954, 2924, 2855, 1724, 1459; **HRMS** no ionisation by ESI.

3,3-Dibenzyldihydrofuran-2(3*H*)-one (26h)

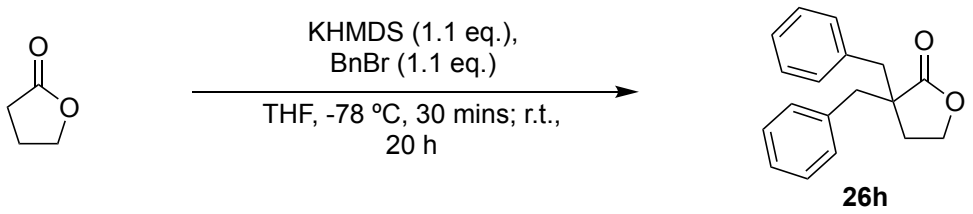

26h

Synthesised using an adapted literature procedure.[11] To a solution of KHMDS in THF (11.0 mL, 1.00 M, 11.0 mmol) at -78 °C was added freshly distilled γ-butyrolactone (762 μL, 10.0 mmol) and the slurry was stirred for 30 minutes. Benzyl bromide (1.30 mL, 11.0 mmol) was then added dropwise over 30 minutes, and the solution was allowed to gradually warm to room temperature. After 20 hours the reaction mixture was diluted with Et_2O (50 mL) and washed with NH_4Cl (50 mL of a saturated aqueous solution). The aqueous was further extracted with Et_2O (3 x 50 mL), and the combined organic phased were dried over anhydrous $MgSO_4$, filtered, and concentrated *in vacuo*. The crude residue was purified by flash column chromatography (20% EtOAc in petrol; R_f 0.42) to give a white solid (489 mg, 1.84 mmol, 33% (using BnBr as the limiting reagent)).

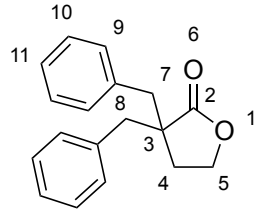

26h

^{1}H NMR (400 MHz, $CDCl_3$) δ 7.36 – 7.27 (m, 6H, H-10, H-11), 7.27 – 7.22 (m, 4H, H-9), 3.39 (t, *J* = 7.4 Hz, 2H, H-5), 3.23 (d, *J* = 13.4 Hz, 2H, H-7), 2.81 (d, *J* = 13.4 Hz, 2H, H-7), 2.18 (t, *J* = 7.4 Hz, 2H, H-4); **^{13}C{^{1}H} NMR** (101 MHz, $CDCl_3$) δ 181.2 (C-2), 136.6 (C-8), 130.3 (C-9), 128.7 (C-10), 127.3 (C-11), 65.4 (C-5), 49.9 (C-3), 44.0 (C-7), 29.2 (C-4); **FTIR** (neat) ν_{max} /cm^{-1} 3084, 3058, 3029, 3004, 2923, 2912, 1756, 1599, 1582, 1494, 1455, 1442; **HRMS** (ESI) *m/z* calc'd for $C_{18}H_{12}O_2$ $[M+H]^+$: 267.1380, found: 267.1387; **m.p.** 129-131 °C (lit. 128-130 °C).[12]

2.6.6 Substrate Scope

General procedure for the $FeCl_3$-catalysed reductive etherification

To a solution of ester (360 μmol) and $FeCl_3$ (11.7 mg, 72.0 μmol) in fluorobenzene (2.00 mL) was added TMDS (128 μL, 720 μmol) and the solution was heated to 40 °C. After 24 hours the reaction is filtered through a silica plug and the organic filtrate was concentrated *in vacuo*.

1-Isobutoxydecane (27d)

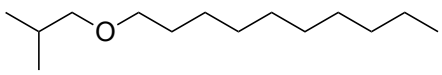

27d

Purification by flash column chromatography (1% EtOAc in petrol; R_f 0.20) to give a colourless oil (64.0 mg, 299 μmol, 83%).

^{1}H NMR (400 MHz, $CDCl_3$) δ 3.39 (t, *J* = 6.7 Hz, 2H, OC*H*$_2$CH$_2$), 3.16 (d, *J* = 6.7 Hz, 2H, OC*H*$_2$CH), 1.94 – 1.76 (nonet, *J* = 6.7 Hz, 1H, C*H*), 1.56 (tt, *J* = 6.9, 6.7 Hz, 2H, OCH$_2$C*H*$_2$), 1.40 – 1.18 (m, 14H, CH_2), 0.90 (d, *J* = 6.7 Hz, 6H, (C*H*$_3$)$_2$CH), 0.88 (t, *J* = 6.9 Hz, 3H, CH$_2$C*H*$_3$); **^{13}C{^{1}H} NMR** (101 MHz, $CDCl_3$) δ 78.0 (CH_2), 71.2 (CH_2), 32.1 (CH_2), 29.9 (CH_2), 29.78 (CH_2), 29.73 (CH_2), 29.66 (CH_2), 29.5 (CH_2), 28.6 (CH), 26.4 (CH_2), 22.8

(CH_2), 19.6 (CH_3), 14.3 (CH_2); **FTIR** (neat) ν_{max} /cm^{-1} 2955, 2924, 2853, 2799, 1467; **GC-HRMS** (EI) *m/z* calc'd for $C_{14}H_{31}O$ $[M+H]^+$: 215.2375, found: 215.1775 (279 ppm error, no ionisation by ESI).

(*E*)-(3-Methoxyprop-1-en-1-yl)benzene (27e)

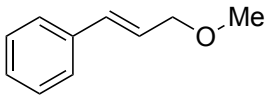

27e

Purification by flash column chromatography (2% EtOAc in petrol; R_f 0.18) to give a colourless oil (14.1 mg, 95.1 μmol, 27%).

^{1}H NMR (400 MHz, $CDCl_3$) δ 7.44 – 7.37 (m, 2H, Ar*H*), 7.36 – 7.29 (m, 2H, Ar*H*), 7.29 – 7.20 (m, 1H, Ar*H*), 6.62 (dt, *J* = 15.9, 1.5 Hz, 1H, ArC*H*CH), 6.30 (dt, *J* = 15.9, 6.0 Hz, 1H, ArCHC*H*), 4.11 (dd, *J* = 6.0, 1.5 Hz, 2H, CH_2), 3.40 (s, 3H, CH_3); **^{13}C{^{1}H} NMR** (101 MHz, $CDCl_3$) δ 136.8 (C_q), 132.6 (CH), 128.7 (CH), 127.8 (CH), 126.6 (CH), 126.1 (CH), 73.2 (CH_2), 58.1 (CH_3); **FTIR** (neat) ν_{max} /cm^{-1} 3026, 2924, 2877, 2844, 2820, 1494, 1449, 1379; **GC-HRMS** (EI) *m/z* calc'd for $C_{10}H_{12}O$ $[M]^+$: 148.0888, found: 148.0434 (307 ppm error, no ionisation by ESI). Data consistent with literature.[13]

1-Indanone (28)

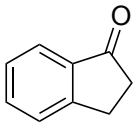

28

Purification by flash column chromatography (2% EtOAc in petrol; R_f 0.11) to give a colourless oil (13.2 mg, 99.9 μmol, 28%).

^{1}H NMR (400 MHz, $CDCl_3$) δ 7.76 (ddd, *J* = 7.7, 1.2, 1.0 Hz, 1H, Ar*H*), 7.59 (ddd, *J* = 7.7, 7.5, 1.2 Hz, 1H, Ar*H*), 7.48 (ddd, *J* = 7.7, 1.0, 1.0 Hz, 1H, Ar*H*), 7.37 (ddd, *J* = 7.7, 7.5, 1.0 Hz, 1H, Ar*H*), 3.19 – 3.11 (m, 2H, C$H_2$$CH_2$CO), 2.73 – 2.66 (m, 2H, CH_2CH_2CO); **^{13}C{^{1}H} NMR** (101 MHz, $CDCl_3$) δ 207.2 (C_q), 155.3 (C_q), 137.2 (C_q), 134.7 (CH), 127.4 (CH), 126.8 (CH), 123.9 (CH), 36.4 (CH_2), 25.9 (CH_2); **FTIR** (neat) ν_{max} /cm^{-1} 3071,

3012, 2927, 1701, 1609, 1463, 1439, 1404; **HRMS** (ESI) *m/z* calc'd for $C_9H_{12}NO$ $[M+NH_4]^+$: 150.0913, found: 150.0903. Data consistent with literature.[14]

((Undecan-2-yloxy)methyl)cyclopropane (27g)

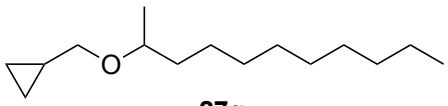

27g

Purification by flash column chromatography (10% DCM in pentane; R_f 0.14) to give a colourless residue (5.3 mg, 23.4 μmol, 6.5%)

^{1}H NMR (400 MHz, $CDCl_3$) δ 3.37 (h, *J* = 6.1 Hz, 1H), 3.29 (dd, *J* = 10.0, 6.9 Hz, 1H), 3.20 (dd, *J* = 10.0, 6.8 Hz, 1H), 1.58 – 1.47 (m, 1H), 1.43 – 1.18 (m, 16H), 1.12 (d, *J* = 6.1 Hz, 3H), 1.04 (ttt, *J* = 8.0, 6.8, 4.8 Hz, 1H), 0.88 (t, *J* = 6.8 Hz, 3H), 0.51 (dtd, *J* = 8.0, 5.0, 1.6 Hz, 2H), 0.18 (q, *J* = 6.1 Hz, 2H); **^{13}C{^{1}H} NMR** (101 MHz, $CDCl_3$) δ 75.3 (CH), 73.4 (CH_2), 36.8 (CH_2), 32.1 (CH_2), 29.9 (CH_2), 29.8 (CH_2), 29.8 (CH_2), 29.5 (CH_2), 25.8 (CH_2), 22.8 (CH_2), 19.9 (CH_3), 14.3 (CH_3), 11.2 (CH_2), 3.2 (2 x CH_2); **FTIR** (neat) ν_{max} /cm^{-1} 3006, 2958, 2924, 2854, 1465; **HRMS** (ESI) *m/z* calc'd for $C_{10}H_{31}O$ $[M+H]^+$: 227.2369, found: 227.2365.

3,3-Dibenzyltetrahydrofuran (27h)

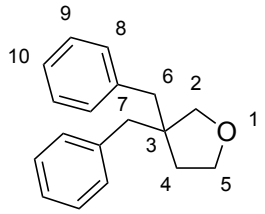

27h

Purification by flash column chromatography (5% acetone in pentane; R_f 0.41) to give a colourless oil (35.5 mg, 120 μmol, 39%).

^{1}H NMR (500 MHz, $CDCl_3$) δ 7.34 – 7.27 (m, 4H, H-9), 7.24 (tt, *J* = 7.4, 1.7 Hz, 2H, H-10), 7.20 – 7.14 (m, 4H, H-8), 3.78 (t, *J* = 7.3 Hz, 2H, H-5), 3.61 (s, 2H, H-2), 2.78 (d, *J* = 13.7 Hz, 2H, H-6), 2.75 (d, *J* = 13.7 Hz, 2H, H-6), 1.81 (t, *J* = 7.3 Hz, 2H, H-4); **^{13}C{^{1}H} NMR** (126 MHz, $CDCl_3$) δ 138.6 (C-7), 130.8 (C-8), 128.3 (C-9), 126.4 (C-10), 75.3 (C-2), 67.4 (C-5), 47.6 (C-3), 42.2 (C-6), 34.9 (C-4); **FTIR** (neat) ν_{max} /cm^{-1} 3084, 3061,

3027, 2964, 2926, 2870, 2856, 1602, 1582, 1495, 1453; **HRMS** (ESI) *m/z* calc'd for $C_{18}H_{21}O$ $[M+H]^+$: 253.1587, found: 253.1582.

1-Fluoro-4-(2-phenoxyethyl)benzene (27b)

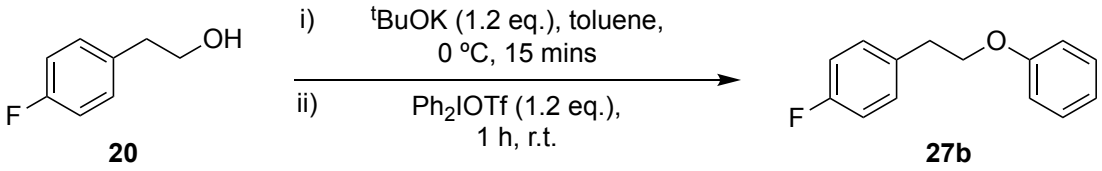

Synthesised using an adapted literature procedure.[15] To a solution of ^{t}BuONa (115 mg, 1.20 mmol) in toluene (5.00 mL) at 0 °C was added 4-fluorophenethyl alcohol (**18**) (125 μL, 1.00 mmol) and the reaction was stirred for 15 minutes. Ph_2IOTf (516 mg, 1.20 mmol) was then added in one portion and the solution was warmed to room temperature. After 1 hour the solution was diluted with Et_2O (5.0 mL) and filtered through a silica plug, washing with Et_2O (20 mL). The organic filtrate was then concentrated *in vacuo* and purified by flash column chromatography (1% Et_2O in pentane; R_f 0.20) to give a pale yellow oil (168 mg, 0.775 mmol, 77%).

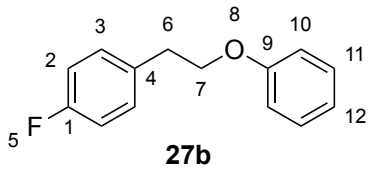

27b

^{1}H NMR (400 MHz, $CDCl_3$) δ 7.35 – 7.24 (m, 4H, H-3, H-11), 7.07 – 7.00 (m, 2H, H-2), 6.98 (tt, *J* = 7.5, 1.1 Hz, 1H, H-12), 6.95 – 6.90 (m, 2H, H-10), 4.18 (t, *J* = 6.9 Hz, 2H, H-7), 3.10 (t, *J* = 6.9 Hz, 2H, H-6); **^{13}C{^{1}H} NMR** (101 MHz, $CDCl_3$) δ 161.8 (d, *J* = 244.2 Hz, C-1), 158.8, (C-9), 134.2 (d, *J* = 3.2 Hz, C-4), 130.5 (d, *J* = 7.8 Hz, C-3), 129.6 (C-11), 121.0 (C-12), 115.4 (d, *J* = 21.1 Hz, C-2), 114.7 (C-10), 68.6 (C-7), 35.1 (C-6); **FTIR** (neat) ν_{max} /cm^{-1} 3063, 3040, 2927, 2871, 1599, 1587, 1509, 1496, 1471, 1417; **GC-HRMS** (EI) *m/z* calc'd for $C_{14}H_{13}OF$ $[M]^+$: 216.0950, found: 216.0418 (246 ppm error, no ionisation by ESI). Data consistent with literature.[16]

2.6.7 References

1 E. L. Stoll, T. Barber, D. J. Hirst and R. M. Denton, *Chem. Commun.*, 2022, **58**, 3509–3512.
2 N. Soga, T. Yoshiki, A. Sato, T. Kawamoto, I. Ryu and H. Matsubara, *Tetrahedron Lett.*, 2021, **69**, 152977.
3 Y. Takeda, K. Narita and T. Katoh, *European J. Org. Chem.*, 2017, **2017**, 901–907.
4 K. J. Kolonko and H. J. Reich, *J. Am. Chem. Soc.*, 2008, **130**, 9668–9669.
5 N. Sakai, T. Moriya and T. Konakahara, *J. Org. Chem.*, 2007, **72**, 5920–5922.
6 Y. Q. Yuan, P. S. Kumar and S. R. Guo, *Synlett*, 2017, **28**, 1620–1623.
7 C. Cheng and M. Brookhart, *Angew. Chem. Int. Ed.*, 2012, **51**, 9422–9424.
8 H. Li, S. Liu, Y. Huang, X. H. Xu and F. L. Qing, *Chem. Commun.*, 2017, **53**, 10136–10139.
9 W. Yu, S. Yang, F. Xiong, T. Fan, Y. Feng, Y. Huang, J. Fu and T. Wang, *Org. Biomol. Chem.*, 2018, **16**, 3099–3103.
10 S. Chun and Y. K. Chung, *Org. Lett.*, 2017, **19**, 3787–3790.
11 S. Thaisrivongs, D. T. Pals, S. R. Turner and L. T. Kroll, *J. Med. Chem.*, 1988, **31**, 1369–1376.
12 L. Miao, I. Haque, M. R. Manzoni, W. S. Tham and S. R. Chemler, *Org. Lett.*, 2010, **12**, 4739–4741.
13 A. J. Argüelles, S. Sun, B. G. Budaitis and P. Nagorny, *Angew. Chem. Int. Ed.*, 2018, **57**, 5325–5329.
14 L. J. Mitchell and C. J. Moody, *J. Org. Chem.*, 2014, **79**, 11091–11100.
15 R. Ghosh, E. Lindstedt, N. Jalalian and B. Olofsson, *ChemistryOpen*, 2014, **3**, 54–57.
16 H. Minami, K. Nogi and H. Yorimitsu, *Synlett*, 2021, **32**, 1542–1546.

Chapter 3

Reductive Beckmann Rearrangements of Oximes

3.1 Introduction

3.1.1 Nitrillium and Keteniminium ions

Nitrilium and keteniminium ions are two closely related compounds which mostly serve as transient intermediates in organic synthesis (Figure 1). Their unique reactivity is dominated by two characteristics: a carboxylic acid oxidation level and a strongly electrophilic carbon. These factors make addition into the imidoyl-like carbon the principal mode of reaction, even with relatively poor nucleophiles such as chloride ions. In the 50 years since "the expected versatile behaviour" of this family of compounds was first noted,[1] hundreds of reports including two recent reviews[2,3] have been published, demonstrating the value of these intermediates in contemporary synthesis.

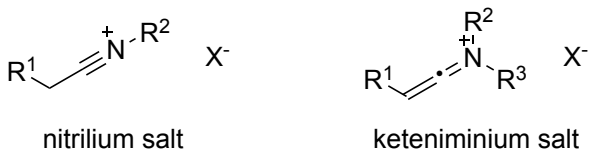

Figure 1. *The generic structures of nitrilium and keteniminium salts.*

Synthesis of Nitrilium and Keteniminium ions

The first reactions to exploit nitrilium ions did so without ever isolating the intermediate. The Beckmann rearrangement[4] and the Ritter reaction[5,6] (Scheme 1) both involve an acid-catalysed hydroxide elimination, facilitating an oxime rearrangement and nitrile alkylation respectively. In both cases this leads to a nitrilium ion which under typical conditions is quickly quenched by water to give the desired amide.

Beckmann Rearrangement (1887):

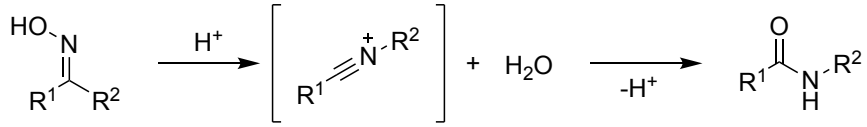

Ritter Reaction with Alcohols (1948):

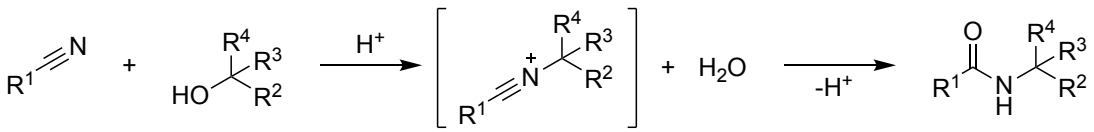

Scheme 1*. Comparison of the Beckmann rearrangement and the Ritter reaction, showing the respective nitrilium ion intermediates.*

Whilst amide formation is certainly useful and industrially important, the desire to use these highly reactive intermediates to perform a greater variety of transformations has led to the development of two general preparative methods for the synthesis and isolation of nitrilium and keteninimium ions. Nitrile alkylation, is one such method which was first reported by Meerwein and co-workers in 1956 (Scheme 2).[7] Using triethyl oxonium tetrafluoroborate (Meerwein's salt), simple nitriles were ethylated to the tetrafluoroborate salt in moderate to high yields. In the same publication it was also shown that nitrile alkylations could be accomplished with Lewis acids such as $FeCl_3$ or $SbCl_5$ and isopropyl-, tert-butyl- and methoxymethyl- chloride, although reactions were slow and often required a large excess of reagents. Since this initial report, dialkoxycarbonium salts,[8] *O*-alkyldibenzofuranium salts,[9] alkyl fluorosulfonates[10] and alkyl triflates[11,12] have all been used as electrophiles, but the main restriction is the instability of the alkylating agent; typically limiting this method to methyl and ethyl alkylations. The reaction rate is also slowed by the association of the Lewis basic nitriles with highly electrophilic nitrilium cations, resulting in some reactions taking days to complete.

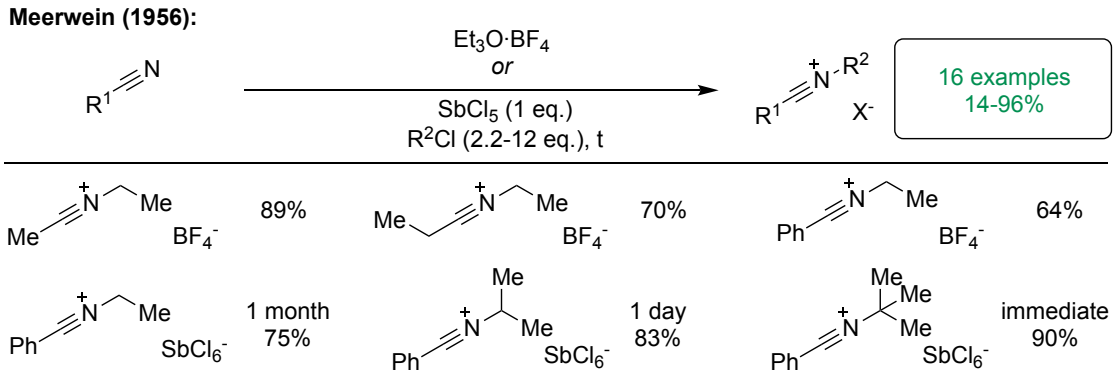

***Scheme 2**. Reaction conditions and scope of Meerwein's nitrile alkylations*

The first and most widespread method for the synthesis of nitrilium and keteniminium ions was the activation of amides. This type of reaction was first reported in 1887, when Wallach used phosphorus pentachloride to transform secondary amides into the corresponding imidoyl chloride (Scheme 3A).[13] 50 years later, von Braun described the analogous reactions with tertiary amides to make α-chloroenamines (Scheme 3B).[14] Importantly, both of these precursors can form the corresponding nitrilium and keteniminium ions upon exposure to a suitable Lewis acid. As such, in 1955 Klages reported in the first isolation of nitrilium ions using

$SbCl_5$.[15] Similarly, many of the [2+2] reactions which Ghosez and co-workers pioneered in the 1970s used $ZnCl_2$ to drive the equilibrium from α-chloroenamines in favour of the more reactive keteniminium ions.[16–18]

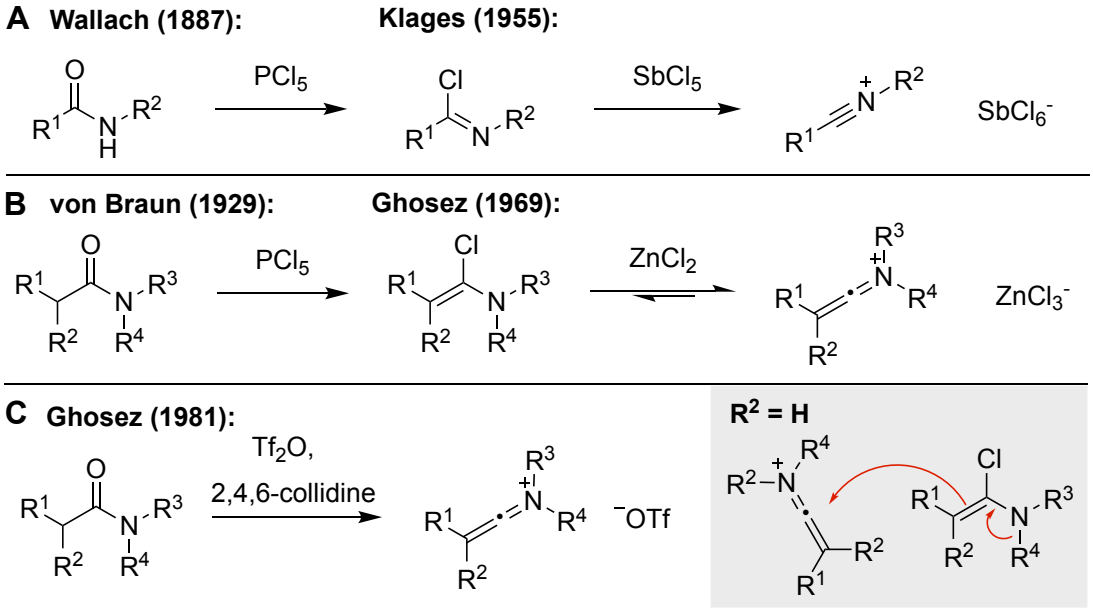

***Scheme 3**. Methods employed in amide activation over time including an aldol-type side reaction.*

Another notable development in amide activation was the use of triflic anhydride in combination with a non-nucleophilic base (Scheme 3C).[19] This procedure allowed the keteniminium ions to be formed directly without the need for an additional Lewis acid. Furthermore, it avoided aldol-type reactions between α-chloroenamines and keteniminium ions which Ghosez found to be a limiting side reaction for less substituted substrates (Scheme 3C, where R^2=H). Non-nucleophilic pyridine-type bases are typically used but interestingly the choice of base has a strong and poorly understood influence on the mechanism of amide activation and the yield of further transformations.[20,21]

Reduction of Nitrilium and Keteniminium ions

Conceptually, the simplest nucleophiles which can be added to nitrilium and keteniminium ions are hydrides; first forming imines and then amines. In a seminal publication, Charette and co-workers activated and then reduced tertiary amides using a Hantzsch ester as both a base and a hydride source (Scheme 4).[22] Whilst the reduction of an amide to amine is certainly not novel, this simple, metal-free procedure was done in one hour at room temperature and could often be purified

with just a simple work up. Moderate to high yields were achieved in most cases but importantly, the reaction had an outstanding functional group tolerance. Ketones, esters, alkynes, nitriles, and epoxides all remained untouched under the reaction conditions and *N*-allyl and *N*-phenyl benzylamides were not reduced to benzyl alcohol which is a common side product of their reduction with typical hydride-based reagents.

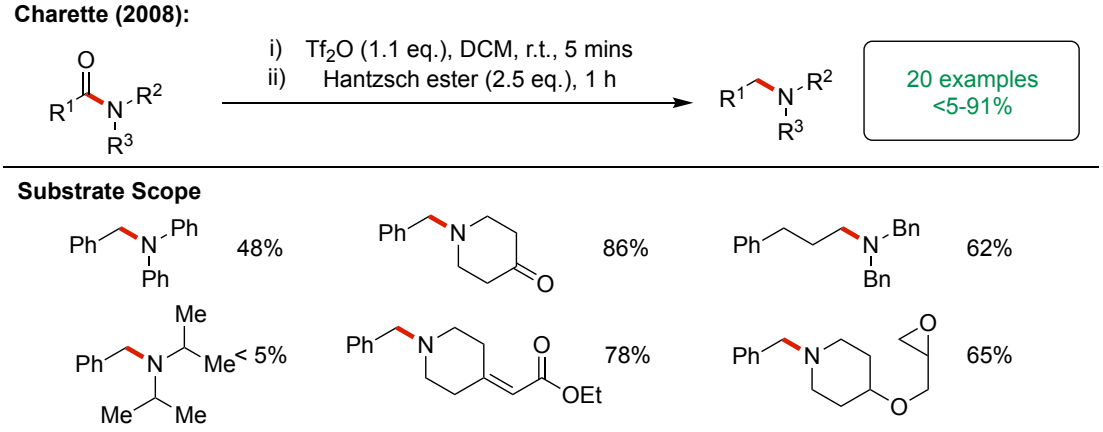

Scheme 4 *General conditions and substrate scope for Charette's tertiary amide reduction.*

Two years later, the method was extended to incorporate secondary amides which had previously been slow to react (Scheme 5).[23] Under similar conditions, triethylsilane cleanly reduced the nitrilium intermediates to imines which could be isolated, hydrolysed to the aldehyde, or reduced again to the amine using a Hantzsch ester.

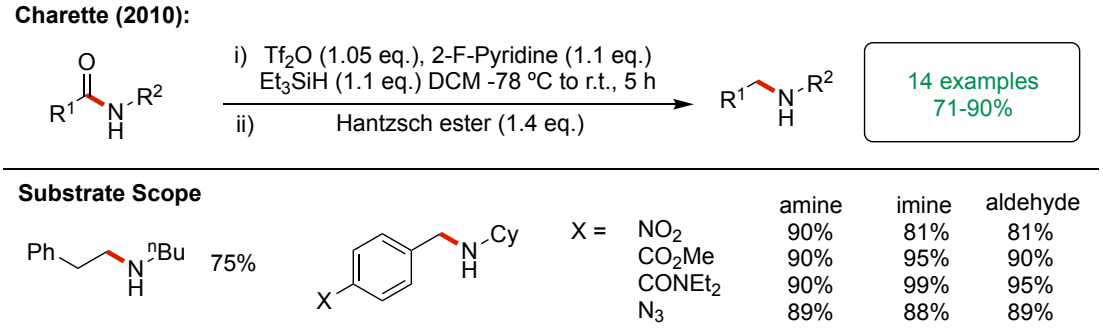

Scheme 5*. General conditions and substrate scope for Charette's secondary amide reduction.*

In the same year, the Huang group reported[24] another reduction of nitrilium and keteniminium triflates using sodium borohydride. Whilst the functional group tolerance was generally poorer than Charette's procedure, the reaction worked for a variety of amides and lactams including a series of sterically hindered *N,N*-

diisopropyl amides which the Hantzsch ester was slow to reduce. Huang subsequently published a second metal-free procedure which combined amide activation with a $B(C_6F_5)_3$-catalysed hydrosilylation to furnish a number of secondary amines in moderate to excellent yields (Scheme 6).[25] Interestingly, the $B(C_6F_5)_3$ catalysed reduction of amides had already been reported twice previously,[26,27] but Huang's 'pre-activation' of the amides with triflic anhydride allowed the reduction to occur with near equimolar silane at room temperature, which in turn resulted in an increase in selectivity for amides over other reducible functional groups. Yields were generally excellent for benzamides containing nitro, methoxy, nitrile, ester and TBDPS ethers, although less substituted aliphatic amides performed slightly worse. Huang presented this as a "mild, metal-free" method, however the use of powerful Brønsted and Lewis acids may well undermine functional group tolerance on more complex substrates.

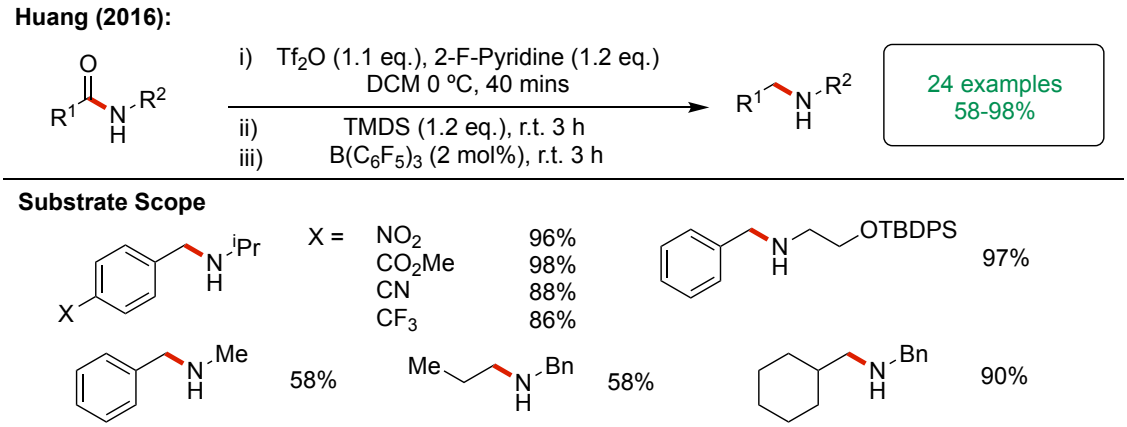

Scheme 6. *General conditions and substrate scope for Huang's secondary amide hydrosilylation.*

3.1.2 The Beckmann Rearrangement

Discovered in 1887, the Beckmann rearrangement is an acid-mediated rearrangement of a ketoxime into a secondary amide.[4] The conditions for this reaction are usually quite forcing; a typical procedure may require high temperatures in concentrated sulfuric acid or a "Beckmann solution" which contains HCl, acetic anhydride and acetic acid. The harsh conditions pose problems for sensitive substrates; however, the reaction reliably gives good yields for many oximes including the archetypal rearrangement of cyclohexanone oxime to ε-caprolactam.[28]

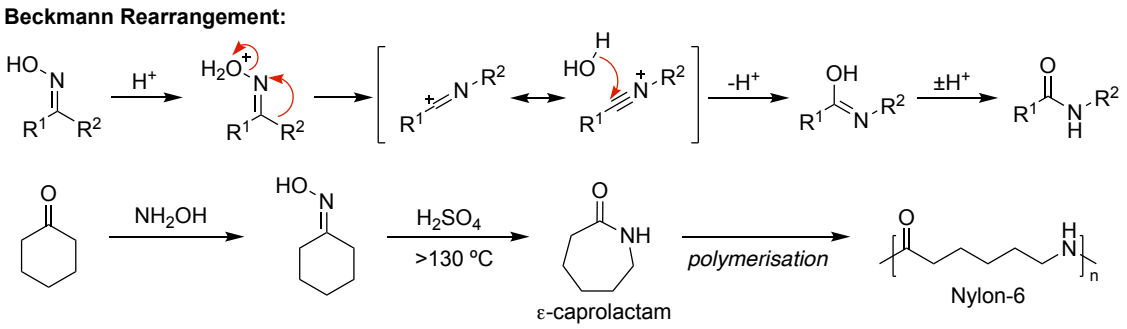

***Scheme 7**. Mechanism of the Beckmann Rearrangement with an example of its use in caprolactam synthesis.*

The first step of the mechanism involves protonation of the oxime which mostly occurs on the nitrogen atom. Unusually, proton transfer from the nitrogen to the oxygen has been calculated to be the rate determining step in sulfuric acid solutions, with an energy barrier of around 100 kJmol^{-1}. Following this, the N-O bond of the *O*-protonated oxime rapidly breaks with a concomitant and stereoselective *[1,2]*-shift of the antiperiplanar R group (Scheme 7).[28,29] Theoretically and in most cases, one oxime stereoisomer only gives a single amide regioisomer. However, under certain reaction conditions the starting material can isomerise, allowing both R groups to migrate. The product of this rearrangement is a nitrilium ion which is quenched by water to give the amide after tautomerisation.

A known side reaction which can occur is the Beckmann elimination, where the carbon nitrogen bond in the nitrilium ion breaks to give a nitrile and an alkene (Scheme 8). This is usually only an issue where the migrating group is particularly good at stabilising a build-up of positive charge and this pathway can be reduced by choice of reagents.

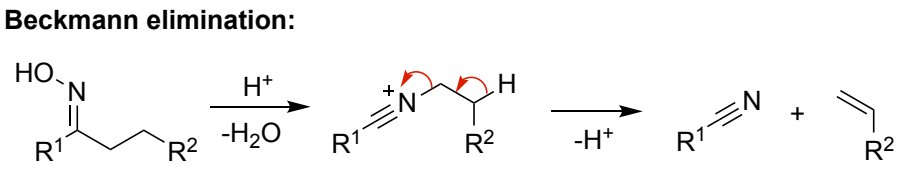

***Scheme 8**. Overview of the Beckmann elimination.*

With more sensitive substrates the same reaction can be accomplished by transforming the hydroxyl into a better leaving group such as a sulfonate ester. This enables the reaction to be performed using milder acids and at lower temperatures. Organic solvents can also be used, and of these, DCM is most common as it is non-nucleophilic and its high dielectric constant enables a faster rate of reaction.[29] There

is also some empirical evidence to suggest that leaving groups which can simultaneously coordinate to the nitrilium ion and form *pseudo*-tetrahedral intermediates give increased reactivity (Scheme 9).[30–32]

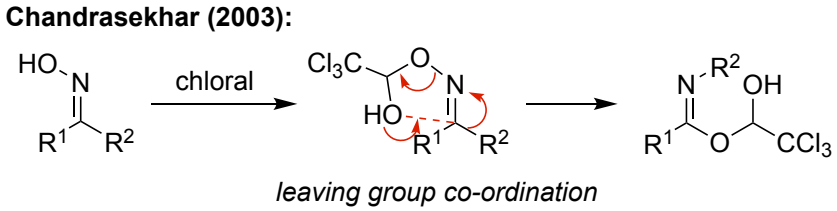

***Scheme 9**. Proposed leaving group co-ordination, leading to enhanced Beckmann Rearrangements.*

This reaction has been exemplified in the synthesis of (+)-codeine by White and co-workers (Scheme 10).[33] As part of this sequence, an oxime is activated to the *O*-brosylate ester which, after heating, selectively forms the least sterically hindered oxime diastereoisomer in an 11:1 ratio. Then, upon dilution with acetic acid, the Beckmann rearrangement occurs in 1 hour at room temperature to give 69% of the desired amide with <10% of its unwanted regioisomer. Interestingly, under numerous conditions, differently activated oximes did not undergo the rearrangement which led the authors to suggest that due to the rigid framework the oxime must become sp^3 hybridised to give the correct orbital alignment.

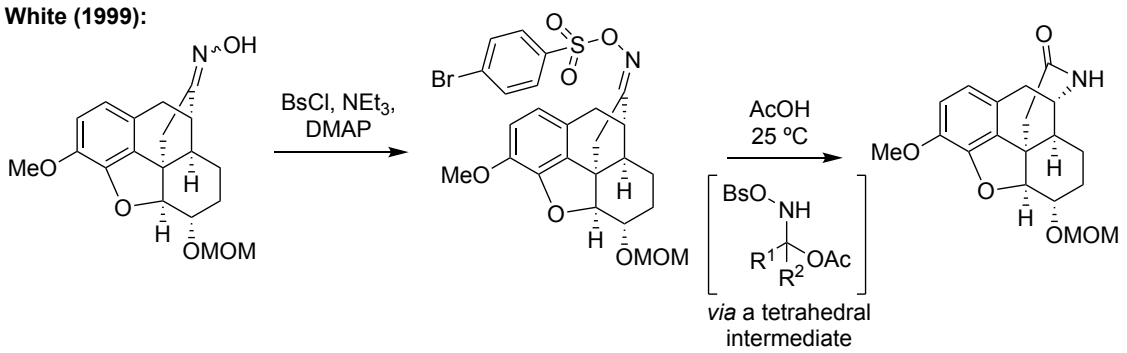

***Scheme 10**. Key step in the White group's synthesis of (+)-codeine involving a Beckmann rearrangement.*

Often, the oxime is activated in a separate step to rearrangement, but as Savanur and co-workers demonstrated as recently as 2015,[34] the two reactions can occur successively in a one-pot transformation (Scheme 11). In their simple procedure, activation of an oxime with triflic anhydride leads to the generation of a nitrilium triflate which forms the amide after quenching with water.

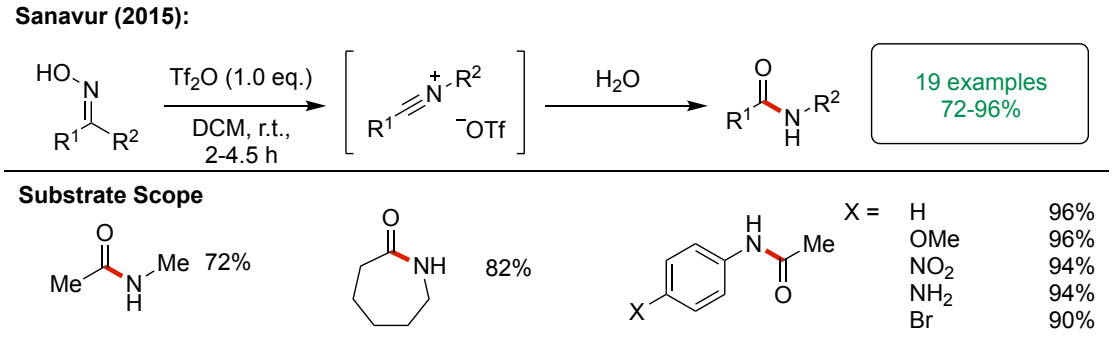

Scheme 11. *General conditions and substrate scope for Sanavur's triflic anhydride mediated Beckmann rearrangement.*

As amides are such a key building blocks in medicinal, agricultural, polymer and supramolecular chemistry, most of the recent developments in Beckmann chemistry still focuses on the fundamental sequence of ketone to oxime to amide. One aspect of this is the development of bespoke catalysts which allow the rearrangement to take place under as mild and as economic conditions as possible. This mostly relies on use of a dehydrating agent such as cyanuric chloride,[35] BOPCl,[36] triphosphazene,[37] TsCl,[38] T3P®,[39] cyclopropenium salts,[40] $[Ph_3PI]^+$, dichloroimidazolidinedione[41] or bespoke esters[42] to initiate a self-propagating reaction mediated by the formation of a substoichiometric amount of imidate.[43]

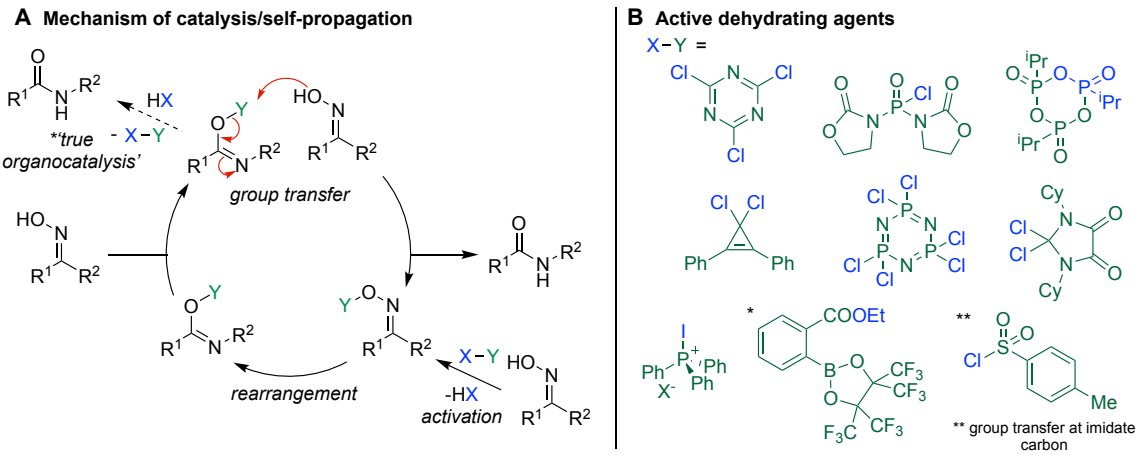

Scheme 12*. General mechanism for catalytic Beckmann rearrangements and the structures of established catalysts.*

Other improvements have focussed on reducing step count by eliminating the need to isolate the oxime intermediate.[44,45] This somewhat blurs the lines between Beckmann and Schmidt reaction, but overall installs an amide through the oxidative rearrangement of a ketone with a nitrogen donor. One of the latest developments

uses nitromethane under reducing conditions to form an acetyl hydroxylamine *in situ* (Scheme 13).[46] This condenses with the ketone to form an *O*-acyl oxime which quickly rearranges to the secondary amide.

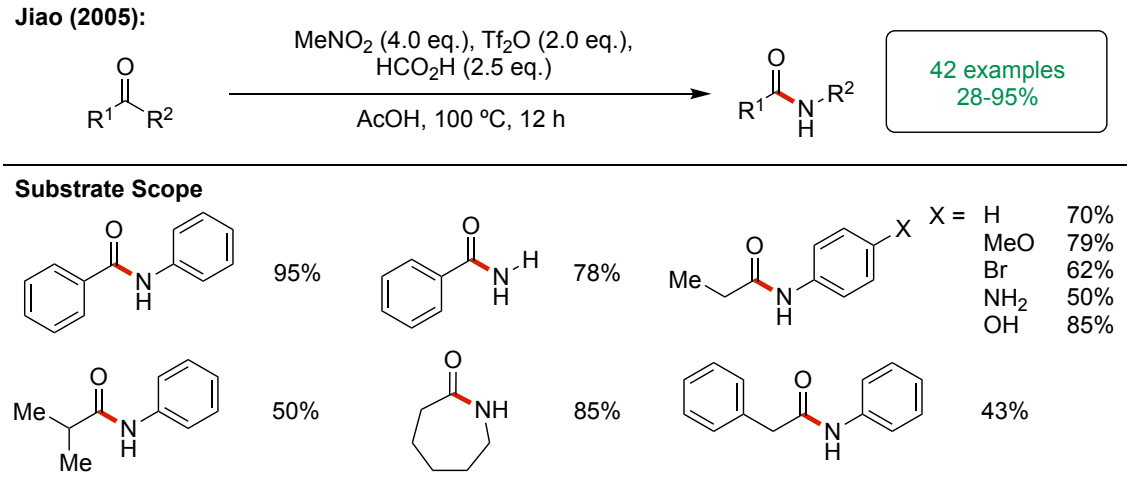

Scheme 13. *A one-pot nitrogen insertion via a Beckmann-type reaction.*

3.1.3 Reductive Beckmann Rearrangements

To widen the scope of the Beckmann rearrangement, efforts have been made to develop a reductive variant, to form an amine product rather than an amide. A simple but convenient example is the Yamamoto group's 1984 DIBAL-H mediated transformation (Scheme 14).[47] The original article was limited in content, however some years later Cho and co-workers revisited the methodology and applied it to heterocycles relevant to medicinal chemistry.[48,49] The scope was restricted to bicyclic and tricyclic oximes with an aromatic migrating group, however ethers, thioethers, indoles and benzothiophenes were all tolerated in the rearrangement. This form of molecular editing was used to probe structure-activity relationships of vasopressin analogues.[50]

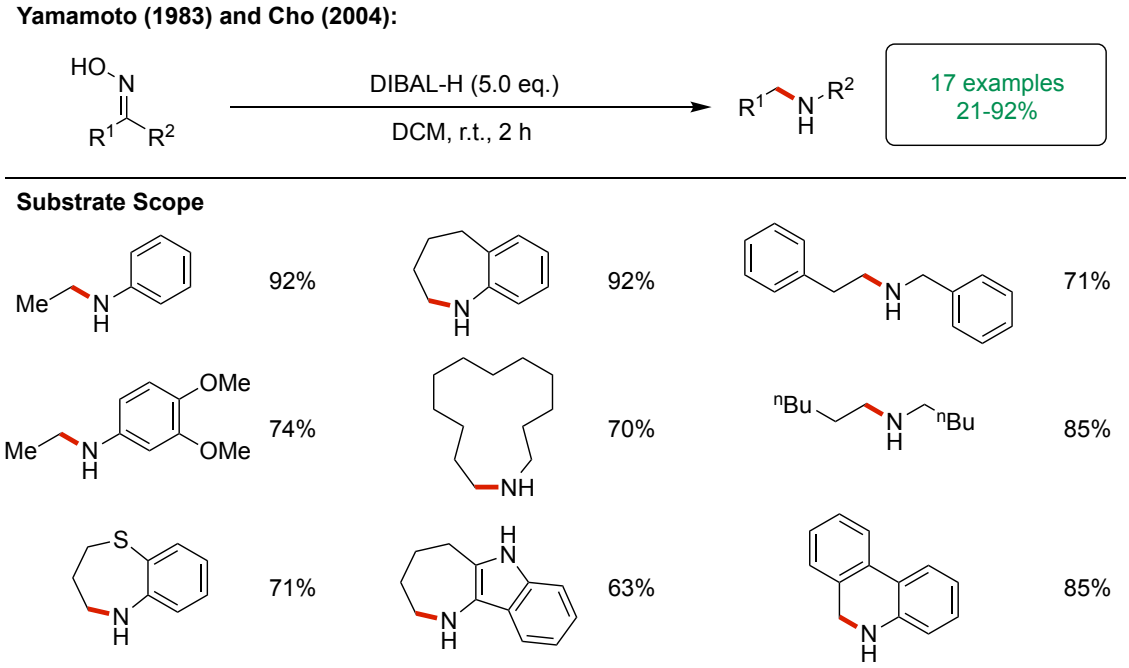

***Scheme 14**. General conditions and substrate scope for Yamamoto's DIBAL-H enabled reductive Beckmann rearrangement.*

Interestingly, despite using a mixture of oxime isomers, the migration occurred with complete regioselectivity. In the proposed mechanism (Scheme 15),[51] the first equivalent of DIBAL-H reacts with the acidic oxime proton to liberate hydrogen and the second reduces the oxime to the hydroxylamine. Due to bond rotation around the newly formed sp^3 centre, both R groups can migrate, and the selectivity is derived from the ability of each group to stabilise a build-up of positive charge in the transition state. The resultant imine-aluminate complex is then reduced with a third DIBAL-H equivalent and a final treatment with sodium fluoride liberates the free amine.

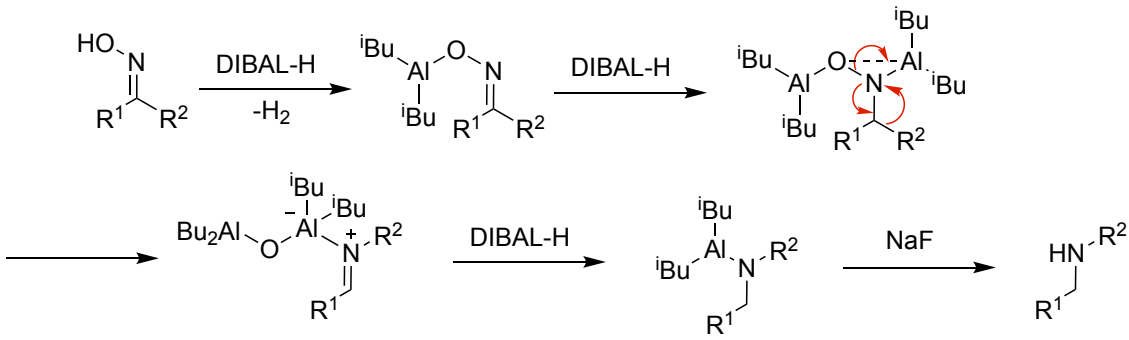

***Scheme 15**. Mechanism for the DIBAL-H mediated reductive Beckmann rearrangement.*

A second reductive Beckmann rearrangement has also been developed for the synthesis of tethered anilines. As Ortiz-Marciales and co-workers described,[52] silylated oximes reductively rearrange upon treatment with a combination of boron trifluoride and borane. However, many side reactions occur, limiting the scope of the protocol. For instance, the synthesis of primary amines from complete reduction of the oxime was a persistent problem with TBS oximes and was further exacerbated if the BF_3 was added before the borane. However, formation of primary amines was completely suppressed using more sterically hindered TIPS protected oximes.

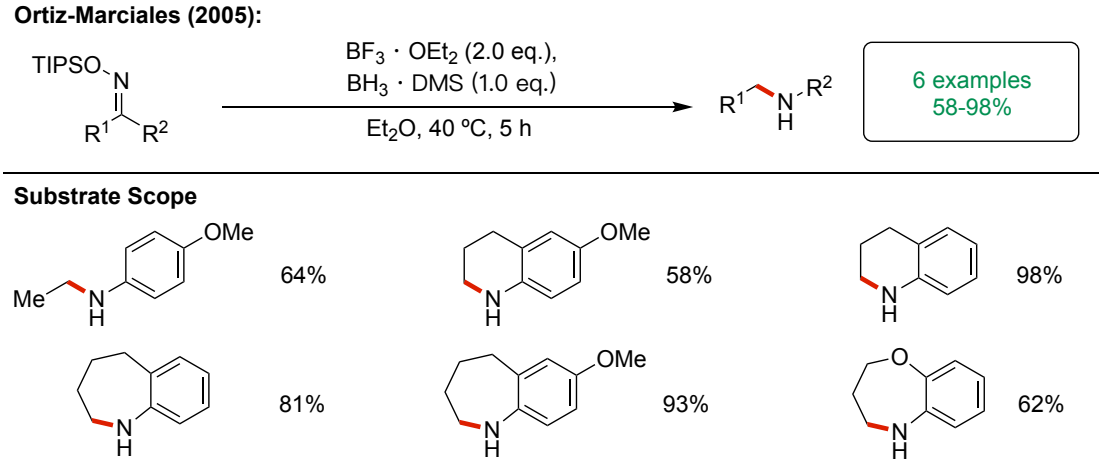

***Scheme 16**. General conditions and scope for the Ortiz-Marciales reductive Beckmann rearrangement.*

Whilst each of these methods give an interesting and novel way to introduce an anime into a carbocycle, the reactions have very niche applications. Firstly, the reported substrate scope in both cases is very limited and yield is considerably variable. Secondly the use of excess strong reducing agents has consequences for functional group tolerance and the atom economy of the reaction. Also, in the BF_3 enabled mechanism, synthesis of the silylated oximes required an additional step which is detrimental to the overall step economy.

3.2 Project Aims

In recent years and particularly over the last decade there has been a resurgence of new chemistry based on nitrilium and keteniminium ions.[2,3] To these reactive intermediates, a plethora of reagents can be added including heteroatom nucleophiles,[53] organometallics,[21,54–58] arenes,[59,60] alkenes,[61] enolates,[62–64] enamines[65–67] and hydrides.[22–25] Furthermore, these powerful electrophiles have enabled the development of new concepts in synthetic methodology including umpolung reactivity of amides,[68] novel pyridine syntheses[69] and enantioselective pyridine activation.[70]

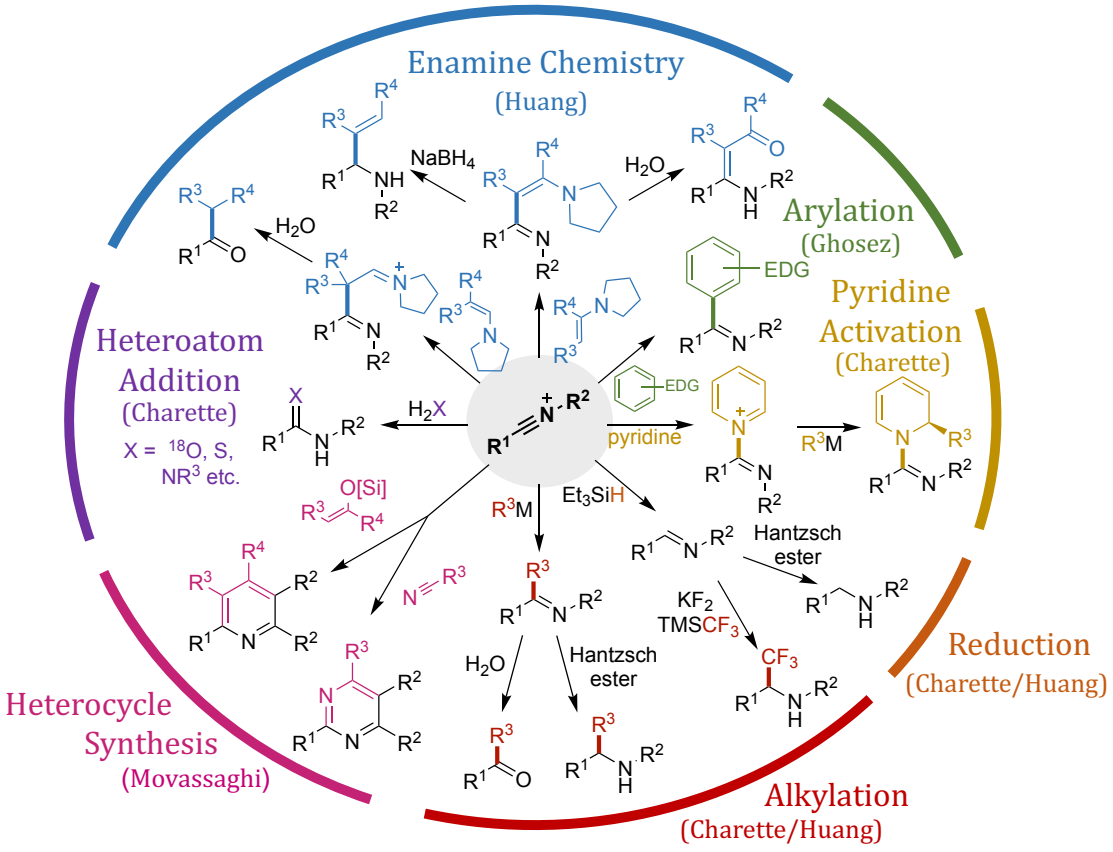

Scheme 17. *A summary of some of the key reactivity of nitrilium ions.*

In all these examples, nitrilium and keteniminium ions are invariably accessed from amide activation. This project aims to generate nitrilium ions from an interrupted Beckmann rearrangement as an alternative and complementary method, which will allow this chemistry to be used more widely. In principle, any of the nucleophiles which have previously been used with nitrilium ions could then be added, but for simplicity the project will begin with the addition of hydrides to make secondary amines.

Although this approach is unlikely to replace general, well-established methods for amine synthesis (alkylation, reductive amination, Buchwald-Hartwig cross-coupling etc.) it may give strategic advantages through its alternative retrosynthetic disconnection. Ketoximes are stable starting materials which are readily accessed from the condensation of a ketone and hydroxylamine- typically in high yields. Ketones themselves are also incredibly versatile reagents, with many diverse syntheses and extensive methods for functionalisation. Additionally, the Beckmann rearrangement belongs to a rare subset of reactions involving the insertion of atoms into a carbon-carbon bond. This unusual feature can constitute an expedient way of accessing larger heterocycles through ring expansion. It may also be a useful method to introduce a nitrogen atom late into a synthesis, with potential applications in late-stage diversification and ^{15}N-isotopic labelling.

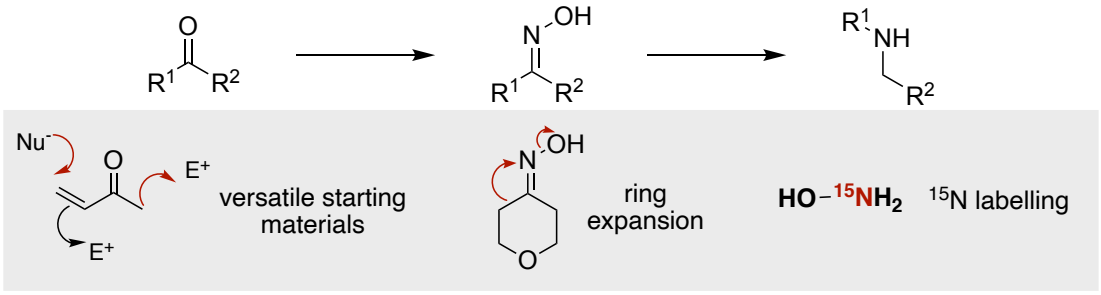

Figure 2. *General sequence for a reductive Beckmann transformation with potential advantages highlighted.*

The proposed reductive Beckmann reaction should be possible by a merger of the triflic anhydride enabled Beckmann rearrangement published by Sanavar and co-workers,[34] and either the Charette[23] or the Huang[24] groups' reduction of secondary amides. Both procedures will be investigated and optimised on a simple substrate before attempting to explore the substrate scope.

Sanavur (2015):

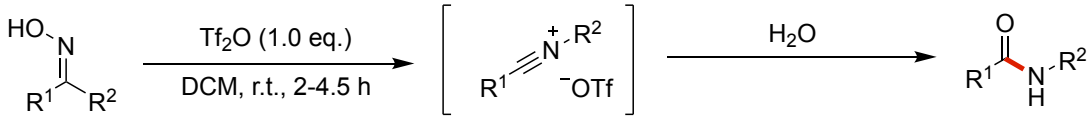

Charette (2010):

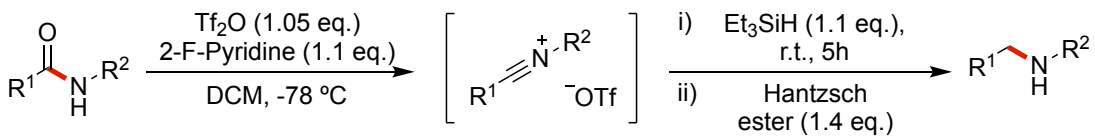

Scheme 18. *Comparison of the Sanavur and Charette reactions, showing both go through the same intermediate.*

3.3 Results and Discussion

3.3.1 Tf_2O-mediated Reductive Beckmann Rearrangement

3.3.1.1 An Interrupted Beckmann Rearrangement

To begin development of the oxime rearrangement, (*E*)-4-fluoroacetophenone oxime, **33**, was chosen as a model substrate as it was already reported to undergo the triflic anhydride-mediated Beckmann rearrangement with 99% conversion in 3.5 hours.[34] Additionally, it could be synthesised as a single disatereoisomer from condensation of the ketone with hydroxylamine and allowed reaction monitoring by LC-MS and ^{19}F NMR spectroscopy.

A small screen was undertaken to investigate optimal conditions for the Beckmann rearrangement (Table 1). In addition to triflic anhydride, milder dehydrating agents were trialled under the same conditions. This included oxalyl chloride and catalytic DMF or triphenylphosphine oxide which previous work in the Denton group had found to enable a dehydrative rearrangement of aldoximes to nitriles.[71]

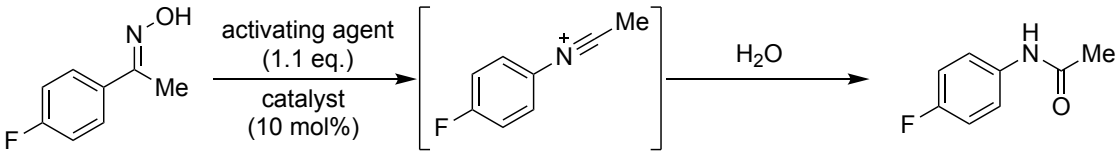

Activator	Catalyst (10 mol%)	Amide (HPLC area) /%
Tf_2O	-	98
Ms_2O	-	91
$SOCl_2$	-	86
$(COCl)_2$	Ph_3PO	0
	DMF	0

***Table 1**. Attempted optimisations of a dehydrative Beckmann rearrangement using HPLC area as a measure of conversion.*

After 15 hours, an NMR of the crude reaction mixture was taken, and a quenched aliquot was analysed by LC-MS. Although not quantitative, a comparison of the LC-MS UV peak areas revealed that after quenching, triflic anhydride appeared to give high conversion of the oxime **33** to amide **34**. In comparison, mesic anhydride and thionyl chloride were both competent activating agents, but also gave numerous unidentified side products. Furthermore, reactions with oxalyl chloride did not

seem to give any product. The same trends were apparent in the crude NMR samples, with numerous unidentified products observed in the spectra for mesic anhydride, thionyl chloride and oxalyl chloride. However, even with triflic anhydride, four aryl fluoride ^{19}F NMR signals were detected (Figure 3), suggesting the mechanism is not as straightforward as Sanavur and co-workers proposed.[34] Despite this, in all further reactions Tf_2O was used to initiate the Beckmann rearrangement as it gave the cleanest reactions and the procedure is almost identical to the conditions used in amide activation. It was subsequently found that the Beckmann rearrangement is very fast, allowing the reaction time to be decreased to 10 minutes at -16 °C which is more comparable to the amide activation performed by the Charette group.[23]

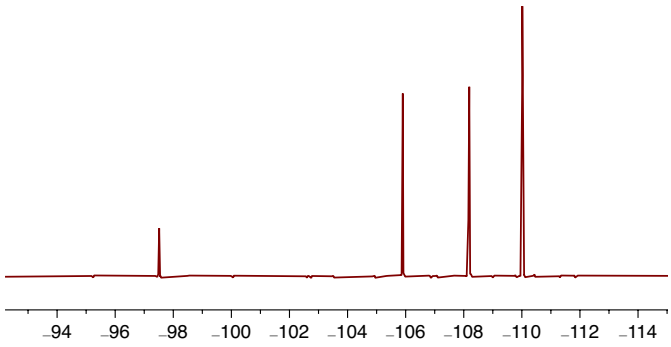

Figure 3. *$^{19}F\{^1H\}$ of the crude reaction mixture of oxime **17** after activation with Tf_2O.*

3.3.1.2 Reduction of Nitrilium ions

With a workable Beckmann rearrangement in hand, attention shifted to the implementation of a reduction for the nitrilium ion. This was first attempted with sodium borohydride since the Huang group had reported its use for the reduction of nitrilium ions.[24]

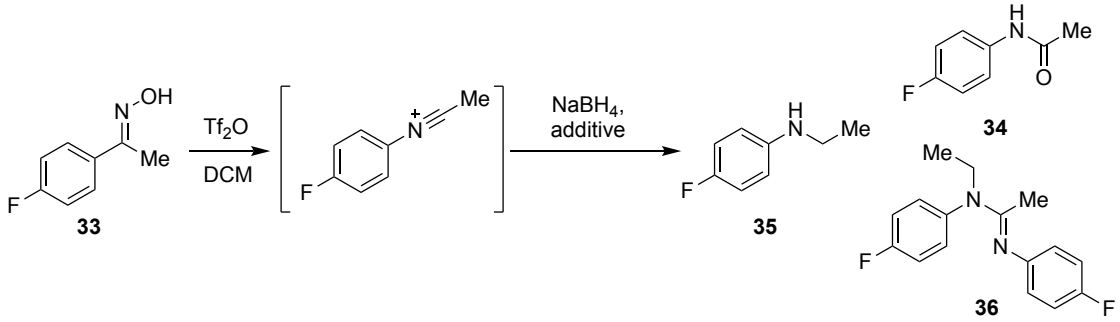

Additive	NMR Yield /%			Theoretical amine after hydrolysis /%
	Amine **35**	Amide **34**	Amidine **36**	
	32	42	2	33
^{i}PrOH (2.0 eq.)	34	44	18	43
CF_3CH_2OH (4.0 eq.)	38	39	0	38
THF (31 eq.)	48	39	0	48

***Table 2**. Reduction of the nitrilium ion to a mixture of products under the conditions of Huang and co-workers.*

However, despite rigorous drying of the solvents and glassware, the reduction did not go smoothly and was plagued by hydration of the nitrilium and formation of amide. One rationalisation for this is that, without a co-solvent the sodium borohydride was poorly soluble, so it was likely that the reduction was slow. To improve reactivity, two equivalents of isopropanol were added with the hope of bringing the reducing agent into solution and forming the more active borohydride ester. However, almost no improvement was observed, with the alcohol presumably adding to the nitrilium ion to form an imidate intermediate. Even using rigorously dried THF and closely following the Huang group's procedure, amide formation could not be avoided. It is not known why yields were poor, however it may stem an underappreciated complexity of the oxime activation, since Huang reported the a near identical amide, acetanilide, in a 78% yield.[24]

Turning to a set of mild conditions developed by the Charette group, triethylsilane was used to reduce the nitrilium ion to an imine followed by further reduction with a Hantzsch ester.[23] Using the literature conditions, the amine was formed in only 33% yield with the amide and a large unidentified impurity still present (Table 3). This is a sizeable reduction from the 71-90% yields that the Charrette group reported, including with many anilines.

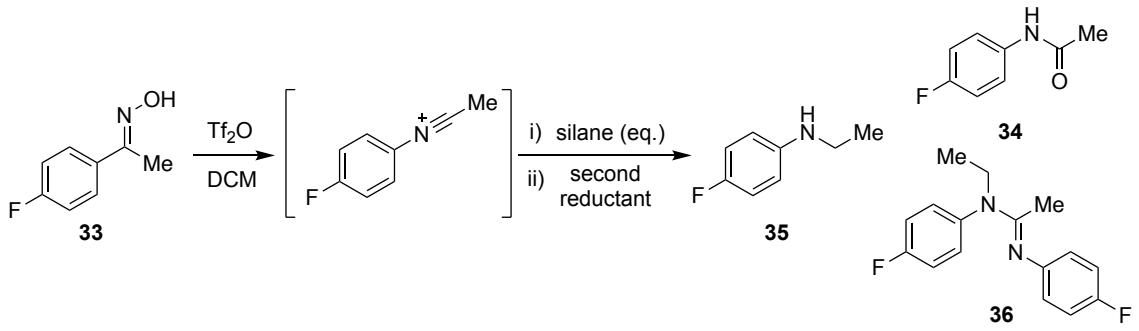

Silane (eq.)	Second reductant (eq.)	NMR Yield /%			Theoretical amine after hydrolysis /%
		Amine **35**	Amide **34**	Amidine **36**	
Et_3SiH (1.1)	Hantzsch ester (1.4)	33	33	0	33
Et_3SiH (1.2)	$NaBH_4$ (1.0), THF	64	20	0	64
TMDS (2.2)	-	57	0	41	77.5
TMDS* (2.2)	-	70	9	15	77.5

***Table 3**. Optimisation of silane mediated nitrilium ion reduction. *Reaction warmed from -45 ℃ to room temperature. NMR yield was calculated using an internal standard of α,α,α-trifluorotoluene.*

A mixed procedure was also investigated using triethylsilane and sodium borohydride, and this gave an improved 64% NMR yield (Table 3). In this reaction, a crude NMR was taken before the addition of sodium borohydride. Unlike as described in the literature, no iminium was present, and it appeared that the nitrilium ion was being reduced directly to the amine. Using TMDS alone – a more sustainable and more reducing hydride – the nitrilium ion could be directly reduced to the amine in a 57% yield over 5 hours. Rather than forming any amide, an amidine was the main side-product in the reaction, which presumably results from the formation of an amine in the presence of a nitrilium ion. However, the selectivity could be improved and amidine minimised by slowly warming the reaction from -45 °C to room temperature.

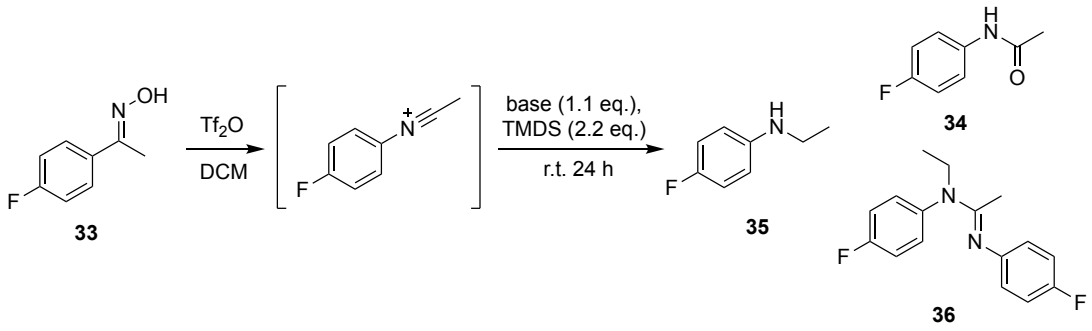

Base	NMR Yield /%			Theoretical amine after hydrolysis /%
	Amine **35**	Amide **34**	Amidine **36**	
-	40	22	34	57
2-F Pyridine	22	30	31	37.5
2-Cl Pyridine	12	13	27	25.5
2-Br Pyridine	14	13	20	24
2-I Pyridine	18	19	9	22.5
PCy_3	28	46	0	28
PPh_3	0	70	0	0
$P(4\text{-}C_6H_4CF_3)_3$	27	61	4	29
$P(C_6F_5)_3$	42	29	16	50

***Table 4**. The effect of base on the reductive Beckmann rearrangement with (E)-4-fluoroacetophenone.*

A minor difference between the developed conditions and the original procedure is that the Charette group[23] used 2-fluoropyridine as a non-nucleophilic base which they found was required to fully activate the secondary amide. In contrast, the procedure used by the Sanavur group did not require a base to initiate the Beckmann rearrangement.[34] Nevertheless, to investigate the effect of buffering the reaction media a number of weak bases were screened under the reaction conditions. It was found that a series of 2-halopyridines did not improve the selectivity of the reduction and furthermore, yields diminished with increasing pyridine basicity. Phosphines also gave reduced yields, although the effect was smallest for $P(C_6F_5)_3$ which itself is a poor base.

The growing disparity between the observed and literature reactivity brought into question whether (*E*)-4-fluoroacetophenone oxime (**33**) was truly a representative substrate. Although benzamides were used by the Charette group,[23] the alkyl group was always larger than an ethyl, which may have suppressed formation of the amidine through steric crowding. Therefore, (*E*)-L-menthone oxime (**37**) was synthesised as it was aliphatic, structurally very different and the steric demand of

the isopropyl group allowed preferential formation of one oxime from its condensation with hydroxylamine.

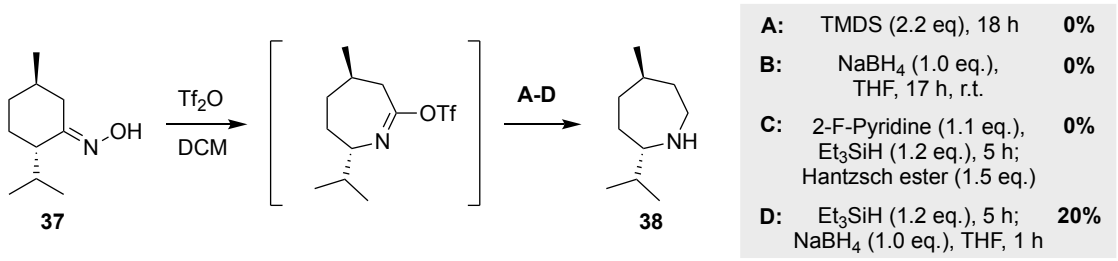

***Scheme 19**. Different conditions for the reductive Beckmann rearrangement on (E)-L-menthone oxime and their yields.*

Upon subjection of the oxime to the previously optimised conditions (Scheme 19, **A**), no amine was isolated following an acid-base work-up. The same was true using the Huang group (**B**) or the Charette group's original conditions (**C**) however a 20% yield was achieved using a combination of both procedures (**D**). Interestingly, in the silane mediated reductions, before the addition of the second reductant, the crude ^{1}H NMR showed a dddd at 8.9 ppm which was consistent with iminium ion **39** (Figure 4).

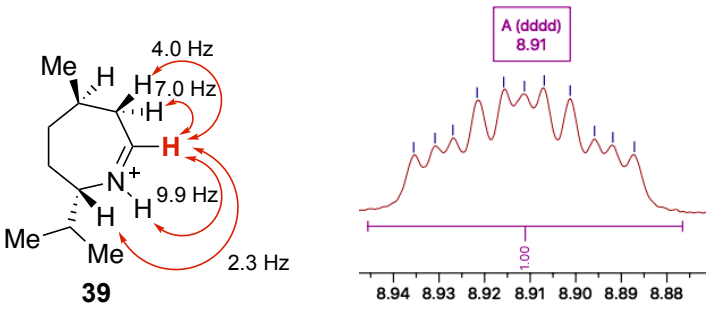

***Figure 4**. Iminium ion (**39**) and its diagnostic ^{1}H NMR peak.*

To obtain slightly simpler NMR spectra the substrate was changed again; this time to the symmetrical dicyclohexyl carbonyl oxime (**40**). Using *p*-difluorobenzene as an internal standard, the hydrosilylation was repeated and gave quantitative formation of the iminium ion after 5 hours with triethylsilane.

Zinc-Catalysed Hydrosilylation

Following the development of an effective iminium ion synthesis, only the final reduction remained. There are many procedures to reduce iminium ions but based

on the previous step, one of the most convenient seemed to be a catalytic hydrosilylation. In this regard, zinc acetate was an ideal choice because, as well as being inexpensive and non-toxic, recent work by both the Beller[72] and the Denton[73] groups had shown that it was a powerful catalyst for silane-mediated amide reduction.

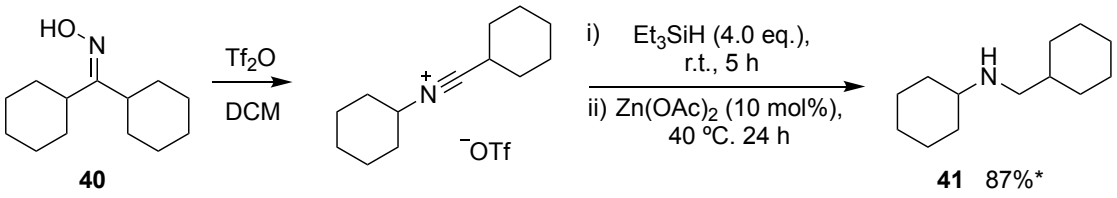

***Scheme 20**. Zinc-catalysed reductive Beckmann rearrangement on dicyclohexylcarbonyl oxime **40**. *NMR yield.*

Pleasingly, after 24 hours at 40 °C the reduction of the nitrilium ion with 10 mol% $Zn(OAc)_2$ gave the desired amine in an NMR yield of 87% (Scheme 20). However, the reaction was slow, giving only 67% after 16 hours. To try and increase the rate of reaction a short optimisation of the silane was performed (Table 5).

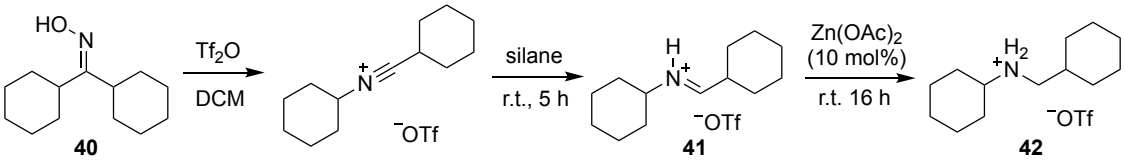

Silane	Equivalents	Iminium (**42**) at 5 h /%	$Zn(OAc)_2$	Ammonium (**43**) at 16 h /%
Et_3SiH	2	77	✓	69
	4	83	✓	77
			×	0
TMDS	2	84	✓	90
	4	89	✓	69*
			×	13
$PhSiH_3$	2	23	✓	0

***Table 5**. Optimisation of the silane in the reductive Beckmann rearrangement of dicyclohexyl carbonyl oxime. *Internal standard signal obscured by ammonium N-H peak.*

Although the Denton group had previously found phenylsilane to be the optimal reducing agent for amides, [73] in this reaction, neither the amine nor the ammonium salt was present after 16 hours. TMDS and Et_3SiH fared much better. Reduction with

triethylsilane was slightly slower but did not give any imine reduction in the absence of a catalyst. In contrast, TMDS was less selective but more reactive, giving slightly higher yields than triethylsilane at every stage (except where the peak of the NMR standard was obscured). A final optimisation of the reaction parameters allowed the catalyst loading to be reduced to 2.5 mol% and the concentration to be increased to 0.4 M with a reaction temperature of 35 °C.

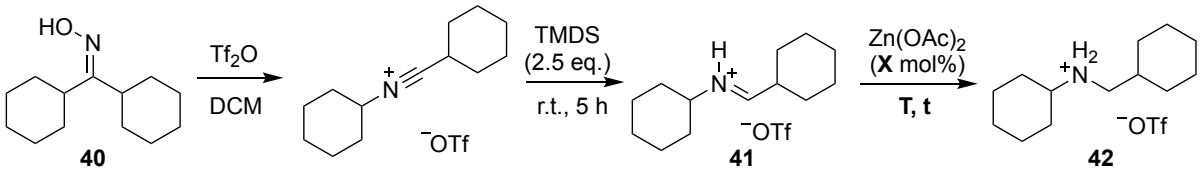

Concentration /M	Catalyst loading /mol%	Temperature /ºC	Time /h	Yield /%
0.25	1.0	r.t.	32	77
0.25	2.5	r.t.	16	65
0.25	2.5	35	16	77
0.40	2.5	35	16	87

***Table 6**. Optimisation of the conditions for the reductive Beckmann rearrangement of dicyclohexyl carbonyl oxime.*

DCM had been used as the reaction solvent as it in previous reports by Charette and Huang it had repeatedly been found to be the optimal solvent for Beckmann rearrangements and for amide activation.[22,74,75] Consequently, a solvent screen was not performed, however in recognition of DCM's less sustainable properties, trifluorotoluene was trialled as less toxic, higher boiling replacement.[76] Based on the poor solubility of the iminium salt, higher temperatures were required for the second reduction which allowed the product was recovered in a 79% yield; only 8% lower than using of DCM (Table 7). Despite the challenges to sustainability, DCM was used in further optimisation due to the more convenient reaction conditions, boiling point, ^{1}H NMR properties, and increased yields.

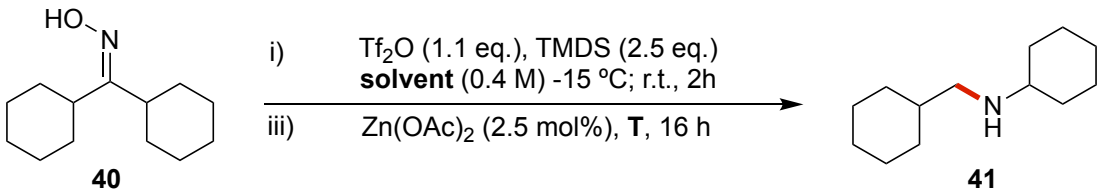

Solvent	Temperature /°C	Yield /%
DCM	35	87
trifluorotoluene	65	79

Table 7. Comparison of the yield for the reductive Beckmann reaction in DCM and trifluorotoluene.

Finally, under the new reaction conditions the use of mesic anhydride as the activating agent was revisited. Although, using 4-fluoroacetophenone (**33**), the activation mixture had seemed more complex, mesic anhydride bares structural similarities to triflic anhydride and gave the next highest conversions. It also much milder and, as a solid, it has practical advantages over handling triflic anhydride which is a volatile and highly reactive liquid.

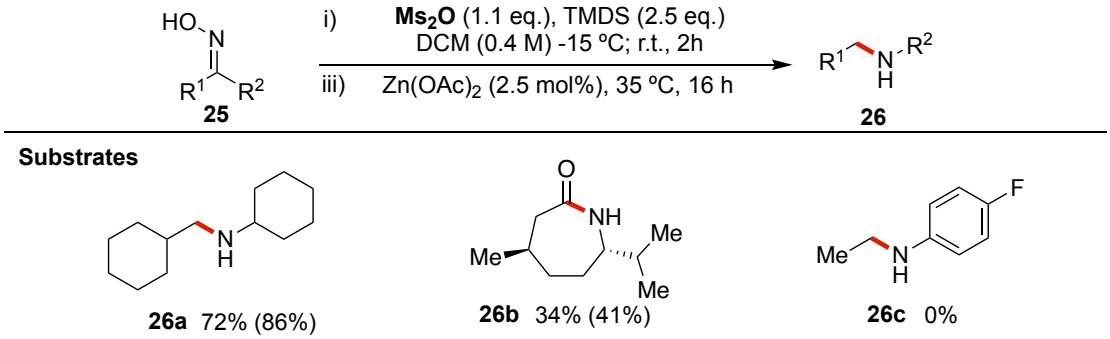

Scheme 21. *Attempted reductive Beckmann reaction with Ms_2O rather than Tf_2O. NMR conversions in parentheses ().*

Although the initial result with dicyclohexanone oxime (**40**) encouragingly gave a 72% isolated yield, the reaction of (*E*)-menthone oxime gave the amide as the only isolable material. Furthermore 4-fluoroacetophenone (**33**) gave a mixture of species by ^{19}F NMR spectroscopy which mainly converged to the amide after work up with no observable product. Use of triflic anhydride was therefore continued in subsequent reactions.

3.3.4 Substrate Synthesis and Scope

With a firm proof-of-concept of the reductive Beckmann rearrangement in hand, a diverse series of oximes were synthesised through the condensation of ketones with

hydroxylamine. Focus was placed on the synthesis of cyclic oximes, as ring expansion is a key aim of this methodology. Therefore 12 cyclic oximes were prepared containing reducible functional groups, electron withdrawing groups and caged structures. Electron-rich and electron-deficient aryl oximes were also synthesised to examine the synthesis of anilines, as well as an α,β-unsaturated ketones to investigate the extent of reduction. In a slightly modified procedure, ^{15}N-labelled cyclohexanone oxime (**46g**) was prepared using just 1.05 equivalents of $^{15}NH_2OH{\cdot}HCl$, reflecting its high cost.

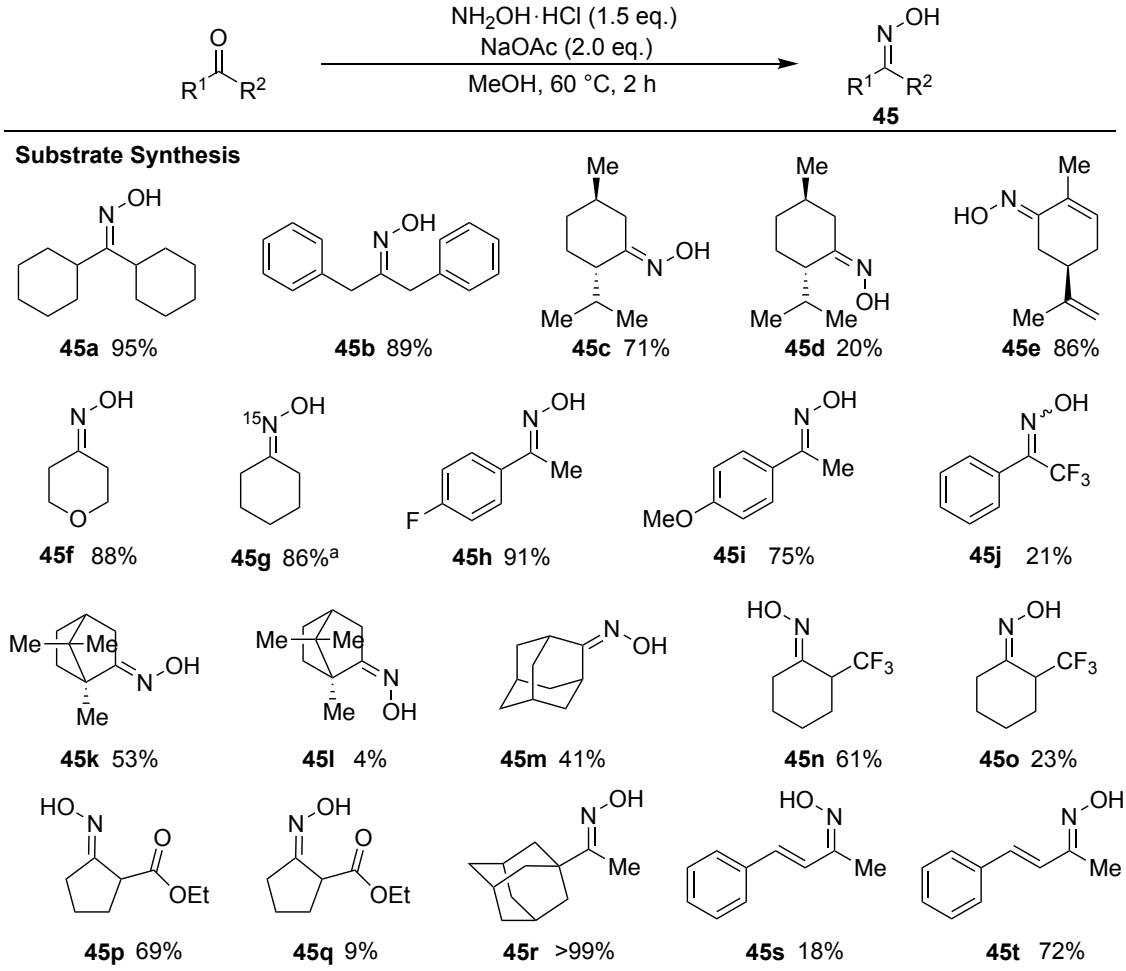

Scheme 22. *Scope of oxime synthesis under standard conditions.* [a] *$^{15}NH_2OH{\cdot}HCl$ (1.05 eq.) and NaOAc (1.20 eq.) were used.*

Generally, using a standard procedure, yields were good to excellent and where mixtures of diastereoisomers formed, separation was usually possible by flash column chromatography. The reaction predominantly gave (*E*)-selectivity and was strongly influenced by sterics as can be seen for **45d** and **45e**, or **45r**. Aryl oximes

gave complete (*E*)-selectivity except for trifluoroacetophenone oxime (**45j**) which formed an a 79:21 ratio of diastereoisomers in an inseparable and rapidly hydrolysed mixture. Some of the lowest yields were given for sterically encumbered, bridged bicyclic ketones such as **45k**, **45l**, and **45m**.

17 of these oximes were then subjected to the optimised reductive Beckmann conditions and, of these, 9 gave the desired secondary amines in yields of 17-87% (Scheme 23). Good yields were established for simple cyclic and acyclic substrates (**46a**, **46b** and **46c**). For dibenzyloxime (**46b**), yield was slightly lower, which may be due to low-level Bischler-Napierlski-type reactivity or Beckmann elimination: although products of these reactions were not observed. Use of both (*E*)- and (*Z*)-menthone oxime (**45b** and **45c**) showed the reaction was regiospecific, and furthermore, isolation of single diastereoisomers precluded epimerisation of either stereocentre.

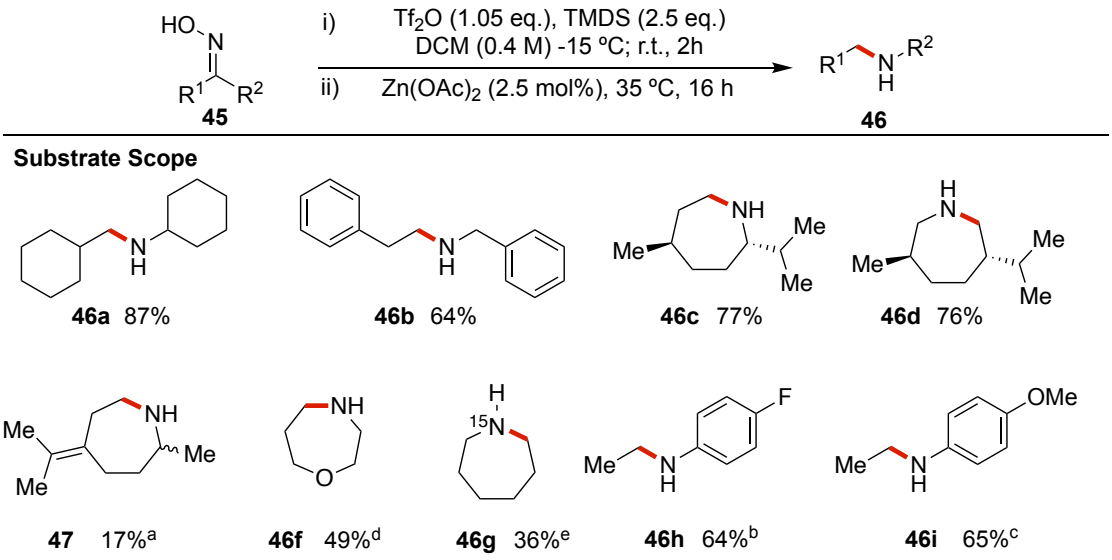

***Scheme 23**. General reaction conditions and preliminary substrate scope for the zinc-catalysed reductive Beckmann rearrangement. [a] TMDS (3.5 eq.); [b] Et_3SiH (2.5 eq.) -15 °C 16 h; [c] TMDS (2.5 eq.) -15 °C 16 h; [d] isolated as HOTf salt; [e] isolated as Boc adduct.*

Carvone oxime (**45e**) was chosen as substrate because in the standard Beckmann conditions the rearrangement of cyclohexenone oximes can compete with the Semmler-Wolff aromatisation (Scheme 24).[77,78] Furthermore, in this system, reduction of the endocyclic and terminal alkenes both seemed plausible *via* enamine or carbocation intermediates. However, the only secondary amine isolated was **47**, resulting from the reductive Beckmann reaction, enamine reduction and alkene

migration. No aromatic protons were visible in the crude NMR spectrum, and the fully reduced azepane was not detected by mass spectrometry, ruling out the Semmler-Wolff or alkene reduction as major side reactions. Nevertheless, the poor yield likely occurs due to numerous side reactions which can compete with the productive reaction.

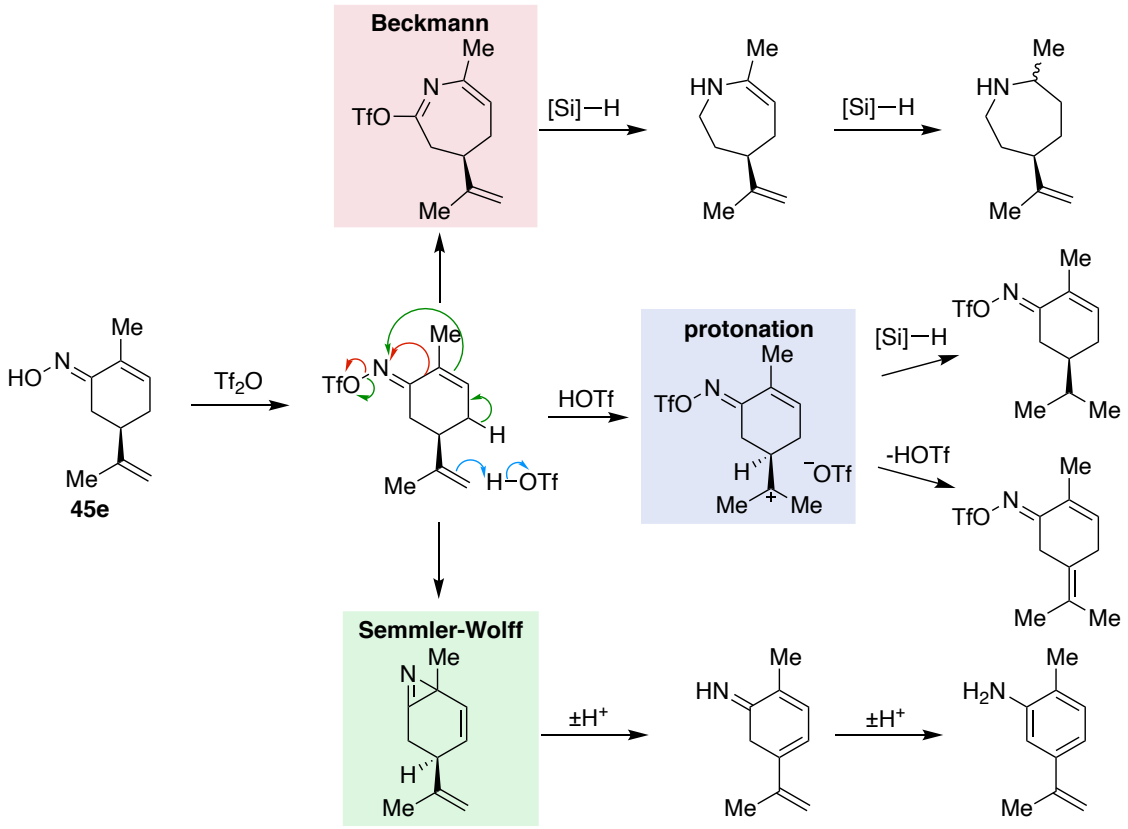

Scheme 24.*Possible pathways in the reductive Beckmann reaction of (E)-carvone oxime,* ***45e****.*

Cyclic oximes with fewer substituents also gave the desired reactivity, yielding homomorpholine (**46f**) and ^{15}N-azepane (**46g**), although the isolation of these simple products proved challenging. Homomorpholine has high polarity which prohibited an aqueous work up, although direct column chromatography of the concentrated reaction mixture enabled isolation of the product albeit as its triflate salt. Some time was spent developing methods to aid the isolation of **46f**, and more generally to avoid column chromatography with cyclic secondary amines. However, direct attempts at an *in situ* protection through base/anhydrides, base/alkylating agent, benzaldehyde/TMDS all failed; as did purification by crystallisation, Kugelrohr distillation and alumina chromatography.

The azepane was more accommodating of an aqueous work up, however, gave low yields following chromatographic purification, possibly due to its partial volatility (boiling point 143 °C). For this substrate, reaction with Boc_2O was possible after an acid-base work up to give the protected azepane (**48**) in a 36% yield (Scheme 25).

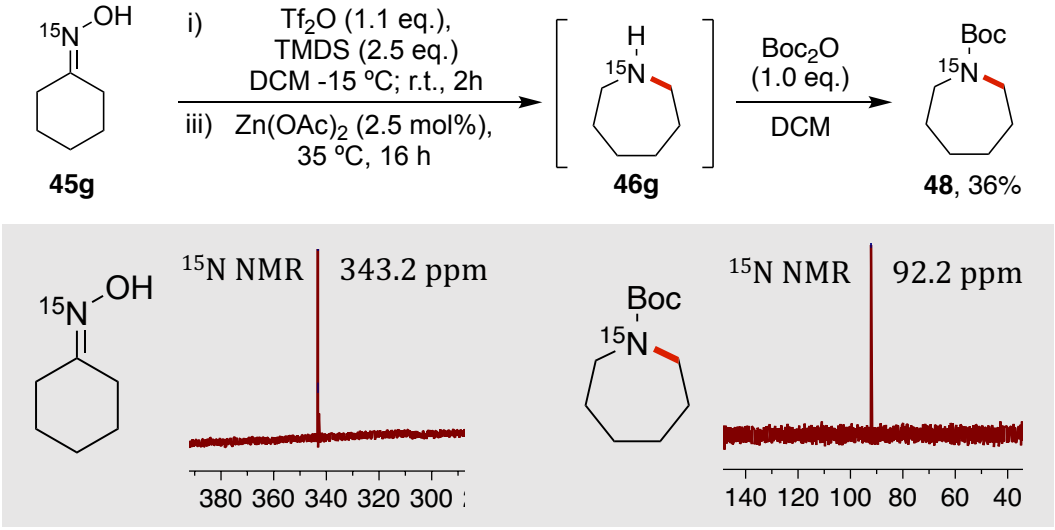

Scheme 25. *Synthesise of ^{15}N-Boc-azepane (**48**) and its ^{15}N NMR spectrum in comparison to the **45g**.*

As discovered in the optimisation, application of this methodology to aniline synthesis suffers from a lack of selectivity of the hydrosilylation, whereby reduction of the nitrilium ion to the iminium ion occurs at a similar rate to reduction of the iminium ion to the ammonium ion. Consequently, amines can be formed in the presence of nitrilium ions, leading to formation of amidines. Selectivity for the amine can be improved using milder reaction conditions, and this approach was used to reoptimize the substrates (Table 8) for electron neutral and electron rich oximes **45h** and **45i** (Hammett constant σ_p = 0.06, -0.27).[79]

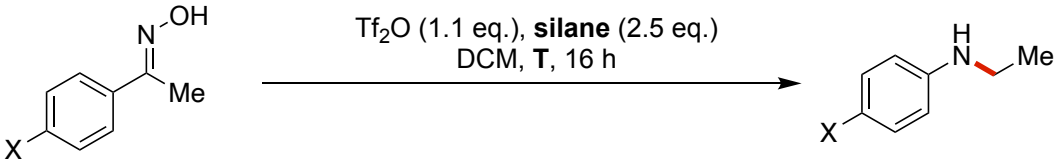

X	Silane	Temperature, T /°C	Yield /%
OMe	TMDS; $Zn(OAc)_2$	r.t.; 35	40
OMe	TMDS	-15	66
OMe	Et_3SiH	-15	34
F	TMDS	-15	60
F	Et_3SiH	-15	64

Table 8. *Optimisation for the reduction Beckman reaction of aryl oximes.*

Similar to the initial optimisation, lower temperatures and Et_3SiH gave better yields of 4-fluoroaniline **46h**. Reduced temperatures also seemed to improve the yield of aryl methoxy ether **46i**, however with triethylsilane, yield dropped significantly and the reaction turned an orange colour. Possibly, this mild silane lowers the rate of hydrosilylation to the point where other side reactions can dominate, especially as in this case anisidine **46i** is highly electron-rich.

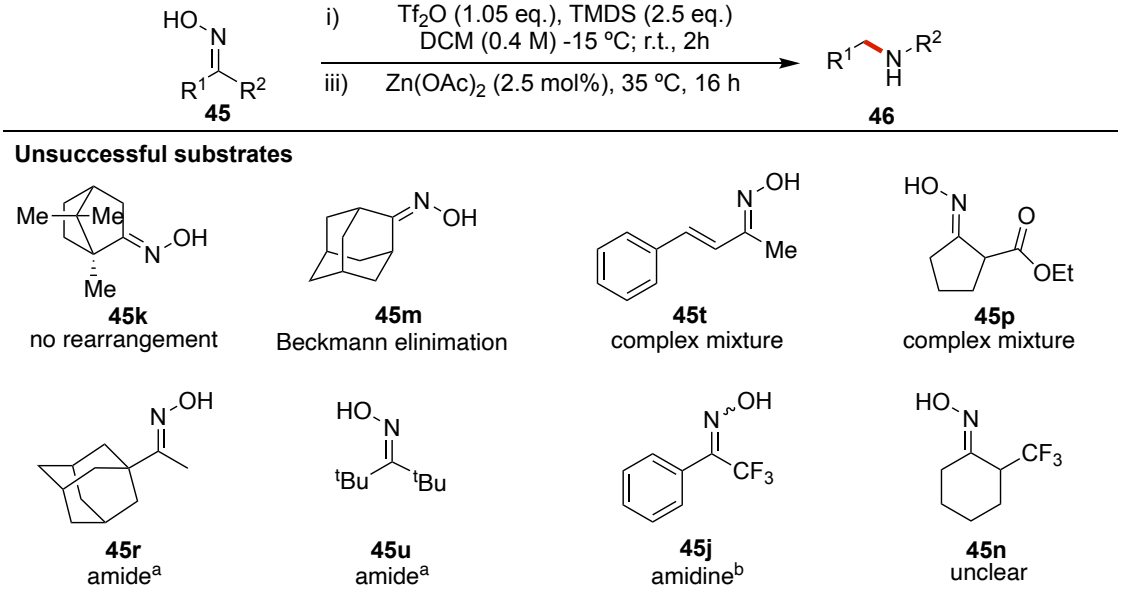

Scheme 26. *Unsuccessful substrates in the reductive Beckmann reaction including major side products where identifiable.* [a] *Products observed by mass spectrometry;* [b] *Products observed by* ^{19}F *NMR spectroscopy.*

A number of substrates failed to give the expected secondary amine product (Scheme 26). (*E*)-camphor oxime (**45k**) was known to be a poor substrate for the Beckmann rearrangement owing to high ring strain in the rearrangement transition state which can only be mitigated by using a nucleophile to generate a tetrahedral intermediate.[33,80] As a result, only the unreacted starting material was recovered despite using triflic anhydride as a powerful activating agent. Tricyclic cyclic oxime **45m**, seemingly tolerated the rearrangement, however only **49** and **50** were isolated from the reaction mixture, indicating Beckmann fragmentation. This potentially results from 2 factors; i) the imidoyl triflate is less stable than the nitrilium ion and ii) the imidoyl nitrogen is conformationally locked in an antiperiplanar position with respect to a hydrogen, leaving no entropic barrier to elimination. Also notable was that the amide was formed in roughly the same yield as the nitrile. This may be explained by the nucleophilic addition of the nitrile to the

imidoyl triflate to generate **51**, which has certainly been previously reported for nitrilium ions (Scheme 27).[81]

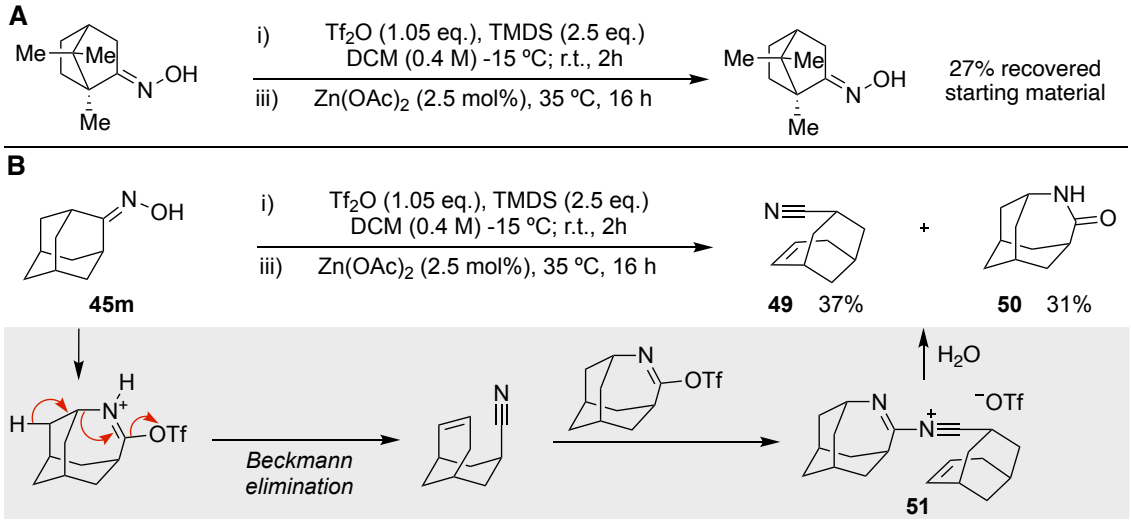

Scheme 27. *The products of the reductive Beckmann.* ***(A)*** *The recovery of (E)-camphor oxime;* ***(B)*** *Rearrangement products of 2-adamantone oxime and a proposed reaction pathway.*

Substrates with α-quaternary centres, **45r** and **45u**, were not viable for the reductive Beckmann reaction, instead giving amides as the major products (identified by mass spectrometry). This was disappointing as a potential benefit of this reaction was the ability to iteratively alkylate ketones which, following rearrangement would give a modular synthesis of α-quaternary amines. Finally, **45t** gave a complex mixture of products, and although a species with the correct mass was recovered for **45p** and **45n**, both were of low yield and purity indicating < 5% conversion.

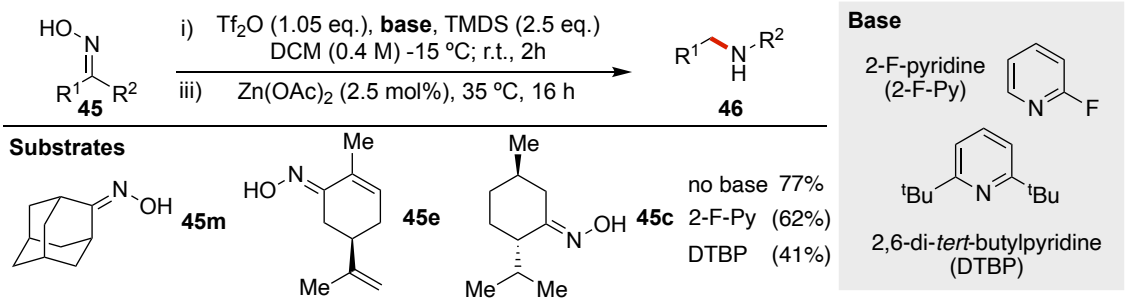

Scheme 28. *Attempted re-optimisation by examining the role of base. NMR yields in parentheses ().*

A short reinvestigation on the inclusion of bases was performed with the aim of minimising acid-catalysed side reactions to increase yield and substrate scope (Scheme 28). Two non-nucleophilic bases with precedent for amide

activation[23,25,82,83] were trialled on the reaction of 3 substrates; 2 which (**45m** and **45e**) resulted in side reactions under standard conditions and one previously successful substrate (**45c**). Both bases were unsuccessful in improving the reactivity for sensitive substrates and furthermore, they diminished the conversion of the **45c** as determined by NMR.

3.3.2 Nitrilium Ion Chemistry through an Interrupted Beckmann Rearrangement

One potential advantage of the interrupted Beckmann rearrangement was the ability to generate highly reactive nitrilium ion intermediates. Reduction of these to the corresponding secondary amines and allowed exploration of the substrate scope of this methodology, however, the diverse reactions of nitrilium ions which were worthy of investigation.

Early development work for the reductive Beckmann reaction showed that using Et_3SiH, nitrilium ions could be selectively reduced to iminium ions in high conversions. Charette and co-workers had demonstrated a similar procedure using amide activation, and found several *C*-aryl imines could be isolated using an aqueous work-up.[23] Applying this to iminium **52** (Scheme 29A) however, led to rapid hydrolysis due to the lower stability of aliphatic imines.[84] Instead, due to the high conversion, it was possible to isolate the iminium triflate by evaporation of the solvent, silane, and silyl triflate by-products at 40 °C under high vacuum for 24 hours.

As nitrilium ions principally react with nucleophiles;[2] amines,[85] thiolates,[86] alkoxides,[87] and ^{18}O-water,[53] have all been reacted to generate the corresponding imidoyl adducts. With confidence in this reactivity, oxime **45r**, which was unsuccessful in the reductive Beckmann, was reacted with Tf_2O followed by addition of pyrrolidine (Scheme 29B). The desired amidine was afforded with 67% yield, with the remaining mass balance being the undesired amide. It was notable that Charrete and Grenon[85] also reported comparable yields (34-84%) from amide activation. This may suggest that in the reductive Beckmann rearrangement of oxime **45r** the reduction is limiting, however additional complexities in oxime activation cannot be ruled out due to the substantial amide formation.

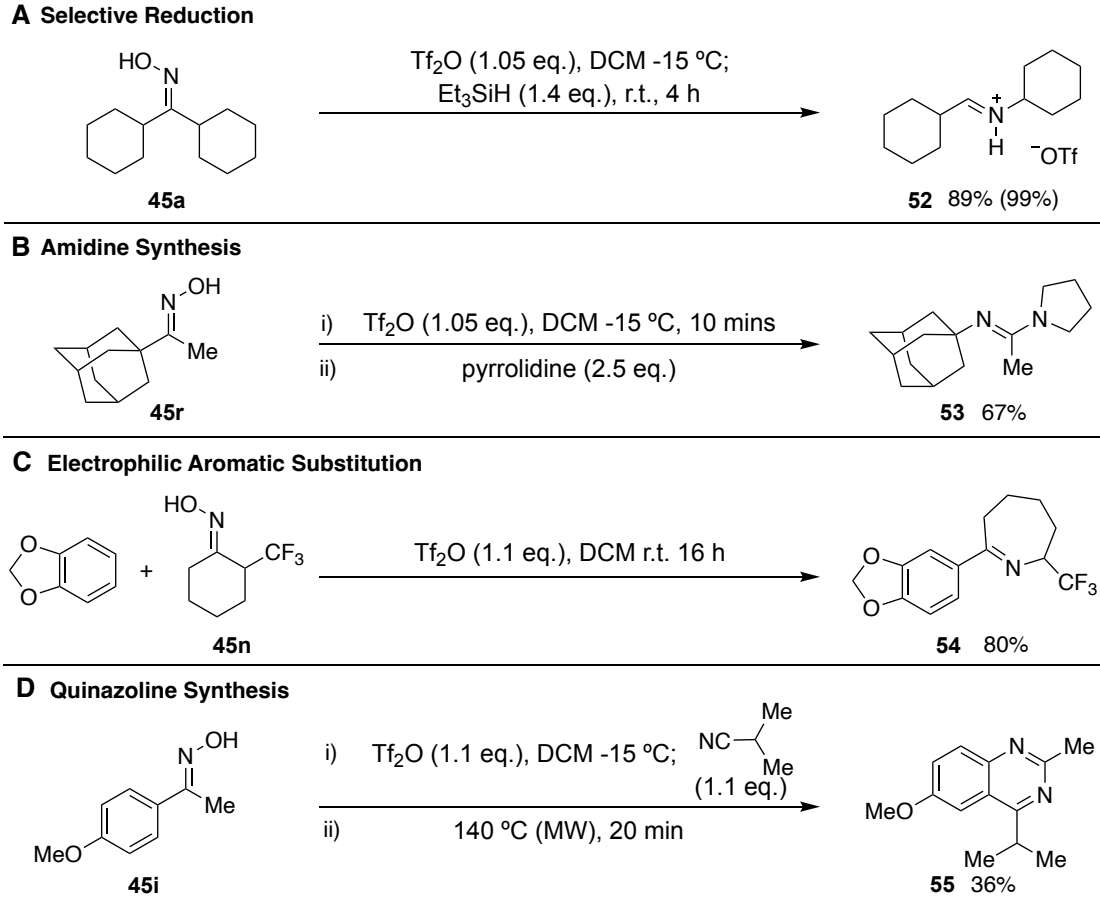

Scheme 29. *Alternative reactions using the nitrilium ion intermediates;* ***(A)*** *Selective reduction to an iminium triflate;* ***(B)*** *Synthesis of an amidine;* ***(C)*** *Electrophilic aromatic substitution;* ***(D)*** *Quinazoline synthesis.*

Nitrilium ions can also participate in electrophilic aromatic substitution – in fact, this reactivity necessitated careful selection of an internal standard. Using 0.5 equivalents of 1,3-benzodioxole to monitor the reductive Beckmann reaction of **45n** (Scheme 29C), a 19% yield (with respect to the oxime) of the S_EAr product was obtained. Interestingly this reactivity was only observed with oxime **45n**, which may reflect the electron withdrawing nature of its trifluoromethyl group. An 80% yield could be obtained when the imine was intentionally made using 1 equivalent of benzodioxole.

Finally, chemical reactivity unique to nitrilium ions was demonstrated through an adaptation of Movassaghi and Hill's quinazoline synthesis.[81] In this reaction, a nitrile adds to an *N*-aryl nitrilium ion followed by electrophilic aromatic substitution to form the aromatic ring. Pleasingly, this could be accomplished using **45i** and isobutyronitrile to give the quinazoline product, albeit in only a 35% yield. Reported yields for this reaction were in the 59-94% range, with 89% for the most similar

substrate. The largest difference between the two procedures was the use of 2-chloropyridine as a base, however as in other oxime activations, this had an inhibitory effect when starting from the oxime (**45i**).

3.3.3 Discovery of a "Dual Catalytic" Reductive Beckmann Reaction

Taking into account both published reductive Beckmann rearrangements and the triflic anhydride enabled reaction, there is no doubt that the limitations to these procedures lie in the scope and functional group tolerance – or lack thereof. Additionally, the requirement for excess strong Lewis acids or stoichiometric triflic anhydride is a barrier to the implementation of this approach in large-scale synthesis.

In recent years a number of procedures have emerged using substoichiometric amounts of dehydrating agents to initiate self-propagating Beckmann rearrangements (Section 3.1.2). In theory, the only by-products of these reaction are the dehydrating agent's hydrolysis products, giving good atom economy for the formation of amides.

It was hypothesised that a reductive Beckmann rearrangement could be affected by the merger of a 'catalytic' Beckmann rearrangement with the Denton group's zinc-catalysed amide reduction (Scheme 30).[73] This may be particularly efficient because the by-products of the 'catalytic' Beckmann are typically acids and, as shown by Stoll *et. al.*, additional carboxylic acids are beneficial to the catalytic amide reduction due to the *in situ* formation of hydrosilyl esters. A similar study conducted within the Denton has recently observed a similar rate enhancement from the formation of hydrosilyl sulfonic acid esters.

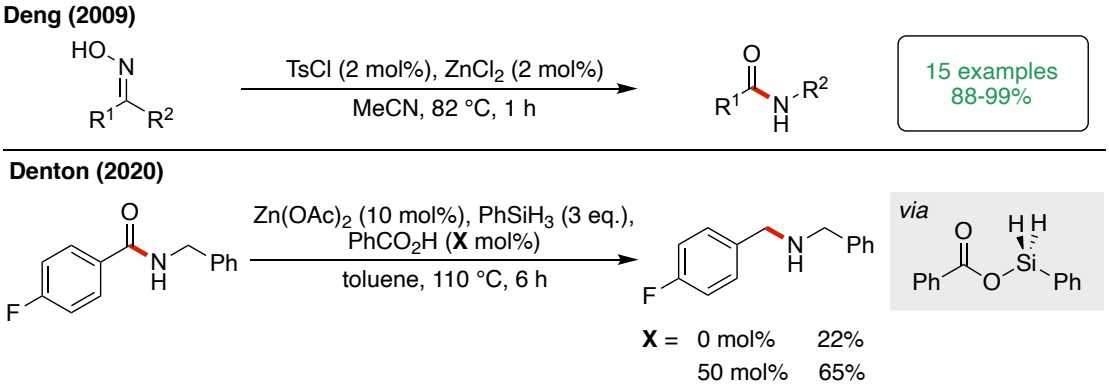

***Scheme 30**. Approached to a 'dual catalytic' Beckmann rearrangement; **(A)** A Beckmann rearrangement using substoichiometric TsCl and; **(B)** A zinc-catalysed amide reduction*

Following a review of reported catalytic Beckmann rearrangements, conditions described by Deng and co-workers seemed most compatible with the amide reduction.[38] Specifically, use of tosyl chloride as the dehydrating agent would generate TsOH as the by-product and furthermore, the rearrangement gave better yields with $ZnCl_2$ as a catalyst.

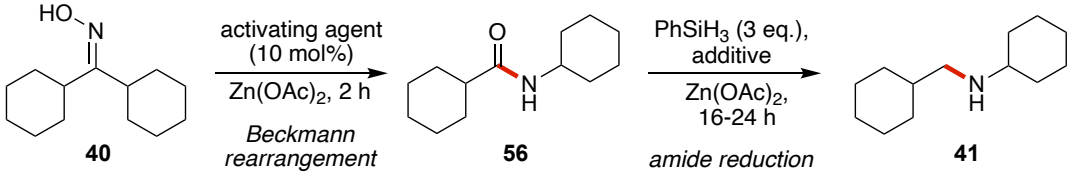

Beckmann Rearrangement				Amide Reduction			
Activating agent	Solvent	$Zn(OAc)_2$ /mol%	Temperature /°C	$Zn(OAc)_2$ /mol%	Additive	Temperature /°C	Yield /%
TsCl	MeCN	10	82	0	-	82	0
Ms_2O	DCM	2.5	40	0	-	40	0
Ms_2O	trifluorotoluene	10	60	0	-	100	55
Ms_2O	toluene	10	60	0	-	111	32
Ms_2O	trifluorotoluene	0	60	10	*N*-methylmorpholoine (10 mol%)	100	79
Ms_2O	trifluorotoluene	0	60	10	$PhCO_2H$ (50 mol%)	100	92
Ms_2O	trifluorotoluene	0	60	10	-	100	94

***Table 9.** Optimisation of a second generation 'dual catalytic' reductive Beckmann reaction.*

Therefore, in a slightly modified procedure, zinc chloride was replaced with zinc acetate and after 2 hours at reflux complete conversion of model substrate **40** to amide **56** was observed. Subsequent addition of phenylsilane however, did not lead to any reduction (Table 9). Encouragingly, substoichiometric mesic anhydride also gave quantitative rearrangement, and this had the benefits of being an easily handled solid which generated two equivalents of sulfonic acid per anhydride.

Although the subsequent amide reduction was not possible in DCM, higher boiling aromatic solvents used by the Denton group, gave the amine in moderate yields. In these solvents the initial Beckmann rearrangement required elevated temperatures to dissolve the oxime.

A further improvement came from the increased segregation of the two steps. Catalytic *N*-methylmorpholine was trialled in the reduction based on the optimised procedure for the reduction of carboxylic acids,[88] whereas a separate addition of carboxylic acid was used to replicate the conditions for reduction of an isolated secondary amide.[73] Both alterations gave improved yields, but the key to each was revealed to be the addition of zinc acetate *after* the Beckmann rearrangement. This was shown in a final control experiment which gave an excellent yield of 94%.

This short investigation provided proof of concept for a more sustainable reductive Beckmann rearrangement which has the potential for widespread us. Due to the time constraints of this PhD studentship, at this stage the project was passed on to a postdoctoral research associate for further development and investigation of the substrate scope. It is anticipated that due to the reduced acidity of the rearrangement and the proven functional group tolerance of the catalytic reduction, a wider variety of substrates may be viable in this reaction. Further advantages include use of non-halogenated solvents, commercial phenylsilane, and substoichiometric mesic anhydride and zinc acetate; both of which are inexpensive and easily handled reagents.

3.3.4 A Reductive Beckmann Approach to the Synthesis of (-)-Meptazinol.

To demonstrate how a reductive Beckmann rearrangement may be implemented in synthesis, a target compound of pharmacological interest was sought. Particular focus was placed on cyclic amines of uncommon ring sizes, which could potentially be problematic to access from conventional C-N bond formation, but for which a ring expansion could be advantageous. To this end, azepanes were attractive, and a suitable target was identified in meptazinol: an active pharmaceutical ingredient which has also been derivatised for prospective multi-target therapies (Figure 5).[89,90]

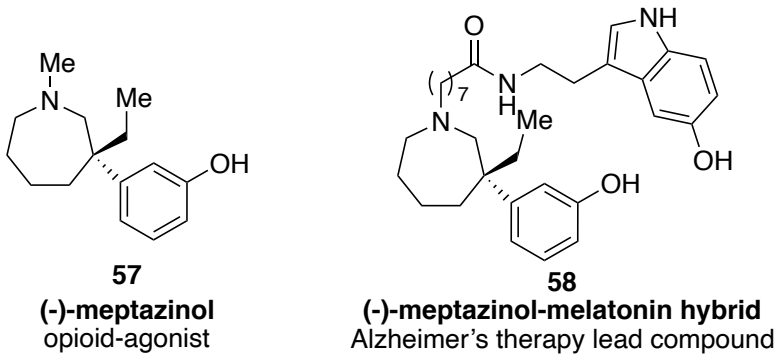

Figure 5. *The structure of meptazinol and a meptazinol-based multi-target-directed ligand as a prospective Alzheimer's therapy.*[90]

Meptazinol is an opioid-type analgesic used for severe postoperative, obstetric or cancer pain which has a low addiction potential and few side effects. It is administered as a racemate; however, the (-)-enantiomer is the more potent opioid-agonist and displays additional analgesic properties resulting from inhibition of acetylcholinesterase.[91,92] Single enantiomers of meptazinol are not commercially available; therefore, to study their properties and develop new lead compounds (such as **58**),[90] resolutions have been developed using either diastereomeric crystallisation, preparative HPLC,[91] or electrophoresis.[93] An enantioselective synthesis has not yet been reported.

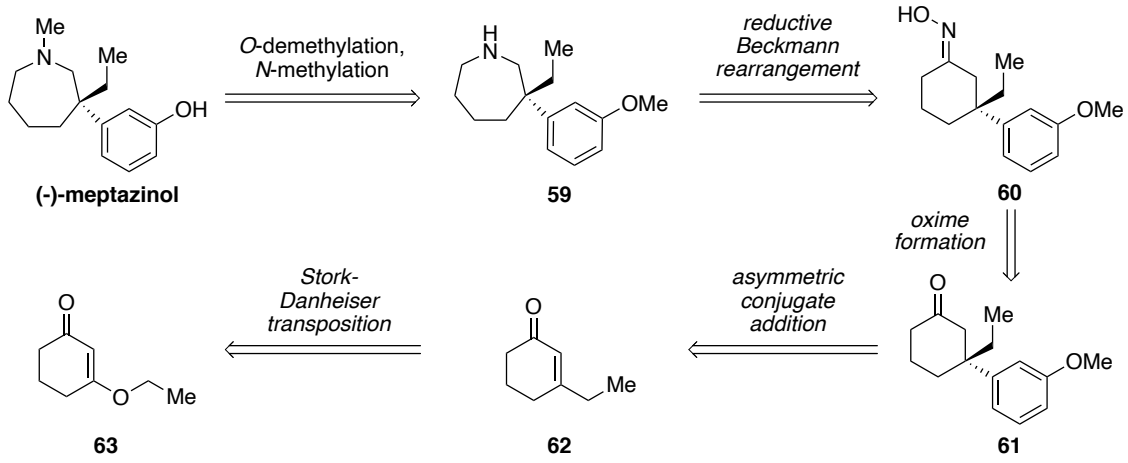

Figure 6. *Retrosynthetic analysis of (-)-meptazinol leading to commercial 3-ethoxycyclohex-2-en-1-one.*

Structurally, meptazinol is a *N*-methyl azepane with a β-quaternary stereocentre consisting of ethyl and 3-hydroxyphenyl groups which branch from the cyclic core. It was envisaged that, through an *N*-methylation and *O*-demethylation sequence (Figure 6), meptazinol could be accessed from a product of the reductive Beckmann reaction (**59**). Formation of this secondary amine requires (*E*)-cyclohexanone oxime

60, which – based on steric interactions – should be the major isomer from the condensation of hydroxylamine with cyclohexanone **61**. Installation of the β-stereocentre was then anticipated to proceed *via* an asymmetric conjugate addition with cyclohexenone **62**; a synthesis of which had been reported from commercial 3-ethoxycyclohex-2-en-1-one, **63**.[94]

To begin the sequence toward meptazinol, a Stork-Danheiser transposition was used to form 3-ethylcyclohex-2-enone (**62**, Scheme 31).[94,95] On larger scales and without Kugelrohr distillation (used in literature), the acid-catalysed, hydrolytic work-up was found to be inefficient, however **62** was obtained in a 74% yield after reprocessing the crude residue with sulfuric acid in acetonitrile.

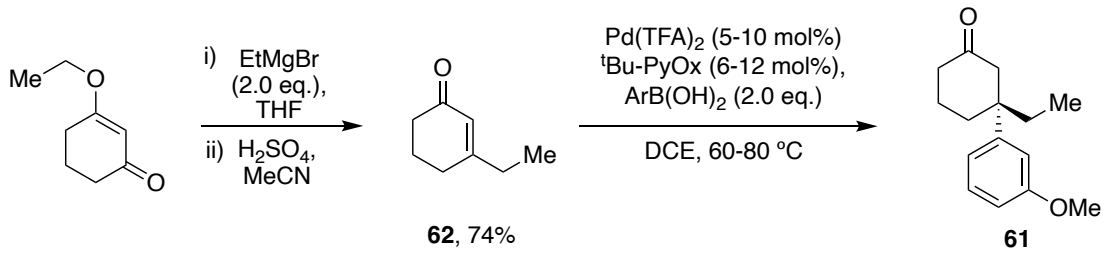

Scale /mmol	Ligand	Temperature /°C	Catalyst Loading /mol%	Time /days	Yield /%	e.e. /%
0.22	(*S*)-*t*-BuPyOx	60	5	1	89	89
0.74	2,2'-bipyridine	80	10	4	74	0
13.2	(*S*)-*t*-BuPyOx	80	10	5	66	92

Scheme 31 and Table 10. *The Stork-Danheiser transposition and asymmetric conjugative addition; and table showing the effect of scale on the conjugate addition.*

Turning to the asymmetric conjugate addition, from a short survey of potential methods, a procedure from the Stoltz group[96] seemed most practical based on the use of a simple palladium (II) precatalyst with a commercial, enantioenriched ^{t}Bu-PyOx ligand. On a 0.22 mmol scale, this furnished the desired cyclohexanone in excellent yield and enantioselectivity (Table 10). The racemic product was also made as an HPLC standard, although full conversion was not reached despite an increased catalyst loading. This was initially ascribed to the change of ligand, however the reaction continued to stall upon scaling up the enantioselective procedure. Although not known at the time, a subsequent publication from the Stoltz group also observed this effect.[97] Contrary to their initial report, stoichiometric

water was found to be essential for catalyst turnover, especially on larger scales where – relative to the reaction size – there is less moisture in the headspace and on the glassware. Due to time and material constraints, the addition of water was not investigated in the synthesis of meptazinol but could be a simple way to improve the yield and lower the catalyst loading of this reaction.

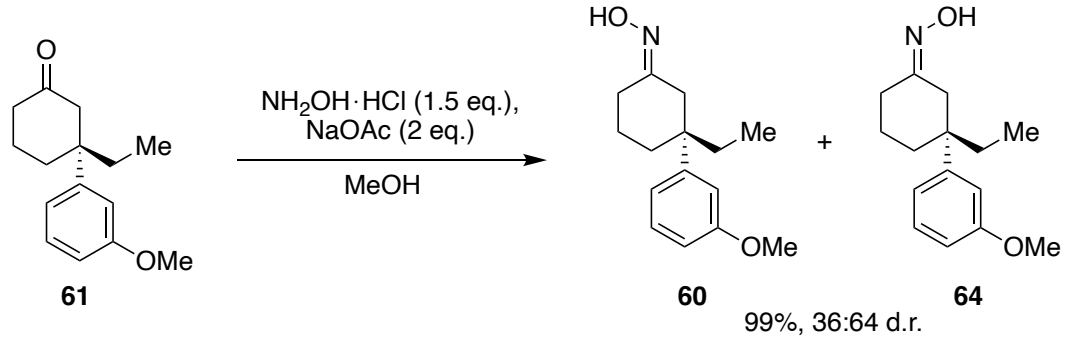

Scheme 32. *Condensation of* ***61*** *with hydroxylamine to generate a mixture of oxime diastereoisomers (****60*** *and* ***64).***

In the next step, the cyclohexanone was reacted with hydroxylamine to generate **60** and **64** (Scheme 32). A near quantitative yield was achieved however the oxime diastereoisomers were inseparable by column chromatography.

The condensation was not expected to be highly selective, yet a preference for the (*E*)-diastereoisomer was anticipated based on a steric argument. However, NMR analysis of the mixture of oximes suggested a diastereoisomeric ratio of 64:36 in favour of the (*Z*)-isomer. The major diastereoisomer was assigned as the (*Z*)-isomer using NOESY (Figure 7). From a conformational analysis of both diastereoisomers, this interaction is only possible in chair A (Figure7); where the aryl group occupies an axial position. Based on similar studies,[98–101] this conformational preference is rationalised by the minimisation of torsional strain around the aryl group; however, the (*Z*)-selectivity was still not understood.

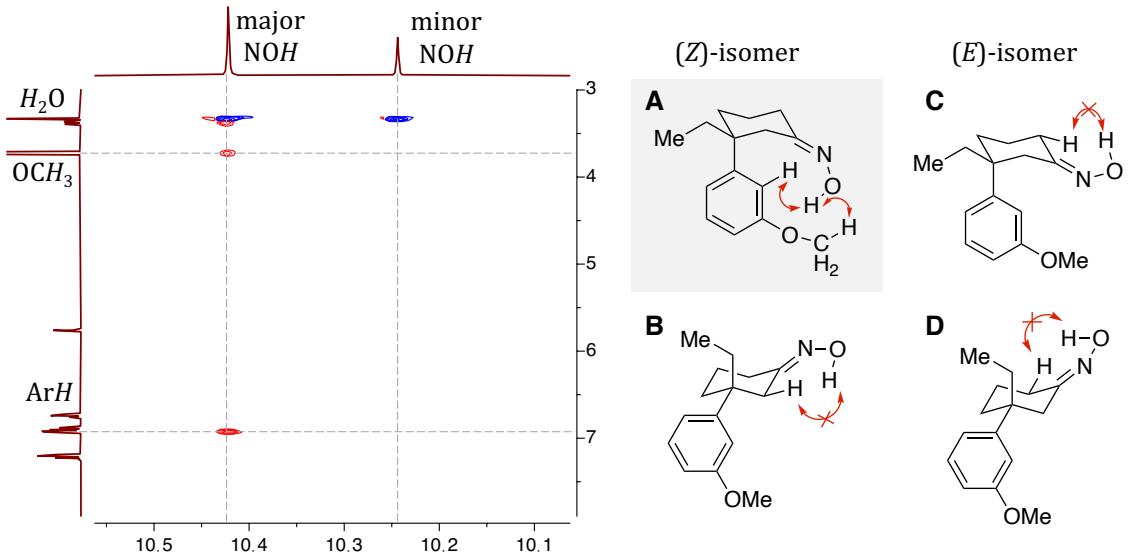

	(*Z*)-isomer		(*E*)-isomer	
	A	**B**	**C**	**D**
Calculated energy /kJ·mol^{-1}	0.00	+5.52	+4.94	+6.19
Calculated distribution /%	75.4	8.1	10.3	6.2
Actual distribution /%	64		36	

Figure 7 and Table 11. *NOESY correlation for the mixture of oxime diastereoisomers (top left); Possible chair conformations for both oxime diastereoisomers including possible NOESY interactions (top right); table showing computed (ωB97XD/6-31G*) energies of each conformer, the predicted Boltzmann distribution, and a comparison with the actual distribution.*

To gain a more accurate representation of these structures, the chair-like conformers were modelled *in silico* using the ωB97XD/6-31G* theoretical. The minimised gas phase electronic energies of these 4 geometries showed that chair A was indeed the most stable form: being almost 5 kJ·mol^{-1} more stable than the other isomers (Table 11). Largely driven by this conformer, a Boltzmann distribution based on these four results predicted an 83.5% selectivity for the (*Z*)-isomer.

Furthermore, analysis of the energy-minimised structure of chair A (Figure 8) revealed the proximity between the oxime oxygen and the aryl ring: in particular the aryl C-H was just 2.43 Å away from the *O* atom. This was consistent with the NOESY correlations and indicated intramolecular non-covalent interactions between a lone pair on oxygen and the electron deficient aryl σ-plane. For comparison, similar interactions between benzene and other hydrogen bond acceptors have been reported with at distances of 2.37-2.55 Å and with stabilisation energies of 4.5-8.6 kJ·mol^{-1}.[102] This type of bonding would explain the calculated stability of chair A and would help to account for to the observed (*Z*)-selectivity in oxime formation.

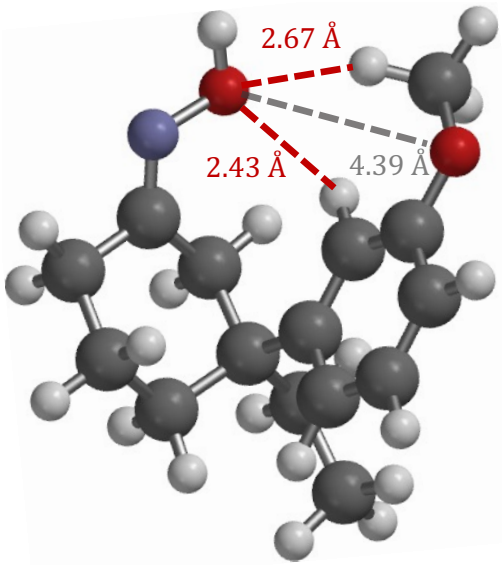

Figure 8. *Lowest energy structure of* ***60*** *calculated using the ωB97XD/6-31G* theoretical, with possible interactions of the oxime oxygen highlighted.*

With both oximes in hand, attention turned to the reductive Beckmann rearrangement. Under the standard reaction conditions, the mixture of diastereoisomers was converted to the corresponding secondary amines in a combined yield of 62% (Scheme 33). At this stage, the two regioisomers could be separated by flash column chromatography (**59** R_f 0.43 and **65** 0.13) to give isolated products in a 37:63 ratio. This distribution is almost identical to the ratio of oximes in the starting material, highlighting the regiospecificity of the reaction. While the major product was not the intended isomer, it is noteworthy that a remote, γ-quarterary stereocentre could be installed using this methodology. However, this undesired pathway detracted from formation of the β-substituted product, which was isolated in just a 23% yield.

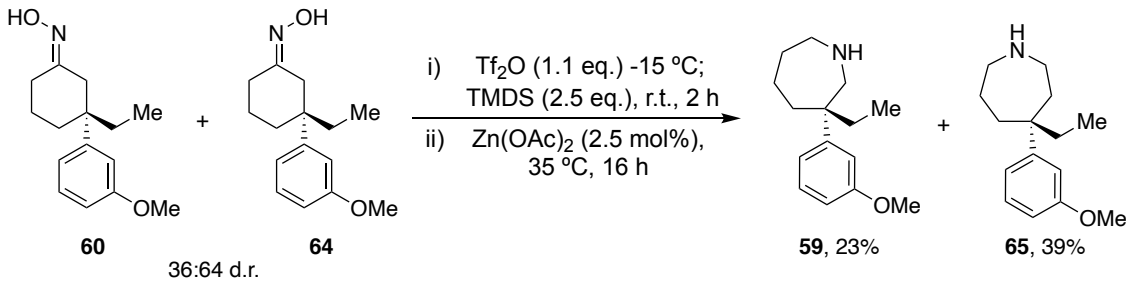

Scheme 33. *The reductive Beckmann rearrangement of a diastereomeric mixture of* ***60*** *and* ***64****.*

With the core scaffold of meptazinol established, the remaining transformations consisted of *N*-methylation and *O*-demethylation. Beginning with the methylation, it was anticipated that this could be achieved using reductive amination. Conventional procedures such as $NaBH_4$/paraformaldehyde or the Eschweiler-Clarke were plausible, however reductive amination using phenylsilane and formic acid was investigated to: i) exemplify previous methods developed in the Denton group,[73] ii) validate formic acid as a previously unexplored coupling partner and iii) demonstrate meptazinol functionalisation with carboxylic acids – an abundant class of electrophiles which may enable further derivatisation.

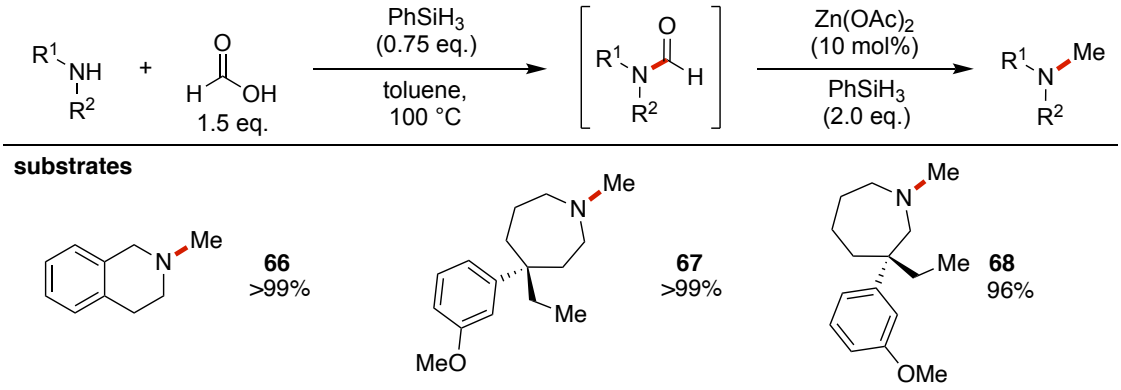

Scheme 34. *The 2-step reductive alkylation of secondary amines with formic acid and phenylsilane.*

Using a slightly lower reaction temperature to avoid evaporation of formic acid (boiling point 101 °C), the procedure was trialled using tetrahydroisoquinoline as a model substrate (Scheme 34). This gave the *N*-methylated product in a quantitative yield which provided encouraging evidence that the route might be viable. Subsequently, **59** and **65** were methylated in excellent yields.

Finally, both *O*-methyl meptazinol (**68**) and its regioisomer (**67**) were demethylated using $BCl_3{\cdot}SMe_2$ to give 67% and 56% yields of **57** and **69** respectively (Scheme 35). In both reactions, a second, less-polar spot was observable by TLC, and while this was naïvely discarded in the purification of **69**, this second species was isolated and characterised in the reaction of **68**. Mass spectrometry and ^{11}B NMR identified this as a meptazinol BCl_3-adduct (**70**) which accounted for the reaction's remaining mass balance. Attempts to hydrolyse this proved unexpectedly difficult: with extended exposure to aqueous acid, base and NH_3 (as a nucleophile) giving only an additional 6% yield of meptazinol (73% total) and leaving the remaining adduct untouched.

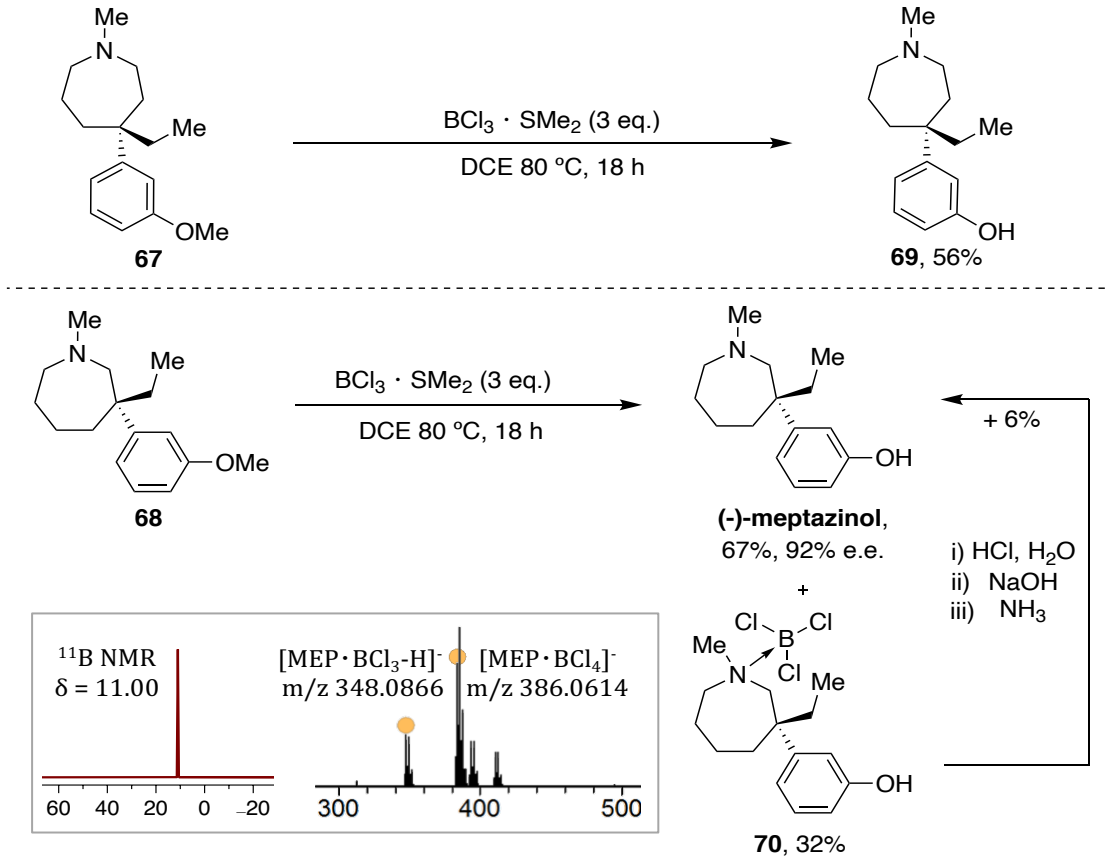

Scheme 35. *Demethylation of **67** and **68** with BCl_3·SMe_2, including the formation of the BCl_3 adduct, its characteristic ^{11}B NMR spectrum and mass spectrum, and attempts to hydrolyse this side product.*

The identity of synthesised (-)-meptazinol was then confirmed through comparison with a commercial sample of (±)-meptazinol·HCl (after treatment with aqueous Na_2CO_3). Comparison of both materials established excellent correlation by ^{13}C NMR and HPLC. Additionally, the synthesised material retained its 92% e.e. and had a negative optical rotation consistent with literature data for (-)-meptazinol ($[\alpha]_D^{25}$ = -14.1°, *c* 0.28 in MeOH at 92% e.e.; lit: -15.1°, *c* 0.46 in MeOH at >99% e.e.[90]). To independently verify the absolute stereochemistry, a crystal structure was sought, however under a variety of conditions small and overlapping crystals were isolated which were unsuitable for single-crystal x-ray diffraction.

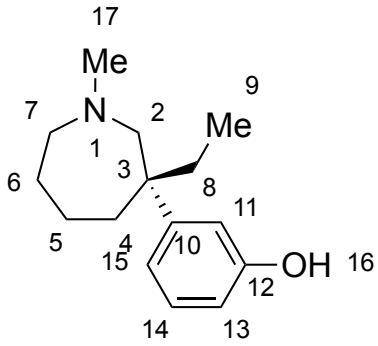

Carbon Number	Meptazinol ^{13}C NMR **δ** /ppm		Difference, **δ** /ppm
	Synthetic	Commercial	
C-12	155.9	156.0	0.1
C-10	148.9	149.1	0.2
C-14	129.2	129.1	-0.1
C-15	119.0	118.9	-0.1
C-11	114.6	114.7	0.1
C-13	112.8	112.8	0.0
C-2	68.9	69.2	0.3
C-7	60.7	60.9	0.2
C-17	49.3	49.4	0.1
C-3	45.4	45.4	0.0
C-4	37.6	37.3	-0.3
C-8	35.2	35.0	-0.2
C-5	30.2	30.5	0.3
C-6	22.5	22.5	0.0
C-9	8.6	8.6	0.0

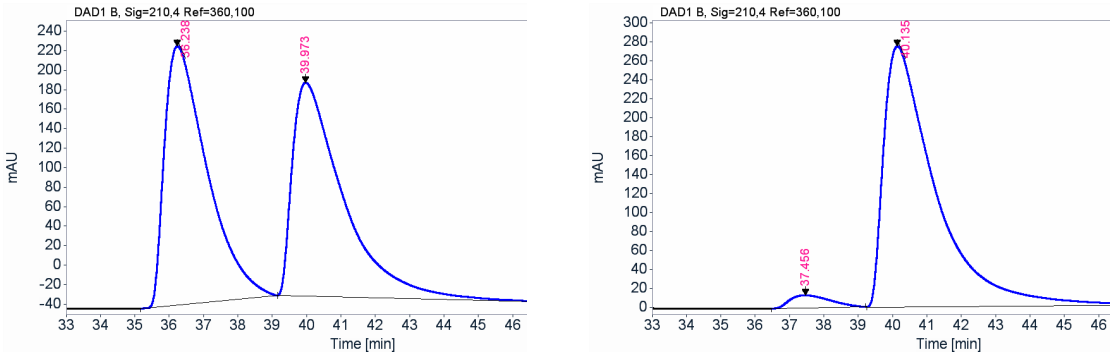

Figure 9. *Comparison of synthesised (-)-meptazinol and commercial (±)-meptazinol; (top) numbered structure of (-)-meptaziol; (middle) table comparing ^{13}C NMR signals; (bottom) chiral HPLC chromatograms for racemic (left) and enantioenriched (right) meptazinol.*

Overall, the first enantioselective synthesis of (-)-meptazinol has been established, using an asymmetric conjugate addition and a reductive Beckmann reaction to form the core azepane scaffold (Scheme 36). Over 6 steps, meptazinol was isolated an 11% yield along with a 14% of a regioisomer which resulted from the unexpected diastereoselectivity of oxime formation. This lack of selectivity, coupled with the limited yield (62% combined), exemplify the current challenges in the development of an efficient reductive Beckmann reaction. However this synthesis also highlights the advantages of such an approach; namely the use of versatile ketone starting materials which enabled formation of a quaternary stereocentre in 92% e.e.. Furthermore, ring expansion enabled 2 challenging azepane scaffolds to be made from an abundant 6-membered carbocycle.

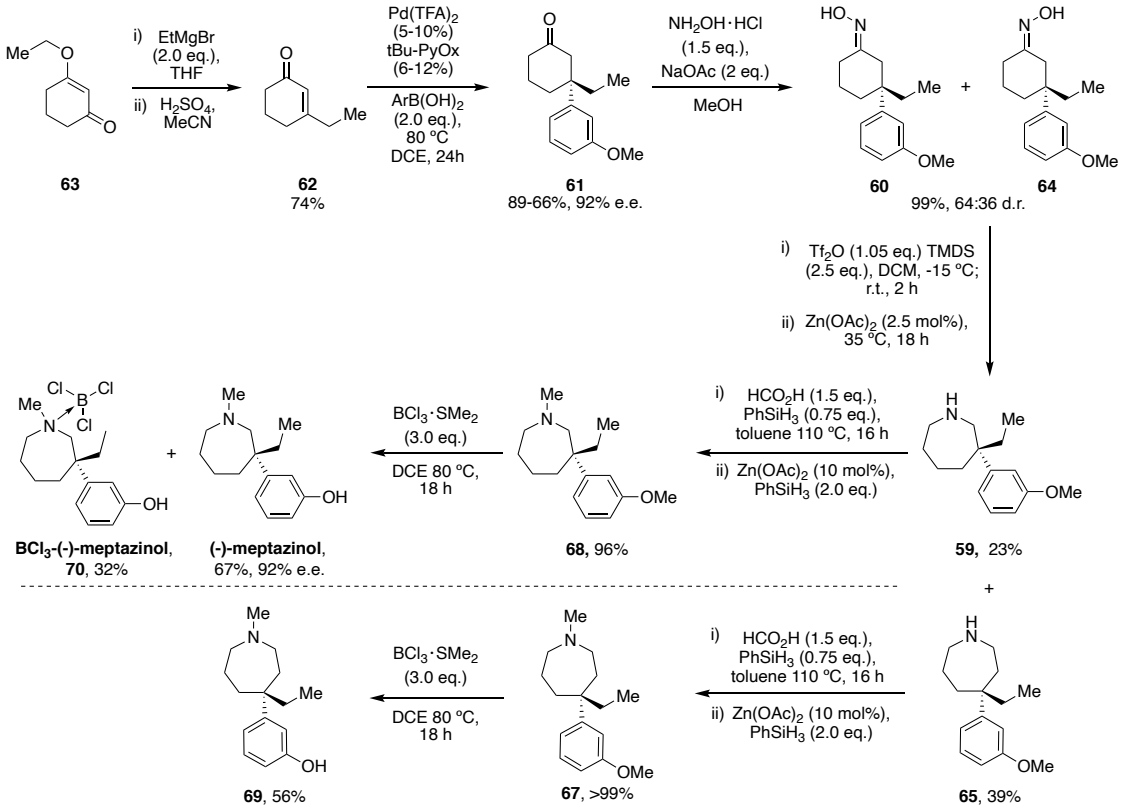

Scheme 36. *Summary of reactions in the synthesis of (-)-meptazinol.*

3.4 Conclusions

A reductive Beckmann rearrangement has been investigated using two reaction manifolds in attempt establish a general approach to the synthesis of secondary, and particularly, cyclic secondary amines by reductive nitrogen insertion. The first strategy used triflic anhydride to generate highly reactive nitrilium ions which could then be reduced under mild conditions. Although this first seemed possible by an amalgamation of two complimentary processes, both the Charette and the Huang group's nitrilium ion reductions were difficult to accomplish using oximes as starting materials and showed disparities, for example, in the role of a base. This resulted in the development of a novel reduction of nitrilium ions using silanes and $Zn(OAc)_2$ catalysis. By optimising this procedure, 9 structurally diverse cyclic and acyclic amines made in yields of 17-87% with characterisation of major side reactions.

It was also possible to intercept the nitrilium ions to diversity the applications of this interrupted Beckmann rearrangement. Accessing these key intermediates enabled selective reduction (to an imine) and electrophilic aromatic substitution as well as the synthesis of an amidine and a quinazoline.

A second iteration of the reductive Beckmann reaction was pursued in which the rearrangement is initiated using sub-stoichiometric amounts of a mesic anhydride to give an amide and mesic acid by-products. These acids were then used to activate phenylsilane towards a $Zn(OAc)_2$-catalysed amide reduction which furnished the product of the model reaction in a 95% yield. This paves the way for a milder and more sustainable method for the reductive Beckmann reaction under dual catalytic conditions and should be pursued in future reaction development.

Finally, the first enantioselective synthesis of (-)-meptazinol, an analgesic active pharmaceutical ingredient, has been achieved using the reductive Beckmann reaction as a key step. This was completed in 6 steps, starting from a commercial 6-membered carbocycle and employed conjugate addition and ring expansion to enantioselectivly form the core β-quaternary azepane scaffold. Overall, this synthesis gave an 11% yield of (-)-meptazinol in 92% e.e., with 14% of a γ-quaternary regioisomer.

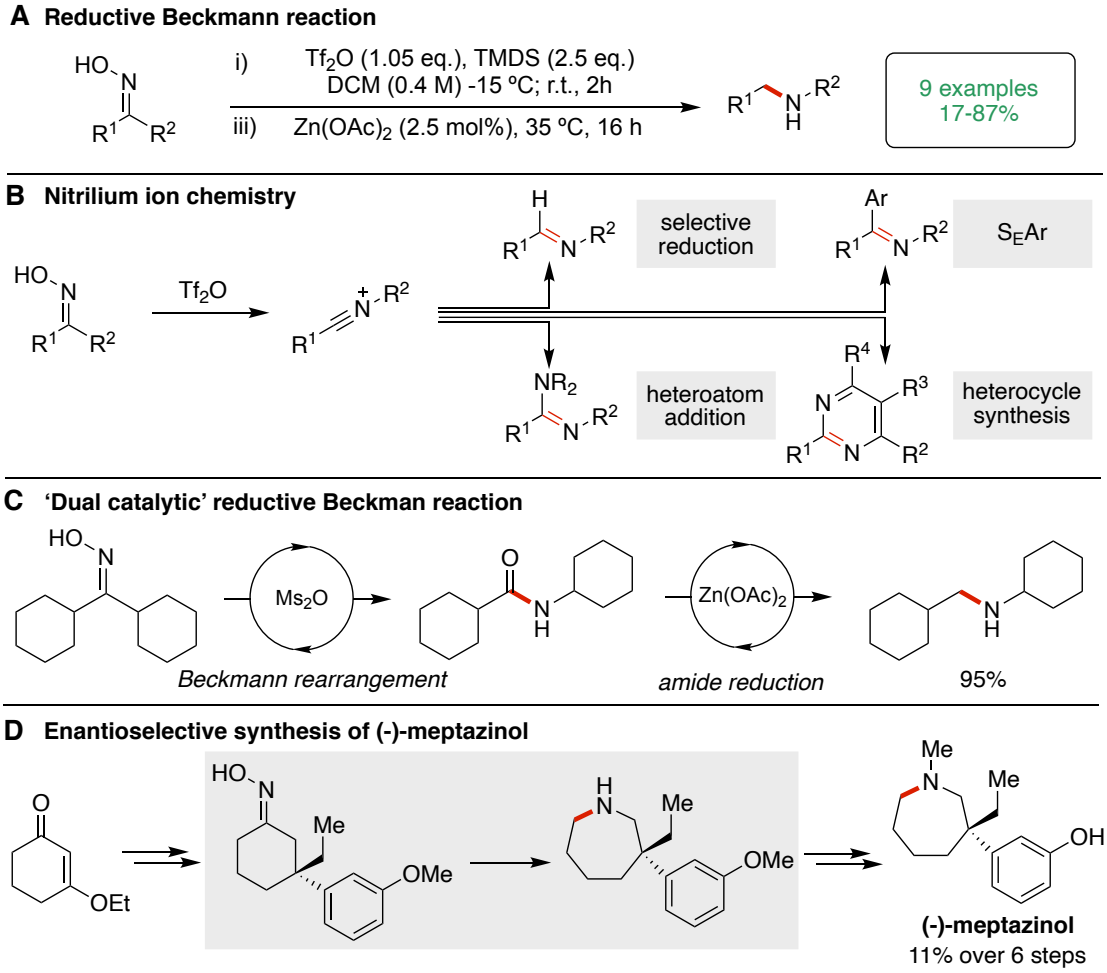

Scheme 37. *Summary of investigations towards a reductive Beckmann reaction; (A) First generation reductive Beckmann reaction; (B) Derivativisations of the nitrilium access through an interrupted Beckmann reaction; (C) A second generation 'dual catalytic' reductive Beckmann reaction; (D) Synthesis of (-)-meptazinol using a reductive Beckmann reaction as the key step.*

3.5 References

1 L. Ghosez, B. Haveuaux and H. G. Viehe, *Angew. Chem. Int. Ed.*, 1969, **8**, 454–455.
2 D. Kaiser, A. Bauer, M. Lemmerer and N. Maulide, *Chem. Soc. Rev.*, 2018, **47**, 7899–7925.
3 T. Van Dijk, J. Chris Slootweg and K. Lammertsma, *Org. Biomol. Chem.*, 2017, **15**, 10134–10144.
4 E. Beckmann, *Ber. Dtsch. Chem. Ges.*, 1887, **20**, 2580–2585.
5 J. J. Ritter and P. Paul Minieri, *J. Am. Chem. Soc.*, 1948, **70**, 4045–4048.
6 J. J. Ritter and J. Kalish, *J. Am. Chem. Soc.*, 1948, **70**, 4048–4050.
7 H. Meerwein, P. Laasch, R. Mersch and J. Spille, *Chem. Ber.*, 1956, **89**, 209–224.
8 S. Kabuß, *Angew. Chem., Int. Ed.* , 1966, **5**, 675–676.
9 A. J. Copson, A. A. Logun and R. P. Sharma, *J. Chem. Soc. Chem. Commun.*, 1972, 315–316.
10 M. Strebelle and R. Fuks, *Bull. des Sociétés Chim. Belges*, 1978, **87**, 717–720.
11 B. L. Booth, K. O. Jibodu and M. F. Proença, *J. Chem. Soc. Chem. Commun.*, 1980, 1151–1153.
12 B. L. Booth, K. O. Jibodu and M. F. J. R. P. Proença, *Perkin Trans. 1*, 1983, 1067–1073.
13 O. Wallach, *Liebigs Ann.* , 1877, **184**, 1–127.
14 J. v. Braun and A. Heymons, *Ber. Dtsch. Chem. Ges.*, 1929, **62**, 409–413.
15 F. Klages and W. Grill, *Liebigs Ann.* , 1955, **594**, 21–32.
16 J. Marchand-Brynaert and L. Ghosez, *J. Am. Chem. Soc.*, 1972, **94**, 2870–2872.
17 J. Marchand-Brynaert and L. Ghosez, *Tetrahedron Lett.*, 1974, **15**, 377–380.
18 A. Sidani, J. Marchand-Brynaert and L. Ghosez, *Angew. Chem., Int. Ed.* , 1974, **13**, 267–267.
19 J. -B Falmagne, J. Escudero, S. Taleb-Sahraoui and L. Ghosez, *Angew. Chem., Int. Ed.* , 1981, **20**, 879–880.
20 A. B. Charette and M. Grenon, *Can. J. Chem.*, 2001, **79**, 1694–1703.
21 K. J. Xiao, J. M. Luo, X. E. Xia, Y. Wang and P. Q. Huang, *Chem. Eur. J.*, 2013, **19**, 13075–13086.
22 G. Barbe and A. B. Charette, *J. Am. Chem. Soc.*, 2008, **130**, 18–19.
23 G. Pelletier, W. S. Bechara and A. B. Charette, *J. Am. Chem. Soc.*, 2010, **132**, 12817–12819.
24 S. H. Xiang, J. Xu, H. Q. Yuan and P. Q. Huang, *Synlett*, 2010, 1829–1832.
25 P. Q. Huang, Q. W. Lang and Y. R. Wang, *J. Org. Chem.*, 2016, **81**, 4235–4243.
26 R. C. Chadwick, V. Kardelis, P. Lim and A. Adronov, *J. Org. Chem.*, 2014, **79**, 7728–7733.
27 E. Blondiaux and T. Cantat, *Chem. Commun.*, 2014, **50**, 9349–9352.
28 M. T. Nguyen, G. Raspoet and L. G. Vanquickenborne, *Perkin Trans. 2*, 1997, 821–825.
29 M. T. Nguyen, G. Raspoet and L. G. Vanquickenborne, *J. Am. Chem. Soc.*, 1997, **119**, 2552–2562.
30 R. Anilkumar and S. Chandrasekhar, *Tetrahedron Lett.*, 2000, **41**, 5427–5429.
31 S. Chandrasekhar and K. Gopalaiah, *Tetrahedron Lett.*, 2003, **44**, 7437–7439.
32 S. Chandrasekhar and K. Gopalaiah, *Tetrahedron Lett.*, 2003, **44**, 755–756.
33 J. D. White, P. Hrnciar and F. Stappenbeck, *J. Org. Chem.*, 1999, **64**, 7871–7884.
34 R. G. Kalkhambkar and H. M. Savanur, *RSC Adv.*, 2015, **5**, 60106–60113.
35 Y. Furuya, K. Ishihara and H. Yamamoto, *J. Am. Chem. Soc.*, 2005, **127**, 11240–11241.
36 M. Zhu, C. Cha, W. P. Deng and X. X. Shi, *Tetrahedron Lett.*, 2006, **47**, 4861–4863.
37 M. Hashimoto, Y. Obora, S. Sakaguchi and Y. Ishii, *J. Org. Chem.*, 2008, **73**, 2894–2897.
38 H. J. Pi, J. D. Dong, N. An, W. Du and W. P. Deng, *Tetrahedron*, 2009, **65**, 7790–7793.
39 J. K. Augustine, R. Kumar, A. Bombrun and A. B. Mandal, *Tetrahedron Lett.*, 2011, **52**, 1074–1077.
40 C. M. Vanos and T. H. Lambert, *Chem. Sci.*, 2010, **1**, 705–708.
41 Y. Gao, J. Liu, Z. Li, T. Guo, S. Xu, H. Zhu, F. Wei, S. Chen, H. Gebru and K. Guo, *J. Org. Chem.*, 2018, **83**, 2040–2049.
42 X. Mo, T. D. R. Morgan, H. T. Ang and D. G. Hall, *J. Am. Chem. Soc.*, 2018, **140**, 5264–5271.
43 N. An, B. X. Tian, H. J. Pi, L. A. Eriksson and W. P. Deng, *J. Org. Chem.*, 2013, **78**, 4297–4302.
44 Y. Tamura, H. Fujiwara, K. Sumoto, M. Ikeda and Y. Kita, *Synth.*, 1973, **1973**, 215–216.
45 K. Hyodo, G. Hasegawa, N. Oishi, K. Kuroda and K. Uchida, *J. Org. Chem.*, 2018, **83**, 13080–13087.
46 J. Liu, C. Zhang, Z. Zhang, X. Wen, X. Dou, J. Wei, X. Qiu, S. Song and N. Jiao, *Science*, 2020, **367**, 281–285.
47 J. Fujiwara, H. Sano, K. Maruoka and H. Yamamoto, *Tetrahedron Lett.*, 1984, **25**, 2367–2370.
48 H. Cho, K. Murakami, H. Nakanishi, H. Isoshima, K. Hayakawa and I. Uchida, *Heterocycles*, 1998, **48**, 919–927.
49 H. Cho, Y. Iwama, K. Sugimoto, S. Mori and H. Tokuyama, *J. Org. Chem.*, 2010, **75**, 627–636.

50 H. Cho, K. Murakami, H. Nakanishi, A. Fujisawa, H. Isoshima, M. Niwa, K. Hayakawa, Y. Hase, I. Uchida, H. Watanabe, K. Wakitani and K. Aisaka, *J. Med. Chem.*, 2004, **47**, 101–109.
51 H. Cho, Y. Iwama, K. Sugimoto, E. Kwon and H. Tokuyama, *Heterocycles*, 2009, **78**, 1183–1190.
52 M. Ortiz-Marciales, L. D. Rivera, M. De Jesús, S. Espinosa, J. A. Benjamin, O. E. Casanova, I. G. Figueroa, S. Rodríguez and W. Correa, *J. Org. Chem.*, 2005, **70**, 10132–10134.
53 A. B. Charette and P. Chua, *Tetrahedron Lett.*, 1998, **39**, 245–248.
54 K. J. Xiao, Y. Wang, K. Y. Ye and P. Q. Huang, *Chem. Eur. J.*, 2010, **16**, 12792–12796.
55 W. S. Bechara, G. Pelletier and A. B. Charette, *Nat. Chem.*, 2012, **4**, 228–234.
56 K. J. Xiao, Y. Wang, Y. H. Huang, X. G. Wang and P. Q. Huang, *J. Org. Chem.*, 2013, **78**, 8305–8311.
57 H. Q. Deng, X. Y. Qian, Y. X. Li, J. F. Zheng, L. Xie and P. Q. Huang, *Org. Chem. Front.*, 2014, **1**, 258–266.
58 P. Q. Huang, Y. H. Huang, K. J. Xiao, Y. Wang and X. E. Xia, *J. Org. Chem.*, 2015, **80**, 2861–2868.
59 J. Marchand-Brynaert and L. Ghosez, *J. Am. Chem. Soc.*, 1972, **94**, 2869–2870.
60 P. Q. Huang, Y. H. Huang and K. J. Xiao, *J. Org. Chem.*, 2016, **81**, 9020–9027.
61 P. Q. Huang, Y. H. Huang, H. Geng and J. L. Ye, *Sci. Rep.*, 2016, **6**, 1–10.
62 P. Q. Huang, W. Ou, K. J. Xiao and A. E. Wang, *Chem. Commun.*, 2014, **50**, 8761–8763.
63 P. Q. Huang and W. Ou, *Eur. J. Org. Chem.*, 2017, **2017**, 582–592.
64 P. Q. Huang and T. Fan, *Eur. J. Org. Chem.*, 2017, **2017**, 6369–6374.
65 Y. P. Liu, C. J. Zhu, C. C. Yu, A. E. Wang and P. Q. Huang, *Eur. J. Org. Chem.*, 2019, **2019**, 7169–7174.
66 Y. P. Liu, S. R. Wang, T. T. Chen, C. C. Yu, A. E. Wang and P. Q. Huang, *Adv. Synth. Catal.*, 2019, **361**, 971–975.
67 A. E. Wang, C. C. Yu, T. T. Chen, Y. P. Liu and P. Q. Huang, *Org. Lett.*, 2018, **20**, 999–1002.
68 C. R. Gonçalves, M. Lemmerer, C. J. Teskey, P. Adler, D. Kaiser, B. Maryasin, L. González and N. Maulide, *J. Am. Chem. Soc.*, 2019, **141**, 18437–18443.
69 M. Movassaghi, M. D. Hill and O. K. Ahmad, *J. Am. Chem. Soc.*, 2007, **129**, 10096–10097.
70 A. B. Charette, M. Grenon, A. Lemire, M. Pourashraf and J. Martel, *J. Am. Chem. Soc.*, 2001, **123**, 11829–11830.
71 R. M. Denton, J. An, P. Lindovska and W. Lewis, *Tetrahedron*, 2012, **68**, 2899–2905.
72 S. Das, D. Addis, K. Junge and M. Beller, *Chem. Eur. J.*, 2011, **17**, 12186–12192.
73 E. L. Stoll, T. Tongue, K. G. Andrews, D. Valette, D. J. Hirst and R. M. Denton, *Chem. Sci.*, 2020, **11**, 9494–9500.
74 C. Madelaine, V. Valerio and N. Maulide, *Angew. Chem. Int. Ed.*, 2010, **49**, 1583–1586.
75 R. G. Kalkhambkar and H. M. Savanur, *RSC Adv.*, 2015, **5**, 60106–60113.
76 J. J. Maul, P. J. Ostrowski, G. a Ublacker, B. Linclau and D. P. Curran, *Mod. Solvents Org. Synth.*, 1999, **206**, 79–105.
77 F. W. Semmler, *Ber. Dtsch. Chem. Ges.*, 1892, **25**, 3352–3354.
78 L. Wolff, *Liebigs Ann.* , 1902, **322**, 351–391.
79 C. Hansch, A. Leo and R. W. Taft, *Chem. Rev.*, 1991, **91**, 165–195.
80 G. R. Krow and S. Szczepanski, *Tetrahedron Lett.*, 1980, **21**, 4593–4596.
81 M. Movassaghi and M. D. Hill, *J. Am. Chem. Soc.*, 2006, **128**, 14254–14255.
82 K. J. Xiao, A. E. Wang and P. Q. Huang, *Angew. Chem. Int. Ed.*, 2012, **51**, 8314–8317.
83 H. Chen, Y. H. Huang, J. L. Ye and P. Q. Huang, *J. Org. Chem.*, 2019, **84**, 9270–9281.
84 C. Godoy-Alcántar, A. K. Yatsimirsky and J. M. Lehn, *J. Phys. Org. Chem.*, 2005, **18**, 979–985.
85 A. B. Charette and M. Grenon, *Tetrahedron Lett.*, 2000, **41**, 1677–1680.
86 A. B. Charette and M. Grenon, *J. Org. Chem.*, 2003, **68**, 5792–5794.
87 A. B. Charette and P. Chua, *Synlett*, 1998, **1998**, 163–165.
88 E. L. Stoll, T. Barber, D. J. Hirst and R. M. Denton, *Chem. Commun.*, 2022, **58**, 3509–3512.
89 G. F. Zha, K. P. Rakesh, H. M. Manukumar, C. S. Shantharam and S. Long, *Eur. J. Med. Chem.*, 2019, **162**, 465–494.
90 S. Cheng, W. Zheng, P. Gong, Q. Zhou, Q. Xie, L. Yu, P. Zhang, L. Chen, J. Li, J. Chen, H. Chen and H. Chen, *Bioorganic Med. Chem.*, 2015, **23**, 3110–3118.
91 C. Rudolphi and G. Blaschke, *J. Chromatogr. B Biomed. Sci. Appl.*, 1995, **663**, 315–326.
92 B. Holmes and A. Ward, *Drugs*, 1985, **30**, 285–312.
93 J. Yu, Z. Jiang, T. Sun, F. Ji, S. Xu, L. Wei and X. Guo, *Biomed. Chromatogr.*, 2014, **28**, 135–141.
94 S. Kehrli, D. Martin, D. Rix, M. Mauduit and A. Alexakis, *Chem. Eur. J.*, 2010, **16**, 9890–9904.
95 G. Stork and R. L. Danheiser, *J. Org. Chem.*, 1973, **38**, 1775–1776.

96 J. C. Holder, A. N. Marziale, M. Gatti, B. Mao and B. M. Stoltz, *Chem. Eur. J.*, 2013, **19**, 74–77.
97 S. E. Shockley, J. C. Holder and B. M. Stoltz, *Org. Process Res. Dev.*, 2015, **19**, 974–981.
98 N. L. Allinger and M. T. Tribble, *Tetrahedron Lett.*, 1971, **12**, 3259–3262.
99 H. Senderowitz, F. Guarnieri and W. C. Still, *J. Am. Chem. Soc.*, 1995, **117**, 8211–8219.
100 K. B. Wiberg, H. Castejon, W. F. Bailey and J. Ochterski, *J. Org. Chem.*, 2000, **65**, 1181–1187.
101 D. J. Hodgson, U. Rychlewska, E. L. Eliel, M. Manoharan, D. E. Knox and E. M. Olefirowicz, *J. Org. Chem.*, 1985, **50**, 4838–4843.
102 A. Gavezzotti, *New J. Chem.*, 2016, **40**, 6848–6853.

3.6 Experimental

3.6.1 General Reaction Information

In addition to the general information in section 2.6. Triflic anhydride was purchased from commercial suppliers and stored at -16 °C for up to 2 months. After this time either a new bottle of Tf_2O was purchased or the remaining liquid was distilled over phosphorus pentoxide. Cooling to -15 °C was affected using an ice/acetone bath (1:1).

3.6.2 General Analysis and Characterisation Information

In addition to the General information in section 2.6 Liquid chromatography-mass spectrometry (LC-MS) analyses were performed using an Agilent 1260 Infinity HPLC with a 6120 Quadrupole mass spectrometer. Chromatography conditions: Waters XBridge C18 3.5µm 2.1 x 30 mm column. Mobile phase A: 0.1% Ammonia in water, mobile phase B: acetonitrile. Flow rate 0.8 mL/min in a gradient of 5 – 95 % mobile phase B over 3.5 minutes with UV detection at 210 – 400 nm reported at 254nm. Column temperature 40 °C. Chiral HPLC analysis was performed on Agilent 1200 Infinity series instruments using 4.6 × 250 mm columns.

3.6.3 The Synthesis of Oximes

General procedure for the synthesis of oximes

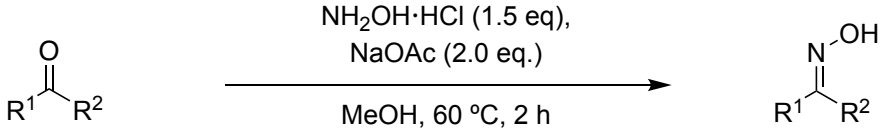

To a suspension of ketone (1.0 eq.) and NaOAc (2.0 eq.) in methanol (0.50 M) was added $NH_2OH{\cdot}HCl$ (1.5 eq.) and the suspension was heated to 60 °C for 2 hours. Upon cooling to room temperature, the reaction mixture was then diluted with diethyl ether (2.0 mL/mmol) and washed successively with NaCl (aqueous solution made from 1.0 mL/mmol saturated NaCl and 1.0 mL/mol water), and $NaHCO_3$ (2.0 mL/mmol of a saturated aqueous solution). The remaining organic layer was dried over anhydrous $MgSO_4$ and concentrated *in vacuo*.

Dicyclohexylmethanone oxime (45a)

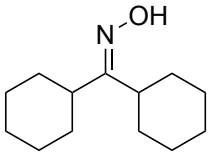

45a

30.0 mmol scale. Purification by flash column chromatography (10% EtOAc in cyclohexane; R_f 0.29) to give a colourless solid (5.97 g, 28.5 mmol, 95%).

^{1}H NMR (500 MHz, DMSO) δ 10.16 (s, 1H, NO*H*), 2.86 (tt, *J* = 12.1, 3.5 Hz, 1H, C*H*), 2.12 (tt, *J* = 8.6, 2.1 Hz, 1H, C*H*), 1.74 – 1.57 (m, 8H), 1.57 – 1.50 (m, 2H), 1.49 – 1.38 (m, 2H), 1.30 – 1.09 (m, 8H); **^{13}C{^{1}H} NMR** (126 MHz, DMSO) δ 164.4 (C_q), 39.9 (CH), 37.1 (CH), 31.8 (CH_2), 28.1 (CH_2), 26.1 (CH_2), 25.9 (CH_2), 25.8 (CH_2), 25.7 (CH_2); **FTIR** (neat) ν_{max} /cm^{-1} 3219 (br.), 3160, 2925, 2847, 1449, 1441; **HRMS** (ESI) *m/z* calc'd for $C_{13}H_{24}NO$ $[M+H]^+$: 210.1852, found: 210.1854; **m.p.:** 160-162 °C (lit. 157-160 °C). Data are consistent with literature.[1]

1,3-Diphenylpropan-2-one oxime (45b)

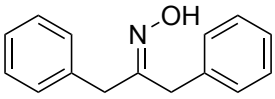

45b

20.0 mmol scale. Purification by flash column chromatography (20% EtOAc in petrol; R_f 0.25) to give a white solid (4.01 g, 17.8 mmol, 89%).

^{1}H NMR (400 MHz, DMSO) δ 10.79 (s, 1H, NO*H*), 7.34 – 7.08 (m, 10H, Ar*H*), 3.52 (s, 2H, CH_2), 3.36 (s, 2H, CH_2); **^{13}C{^{1}H} NMR** (101 MHz, DMSO) δ 155.9 (C_q), 137.3 (C_q), 136.8 (C_q), 129.0 (CH), 128.9 (CH), 128.39 (CH), 128.38 (CH), 126.4 (CH), 126.1 (CH), 39.2 (CH_2), 32.3 (CH_2); **FTIR** (neat) ν_{max} /cm^{-1} 3244 (br.), 3086, 3059, 3028, 2905, 1659, 1602, 1584, 1496, 1452, 1425; **HRMS (ESI):** *m/z* calc'd for $C_{15}H_{16}NO$ $[M+H]^+$; 226.1226, found; 226.1225; **m.p.:** 122-124 °C (lit. 121-123 °C). Data consistent with literature.[2]

(*E*)- and (*Z*)-*L*-Menthone oxime, (45c) and (45d)

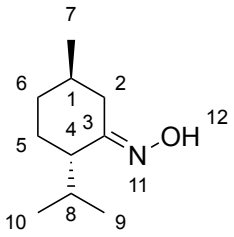

45c

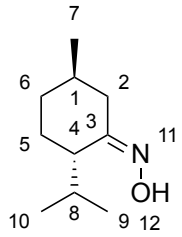

45d

6.50 mmol scale. Purification by flash column chromatography (10% EtOAc in petrol) to give 2 colourless solids: (*E*)-*L*-menthone oxime (**45c**) (R_f 0.31; 790 mg, 4.67 mmol, 71%), and (*Z*)-*L*-menthone oxime (**45d**) (R_f 0.14; 222 mg, 1.31 mmol, 20%).

(*E*)-*L*-Menthone oxime (**45c**): **^{1}H NMR** (500 MHz, DMSO) 10.22 (s, 1H, H-12), 2.96 – 2.87 (m, 1H, H-2), 2.11 (apparent octet, *J* = 6.9 Hz, 1H, H-8), 1.87 – 1.72 (m, 3H, H-4, H-5, H-6), 1.63 – 1.53 (m, 1H, H-1), 1.55 – 1.49 (m, 1H, H-2), 1.30 – 1.19 (m, 1H, H-2), 1.16 – 1.06 (m, 1H, H-6), 0.90 (d, *J* = 6.2 Hz, 3H, H-7), 0.88 (d, *J* = 6.9 Hz, 3H, H-9), 0.86 (d, *J* = 6.9 Hz, 3H, H-10); **^{13}C{^{1}H} NMR** (126 MHz, DMSO) δ 158.1 (C-3), 47.8 (C-4), 32.4 (C-6), 31.9 (C-1), 31.4 (C-2), 26.6 (C-5), 25.9 (C-8), 21.6 (C-7), 21.4 (C-9), 19.1 (C-10); **FTIR** (neat) ν_{max} /cm^{-1} 3265 (br.), 3146, 2951, 2923, 2868, 2841, 1666, 1442; **HRMS** (ESI) *m/z* calc'd for $C_{10}H_{19}NO$ $[M+H]^+$: 170.1539, found: 170.1546; **m.p.:** 60-63 °C (lit. 60-61 °C); **$[\alpha]_D^{25}$** -20.1° (*c*. 1.0, $CHCl_3$). Data consistent with literature.[3]

(*Z*)-*L*-Menthone oxime (**45d**): **^{1}H NMR** (500 MHz, DMSO) 10.06 (s, 1H, H-12), 2.90 (ddd, *J* = 10.4, 5.1, 2.5 Hz, 1H, H-4), 2.32 (dd, *J* = 13.4, 5.5 Hz, 1H, H-2), 2.11 (qdddd, *J* = 7.3, 5.5, 4.5, 2.4, 1.5 Hz, 1H, H-1), 1.87 (dhept, *J* = 10.4, 6.6 Hz, 1H, H-8), 1.80 (dd, *J* = 13.4, 1.5 Hz, 1H, H-2), 1.77 (apparent ddt, *J* = 13.8, 13.7, 4.5 Hz, 1H, H-6), 1.58 (apparent dtd, *J* = 13.8, 3.8, 2.5 Hz, 1H, H-5), 1.48 (apparent dddd, *J* = 13.8, 13.7, 5.1, 3.8 Hz, 1H, H-5), 1.19 (apparent dtt, *J* = 13.7, 3.8, 2.4 Hz, 1H, H-6), 0.92 (d, *J* = 6.6 Hz, 3H, H-10), 0.85 (d, *J* = 7.1 Hz, 3H, H-7), 0.76 (d, *J* = 6.6 Hz, 3H, H-9); **^{13}C{^{1}H} NMR** (126 MHz, DMSO) 158.0 (C-3), 39.2 (C-4, assigned from HSQC), 34.5 (C-2), 28.7 (C-1), 26.1 (C-6), 25.8 (C-8), 21.4 (C-5), 20.7 (C-9), 20.4 (C-10), 17.9 (C-7); **IR ν_{max} /cm^{-1}** 3194 (br.), 3084, 2953, 2932, 2913, 2868, 2765, 1661, 1465, 1428; **HRMS** (ESI)

m/z calc'd for $C_{10}H_{19}NO$ $[M+H]^+$: 170.1539, found: 170.1537; **m.p.:** 79-80 °C; **$[\alpha]_D^{25}$** -72.4° (*c*. 0.50, $CHCl_3$).

(*R,E*)-Carvone oxime (45e)

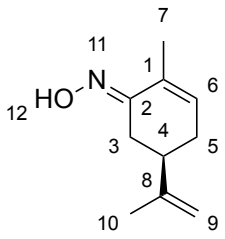

45e

20.0 mmol scale. No further purification required to exclusively give the *E*-isomer as a pale-yellow solid (2.86 g, 17.1 mmol, 86%).

^{1}H NMR (400 MHz, DMSO) δ 10.85 (s, 1H, H-12), 5.96 (ddd, *J* = 5.8, 2.8, 1.4 Hz, 1H, H-6), 4.75 (m, 2H, H-9), 3.01 (ddd, *J* = 16.3, 4.0, 1.8 Hz, 1H, H-3), 2.31 – 2.14 (m, 2H, H-4, H-5), 2.04 (ddt, *J* = 17.3, 10.5, 2.8 Hz, 1H, H-5), 1.95 (dd, *J* = 16.3, 12.4 Hz, 1H, H-3), 1.77 (m, 3H, H-7), 1.72 (t, *J* = 1.0 Hz, 3H, H-10); **^{13}C{^{1}H} NMR** (101 MHz, DMSO) δ 154.4 (C-2), 147.9 (C-8), 130.7 (C-6), 130.3 (C-1), 109.8 (C-9), 39.8 (C-4), 29.7 (C-5), 26.9 (C-3), 20.5 (C-10), 17.6 (C-7); **FTIR** (neat) ν_{max} /cm^{-1} 3251 (br.), 3209, 3078, 2939, 2903, 1432, 1370; **HRMS** (ESI) *m/z* calc'd for $C_{10}H_{16}NO$ $[M+H]^+$: 166.1226, found: 166.1226; **m.p.:** 72-74 °C (lit. 71-72°C); **$[\alpha]_D^{25}$** -43.8° (*c*. 1.0, $CHCl_3$), lit. -43.0° (*c*. 0.40, $CHCl_3$). Data are consistent with literature.[4]

Tetrahydro-4*H*-pyran-4-one oxime (45f)

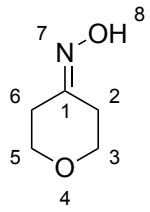

45f

20.0 mmol scale. Purification by flash column chromatography (50% EtOAc in petrol; R_f 0.38) to give a colourless solid (2.04 g, 17.7 mmol, 88%).

^{1}H NMR (400 MHz, DMSO) δ 10.38 (s, 1H, H-8), 3.68 (t, *J* = 5.7 Hz, 2H, H-5), 3.60 (t, *J* = 5.9 Hz, 2H, H-3), 2.49 (t, *J* = 5.9 Hz, 2H, H-2), 2.23 (t, *J* = 5.7 Hz, 2H, H-6); **^{13}C{^{1}H} NMR** (101 MHz, DMSO) δ 153.0 (C-1), 67.6 (C-5), 66.0 (C-3), 31.9 (C-6), 25.6 (C-2); **FTIR** (neat) ν_{max} /cm^{-1} 3274 (br.), 2972, 2925, 2859, 1663, 1653, 1475, 1440, 1415; **HRMS** (ESI) *m/z* calc'd for $C_5H_{10}NO_2$ $[M+H]^+$: 116.0706, found: 116.0698; **m.p.:** 89-91 °C, (lit. 87-88 °C). Data consistent with literature.[5,6]

^{15}*N*-Cyclohexanone oxime (45g)

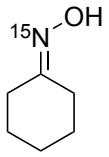

45g

The general procedure was applied with a modified stoichiometry of cyclohexanone (245 mg, 2.50 mmol), $^{15}NH_2OH{\cdot}HCl$ (185 mg, 2.63 mmol) and NaOAc (246 mg, 3.00 mmol). Purification by flash column chromatography (40% Et_2O in petrol; R_f 0.25) to give a colourless solid (247 mg, 2.16 mmol, 86%).

^{1}H NMR (500 MHz, DMSO) δ 10.09 (d, *J* = 1.8 Hz, 1H), 2.36 (ddd, *J* = 7.1, 5.6, 1.6 Hz, 2H), 2.14 – 2.05 (m, 2H), 1.60 – 1.45 (m, 4H); **^{13}C{^{1}H} NMR** (126 MHz, DMSO) δ 157.1 (d, *J* = 1.8 Hz), 31.6 (d, *J* = 11.8 Hz), 26.7 (d, *J* = 2.1 Hz), 25.4, 25.3, 23.8 (d, *J* = 1.8 Hz); **^{15}N NMR** (51 MHz, DMSO) δ 343.2 (lit. δ 329.2 in $CDCl_3$); **FTIR** (neat) ν_{max} /cm^{-1} 3167, 3093, 2929, 2887, 2858, 1644, 1478, 1447, 1435; **HRMS (ESI):** *m/z* calc'd for $C_6H_{12}{}^{15}NO$ $[M+H]^+$; 115.0884, found; 115.0892; **m.p.:** 91-93 °C (lit. 88-89 °C). Data consistent with literature.[7]

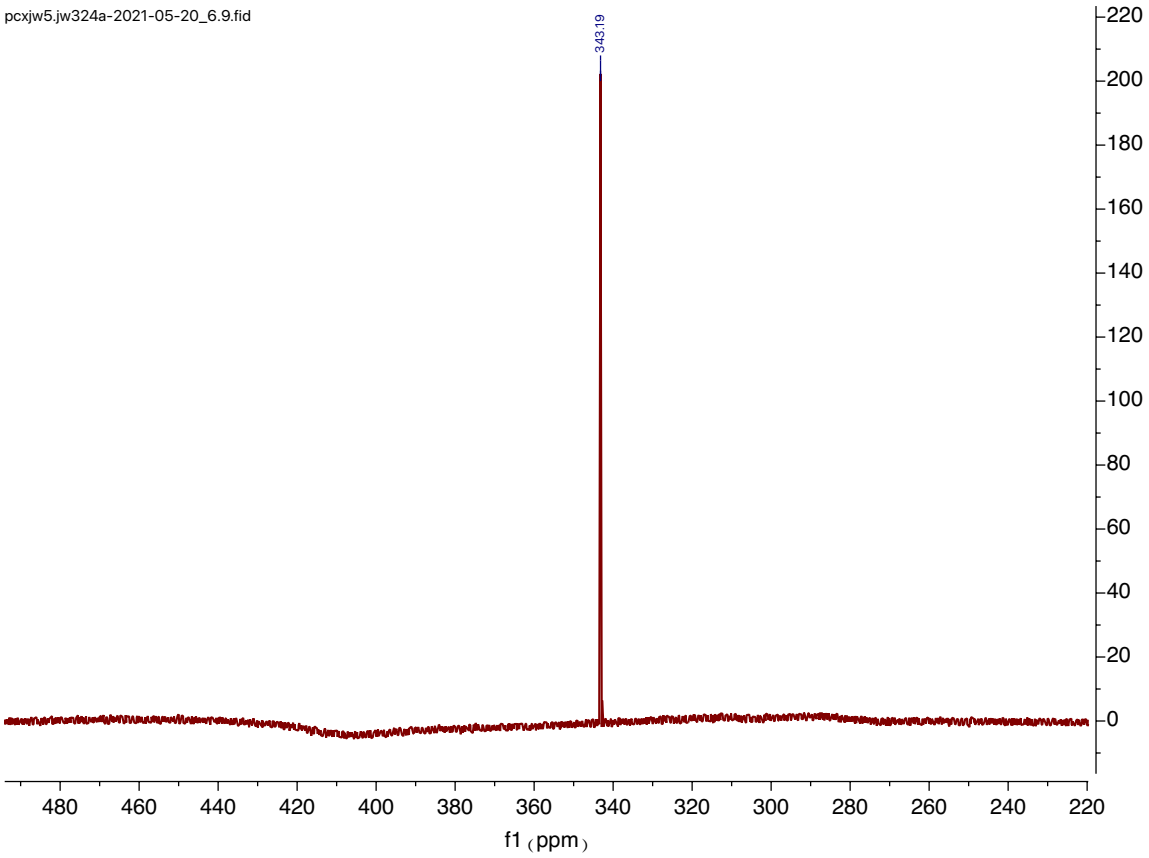

Figure 1. *$^{15}N\{^1H\}$ NMR of 15N-cyclohexanone oxime (**45g**)*

(*E*)-4-Fluoroacetophenone oxime (45h)

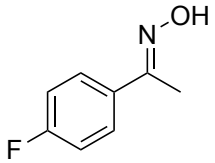

45h

4.00 mmol scale. Purification by flash column chromatography (20% EtOAc in petrol; R_f 0.20) to give a colourless solid (558 mg, 3.84 mmol, 91%).

^{1}H NMR (400 MHz, $CDCl_3$) δ 7.62 (dd, *J* = 8.8, 5.2 Hz, 2H, Ar*H*), 7.07 (dd, *J* = 8.8, 8.8 Hz, 2H, Ar*H*), 2.27 (s, 3H, C*H*$_3$). **^{13}C{^{1}H} NMR** (101 MHz, $CDCl_3$) δ 163.6 (d, *J* = 248.8 Hz, C_q), 155.4 (C_q), 132.8 (d, *J* = 3.3 Hz, C_q), 128.0 (d, *J* = 8.4 Hz, CH), 115.6 (d, *J* = 21.6 Hz, CH), 12.2 (CH_3); **^{19}F{^{1}H} NMR** (376 MHz, $CDCl_3$) δ -112.19; **FTIR** (neat) ν_{max} /cm^{-1} 3217 (br.), 3093, 3066, 2928, 1598, 1511; **HRMS** (ESI) *m/z* calc'd for C_8H_9NOF $[M+H]^+$: 154.0663, found: 154.0660; **m.p.:** 77-79 °C (lit. 74-76 °C). Data are consistent with literature.[8,9]

(*E*)-1-(4-Methoxyphenyl)ethan-1-one oxime (45i)

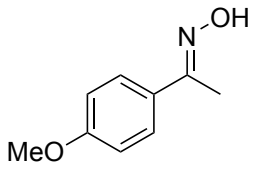

45i

20.0 mmol scale. Purification by recrystallisation from toluene (5.0 mL, 49 °C supersaturation point) to give a colourless solid (2.48 g, 15.0 mmol, 75%).

^{1}H NMR (500 MHz, DMSO) δ 10.96 (s, 1H, NO*H*), 7.62 – 7.55 (m, 2H, Ar*H*), 6.97 – 6.89 (m, 2H, Ar*H*), 3.77 (s, 3H, OCH_3), 2.11 (s, 3H, CH_3); **^{13}C{^{1}H} NMR** (126 MHz, DMSO) δ 159.6 (C_q), 152.4 (C_q), 129.4 (C_q), 126.8 (CH), 113.7 (CH), 55.1 (CH_3), 11.5 (CH_3); **FTIR** (neat) ν_{max} /cm^{-1} 3290, 3238, 3129, 3071, 3009, 2959, 2928, 2829, 1607, 1578, 1512, 1451; **HRMS (ESI):** *m/z* calc'd for $C_9H_{12}NO_2$ $[M+H]^+$; 166.0863, found; 166.0858; **m.p.:** 86-90 °C (lit. 86-87 °C). Data consistent with literature.[10]

2,2,2-Trifluoro-1-phenylethan-1-one oxime (45j)

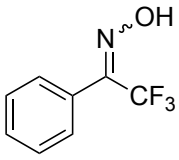

45j

20.0 mmol scale. Purification by flash column chromatography (50% DCM in petrol; R_f 0.24) to give a colourless solid (797 mg, 4.21 mmol, 21%, 78:22 ratio of diastereoisomers). Ratio of diastereoisomers determined by ^{1}H NMR.

^{1}H NMR (400 MHz, $CDCl_3$) δ 8.29 (minor) (s, 1H, NO*H*), 8.15 (major) (s, 1H, NO*H*), 6.94 – 6.71 (m, 5H); **^{13}C{^{1}H} NMR** (101 MHz, $CDCl_3$) major isomer δ 147.9 (q, *J* = 32.5 Hz), 130.6, 128.6, 128.6, 128.4, 120.6 (q, *J* = 274.6 Hz); **^{19}F{^{1}H} NMR** (376 MHz, $CDCl_3$) δ -62.39 (minor), -66.72 (major); **FTIR** (neat) ν_{max} /cm^{-1} 3299 (br.), 3067, 3023, 2911, 1496, 1441; **HRMS** (ESI) *m/z* calc'd for $C_8H_7NOF_3$ $[M+H]^+$: 190.0474, found: 190.0474; **m.p.:** 76-78 °C, (lit. 79-81 °C). Data consistent with literature.[11]

(*E*) and (*Z*)-(*R,R*)-Camphor oxime, (45k) and (45l)

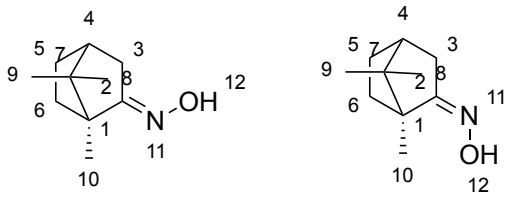

45k **45l**

20.0 mmol scale. Purification by flash column chromatography (10% EtOAc in petrol) to give 2 colourless solids: (*E,R,R*)-camphor oxime (**45k**) (R_f 0.19; 1.78 g, 10.6 mmol, 53%) and (*Z,R,R*)-camphor oxime (**45l**) (R_f 0.08; 130 mg, 0.777 mmol, 3.9%).

(*E,R,R*)-Camphor oxime (**45k**): **^{1}H NMR** (500 MHz, DMSO) δ 10.00 (s, 1H, H-12), 2.35 (ddd, *J* = 17.5, 4.6, 3.1 Hz, 1H, H-3), 1.87 (d, *J* = 17.5 Hz, 1H, H-3), 1.84 (dd, *J* = 4.6, 4.2 Hz, 1H, H-4), 1.77 (apparent ttd, *J* = 11.9, 4.2, 3.1 Hz, 1H, H-5), 1.66 (dddd, *J* = 12.4, 11.9, 4.2, 0.9 Hz, 1H, H-6), 1.30 (ddd, *J* = 12.4, 9.3, 4.1 Hz, 1H, H-6), 1.17 (ddd, *J* = 11.9, 9.3, 4.1 Hz, 1H, H-5), 0.91 (s, 3H, H-10), 0.87 (s, 3H, H-8), 0.71 (s, 3H, H-9); **^{13}C{^{1}H} NMR** (126 MHz, DMSO) δ 166.3 (C-2), 50.8 (C-1), 47.5 (C-7), 43.1 (C-4), 32.8 (C-3), 32.7 (C-6), 26.9 (C-5), 19.2 (C-8), 18.3 (C-9), 11.4 (C-10); **FTIR** (neat) ν_{max} /cm^{-1} 3288 (br.), 3145, 3013, 2957, 2876, 1681, 1473, 1444; **HRMS** (ESI) *m/z* calc'd for $C_{10}H_{16}NO$ $[M+H]^+$: 168.1383, found: 168.1383; **m.p.:** 119-121 °C (lit. 118-119 °C); **$[\alpha]_D^{25}$** -51.6° (*c*. 1.0, $CHCl_3$). Data consistent with literature.[12]

(*Z,R,R*)-Camphor oxime (**45l**): **^{1}H NMR** (500 MHz, DMSO) δ 9.74 (s, 1H, H-12), 2.34 (dddd, *J* = 16.0, 4.0, 3.4, 0.9 Hz, 1H, H-3), 1.82 – 1.72 (m, 3H, H-3, H-4, H-5), 1.60 – 1.49 (m, 1H, H-6), 1.48 (ddd, *J* = 12.9, 9.3, 4.3 Hz, 1H, H-6), 1.27 (s, 3H, H-10), 1.25 – 1.17 (m, 1H, H-5), 0.83 (s, 3H, H-8), 0.80 (s, 3H, H-9); **^{13}C{^{1}H} NMR** (126 MHz, DMSO) δ 161.9 (C-2), 53.4 (C-1), 48.1 (C-7), 43.3 (C-4), 35.9 (C-3), 32.3 (C-6), 27.0 (C-5), 20.1 (C-8), 18.0 (C-9), 14.1 (C-10); **FTIR** (neat) ν_{max} /cm^{-1} 3282 (br.), 3163, 2957, 2926, 2875, 1452; **HRMS** (ESI) *m/z* calc'd for $C_{10}H_{16}NO$ $[M+H]^+$: 168.1383, found: 168.1398; **m.p.:** 110-112 °C; **$[\alpha]_D^{25}$** -103° (*c*. 1.0, $CHCl_3$).

2-Adamantanone oxime (45m)

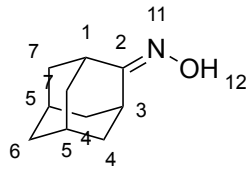

45m

20.0 mmol scale. No further purification required to give the product as a colourless solid (1.34 g, 8.14 mmol, 41%).

^{1}H NMR (500 MHz, DMSO) δ 9.92 (s, 1H, H-9), 3.42 (tt, *J* = 3.0, 2.8 Hz, 1H, H-3), 2.43 (tt, *J* = 3.1, 2.8 Hz, 1H, H-1), 1.93 (td, *J* = 2.8, 2.7 Hz, 2H, H-6), 1.90 (apparent ddt, *J* = 12.2, 3.1, 2.8 Hz, 2H, H-7), 1.84 (apparent ddt, *J* = 12.3, 3.0, 2.8 Hz, 2H, H-4), 1.80 (apparent pt, *J* = 2.8, 1.8 Hz, 2H, H-5), 1.71 (apparent dt, *J* = 12.2, 2.8 Hz, 2H, H-7), 1.65 (ddd, *J* = 12.3, 2.8, 1.8 Hz, 2H, H-4); **^{13}C{^{1}H} NMR** (126 MHz, DMSO) δ 163.1 (C-2), 38.4 (C-7), 36.9 (C-4), 36.0 (C-5), 35.6 (C-1), 28.0 (C-3), 27.4 (C-6); **FTIR** (neat) ν_{max} /cm^{-1} 3183 (br.), 3108, 2907, 2848, 1671, 1479, 1449; **HRMS** (ESI) *m/z* calc'd for $C_{10}H_{16}NO$ $[M+H]^+$: 166.1226, found: 166.1219; **m.p.:** 167-169 °C (lit. 165-166°C). Data are consistent with literature.[13]

(*E*) and (*Z*)-2-(Trifluoromethyl)cyclohexan-1-one oxime, (45n) and (45o)

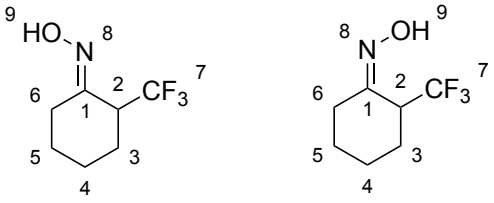

45n **45o**

10.0 mmol scale. Purification by flash column chromatography (20% EtOAc in petrol) to give (*E*)-2-(trifluoromethyl)cyclohexan-1-one oxime (**45n**) as a colourless solid (R_f 0.31, 1.11 g, 6.14 mmol, 61%) and (*Z*)-2-(trifluoromethyl)cyclohexan-1-one oxime (**45o**) as a colourless solid (R_f 0.24, 411 mg, 2.27 mmol, 23%).

(*E*)-isomer (45n): ^{1}H NMR (400 MHz, DMSO) δ 10.98 (s, 1H, H-9), 3.22 (qdd, *J* = 10.1, 6.8, 5.5 Hz, 1H, H-2), 2.44 (t, *J* = 6.2 Hz, 2H, H-6), 1.89 (dddd, *J* = 13.5, 8.5, 5.5, 4.5 Hz, 1H, H-3), 1.77 (dddd, *J* = 13.5, 7.8, 6.8, 4.1 Hz, 1H, H-3), 1.72 – 1.62 (m, 1H, H-

4), 1.62 – 1.47 (m, 3H, H-4, H-5); **^{13}C{^{1}H} NMR** (101 MHz, DMSO) δ 151.5 (C-6), 126.6 (q, *J* = 280.7 Hz, C-7), 44.1 (q, *J* = 25.9 Hz, C-2), 25.9 (q, *J* = 2.2 Hz, C-3), 24.5 (C-5), 22.7 (C-6), 22.3 (C-4); **^{19}F{^{1}H} NMR** (376 MHz, DMSO) δ -65.82; **FTIR** (neat) ν_{max} /cm^{-1} 3287 (br.), 2938, 2876, 2860, 1662, 1451; **HRMS** (ESI) *m/z* calc'd for $C_7H_{11}NOF_3$ $[M+H]^+$: 182.0787, found: 182.0792; **m.p.:** 92-94 °C.

(*Z*)-isomer (45o): ^{1}H NMR (400 MHz, DMSO) δ 11.02 (s, 1H, H-9), 4.19 (qd, *J* = 11.4, 5.3 Hz, 1H, H-2), 2.37 (apparent dt, *J* = 14.4, 3.4 Hz, 1H, H-6), 2.12 (ddd, *J* = 14.4, 13.2, 4.9 Hz, 1H, H-6), 2.08 – 1.94 (m, 1H, H-3), 1.88 (dddd, *J* = 12.7, 4.9, 3.4, 2.3 Hz, 1H, H-5), 1.67 – 1.48 (m, 3H, H-4, H-3), 1.35 (apparent dddt, *J* = 13.7, 12.7, 11.8, 4.3 Hz, 1H, H-5); **^{13}C{^{1}H} NMR** (101 MHz, DMSO) δ 149.8, (C-1), 126.6 (q, *J* = 281.9 Hz, C-7), 35.0 (q, *J* = 26.9 Hz, C-2), 29.6, (C-6), 25.6 (C-5), 24.2 (q, *J* = 2.1 Hz, C-3), 21.2 (C-4); **^{19}F{^{1}H} NMR** (376 MHz, DMSO) δ -63.86; **FTIR** (neat) ν_{max} /cm^{-1} 3196 (br.), 3093, 2947, 2874, 1660, 1479, 1451; **HRMS** (ESI) *m/z* calc'd for $C_7H_{11}NOF_3$ $[M+H]^+$: 182.0787, found: 182.0779; **m.p.:** 38-40 °C.

Ethyl (*E*) and (*Z*)-2-(hydroxyimino)cyclopentane-1-carboxylate, XX and XX

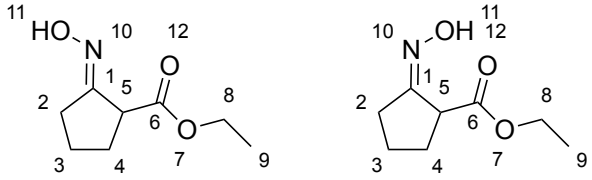

20.0 mmol scale. Purification by flash column chromatography (20% EtOAc in petrol) to give ethyl (*E*)-2-(hydroxyimino)cyclopentane-1-carboxylate (**45p**) as a colourless solid (R_f 0.21, 2.38 g, 13.9 mmol, 69%) and ethyl (*Z*)-2-(hydroxyimino)cyclopentane-1-carboxylate (**45q**) as a pale yellow oil (R_f 0.10, 318 mg, 1.85 mmol, 9.3%).

(*E*) isomer (46p): ^{1}H NMR (400 MHz, DMSO) δ 10.65 (s, 1H, H-11), 4.07 (q, *J* = 7.1 Hz, 2H, H-8), 3.37 (td, *J* = 7.6, 1.8 Hz, 1H, H-5), 2.39 (ddd, *J* = 18.1, 8.4, 4.6 Hz, 1H, H-2), 2.29 (apparent dtd, *J* = 18.1, 7.9, 1.8 Hz, 1H, H-2), 2.05 – 1.94 (m, 1H, H-4), 1.93 – 1.79 (m, 2H, H-3, H-4), 1.73 – 1.57 (m, 1H, H-3), 1.18 (t, *J* = 7.1 Hz, 3H, H-9); **^{13}C{^{1}H} NMR** (101 MHz, DMSO) δ 172.1 (C-6), 161.8 (C-1), 60.2 (C-10), 47.3 (C-5), 29.5 (C-4), 26.9 (C-2), 22.6 (C-3), 14.1 (C-9); **FTIR** (neat) ν_{max} /cm^{-1} 3238 (br.), 2976, 2939,

2900, 1730, 2689, 1449, 1416; **HRMS** (ESI) *m/z* calc'd for $C_8H_{13}NO_3Na$ $[M+Na]^+$: 194.0788, found: 194.0797; **m.p.:** 56-58 °C.

(*Z*) isomer (46q): ^{1}H NMR (400 MHz, DMSO) δ 10.50 (s, 1H, H-11), 4.04 (q, *J* = 7.1, Hz, 2H, H-8), 3.40 (dd, *J* = 9.0, 7.0 Hz, 1H, H-5), 2.34 (ddd, *J* = 7.7, 6.4, 1.1 Hz, 2H, H-2), 2.11 (apparent ddt, *J* = 12.0, 9.0, 6.4 Hz, 1H, H-4), 1.84 (apparent dp, *J* = 11.9, 6.4 Hz, 1H, H-3), 1.75 (dddd, *J* = 12.0, 7.0, 6.5, 6.4 Hz, 1H, H-4), 1.64 (apparent dtdd, *J* = 11.9, 7.7, 6.5, 5.2 Hz, 1H, H-3), 1.16 (t, *J* = 7.1 Hz, 3H, H-9); **^{13}C{^{1}H} NMR** (101 MHz, DMSO) δ 172.0 (C-6), 160.5 (C-1), 59.9 (C-8), 44.6 (C-5), 30.4 (C-2), 30.2 (C-4), 23.8 (C-3), 14.0 (C-9); **FTIR** (neat) ν_{max} /cm^{-1} 3240 (br.), 2972, 2875, 1730, 1449; **HRMS** (ESI) *m/z* calc'd for $C_8H_{13}NO_3Na$ $[M+Na]^+$: 194.0788, found: 194.0798.

(*E*)-1-Adamantan-1-yl)ethan-1-one oxime (45r)

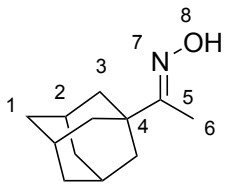

45r

15.0 mmol scale. Purification by flash column chromatography (20% EtOAc in petrol; R_f 0.44) to give a colourless solid (2.89 g, 14.9 mmol, >99%).

^{1}H NMR (500 MHz, DMSO) δ 10.30 (s, 1H, H-8), 1.97 (apparent hept, *J* = 3.2 Hz, 3H, H-2), 1.73 – 1.68 (m, 9H, H-1, H-3), 1.67 (s, 3H, H-6), 1.67 – 1.62 (m, 3H, H-1); **^{13}C{^{1}H} NMR** (126 MHz, DMSO) δ 161.2 (C-5), 39.3 (C-3, assigned through HSQC), 38.4 (C-4), 36.3 (C-1), 27.7 (C-2), 8.7 (C-6); **FTIR** (neat) ν_{max} /cm^{-1} 3219 (br.), 2913, 2897, 2847, 1659, 1445; **HRMS (ESI):** *m/z* calc'd for $C_{12}H_{20}NO$ $[M+H]^+$; 194.1539, found; 194.1536; **m.p.:** 180-182 °C (lit. 182-184 °C). Data consistent with literature.[14]

(2*E*,3*E*)-4-Phenylbut-3-en-2-one oxime (45s) and (2*Z*,3*E*)-4-phenylbut-3-en-2-one oxime (45t)

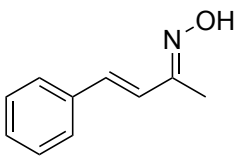

45s

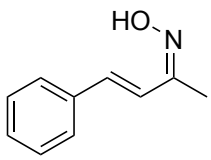

45t

20 mmol scale. Purification by flash column chromatography (25% Et_2O in petrol) to give (2*E*,3*E*)-4-phenylbut-3-en-2-one oxime (**45s**) as a colourless solid (R_f 0.21, 2.33 g, 14.4 mmol, 72%) and (2*Z*,3*E*)-4-phenylbut-3-en-2-one oxime (**45t**) as a colourless solid (R_f 0.14, 592 mg, 3.67 mmol, 18%).

(2*E*,3*E*)-isomer (45s): ^{1}H NMR (500 MHz, DMSO) δ 11.17 – 11.12 (m, 1H, NO*H*), 7.59 – 7.51 (m, 2H, Ar*H*), 7.39 – 7.32 (m, 2H, Ar*H*), 7.31 – 7.24 (m, 1H, Ar*H*), 6.94 (d, *J* = 16.6 Hz, 1H, PhC*H*), 6.85 (apparent dd, *J* = 16.6, 1.3 Hz, 1H, PhCHC*H*), 2.00 (d, *J* = 1.3 Hz, 3H, CH_3); **^{13}C{^{1}H} NMR** δ 154.4 (C_q), 136.5 (C_q), 131.4 (CH), 128.7 (CH), 128.0 (CH), 126.7 (CH), 126.6 (CH), 9.4 (CH_3); **FTIR** (neat) ν_{max} /cm^{-1} 3155, 3052, 2833, 1619, 1574, 1492, 1448, 1434, 1415; **HRMS (ESI):** *m/z* calc'd for $C_{10}H_{12}NO$ $[M+H]^+$: 162.0913, found: 162.0914; **m.p.:** 125-127 °C (lit. 123-125 °C). Data consistent with literature.[15,16]

(2*Z*,3*E*)-isomer (45t): ^{1}H NMR (500 MHz, DMSO) δ 10.88 – 10.83 (m, 1H, NO*H*), 7.60 – 7.55 (m, 2H, Ar*H*), 7.53 – 7.45 (m, 1H, PhCHC*H*), 7.42 – 7.35 (m, 2H, Ar*H*), 7.36 – 7.29 (m, 1H, Ar*H*), 6.99 (d, *J* = 16.7 Hz, 1H, PhC*H*CH), 2.03 (d, *J* = 0.9 Hz, 3H, CH_3); **^{13}C{^{1}H} NMR** (126 MHz, DMSO) δ 150.8 (Cq), 136.3 (Cq), 134.5 (CH), 128.9 (CH), 128.8 (CH), 127.1 (CH), 116.9 (CH), 16.7 (CH_3); **FTIR** (neat) ν_{max} /cm^{-1} 3259, 3205, 3034, 2922, 1627, 1493, 1445; **HRMS (ESI):** *m/z* calc'd for $C_{10}H_{12}NO$ $[M+H]^+$; 162.0913, found; 162.0911; **m.p.:** 106-108 °C (lit. 102 °C). Data consistent with literature.[17]

3.6.4 Reductive Beckmann Substrate Scope

General procedure for the Reductive Beckmann Rearrangement

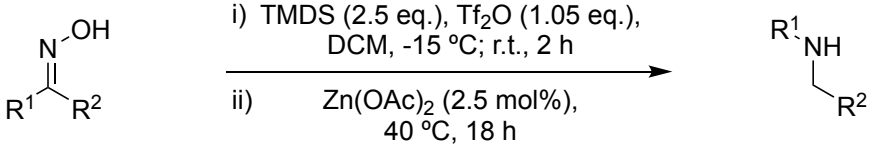

To a flame dried microwave vial was added oxime (1.00 mmol), DCM (2.5 mL) and TMDS (442 μL, 2.50 mmol) and the mixture was cooled to -15 °C. Tf_2O (176 μL, 1.05 mmol) was then added in one portion and stirred for 15 minutes at -15 °C before warming to room temperature. After 2 hours, $Zn(OAc)_2$ (4.6 mg, 2.50 mol%) was

added and the reaction is warmed to 35 °C for a further 18 hours. After cooling to room temperature, the reaction was quenched with NaOH (2.5 mL of a 1.0 M aqueous solution). The organic layer was diluted with DCM (2.5 mL), extracted, and the aqueous layer was washed with DCM (3 x 2.5 mL). The combined organic phases were dried over anhydrous $MgSO_4$, filtered, and concentrated *in vacuo*.

N-(Cyclohexylmethyl)cyclohexanamine (46a)

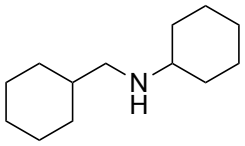

46a

Purification by flash column chromatography (90:9:0.7:0.3 DCM:MeOH:H_2O:NH_3; R_f 0.50) to give a yellow oil (171 mg, 0.873 mmol, 87%).

^{1}H NMR (400 MHz, $CDCl_3$) δ 2.44 (d, *J* = 6.8 Hz, 2H, C*H*$_2$NH), 2.36 (tt, *J* = 10.5, 3.8 Hz, 1H, NHC*H*), 1.91 – 1.81 (m, 2H), 1.76 – 1.65 (m, 6H), 1.65 – 1.53 (m, 2H), 1.42 (ttt, *J* = 10.3, 6.8, 3.3 Hz, 1H), 1.31 – 1.10 (m, 6H), 1.05 (qd, *J* = 10.5, 3.6 Hz, 2H), 0.88 (qd, *J* = 13.7, 3.8 Hz, 2H); **^{13}C{^{1}H} NMR** (101 MHz, $CDCl_3$) δ 57.1 (CH), 53.8 (CH_2), 38.2 (CH), 33.6 (CH_2), 31.8 (CH_2), 31.7 (CH_2), 26.8 (CH_2), 26.3 (CH_2), 26.2 (CH_2), 25.2 (CH_2); **FTIR** (neat) ν_{max} /cm^{-1} 2919, 2850, 1447; **HRMS (ESI):** *m/z* calc'd for $C_{13}H_{26}N$ $[M+H]^+$; 196.2060, found; 196.2067. Data consistent with literature.[18]

N-Benzyl-2-phenylethan-1-amine (46b)

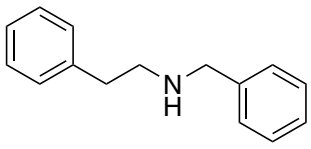

46b

Purification by flash column chromatography (98:1.8:0.15:0.05 DCM:MeOH:H_2O:NH_3; R_f 0.20) to give a yellow oil (135 mg, 0.637 mmol, 64%).

^{1}H NMR (400 MHz, $CDCl_3$) δ 7.45 – 7.16 (m, 10H, Ar*H*), 3.83 (s, 2H, ArC*H*$_2$NH), 2.94 (t, *J* = 6.8 Hz, 2H, NHC*H*$_2$CH$_2$), 2.86 (t, *J* = 6.8 Hz, 2H, NHCH$_2$C*H*$_2$), 1.47 (s, 1H, N*H*); **^{13}C{^{1}H} NMR** (101 MHz, $CDCl_3$) δ 140.4 (C_q), 140.2 (C_q), 128.9 (CH), 128.6 (CH),

128.5 (CH), 128.2 (CH), 127.0 (CH), 126.3 (CH), 54.0 (CH_2), 50.7 (CH_2), 36.5 (CH_2); **FTIR** (neat) ν_{max} /cm^{-1} 3084, 3061, 3026, 2926, 2817, 1661, 1603, 1495, 1453; **HRMS (ESI):** *m/z* calc'd for $C_{15}H_{18}N$ $[M+H]^+$; 212.1434, found; 212.1440. Data consistent with literature.[19]

(2*S*,5*R*)-2-Isopropyl-5-methylazepane (46c)

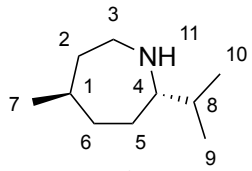

46c

Purification by flash column chromatography (90:9:0.7:0.3 DCM:MeOH:H_2O:NH_3; R_f 0.22) to give a yellow oil (119 mg, 0.768 mmol, 77%).

^{1}H NMR (500 MHz, $CDCl_3$) δ 2.89 (ddd, *J* = 14.0, 8.4, 4.1 Hz, 1H, H-3), 2.82 (ddd, *J* = 14.0, 6.6, 4.3 Hz, 1H, H-3), 2.43 (ddd, *J* = 10.7, 5.1, 2.6 Hz, 1H, H-4), 1.81 (s, 1H, H-11), 1.81 – 1.67 (m, 3H, H-2, H-5, H-6), 1.68 – 1.53 (m, 2H, H-1, H-8), 1.34 – 1.13 (m, 3H, H-2, H-5, H-6), 0.92 (d, *J* = 6.7 Hz, 3H, H-7), 0.88 (d, *J* = 6.8 Hz, 3H, H-9/10), 0.87 (d, *J* = 6.8 Hz, 3H, H-9/10); **^{13}C{^{1}H} NMR** (126 MHz, $CDCl_3$) δ 64.4 (C-4), 45.2 (C-3), 39.3 (C-2), 36.1 (C-6), 34.4 (C-8), 34.3 (C-1), 31.8 (C-5), 24.0 (C-7), 19.1 C-9/10), 19.0 (C-9/10); **FTIR** (neat) ν_{max} /cm^{-1} 2951, 2908, 2869, 1642, 1457; **HRMS (ESI):** *m/z* calc'd for $C_{13}H_{26}N$ $[M+H]^+$; 156.1747, found; 156.1752; **$[\alpha]_D^{25}$** -9.00° (*c*. 1.0, $CHCl_3$). Data consistent with literature.[20]

(3*S*,6*R*)-3-Isopropyl-6-methylazepane (46d)

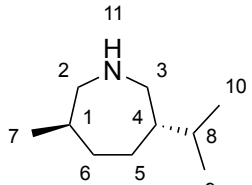

46d

Purification by flash column chromatography (5% 7.0 M NH_3 in MeOH, in DCM R_f 0.22) to give a yellow oil (119 mg, 0.764 mmol, 76%).

^{1}H NMR (400 MHz, $CDCl_3$) δ 2.93 (ddd, *J* = 13.5, 4.4, 1.2 Hz, 2H, H-2), 2.90 (ddd, *J* = 13.5, 5.5, 0.8 Hz, 2H, H-3), 2.65 (dd, *J* = 13.5, 8.6 Hz, 1H, H-3), 2.37 (dd, *J* = 13.5, 9.3 Hz, 1H, H-2), 2.25 (s, 1H, H-11), 1.77 (ddddd, *J* = 13.6, 6.9, 3.8, 1.5, 1.2 Hz, 1H, H-6), 1.68 – 1.57 (m, 2H, H-5, H-1), 1.54 (heptd, *J* = 6.9, 4.0 Hz, 1H, H-8), 1.50 – 1.34 (m, 1H, H-4), 1.29 (dddd, *J* = 13.6, 12.3 10.7, 1.7 Hz, 1H, H-5), 1.11 (ddd, *J* = 13.6, 11.5, 11.3, 1.7 Hz, 1H, H-6), 0.85 (d, *J* = 6.8 Hz, 3H, H-7), 0.84 (t, *J* = 6.9 Hz, 6H, H-19, H-10); **^{13}C{^{1}H} NMR** (101 MHz, $CDCl_3$) δ 56.1 (C-2), 51.5 (C-3), 47.4 (C-4), 37.3 (C-1), 36.0 (C-6), 32.0 (C-8), 28.5 (C-5), 20.8 (C-9/10), 20.0 (C-7), 19.4 (C-9/10); **FTIR** (neat) ν_{max} /cm^{-1} 3390 (br.), 2954, 2918, 2871, 1614, 1549, 1459, 1409; **HRMS (ESI):** *m/z* calc'd for $C_{13}H_{26}N$ $[M+H]^+$; 156.1747, found; 156.1748; **$[\alpha]_D^{25}$** +37.6° (*c*. 1.0, $CHCl_3$).

2-Methyl-5-(propan-2-ylidene)azepane (47)

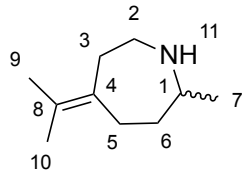

47

Synthesized according to the general procedure using 3.50 mmol TMDS. Purification by flash column chromatography (90:9:0.7:0.3 DCM:MeOH:H_2O:NH_3; R_f 0.12) to give a yellow residue (26.2 mg, 0.171 mmol, 17%).

^{1}H NMR (500 MHz, $CDCl_3$) δ 7.08 (s, 1H, H-11), 3.30 (ddd, *J* = 13.3, 5.5, 4.0 Hz, 1H, H-2), 3.02 (dqd, *J* = 10.4, 6.6, 2.5 Hz, 1H, H-1), 2.84 (ddd, *J* = 13.3, 9.7, 4.0 Hz, 1H, H-1), 2.61 – 2.50 (m, 2H, H-3), 2.47 (ddd, *J* = 15.4, 6.8, 4.3 Hz, 1H, H-5), 2.22 (ddd, *J* = 15.4, 10.0, 4.4 Hz, 1H, H-5), 1.84 (dddd, *J* = 14.9, 6.8, 4.4, 2.5 Hz, 1H, H-6), 1.69 (dddd, *J* = 14.9, 10.4, 10.0, 4.3 Hz, 1H, H-6), 1.65 (s, 3H, H-9/10), 1.64 (s, 3H, H-9/10), 1.34 (d, *J* = 6.6 Hz, 3H, H-7); **^{13}C{^{1}H} NMR** (126 MHz, $CDCl_3$) δ 128.6 (C-4), 127.1 (C-8), 56.0 (C-1), 46.3 (C-2), 34.0 (C-6), 30.5 (C-3), 28.9 (C-5), 21.3 (C-7), 20.43 (C-9/10), 20.42 (C-9/10); **FTIR** (neat) ν_{max} /cm^{-1} 3382 (br.), 2964, 2925, 2857, 2735, 1641, 1589, 1455; **HRMS (ESI):** *m/z* calc'd for $C_{10}H_{20}N$ $[M+H]^+$; 154.1590, found; 156.1608.

1,4-oxazepan-4-ium triflate (46f)

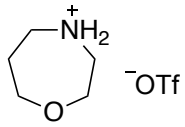

46f

Performed on a 1.50 mmol scale without NaOH wash. Purification by flash column chromatography (90:9:0.7:0.3 DCM:MeOH:H_2O:NH_3; R_f 0.13) to give a yellow residue (185 mg, 0.736 mmol, 49%).

^{1}H NMR (400 MHz, $CDCl_3$) δ 4.85 (s, 2H, N*H*$_2$), 3.83 (t, *J* = 6.0 Hz, 2H, OC*H*$_2$$CH_2CH_2$), 3.80 (t, *J* = 4.5 Hz, 2H, OC*H*$_2$$CH_2NH_2$), 3.15 (t, *J* = 6.0 Hz, 2H, OCH_2CH_2C*H*$_2$), 3.12 (t, *J* = 4.5 Hz, 2H, OCH_2C*H*$_2$$NH_2$), 2.00 (p, *J* = 6.0 Hz, 2H, CH_2C*H*$_2$$CH_2$); **^{13}C{^{1}H} NMR** (101 MHz, $CDCl_3$) δ 120.1 (q, *J* = 318.0 Hz, C_q), 69.5 (CH_2), 68.9 (CH_2), 50.3 (CH_2), 46.5 (CH_2), 30.6 (CH_2); **FTIR** (neat) ν_{max} /cm^{-1} 3481, 3192, 3075, 2925, 2854, 1686, 1618, 1447; **HRMS (ESI):** *m/z* calc'd for $C_5H_{12}NO$ $[M+H]^+$; 101.0913, found; 101.0918.

***N*-Ethyl-4-fluoroaniline (46h)**

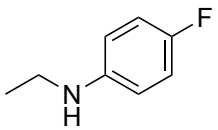

46h

To a flame dried microwave vial was added (*E*)-4-fluoroacetophenone oxime (**45h**) (153 mg, 1.00 mmol), DCM (2.5 mL) and Et_3SiH (399 μL, 2.50 mmol), and the mixture was cooled to -15 °C. Tf_2O (176 μL, 1.05 mmol) was then added in one portion and stirred for 16 hours at -15 °C. After warming to room temperature, the reaction was quenched with NaOH (2.5 mL of a 1.0 M aqueous solution). The organic layer was diluted with DCM (2.5 mL), extracted, and the aqueous layer was washed with DCM (3 x 2.5 mL). The combined organic phases were dried over anhydrous $MgSO_4$, filtered, and concentrated *in vacuo*. The crude residue was purified by flash column chromatography (10% Et_2O in petrol; R_f 0.28) to give a colourless oil (89.2 mg, 0.641 mmol, 64%).

^{1}H NMR (400 MHz, $CDCl_3$) δ 6.94 – 6.84 (m, 2H, Ar*H*), 6.57 – 6.50 (m, 2H, Ar*H*), 3.41 (s, 1H, N*H*), 3.12 (q, *J* = 7.1 Hz, 2H, CH_2), 1.25 (t, *J* = 7.1 Hz, 3H, CH_3); **^{13}C{^{1}H} NMR** (101 MHz, $CDCl_3$) δ 155.9 (d, *J* = 234.5 Hz, C_q), 145.0 (d, *J* = 1.9 Hz, C_q), 115.7 (d, *J* = 22.3 Hz, Ar*H*), 113.6 (d, *J* = 7.4 Hz, Ar*H*), 39.3 (CH_2), 15.0 (CH_3); **^{19}F{^{1}H} NMR** (376 MHz, $CDCl_3$) δ -128.42. **FTIR** (neat) ν_{max} /cm^{-1} 3414 (br.), 3058, 3034, 2970, 2926, 2874, 2851, 1614, 1509, 1483, 1454, 1403; **HRMS (ESI):** *m/z* calc'd for $C_8H_{11}NF$ $[M+H]^+$; 140.0870, found; 140.0882. Data consistent with literature.[21]

N-Ethyl-4-methoxyaniline (46i)

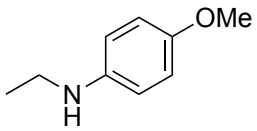

46i

To a flame dried microwave vial was added (*E*)-1-(4-methoxyphenyl)ethan-1-one oxime (**45i**) (165 mg, 1.00 mmol), DCM (2.5 mL) and TMDS (442 μL, 2.50 mmol), and the mixture was cooled to -15 °C. Tf_2O (176 μL, 1.05 mmol) was then added in one portion and stirred for 16 hours at -15 °C. After warming to room temperature, the reaction was quenched with NaOH (2.5 mL of a 1.0 M aqueous solution). The organic layer was diluted with DCM (2.5 mL), extracted, and the aqueous layer was washed with DCM (3 x 2.5 mL). The combined organic phases were dried over anhydrous $MgSO_4$, filtered, and concentrated *in vacuo*. The crude residue was purified by flash column chromatography (5% EtOAc in petrol; R_f 0.18) to give a dark brown oil (99.0 mg, 0.655 mmol, 65%).

^{1}H NMR (400 MHz, $CDCl_3$) δ 6.83 – 6.74 (m, 2H, Ar*H*), 6.64 – 6.57 (m, 2H, Ar*H*), 5.25 (s, 1H, N*H*), 3.75 (s, 3H, OCH_3), 3.12 (q, *J* = 7.1 Hz, 2H, CH_2), 1.24 (t, *J* = 7.1 Hz, 3H, CH_2CH_3); **^{13}C{^{1}H} NMR** (101 MHz, $CDCl_3$) δ 152.38 (C_q), 142.68 (C_q), 115.03 (CH), 114.54 (CH), 55.96 (CH_3), 39.75 (CH_2), 15.09 (CH_3); **FTIR** (neat) ν_{max} /cm^{-1} 3370, 2967, 2934, 2907, 2874, 2833, 1604, 1509, 1464, 1407; **HRMS (ESI):** *m/z* calc'd for $C_9H_{14}NO$ $[M+H]^+$; 152.1070, found; 152.1063. Data consistent with literature.[21]

^{15}N-Boc-azepane (48)

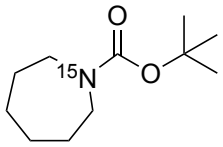

48

To a flame dried microwave vial was added ^{15}N-cyclohexanone oxime (**45g**) (114 mg, 1.00 mmol), DCM (2.5 mL) and TMDS (442 μL, 2.50 mmol) and the mixture was cooled to -15 °C. Tf_2O (176 μL, 1.05 mmol) was then added in one portion and stirred for 15 minutes at -15 °C before warming to room temperature. After 2 hours, $Zn(OAc)_2$ (2.50 mol%, 4.6 mg) was added and the reaction is warmed to 35 °C for a further 18 hours. After cooling to room temperature, the reaction was quenched with water (0.5 mL) and allowed to stir for 30 minutes. The reaction mixture was then diluted with Et_2O (2.5 mL) and extracted with NH_4Cl (3 x 2.5 mL of a 0.5 M aqueous solution). The combined aqueous phases were then basified with NaOH (6.0 M of an aqueous solution) until the pH reached 14 and then re-extracted with DCM (4 x 2.5 mL). The combined organic phases were then dried over anhydrous Na_2SO_4, and carefully concentrated *in vacuo* (azepane bp = 143 °C). To a solution of this crude residue in DCM (5.0 mL) was then added Boc_2O (218 mg, 1.00 mmol) and the reaction mixture was stirred at room temperature. After 16 hours, the organic layer was diluted with H_2O (5.0 mL), extracted, and the aqueous layer was washed with DCM (3 x 2.5 mL). The combined organic phases were dried over anhydrous $MgSO_4$, filtered, and concentrated *in vacuo*. The crude residue was then purified by flash column chromatography (10% Et_2O in petrol; R_f 0.35) to give a colourless oil (72.6 mg, 0.362 mg, 36%).

^{1}H NMR (400 MHz, $CDCl_3$) δ 3.35 (t, *J* = 6.0 Hz, 4H, CH_2), 1.73 – 1.60 (m, 4H, CH_2), 1.57 – 1.49 (m, 4H, CH_2), 1.45 (s, 9H, CH_3); **^{13}C{^{1}H} NMR** (101 MHz, $CDCl_3$) δ 155.8 (d, *J* = 25.9 Hz, (C_q), 79.0 (C_q), 46.9 (d, *J* = 10.1 Hz, CH_2), 28.7 (CH_2), 28.6 (CH_2), 27.3 (CH_2); **^{15}N NMR** (41 MHz, $CDCl_3$) δ 92.15; **FTIR** (neat) ν_{max} /cm^{-1} 2973, 2927, 2856, 1687, 1469, 1452, 1401; **HRMS (ESI):** *m/z* calc'd for $C_{11}H_{22}{}^{15}NO_2$ $[M+H]^+$; 201.1615, found; 201.1614. Data comparable to ^{14}N-Boc-azepane.[22]

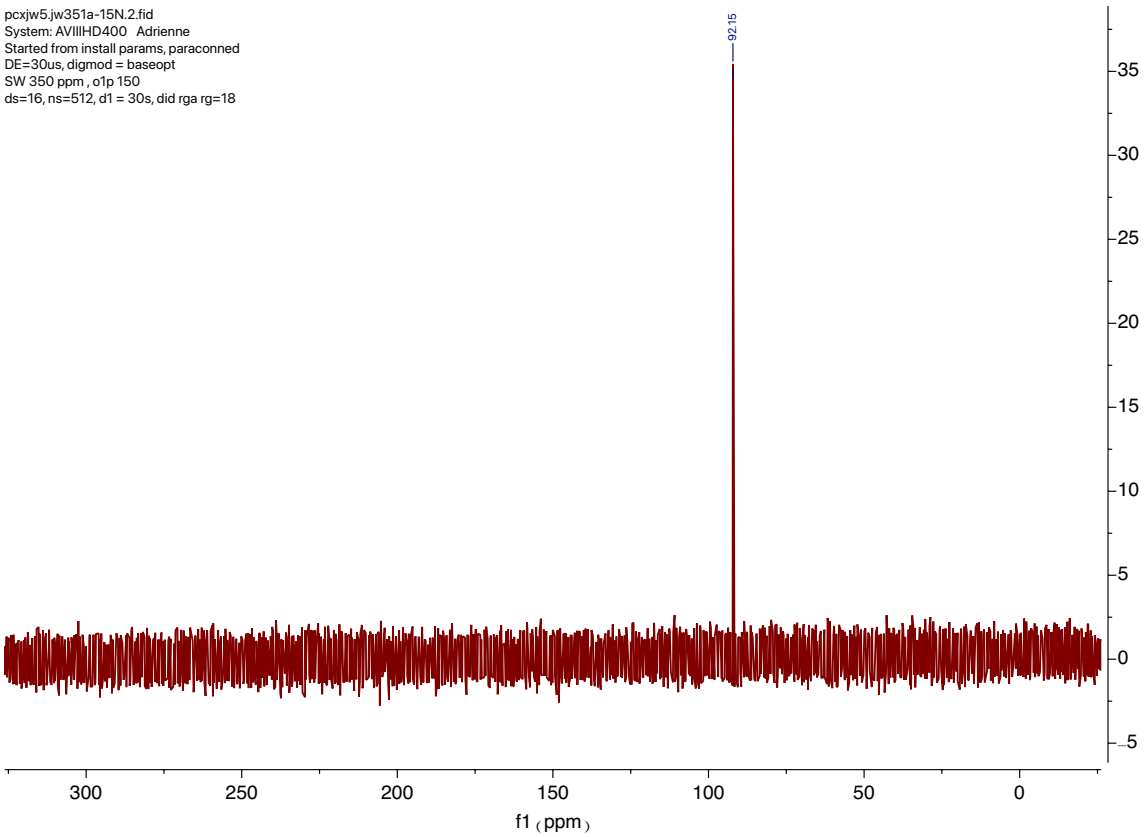

Figure 2. *$^{15}N\{^1H\}$ NMR of ^{15}N-Boc-azepane (**48**)*

(1*S*,3*S*,5*R*)-Bicyclo[3.3.1]non-6-ene-3-carbonitrile (49)

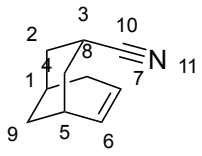

49

Purification by flash column chromatography (5% EtOAc in petrol; R_f 0.20) to give a yellow solid (54.8 mg, 0.372 mmol, 37%).

^{1}H NMR (400 MHz, $CDCl_3$) δ 5.93 (ddd, *J* = 10.0, 3.9, 2.6 Hz, 1H, H-7), 5.87 (apparent ddt, *J* = 10.0, 5.9, 1.7 Hz, 1H, H-6), 2.96 (apparent tt, *J* = 6.8, 1.8 Hz, 1H, H-3), 2.46 (apparent dt, *J* = 19.0, 7.4 Hz, 1H, H-8), 2.40 (m, 1H, H-5), 2.24 (apparent dt, *J* = 19.0, 3.9 Hz, 1H, H-8), 2.25 – 2.14 (m, 1H, H-1), 2.03 (apparent dp, *J* = 14.3, 1.8 Hz, 1H, H-2), 1.98 – 1.87 (m, 2H, H-2, H-4), 1.82 – 1.70 (m, 2H, H-7, H-9), 1.52 (apparent dtd, *J* = 12.5, 3.8, 1.5 Hz, 1H, H-9); **^{13}C{^{1}H} NMR** (101 MHz, $CDCl_3$) δ 131.8 (C-7), 129.4 (C-6), 124.2 (C-10), 34.5 (C-2), 31.9 (C-8), 30.5 (C-9), 30.4 (C-4), 27.5 (C-5), 25.7 (C-1), 21.1 (C-3); **FTIR** (neat) ν_{max} /cm^{-1} 3024, 2962, 2923, 2853, 2229 (CN), 2126, 1458;

HRMS (ESI): *m/z* calc'd for $C_{10}H_{13}NNa$ $[M+H]^+$; 170.0940, found; 170.0954; **m.p.:** 179-183 °C.

4-Azatricyclo[4.3.1.1^{3,8}]undecan-5-one (50)

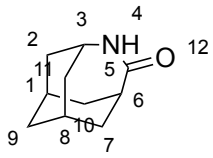

50

Purification by flash column chromatography (5% EtOAc in petrol; R_f 0.20) to give a yellow oil (50.8 mg, 0.307 mmol, 31%).

^{1}H NMR (500 MHz, $CDCl_3$) δ 4.58 (t, *J* = 5.7 Hz, 1H, H-3), 3.06 (t, *J* = 6.3 Hz, 1H, H-6), 2.18 – 2.07 (m, 4H, H-4, H-2, H-11), 2.04 – 1.98 (m, 2H, H-7, H-10), 1.98 – 1.89 (m, 4H, H-4, H-2, H-7, H-10, H-11), 1.77 – 1.68 (m, 2H, H-1, H-8); **^{13}C{^{1}H} NMR** (126 MHz, $CDCl_3$) δ 178.4 (C-5), 52.9 (C-3), 43.4 (C-6), 36.2 (C-2, C-11), 33.5 (C-1, C-10), 30.8 (C-7, C-10), 25.5 (C-9); **FTIR** (neat) ν_{max} /cm^{-1} 2923, 2858, 1719, 1445, 1388; **HRMS (ESI):** *m/z* calc'd for $C_{10}H_{16}NO$ $[M+H]^+$; 166.1226, found; 166.1229.

***N*-Ethyl-*N*,*N*'-bis(4-fluorophenyl)acetimidamide (36)**

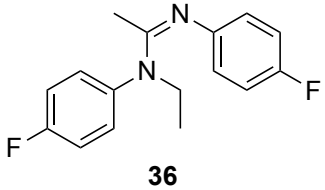

36

To a flame dried microwave vial was added (*E*)-4-fluoroacetophenone oxime (**45h**) (153 mg, 1.00 mmol), DCM (2.5 mL) and TMDS (442 μL, 2.50 mmol), and the mixture was cooled to -15 °C. Tf_2O (176 μL, 1.05 mmol) was then added in one portion and stirred for 5 hours at -15 °C and 16 hours at room temperature. The reaction was quenched with NaOH (2.5 mL of a 1.0 M aqueous solution). The organic layer was diluted with DCM (2.5 mL), extracted, and the aqueous layer was washed with DCM (3 x 2.5 mL). The combined organic phases were dried over anhydrous $MgSO_4$, filtered, and concentrated *in vacuo*. The crude residue was purified by flash column

chromatography (10% Et_2O in petrol; R_f 0.14) to give an off-white solid (66.4 mg, 0.242 mmol, 48%).

^{1}H NMR (400 MHz, $CDCl_3$) δ 7.20 – 7.13 (m, 2H, Ar*H*), 7.13 – 7.04 (m, 2H, Ar*H*), 6.98 – 6.90 (m, 2H, Ar*H*), 6.75 – 6.67 (m, 2H, Ar*H*), 3.85 (q, *J* = 7.1 Hz, 2H, CH_2), 1.59 (s, 3H, CH_3), 1.16 (t, *J* = 7.1 Hz, 3H, CH_3); **^{13}C{^{1}H} NMR** (101 MHz, $CDCl_3$) δ 161.4 (d, *J* = 246.8 Hz, C_q), 158.7 (d, *J* = 239.0 Hz, C_q), 156.3 (C_q), 148.0 (d, *J* = 2.4 Hz, C_q), 140.6 (d, *J* = 3.4 Hz, C_q), 130.6 (d, *J* = 8.5 Hz, C*H*), 123.1 (d, *J* = 7.8 Hz, C*H*), 116.4 (d, *J* = 22.6 Hz, C*H*), 115.5 (d, *J* = 22.0 Hz, C*H*), 45.3 (CH_2), 16.9 (CH_3), 12.7 (CH_3); **^{19}F{^{1}H} NMR** (376 MHz, $CDCl_3$) δ -114.88, -123.43. **FTIR** (neat) ν_{max} /cm^{-1} 3046, 2972, 2929, 2872, 2853, 1620, 1600, 1501, 1443, 1411; **HRMS (ESI):** *m/z* calc'd for $C_{16}H_{17}N_2F_2$ $[M+H]^+$; 275.1354, found; 275.1361; **m.p.:** 109-111 °C.

3.6.5 Nitrilium Ion Chemistry

N-(Cyclohexylmethylene)cyclohexanaminium triflate (52)

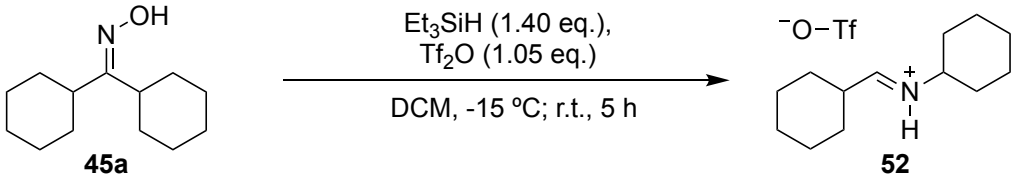

45a **52**

To a flame dried microwave vial was added dicyclohexylmethanone oxime (**45a**) (209 mg, 1.00 mmol), DCM (2.5 mL) and Et_3SiH (223 μL, 1.40 mmol) and the mixture was cooled to -15 °C. Tf_2O (176 μL, 1.05 mmol) was then added in one portion and stirred for 15 minutes at -15 °C before warming to room temperature. After 5 hours, NaOMe (135 mg, 2.50 mmol) was added and stirred for 10 minutes at room temperature. The reaction mixture was then filtered through celite and concentrated *in vacuo*. Excess silane and silicon-containing by-products were removed by warming the crude residue to 40 °C under high vacuum (< 20 mbar) for 24 hours to give a white solid (306 mg, 0.890 mmol, 89%).

^{1}H NMR (400 MHz, $CDCl_3$) δ 12.42 (s, 1H, N$^+$*H*), 8.13 (dd, *J* = 17.1, 8.0 Hz, 1H, C*H*N), 3.76 (tdt, *J* = 11.2, 7.5, 4.0 Hz, 1H, N$^+$C*H*(CH_2)$_2$), 2.90 (dtd, *J* = 11.2, 8.0, 4.0 Hz, 1H, C*H*CHN), 2.02 (apparent dd, *J* = 11.2, 3.7 Hz, 2H, N$^+$CH(C*H*H')$_2$), 1.97 – 1.78 (m, 6H, CH_2), 1.78 – 1.57 (m, 4H, CH_2), 1.48 – 1.15 (m, 8H, CH_2); **^{13}C{^{1}H} NMR** (101 MHz,

$CDCl_3$) δ 182.5 (C*H*), 120.4 (q, *J* = 318.8 Hz, C_q), 63.9 (CH), 42.4 (CH), 31.4 (CH_2), 28.5 (CH_2), 24.9 (CH_2), 24.4 (CH_2), 24.3 (CH_2), 24.2 (CH_2); **FTIR** (neat) ν_{max} /cm^{-1} 3189, 3039, 2931, 2857, 1698, 1450, 1401; **HRMS (ESI):** *m/z* calc'd for $C_{10}H_{16}NO$ $[M+H]^+$; 194.1904, found; 184.1896; **m.p.:** 126-132 °C.

N-(Adamantan-1-yl)-1-(pyrrolidin-1-yl)ethan-1-imine (53)

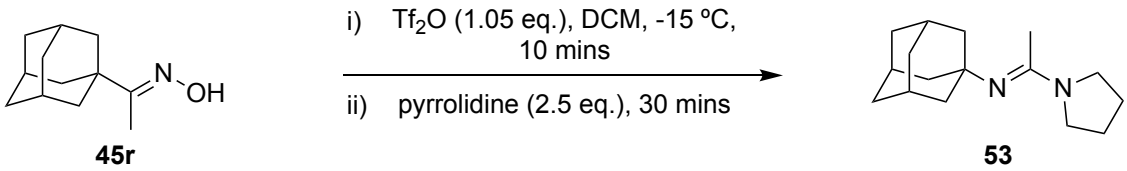

45r **53**

To a flame-dried microwave vial was added **(***E*)-1-(adamantan-1-yl)ethan-1-one oxime (**45r**) (193 mg, 1.00 mmol) and DCM (2.5 mL) and the solution was cooled to -15 °C. Tf_2O (176 μL, 1.05 mmol) was then added in one portion and stirred for 10 minutes at -15 °C. Pyrrolidine (209 μL, 2.50 mmol) was then added and stirred for 30 minutes. The reaction mixture was then warmed to room temperature and quenched with NaOH (2.5 mL of a 1.0 M aqueous solution) which was allowed to stir at room temperature for 10 minutes. The mixture was then diluted with DCM (2.5 mL) and extracted, washing the aqueous with DCM (2 x 5.0 mL). The combined organic phases were then dried over anhydrous $MgSO_4$ and concentrated *in vacuo*. The crude residue was purified by flash column chromatography (95:4.5:0.4:0.1 DCM:MeOH:H_2O:NH_3; R_f 0.20) to give a white solid (165 mg, 0.670 mmol, 67%).

^{1}H NMR (400 MHz, $CDCl_3$) δ 3.69 – 3.56 (m, 4H, CH_2NCH_2), 2.46 (s, 3H, CH_3), 2.20 – 2.14 (m, 3H, C*H*), 2.11 – 2.04 (m, 10H, CH_2), 1.73 – 1.64 (m, 6H, CH_2); **^{13}C{^{1}H} NMR** (101 MHz, $CDCl_3$) δ 161.4 (C_q), 57.1 (C_q), 50.7 (CH_2), 48.6 (CH_2), 42.7 (CH_2), 35.7 (CH_2), 29.7 (CH), 25.1 (CH_2), 24.9 (CH_2), 18.6 (CH_3); **FTIR** (neat) ν_{max} /cm^{-1} 3344, 2910, 2849, 1638, 1505, 1453, 1425; **HRMS (ESI):** *m/z* calc'd for $C_{16}H_{27}N_2$ $[M+H]^+$; 247.2169, found; 247.2171; **m.p.:** 134-136 °C.

7-(Benzo[*d*][1,3]dioxol-5-yl)-2-(trifluoromethyl)-3,4,5,6-tetrahydro-2*H*-azepine (54)

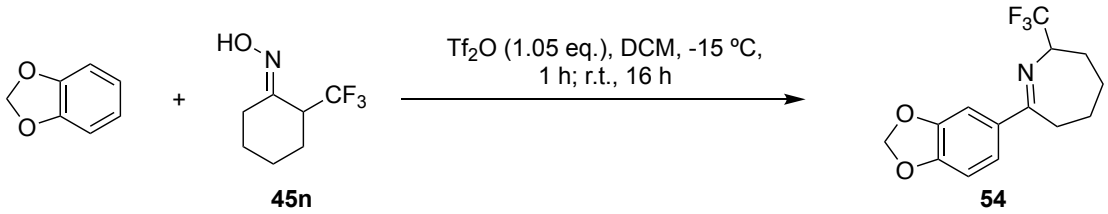

45n **54**

To a flame-dried microwave vial was added (*E*)-2-(trifluoromethyl)cyclohexan-1-one oxime (**45n**) (90.6 mg, 500 μmol), 1,3 benzodioxole (72.3 mg, 592 μmol) and DCM (1.3 mL), and the solution was cooled to -15 °C. Tf_2O (88.2 μL, 0.550 mmol) was added in 1 portion and was stirred for 1 hour at -15 °C, then 16 hours at room temperature. The reaction was then quenched with Na_2CO_3 (1.0 mL of a saturated aqueous solution), diluted with DCM (5.0 mL) and Na_2CO_3 (5.0 mL of a saturated aqueous solution) and separated. The organic phase was dried over anhydrous $MgSO_4$ and concentrated *in vacuo*. The crude residue was purified by flash column chromatography to give a colourless oil (55.0 mg, 0.193 mmol, 39%)

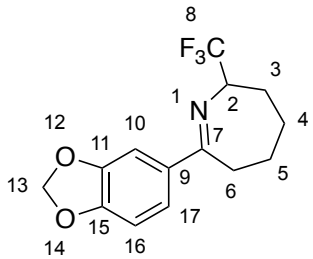

54

^{1}H NMR (400 MHz, $CDCl_3$) δ 7.40 (d, *J* = 1.8 Hz, 1H, H-10), 7.27 (dd, *J* = 8.1, 1.8 Hz, 1H, H-17), 6.80 (d, *J* = 8.1 Hz, 1H, H-16), 5.98 (d, *J* = 4.1 Hz, 1H, H-13), 5.98 (d, *J* = 4.1 Hz, 1H, H-13), 4.00 (qd, *J* = 9.1, 8.2 Hz, 1H, H-2), 3.10 (ddt, *J* = 14.6, 6.8, 1.5 Hz, 1H, H-6), 2.51 (ddd, *J* = 14.6, 12.5, 1.9 Hz, 1H, H-6), 2.10 (ddd, *J* = 13.3, 4.0, 3.9 Hz, 1H, H-4), 2.06 (ddd, *J* = 13.9, 4.2, 4.0 Hz, 1H, H-3), 1.96 – 1.85 (m, 1H, H-5), 1.79 (ddddd, *J* = 13.3, 13.1, 12.4, 4.2, 3.4 Hz, 1H, H-4), 1.45 (dddd, *J* = 13.9, 13.1, 8.2, 2.4 Hz, 1H, H-3), 1.33 (dddd, *J* = 13.9, 12.5, 3.8, 1.5 Hz, 1H, H-5); **^{13}C{^{1}H} NMR** (101 MHz, $CDCl_3$) δ 173.5 (C-7), 149.6 (C-9), 148.2 (C-11), 134.6 (C-15), 126.6 (q, *J* = 271.7 Hz, C-8), 121.7 (C-17), 107.8 (C-16), 107.6 (C-10), 101.5 (C-13), 63.7 (q, *J* = 27.6 Hz, C-2), 30.7 (C-6), 29.6 (C-4), 25.2 (q, *J* = 2.0 Hz, C-3), 23.1 (C-5); **^{19}F NMR** (376 MHz, $CDCl_3$) δ -

77.2; **FTIR** (neat) ν_{max} /cm^{-1} 2931, 2863, 1633, 1607, 1505, 1490, 1461, 1438; **HRMS (ESI):** *m/z* calc'd for $C_{14}H_{15}NO_2F_3$ $[M+H]^+$; 286.1049, found; 286.1050.

4-Isopropyl-6-methoxy-2-methylquinazoline (55)

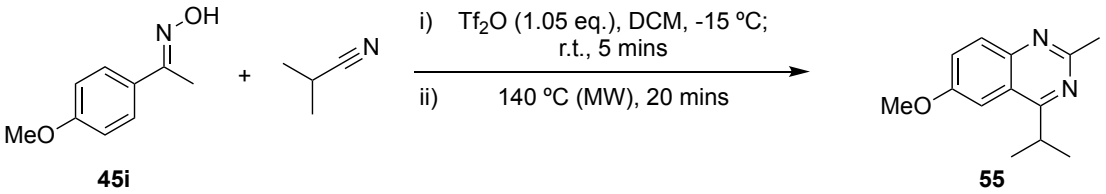

45i **55**

Synthesised using an adapted literature procedure.[23] To a flame-dried microwave vial was added (*E*)-1-(4-methoxyphenyl)ethan-1-one oxime (**45i**) (165 mg, 1.00 mmol) and DCM (2.5 mL), and the solution was cooled to -15 °C. Tf_2O (176 μL, 1.05 mmol) and isobutyronitrile (98.7 μL, 1.10 mmol) were then sequentially added and the solution was stirred at room temperature for 5 minutes. The sealed reaction mixture was then heated in a microwave to 140 °C for 20 minutes. After cooling to room temperature, the mixture was diluted with DCM (5.0 mL) and washed with NaOH (2.5 mL of a 1.0 M aqueous solution) and NaCl (4.0 mL of a saturated aqueous solution). The organic phase was then dried over anhydrous $MgSO_4$ and concentrated *in vacuo*. The crude residue was purified by flash column chromatography (20% EtOAc in petrol; R_f 0.43) to give an orange oil (77.9 mg, 0.360 mmol, 36%).

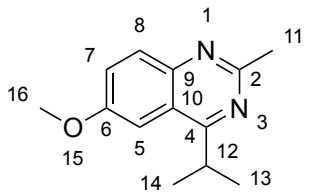

55

^{1}H NMR (500 MHz, $CDCl_3$) δ 7.87 (d, *J* = 9.2 Hz, 1H, H-8), 7.47 (dd, *J* = 9.2, 2.7 Hz, 1H, H-7), 7.32 (d, *J* = 2.7 Hz, 1H, H-5), 3.95 (s, 3H, H-10), 3.79 (hept, *J* = 6.8 Hz, 1H, H-13), 2.83 (s, 3H, H-11), 1.42 (d, *J* = 6.8 Hz, 6H, H-13, H-14); **^{13}C{^{1}H} NMR** (126 MHz, $CDCl_3$) δ 174.1 (C-4), 161.9 (C-2), 157.6 (C-6), 146.4 (C-9), 130.0 (C-8), 125.7 (C-7), 121.7 (C-10), 102.1 (C-5), 55.8 (C-16), 31.1 (C-12), 26.4 (C-11), 21.7 (C-13, C-14); **FTIR** (neat) ν_{max} /cm^{-1} 2966, 2930, 2870, 1621, 1499, 1453, 1429, 1406; **HRMS (ESI):** *m/z* calc'd for $C_{13}H_{17}N_2O$ $[M+H]^+$; 217.1335, found; 217.1338.

Procedure for the 'Second Generation' Reductive Beckmann Reaction

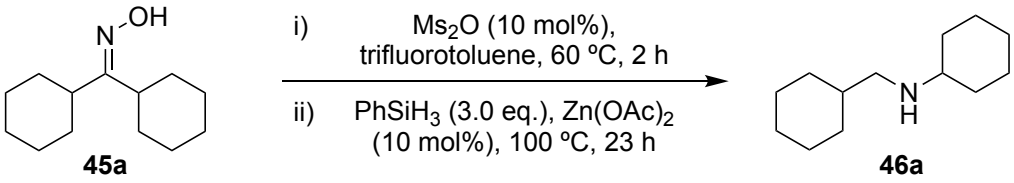

To a flame dried microwave vial was added dicyclohexylmethanone oxime (**45a**) (209 mg, 1.00 mmol), methanesulfonic anhydride (17.4 mg, 0.100 mmol) and trifluorotoluene (2.5 mL). The reaction mixture was heated to 60 °C. After 2 hours, phenylsilane (370 μL, 3.00 mmol) and $Zn(OAc)_2$ (18.3 mg, 0.100 mmol) were added and the reaction was heated to 100 °C for a further 23 hours. After cooling to room temperature, the reaction was quenched with NaOH (2.5 mL of a 1.0 M aqueous solution) (caution: hydrogen evolution). The organic layer was diluted with DCM (2.5 mL), extracted, and the aqueous layer was washed with DCM (3 x 2.5 mL). The combined organic phases were dried over anhydrous $MgSO_4$, filtered, and concentrated *in vacuo*. The crude residue was purified using flash column chromatography (90:9:0.7:0.3 DCM:MeOH:H_2O:NH_3; R_f 0.50) to give a yellow oil (184 mg, 0.942 mmol, 94%). Characterisation provided above.

3.6.6 Meptazinol Experimental

3-Ethylcyclohex-2-en-1-one (62)

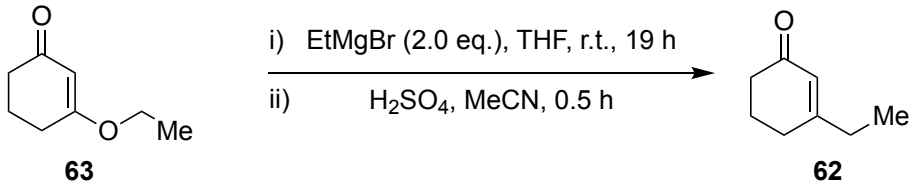

63 **62**

Synthesised using an adapted literature procedure.[24] To a flame-dried flask was added EtMgBr (18.4 mL, 55.2 mmol of a 3.0 M solution in Et_2O). The solution was cooled to 0 °C and a solution of 3-ethoxycyclohex-2-en-1-one (**63**) (3.86 g, 27.5 mmol) in THF (10.0 mL) was added dropwise over 30 minutes. The reaction mixture was then warmed to room temperature and for 19 hours. The reaction was then quenched with sulfuric acid (0.5 M, 10 mL of an aqueous solution), diluted with Et_2O (20 mL), and separated. The aqueous phase was extracted with additional Et_2O (20 mL) and the combined organic layers were washed with $NaHCO_3$ (20 mL of a saturated aqueous solution), dried over anhydrous $MgSO_4$, filtered and concentrated *in vacuo*. The partially hydrolysed intermediates were then diluted with MeCN (10 mL) and sulfuric acid (5.0 mL of a 2.0 M aqueous solution) and stirred for 30 minutes at room temperature. Following complete hydrolysis (monitored by TLC), the solution was diluted with brine (10 mL of a saturated solution) and extracted with Et_2O (3 x 20 mL). The combined organic phases were dried over anhydrous $MgSO_4$, filtered, and concentrated *in vacuo*. The crude residue was purified by flash column chromatography (50% Et_2O in petrol; R_f 0.29) to give a clear pale-yellow oil (2.54 g, 20.3 mmol, 74%).

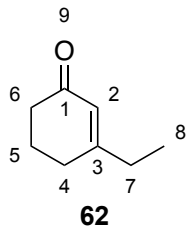

62

^{1}H NMR (500 MHz, $CDCl_3$) δ 5.86 (s, 1H, H-2), 2.34 (t, *J* = 6.7 Hz, 2H, H-6), 2.28 (t, *J* = 5.9 Hz, 2H, H-4), 2.22 (q, *J* = 7.5 Hz, 2H, H-7), 1.97 (p, *J* = 6.5 Hz, 2H, H-5), 1.08 (t, *J* = 7.5 Hz, 3H, H-8); **^{13}C{^{1}H} NMR** (126 MHz, DMSO) δ 200.2 (C-1), 168.0 (C-3), 124.7

(C-2), 37.5 (C-6), 31.0 (C-7), 29.8 (C-4), 22.8 (C-5), 11.4 (C-8); **FTIR** (neat) ν_{max} /cm^{-1} 2968, 2967, 2878, 2827, 1662, 1623, 1457, 1428; **HRMS** (ESI) *m/z* calc'd for $C_8H_{13}O$ $[M+H]^+$: 125.0961, found: 125.0971. Data are consistent with literature.[24]

(*R*)-3-Ethyl-3-(3-methoxyphenyl)cyclohexan-1-one (61)

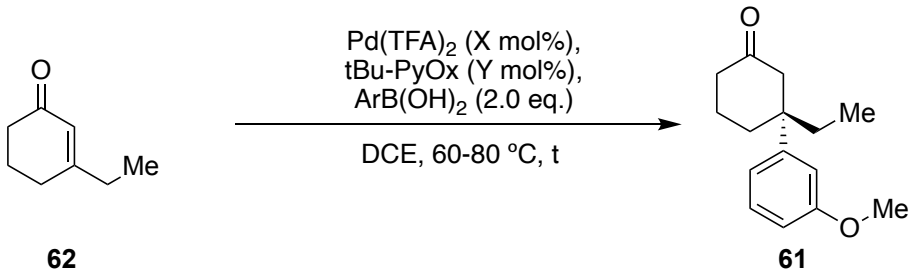

62 **61**

Synthesised using an adapted literature procedure.[25] To a solution of 3-ethylcyclohex-2-en-1-one (**62**) (31.0 mg, 25.0 μmol), (*S*)-4-*tert*-Butyl-2-(2-pyridyl)oxazoline (3.1 mg, 15 μmol) and $Pd(TFA)_2$ (4.2 mg, 12.5 μmol) in DCE (500 μL) was added 3-methoxyphenylboronic acid (76.0 mg, 0.50 mmol) and the reaction mixture was heated at 80 °C for 30 hours. After cooling to room temperature, the reaction mixture was concentrated *in vacuo* and purified directly by flash column chromatography (100% DCM; R_f 0.17) to give a yellow oil (51.9 mg, 22.3 μmol, 89%, 89% e.e.).

Scale /mmol	Ligand	Temperature /°C	Catalyst Loading /mol%	Time /days	Yield /%	e.e. /%
0.22	(*S*)-*t*-BuPyOx	60	5	1	89	89
0.74	2,2'-bipyridine	80	10	4	74	0
13.2	(*S*)-*t*-BuPyOx	80	10	5	66	92

Table 1. *The effect of reaction scale on yield and e.e.*

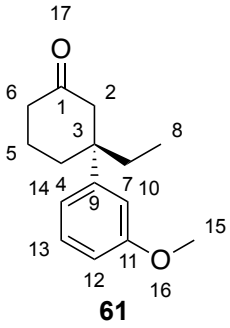

61

^{1}H NMR (500 MHz, $CDCl_3$) δ 7.23 (dd, *J* = 7.8, 8.0 Hz, 1H, H-13), 6.84 (ddd, *J* = 7.8, 1.9, 0.9 Hz, 1H, H-14), 6.81 (dd, *J* = 2.5, 1.9 Hz, 1H, H-10), 6.74 (ddd, *J* = 8.0, 2.5, 0.9 Hz, 1H, H-12), 3.79 (s, 3H, H-15), 2.89 (apparent dddt, *J* = 14.3, 1.9, 1.1, 0.6 Hz, 1H, H-2), 2.40 (d, *J* = 14.3 Hz, 1H, H-2), 2.31 – 2.27 (m, 2H, H-6), 2.14 (dddd, *J* = 13.7, 6.5, 3.6, 1.9 Hz, 1H, H-4), 1.96 (dddd, *J* = 13.7, 10.0, 3.6, 0.6 Hz, 1H, H-4), 1.82 (ddddd, *J* = 13.8, 6.5, 6.2, 5.9, 3.6 Hz, 1H, H-5), 1.75 (dq, *J* = 13.7, 7.4 Hz, 1H, H-7), 1.63 (apparent dq, *J* = 13.7, 7.4 Hz, 1H, H-7), 1.66 – 1.54 (m, 1H, H-5), 0.61 (t, *J* = 7.4 Hz, 3H, H-8); **^{13}C{^{1}H} NMR** ^{13}C NMR (126 MHz, $CDCl_3$) δ 211.6 (C-1), 159.8 (C-11), 146.9 (C-9), 129.5 (C-13), 119.2 (C-14), 113.2 (C-10), 110.9 (C-12), 55.3 (C-15), 50.8 (C-2), 46.6 (C-3), 41.2 (C-6), 36.5 (C-4), 35.7 (C-7), 21.7 (C-5), 8.1 (C-8); **FTIR** (neat) ν_{max} /cm^{-1} 2961, 2937, 2876, 2835, 1705, 1600, 1582, 1488, 1459, 1430; **HRMS** (ESI) *m/z* calc'd for $C_{15}H_{21}O_2$ $[M+H]^+$: 233.1536, found: 233.1534; **Chiral HPLC** column: ODH (4.6 mm × 250 mm, 5 μm), mobile phase: 9:1 isohexane:isopropanol (isocratic), flow rate: 1.0 mL/min, temperature: 40 °C, t_R 10.81 mins (major), 13.01 mins (minor), 92% e.e.; **$[\alpha]_D^{25}$** -54.3° (*c*. 1.0, $CHCl_3$, at 92% e.e.).

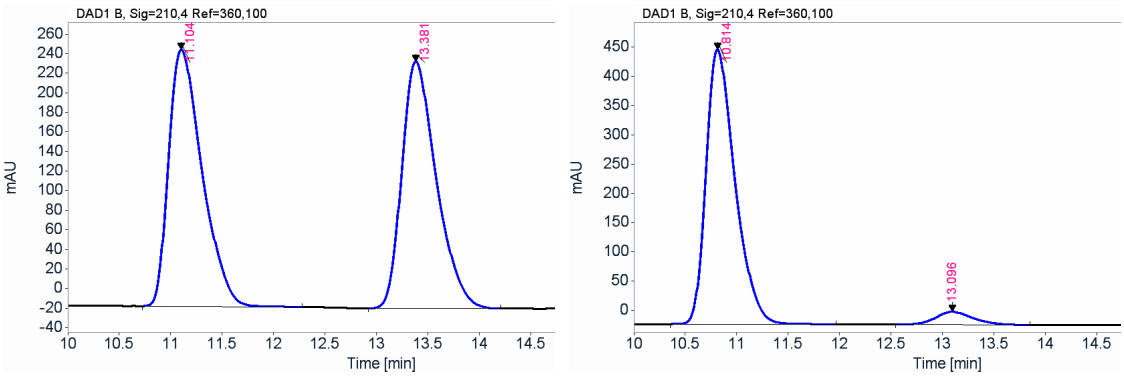

Signal:	DAD1 B, Sig=210,4 Ref=360,100				
RT [min]	Type	Width [min]	Area	Height	Area%
11.104	BB	0.3459	5932.257	262.2860	50.23
13.381	BB	0.3516	5877.530	252.4673	49.77

Signal:	DAD1 B, Sig=210,4 Ref=360,100				
RT [min]	Type	Width [min]	Area	Height	Area%
10.814	BB	0.2963	9191.006	469.6252	94.35
13.096	BB	0.3711	550.201	22.0481	5.65

Figure 3. *Chiral HPLC chromatograms of racemic (left) and enantioenriched (R)-**61** at 89% e.e.*

(*R*)-3-Ethyl-3-(3-methoxyphenyl)cyclohexan-1-one oxime; (*Z*)-isomer (64) and (*E*)-isomer (60)

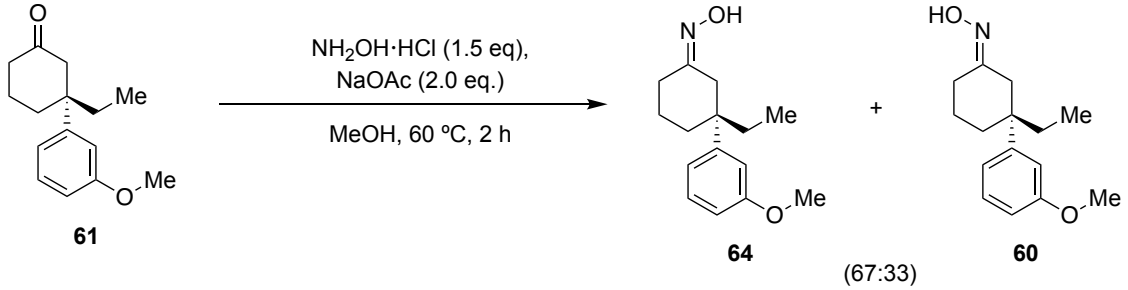

To a suspension of (*R*)-3-ethyl-3-(3-methoxyphenyl)cyclohexan-1-one (**61**) (582 mg, 2.50 mmol), and NaOAc (410 mg, 5.00 mmol) in MeOH (5.0 mL), was added $NH_2OH{\cdot}HCl$ (261 mg, 3.76 mmol) and the reaction mixture was heated to 60 °C for 2 hours. After cooling to room temperature, the reaction mixture was diluted with Et_2O (5.0 mL) and successively washed with brine (solution containing 2.5 mL of a saturated solution and 2.5 mL of water) and $NaHCO_3$ (5.0 mL of a saturated solution). The organic layer was dried over anhydrous $MgSO_4$, filtered, and concentrated *in vacuo*. The crude residue was purified by flash column chromatography (98:2 DCM:MeOH; R_f 0.19, 0.17) to give a yellow oil (613 mg, 2.48 mmol, 99%, 67:33 *Z*:*E* mixture of diastereoisomers; **64:60**).

Ratio of diastereoisomers determined by ^1H spectroscopy and assigned by NOESY correlations. Individual ^1H NMR signals quoted from the mixture of diastereoisomers.

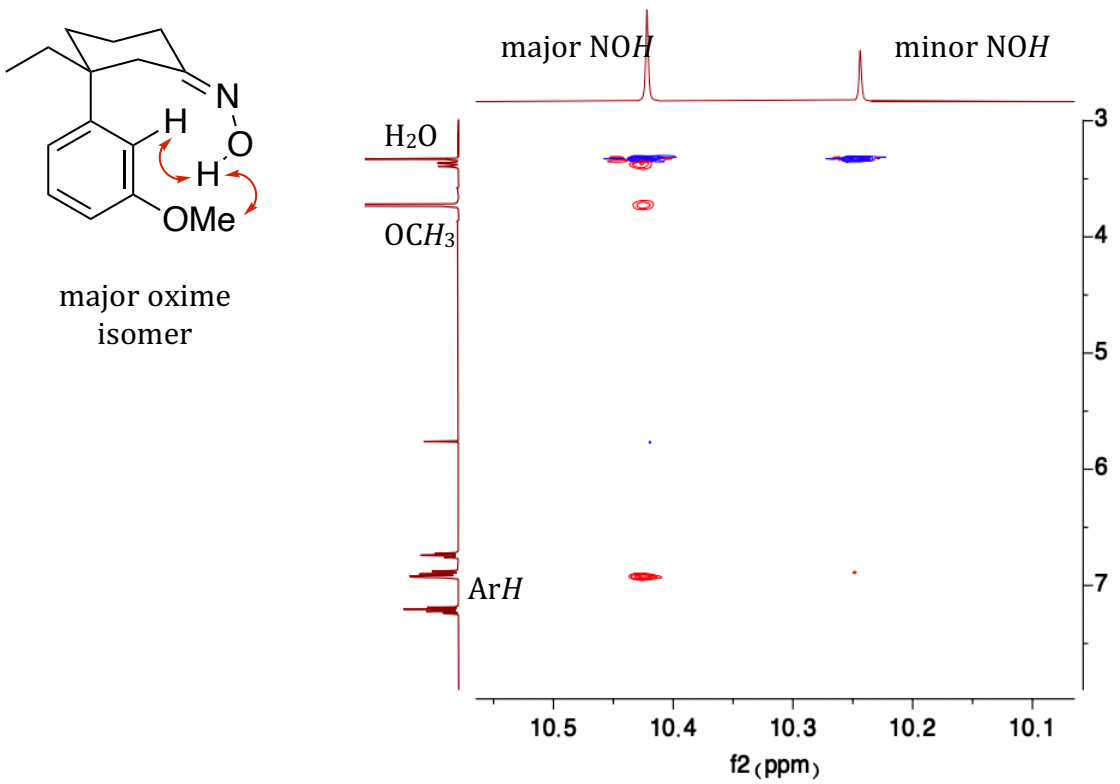

Figure 4. *NOESY correlation for the mixture of oxime diastereoisomers* ***64*****:*****60***

Major (*Z*)-isomer (64)

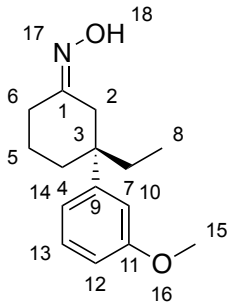

64

^{1}H NMR (500 MHz, DMSO) δ 10.41 (s, 1H, H-18), 7.20 (dd, *J* = 8.0, 7.9 Hz, 1H, H-13), 6.92 (dd, *J* = 2.3, 1.8 Hz, 1H, H-10), 6.90 (ddd, *J* = 7.9, 1.8, 0.9 Hz, 1H, H-14), 6.72 (ddd, *J* = 8.0, 2.3, 0.9 Hz, 1H, H-12), 3.72 (s, 3H, H-15), 3.37 (apparent dt, *J* = 14.2, 1.4 Hz, 1H, H-2), 2.11 (apparent dt, *J* = 14.4, 5.1 Hz, 1H, H-6), 2.09 – 2.01 (m, 2H, H-6, H-3), 1.97 (d, *J* = 14.2 Hz, 1H, H-2), 1.71 (ddd, *J* = 13.6, 11.4, 3.5 Hz, 1H, H-4), 1.59 – 1.46 (m, 3H, H-5, H-7), 1.13 (apparent dtdd, *J* = 13.9, 11.0, 5.1, 3.3 Hz, 1H, H-5), 0.53 (t, *J* = 7.4 Hz, 3H, H-8); **^{13}C{^{1}H} NMR** (126 MHz, DMSO) δ 159.1 (C-11), 156.0 (C-1), 147.1

(C-9), 129.0 (C-13), 118.5 (C-14), 112.9 (C-10), 110.7 (C-12), 54.8 (C-15), 44.2 (C-3), 37.7 (C-4), 36.0 (C-7), 31.6 (C-2), 31.2 (C-6), 21.8 (C-5), 8.0 (C-10).

Minor (*E*)-Isomer (60)

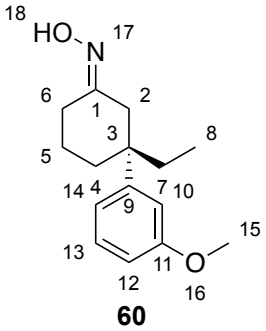

60

^{1}H NMR (500 MHz, DMSO) δ 10.24 (s, 1H, H-18), 7.22 (dd, *J* = 8.0, 7.8 Hz, 1H, H-13), 6.90 (ddd, *J* = 7.8, 2.0, 0.8 Hz, 3H, H-14), 6.87 (dd, *J* = 2.6, 2.0 Hz, 1H, H-10), 6.74 (ddd, *J* = 8.0, 2.6, 0.8 Hz, 2H, H-12), 3.72 (s, 3H, H-15), 2.66 (d, *J* = 14.2 Hz, 1H, H-2), 2.49 (ddd, *J* = 14.7, 6.1, 5.6 Hz, 1H, H-6), 2.23 (d, *J* = 14.0 Hz, 1H, H-2), 2.18 (ddd, *J* = 14.7, 9.4, 5.7 Hz, 1H, H-6), 1.75 (ddd, *J* = 13.6, 9.9, 3.5 Hz, 1H, H-4), 1.68 – 1.60 (m, 1H, H-4), 1.60 – 1.47 (m, 3H, H-5, H-7), 1.24 (ddddd, *J* = 13.4, 9.9, 9.4, 5.6, 3.5 Hz, 1H, H-5), 0.51 (t, *J* = 7.4 Hz, 3H, H-8); **^{13}C{^{1}H} NMR** (126 MHz, DMSO) δ 159.0 (C-11), 155.9 (C-1), 147.3 (C-9), 129.0 (C-13), 119.0 (C-14), 113.5 (C-10), 110.2 (C-12), 54.8 (C-15), 43.1 (C-3), 39.9 (C-2), 36.0 (C-4), 34.4 (C-7), 23.3 (C-6), 20.4 (C-5), 7.9 (C-8).

FTIR (neat) ν_{max} /cm^{-1} 3216, 3084, 2959, 2934, 2876, 1660, 1599, 1581, 1488, 1449, 1429; **HRMS** (ESI) *m/z* calc'd for $C_{15}H_{22}NO_2$ $[M+H]^+$: 248.1645, found: 248.1647.

(*R*)-4-Ethyl-4-(3-methoxyphenyl)azepane (65) and (*S*)-3-ethyl-3-(3-methoxyphenyl)azepane (59)

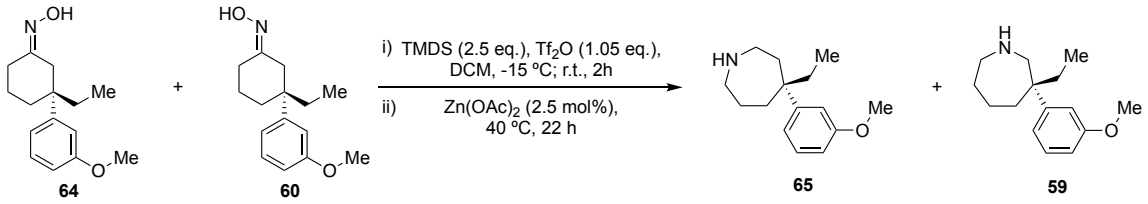

To a flame dried microwave vial was added **64** and **60** (67:33 d.r., 435 mg, 1.76 mmol), DCM (4.4 mL) and TMDS (777 μL, 4.40 mmol) which was cooled to -15 °C. Tf_2O (310 μL, 1.85 mmol) was then added in one portion and the solution was

stirred for 15 mins at -15 °C before warming to room temperature. After a 2 hours, $Zn(OAc)_2$ (8.1 mg, 44 μmol) was added and the suspension was heated to 35 °C. After a further 22 hours, the reaction was cooled to room temperature and quenched with NaOH (4.4 mL of a 1.0 M aqueous solution). The organic layer was diluted with DCM (4.4 mL), extracted, and the aqueous layer was washed with DCM (3 x 4.4 mL). The combined organic phases were dried over anhydrous $MgSO_4$, filtered, and concentrated *in vacuo*. The crude residue was purified using flash column chromatography (90:9:0.8:0.2 DCM:MeOH:H_2O:NH_3) to give **59** as a dark brown oil (R_f 0.43, 93.3 mg, 365 μmol, 23%) and **65** as a light brown oil (R_f 0.13, 159 mg, 525 μmol, 39%).

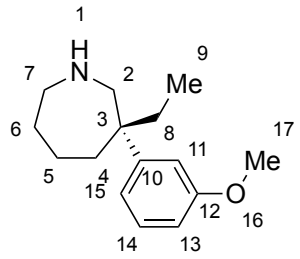

59

^{1}H NMR (400 MHz, $CDCl_3$) δ 7.24 (dd, *J* = 8.2, 7.8 Hz, 1H, H-14), 6.91 (ddd, *J* = 7.8, 1.9, 0.9 Hz, 1H, H-15), 6.87 (dd, *J* = 2.6, 1.9 Hz, 1H, H-11), 6.73 (ddd, *J* = 8.2, 2.6, 0.9 Hz, 1H, H-13), 3.80 (s, 3H, H-17), 3.21 (d, *J* = 14.3 Hz, 1H, H-2), 2.91 (apparent dt, *J* = 13.2, 5.5 Hz, 1H, H-7), 2.86 (d, *J* = 14.3 Hz, 1H, H-2), 2.76 (apparent dt, *J* = 13.2, 6.6 Hz, 1H, H-7), 2.22 (dd, *J* = 14.2, 8.4 Hz, 1H, H-4), 1.78 – 1.46 (m, 7H, H-4, H-5, H-6, H-8), 0.60 (t, *J* = 7.5 Hz, 3H, H-9). **^{13}C{^{1}H} NMR** (101 MHz, $CDCl_3$) δ 159.7 (C-12), 148.7 (C-10), 129.2 (C-14), 119.7 (C-15), 113.9 (C-11), 110.0 (C-13), 59.2 (C-2), 55.2 (C-17), 50.9 (C-7), 47.0 (C-3), 37.8 (C-4), 35.5 (C-8), 32.2 (C-6), 22.8 (C-5), 8.7 (C-9). **FTIR** (neat) ν_{max} /cm^{-1} 3342, 3078, 2957, 2926, 2875, 2857, 2833, 1605, 1580, 1487, 1462; **HRMS** (ESI) *m/z* calc'd for $C_{15}H_{24}NO$ $[M+H]^+$: 234.1852, found: 234.1855; **$[\alpha]_D^{25}$** -3.6° (*c*. 0.99, $CHCl_3$).

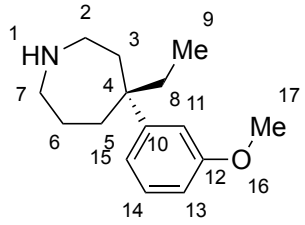

65

^{1}H NMR (400 MHz, $CDCl_3$) δ 7.23 (dd, *J* = 8.2, 7.9 Hz, 1H, H-14), 6.86 (ddd, *J* = 7.9, 1.9, 0.9 Hz, 1H, H-15), 6.82 (dd, *J* = 2.5, 1.9 Hz, 1H, H-11), 6.72 (ddd, *J* = 8.2, 2.5, 0.9 Hz, 1H, H-13), 3.80 (s, 3H, H-17), 2.94 (ddd, *J* = 14.1, 6.6, 2.8 Hz, 1H, H-2), 2.87 – 2.73 (m, 3H, H-2, H-7), 2.27 (dddd, *J* = 15.1, 6.6, 2.4, 1.1 Hz, 1H, H-3), 2.20 (dddd, *J* = 14.6, 7.8, 2.5, 1.1 Hz, 1H, H-5), 1.81 – 1.65 (m, 3H, H-3, H-5, H-6), 1.65 – 1.54 (m, 3H, H-6, H-8), 0.59 (t, *J* = 7.4 Hz, 3H, H-9). **^{13}C{^{1}H} NMR** (101 MHz, $CDCl_3$) δ 159.6 (C-12), 149.3 (C-10), 129.0 (C-14), 119.6 (C-15), 114.0 (C-11), 109.7 (C-13), 55.2 (C-17), 49.6 (C-7), 44.62 (C-5), 44.59 (C-2), 42.0 (C-3), 38.5 (C-8), 37.7 (C-5), 26.5 (C-6), 8.8 (C-9); **FTIR** (neat) ν_{max} /cm^{-1} 3304, 2960, 2932, 2875, 2858, 2834, 1605, 1580, 1546, 1463, 1430, 1409; **HRMS** (ESI) *m/z* calc'd for $C_{15}H_{24}NO$ $[M+H]^+$: 234.1852, found: 234.1851; **$[\alpha]_D^{25}$** +1.6° (*c*. 0.96, $CHCl_3$).

2-Methyl-1,2,3,4-tetrahydroisoquinoline (66)

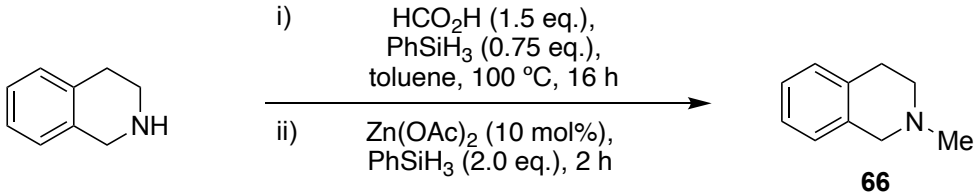

66

Synthesised using an adapted literature procedure.[26] To a biphasic mixture of HCO_2H (113 μL, 2.00 mmol) and phenylsilane (185 μL, 1.50 mmol) in toluene (2.0 mL) at 80 °C was added 1,2,3,4-tetrahydroisoquinoline (266 mg, 2.00 mmol) using a toluene (400 μL) rinse to ensure full transferal. After the effervescence eased (5 mins) the mixture was heated to 100 °C for 16 hours after which time $Zn(OAc)_2$ (36.7 mg, 200 μmol) and phenylsilane (500 μL, 4.05 mmol) were then added. The mixture was heated to 100 °C for an additional 2 hours, then, after cooling to room temperature, the reaction was quenched by slow addition of NaOH (1.0 mL of a 1.0 M aqueous solution). After 30 minutes of stirring, the mixture was diluted with DCM

(5.0 mL) and NaOH (5.0 mL of a 1.0 M aqueous solution) which was separated, washing the aqueous phase with additional DCM (3 x 5.0 mL). The combined organic phases were dried over anhydrous $MgSO_4$, filtered, and concentrated *in vacuo*. The crude residue was purified by flash column chromatography (95:4.5:0.4:0.1 DCM:MeOH:H_2O:NH_3; R_f 0.20) to give a white solid (293 mg, 1.99 mol, 99%).

^{1}H NMR (400 MHz, $CDCl_3$) δ 7.16 – 7.07 (m, 3H, Ar*H*), 7.05 – 6.97 (m, 1H, Ar*H*), 3.57 (s, 2H, ArC*H*$_2$N), 2.92 (t, *J* = 6.0 Hz, 2H, ArC*H*$_2$CH$_2$N), 2.68 (t, *J* = 6.0 Hz, 2H, ArCH$_2$C*H*$_2$N), 2.45 (s, 3H, C*H*$_3$); **^{13}C{^{1}H} NMR** (101 MHz, $CDCl_3$) δ 134.9 (C_q), 133.9 (C_q), 128.8 (CH), 126.5 (CH), 126.2 (CH), 125.7 (CH), 58.1 (CH_2), 53.0 (CH_2), 46.2 (CH_3), 29.3 (CH_2); **FTIR** (neat) ν_{max} /cm^{-1} 3071, 3047, 3022, 2966, 2938, 2920, 2839, 2780, 2737, 2683, 1594, 1498, 1454, 1430; **HRMS** (ESI) *m/z* calc'd for $C_{10}H_{14}N$ $[M+H]^+$: 148.1121, found: 148.1113; **m.p.:** 121-123 °C (lit 121-122 °C). Data are consistent with literature.[27]

(*S*)-3-Ethyl-3-(3-methoxyphenyl)-1-methylazepane (68)

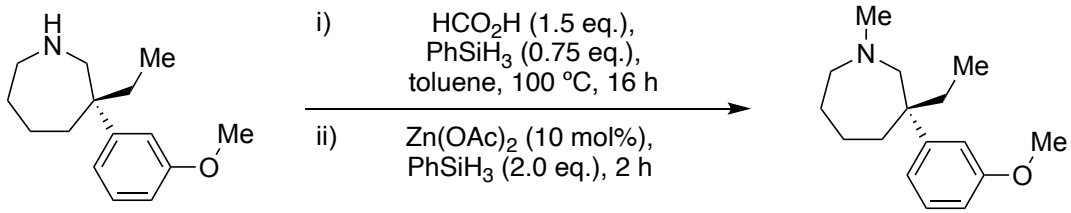

59 **68**

Synthesised using an adapted literature procedure.[26] To a biphasic mixture of HCO_2H (19.4 μL, 514 μmol) and phenylsilane (31.7 μL, 257 μmol) in toluene (200 μL) at 80 °C was added **59** (79.9 mg, 342 μmol) using a toluene (210 μL) rinse to ensure full transferal. After the effervescence eased (5 mins) the mixture was heated to 100 °C for 16 hours after which time $Zn(OAc)_2$ (6.3 mg, 34 μmol) and phenylsilane (84.4 μL, 684 μmol) were then added. The mixture was heated to 100 °C for an additional 2 hours, then, after cooling to room temperature, the reaction was quenched by slow addition of the reaction mixture onto vigorously stirred water (400 μL). After 30 minutes of stirring, the mixture was diluted with DCM (5.0 mL) and NaOH (5.0 mL of a 1.0 M aqueous solution) which was separated, washing the aqueous phase with additional DCM (3 x 2.5 mL). The combined organic phases

were dried over anhydrous $MgSO_4$, filtered, and concentrated *in vacuo*. The crude residue was purified by flash column chromatography (97.5:2.3:0.2:0.1 DCM:MeOH:H_2O:NH_3; R_f 0.17) to give a pale yellow oil (81.0 mg, 327 μmol, 96%)

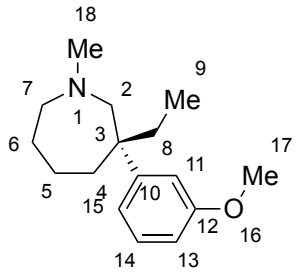

68

^{1}H NMR (400 MHz, $CDCl_3$) δ 7.23 (dd, *J* = 8.2, 7.9 Hz, 1H, H-14), 6.91 (ddd, *J* = 7.9, 1.9, 0.9 Hz, 1H, H-15), 6.88 (dd, *J* = 2.5, 1.9 Hz, 1H, H-11), 6.72 (ddd, *J* = 8.2, 2.5, 0.9 Hz, 1H, H-13), 3.81 (s, 3H, H-17), 2.84 (d, *J* = 13.9 Hz, 1H, H-2), 2.56 (ddd, *J* = 11.9, 6.6, 5.2 Hz, 1H, H-7), 2.55 (d, *J* = 13.9 Hz, 1H, H-2), 2.46 (ddd, *J* = 11.9, 6.6, 5.2 Hz, 1H, H-7), 2.40 (s, 3H, H-18), 2.13 (dd, *J* = 14.3, 8.1 Hz, 1H, H-4), 1.79 – 1.60 (m, 5H, H-4, H-5, H-8), 1.60 – 1.47 (m, 1H, H-5), 0.59 (t, *J* = 7.5 Hz, 3H, H-9). **^{13}C{^{1}H} NMR** (101 MHz, $CDCl_3$) δ 159.5 (C-12), 149.5 (C-10), 129.0 (C-14), 119.5 (C-15), 113.8 (C-11), 109.8 (C-13), 69.0 (C-2), 61.1 (C-7), 55.2 (C-17), 49.6 (C-18), 45.6 (C-3), 38.2 (C-4), 34.9 (C-8), 31.2 (C-6), 22.5 (C-5), 8.7 (C-17); **FTIR** (neat) ν_{max} /cm^{-1} 2961, 2932, 2876, 2843, 2790, 2764, 1600, 1581, 1488, 1462, 1451, 1430; **HRMS** (ESI) *m/z* calc'd for $C_{16}H_{26}NO$ $[M+H]^+$: 248.2009, found: 248.2009; **$[\alpha]_D^{25}$** -27.6° (*c*. 0.83, $CHCl_3$).

(*S*)-Meptazinol (57) and (*S*)-Meptazinol·BCl_3 (70)

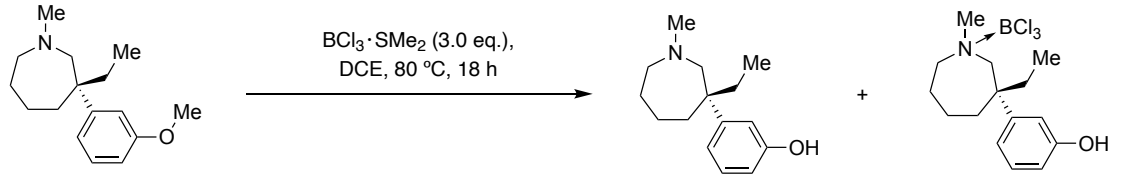

Synthesised using an adapted literature procedure.[28] To a solution of **68** (56.9 mg, 230 μmol) in DCE (1.0 mL) was added BCl_3·SMe_2 (345 μL of a 2.00 M solution in DCM, 690 μmol) and the solution was heated to 80 °C. After 18 hours the reaction was cooled to room temperature and added to a stirred solution of Na_2CO_3 (1.0 mL of a saturated aqueous solution). After 30 minutes the mixture was diluted with

DCM (4.0 mL) and Na_2CO_3 (4.0 mL of a saturated aqueous solution) and separated. The aqueous layer was washed with DCM (2 x 5 mL), then the combined organic phases were dried over anhydrous $MgSO_4$, filtered, and concentrated *in vacuo*. The crude residue was purified using flash column chromatography (95:4.5:0.4:0.1 DCM:MeOH:H_2O:NH_3) to give (-)-meptazinol **57** as a white solid (R_f 0.14, 39.1 mg, 168 μmol, 73%) and meptazinol·BCl_3 complex **70** as a yellow solid (R_f 0.60, 21.1 mg, 60.0 μmol, 26%).

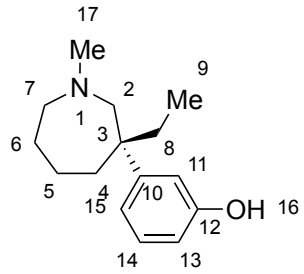

(-)-meptazinol, 57

1H NMR (500 MHz, $CDCl_3$) δ 7.13 (dd, *J* = 8.1, 7.8 Hz, 1H, H-14), 6.86 – 6.79 (m, 2H, H-15, H-11), 6.60 (ddd, *J* = 8.1, 2.4, 1.0 Hz, 1H, H-13), 5.48 (s (br.), 1H, H-16), 2.97 (d, *J* = 13.9 Hz, 1H, H-2), 2.63 – 2.50 (m, 3H, H-2, H-7), 2.44 (s, 3H, H-17), 2.17 (ddd, *J* = 14.2, 8.3, 1.5 Hz, 1H, H-4), 1.75 – 1.53 (m, 7H, H-4, H-5, H-6, H-8), 0.58 (t, *J* = 7.4 Hz, 3H, H-9); **$^{13}C\{^1H\}$ NMR** (126 MHz, $CDCl_3$) δ 155.9 (C-12), 148.9 (C-10), 129.2 (C-14), 119.0 (C-15), 114.6 (C-11), 112.8 (C-13), 68.9 (C-2), 60.7 (C-7), 49.3 (C-17), 45.4 (C-3), 37.6 (C-4), 35.2 (C-8), 30.2 (C-5), 22.5 (C-6), 8.6 (C-9); **FTIR** (neat) ν_{max} /cm^{-1} 3249 (br.), 3032, 2932, 2875, 2557, 2801, 1597, 1584, 1452; **HRMS** (ESI) *m/z* calc'd for $C_{15}H_{24}NO$ $[M+H]^+$: 234.1852, found: 234.1852; **m.p.** 120-122 °C; **Chiral HPLC** column: ODH (4.6 mm × 250 mm, 5 μm), mobile phase: 98:2 isohexane:isopropanol (isocratic), flow rate: 0.5 mL/min, temperature: 40 °C, t_R 36.24 mins (minor), 39.97 mins (major), 92% e.e; **$[\alpha]_D^{25}$** -20.0° (*c*. 1.0, $CHCl_3$, 92% e.e.), -14.1° (*c*. 0.28, MeOH, 92% e.e.), lit. -15.1 (*c*. 0.46, MeOH, >99% e.e.).[29]

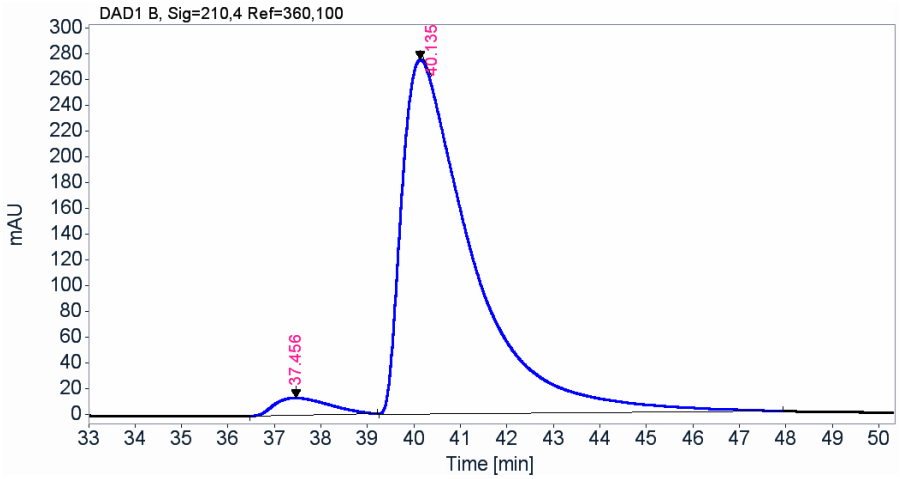

Signal: DAD1 B, Sig=210,4 Ref=360,100

RT [min]	Type	Width [min]	Area	Height	Area%
37.456	MM	0.9802	1131.618	13.6768	3.79
40.135	MM	1.7424	28720.703	274.7285	96.21

Figure 5. *Chiral HPLC chromatogram for (-)-meptazinol in 92% e.e.*

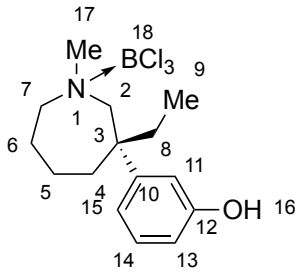

(-)-meptazinol·BCl_3, 70

^{1}H NMR (500 MHz, $CDCl_3$) δ 7.23 (dd, *J* = 8.2, 7.9 Hz, 1H, H-14), 6.97 (ddd, *J* = 8.2, 1.9, 0.8 Hz, 1H, H-15), 6.88 (dd, *J* = 2.5, 1.9 Hz, 1H, H-11), 6.72 (ddd, *J* = 7.9, 2.4, 0.8 Hz, 1H, H-13), 4.58 (dq(1:1:1:1), *J* = 15.2, 2.9 Hz, 1H, H-2), 3.67 (d, *J* = 13.7 Hz, 1H, H-7), 3.54 (dd, *J* = 13.7, 12.8 Hz, 1H, H-7), 3.26 (d, *J* = 15.2 Hz, 1H, H-2), 2.51 (q(1:1:1:1), *J* = 3.1 Hz, 3H, H-17), 2.32 (ddd, *J* = 14.6, 7.2, 1.3 Hz, 1H, H-4), 2.17 – 1.98 (m, 3H, H-4, H-5, H-6), 1.87 (ddddd, *J* = 15.7, 12.8, 10.5, 4.4, 2.8 Hz, 1H, H-6), 1.70 (ddddd, *J* = 14.2, 12.4, 10.5, 2.5, 1.3 Hz, 1H, H-5), 1.47 (q, *J* = 7.3 Hz, 2H, H-8), 0.50 (t, *J* = 7.3 Hz, 3H, H-9); **^{13}C{^{1}H} NMR** (126 MHz, $CDCl_3$) δ 155.9 (C-12), 146.4 (C-10), 129.9 (C-14), 118.8 (C-15), 113.6 (C-11, C-13), 63.4 (C-2), 60.5 (C-7), 44.4 (q, *J* = 1.8 Hz, C-3), 40.6 (C-17), 36.2 (C-8), 34.3 (C-4), 26.9 (q, *J* = 2.1 Hz, C-6), 22.1 (C-5), 8.0 (C-9); **^{11}B NMR** (160 MHz, $CDCl_3$) δ 11.00; **FTIR** (neat) ν_{max} /cm^{-1} 3346 (br.), 2970, 2930, 2876, 2861, 1588, 1495, 1477, 1452; **HRMS** (ESI) *m/z* calc'd for $C_{15}H_{23}BCl_4NO$ [M+Cl]$^-$:

384.0632, found: 384.0632, *m/z* calc'd for $C_{15}H_{22}BCl_3NO$ $[M-H]^-$: 348.0866, found: 348.0866; **m.p.** 202-207 °C; **$[\alpha]_D^{25}$** +5.0° (*c*. 1.0, 9:1 DCM:MeOH, 92% e.e.).

(±)-Meptazinol

Acquired from a salt break of commercially available (±)-meptazinol·HCl. (±)-meptazinol·HCl (25.0 mg, 92.7 μL) was dissolved in water (1.0 mL) and diluted with Na_2CO_3 (4.0 ml of a saturated aqueous solution) and DCM (4.0 mL). The organic layer was extracted and the aqueous was washed with DCM (3 x 2.5 mL). The combined organic layers were dried over anhydrous $MgSO_4$ and concentrated *in vacuo* to give the free base as a white solid (21.6 mg, 92.6 μmol, >99% recovery).

m.p. 133-137 °C (lit. 127-133).[30] Data consistent with enantiopure material.

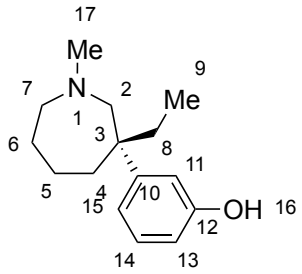

Carbon Number	Meptazinol ^{13}C NMR **δ** /ppm		Difference, **δ** /ppm
	Synthetic	Commercial	
C-12	155.9	156.0	0.1
C-10	148.9	149.1	0.2
C-14	129.2	129.1	-0.1
C-15	119.0	118.9	-0.1
C-11	114.6	114.7	0.1
C-13	112.8	112.8	0.0
C-2	68.9	69.2	0.3
C-7	60.7	60.9	0.2
C-17	49.3	49.4	0.1
C-3	45.4	45.4	0.0
C-4	37.6	37.3	-0.3
C-8	35.2	35.0	-0.2
C-5	30.2	30.5	0.3
C-6	22.5	22.5	0.0
C-9	8.6	8.6	0.0

Table 2. *Comparison of ^{13}C NMR shifts for synthetic (**57**) and commercial meptazinol*

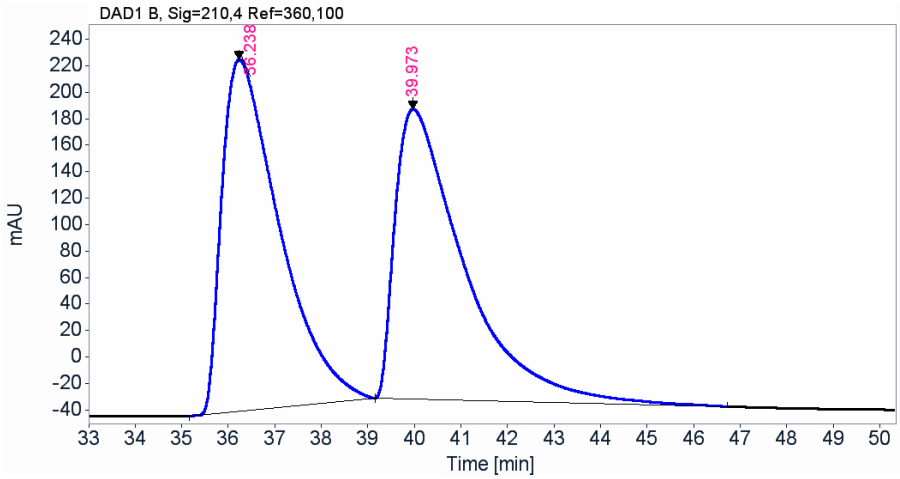

Signal:	DAD1 B, Sig=210,4 Ref=360,100				
RT [min]	Type	Width [min]	Area	Height	Area%
36.238	MM	1.4325	22822.555	265.5333	50.31
39.973	MM	1.7152	22543.566	219.0609	49.69

Figure 6. *Chiral HPLC chromatogram for racemic meptazinol.*

(*R*)-4-Ethyl-4-(3-methoxyphenyl)-1-methylazepane (67)

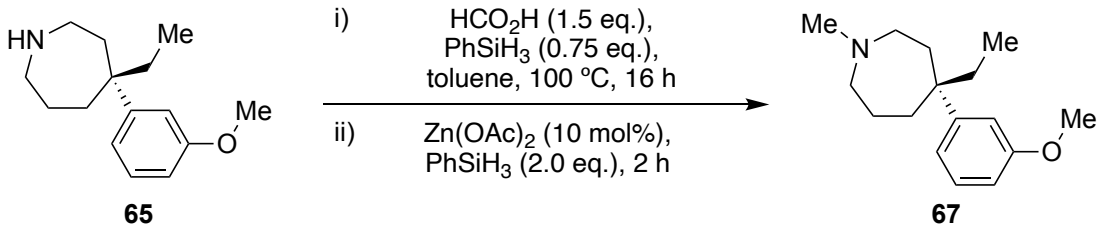

65 **67**

Synthesised using an adapted literature procedure.[26] To a biphasic mixture of HCO_2H (26.7 µL, 706 µmol) and phenylsilane (43.6 µL, 353 µmol) in toluene (300 µL) at 80 °C was added **65** (110 mg, 471 µmol) using a toluene (300 µL) rinse to ensure full transferral. After the effervescence eased (5 mins) the mixture was heated to 100 °C for 16 hours after which time $Zn(OAc)_2$ (8.6 mg, 47 µmol) and phenylsilane (116 µL, 942 µmol) were then added. The mixture was heated to 100 °C for an additional 2 hours then, after cooling to room temperature, the reaction was quenched by slow addition of the reaction mixture onto vigorously stirred water (600 µL). After 30 minutes of stirring, the mixture was diluted with DCM (5.0 mL) and NaOH (5.0 mL of a 1.0 M aqueous solution) which was separated, washing the aqueous phase with DCM (3 x 2.5 mL). The combined organic phases were dried over anhydrous $MgSO_4$, filtered, and concentrated *in vacuo*. The crude residue was

purified by flash column chromatography (90:9:0.8:0.2 DCM:MeOH:H_2O:NH_3; R_f 0.25) to give a pale yellow oil (116 mg, 469 μmol, 99%).

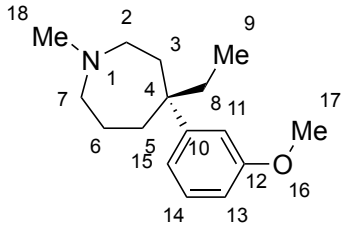

67

^{1}H NMR (400 MHz, $CDCl_3$) δ 7.22 (dd, *J* = 8.2, 7.8 Hz, 1H, H-14), 6.85 (ddd, *J* = 7.8, 1.9, 0.9 Hz, 1H, H-15), 6.81 (dd, *J* = 2.5, 1.9 Hz, 1H, H-11), 6.71 (ddd, *J* = 8.2, 2.5, 0.9 Hz, 1H, H-13), 3.80 (s, 3H, H-17), 2.70 (ddd, *J* = 11.9, 7.5, 3.0 Hz, 1H, H-7), 2.67 (dddd, *J* = 13.2, 8.7, 1.5, 1.2 Hz, 1H, H-2), 2.45 (dd, *J* = 13.2, 9.3 Hz, 1H, H-2), 2.40 (ddd, *J* = 11.9, 8.7, 2.7 Hz, 1H, H-7), 2.32 (s, 3H, H-18), 2.31 (ddd, *J* = 15.2, 8.7, 1.2 Hz, 1H, H-3), 2.10 (ddd, *J* = 14.6, 9.4, 1.8 Hz, 1H, H-5), 1.88 (ddd, *J* = 15.2, 9.3, 1.5 Hz, 1H, H-3), 1.85 (ddd, *J* = 14.6, 9.5, 1.7 Hz, 1H, H-5), 1.81 – 1.71 (m, 1H, H-6), 1.69 – 1.55 (m, 3H, H-6, H-8), 0.56 (t, *J* = 7.4 Hz, 3H, H-9); **^{13}C{^{1}H} NMR** (101 MHz, $CDCl_3$) δ 159.5 (C-12), 150.1 (C-10), 129.0 (C-14), 119.4 (C-15), 113.7 (C-11), 109.7 (C-13), 60.6 (C-7), 55.2 (C-17), 53.4 (C-2), 47.1 (C-18), 44.4 (C-4), 38.4 (C-5), 37.53 (C-8), 37.50 (C-3), 23.7 (C-6), 8.7 (C-9); **FTIR** (neat) ν_{max} /cm^{-1} 2960, 2933, 287, 2836, 2788, 2750, 2705, 1605, 1581, 1486, 1463, 1449, 1430; **HRMS** (ESI) *m/z* calc'd for $C_{16}H_{26}NO$ $[M+H]^+$: 248.2009, found: 234.2005; **$[\alpha]_D^{25}$** -5.1° (*c*. 1.0, $CHCl_3$).

(*R*)-3-(4-Ethyl-1-methylazepan-4-yl)phenol (69)

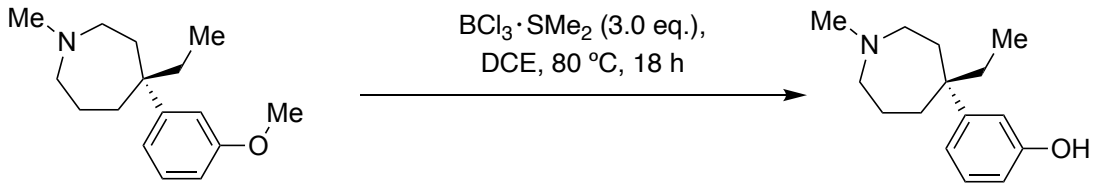

67 **69**

Synthesised using an adapted literature procedure.[28] To a solution of **67** (56.8 mg, 230 μmol) in DCE (1.0 mL) was added BCl_3·SMe_2 (344 μL of a 2.00 M solution in DCM, 689 μmol) and the solution was heated to 80 °C. After 18 hours the reaction was cooled to room temperature and added to a stirred solution of Na_2CO_3 (1.0 mL

of a saturated aqueous solution). After 30 minutes the mixture was diluted with DCM (4.0 mL) and Na_2CO_3 (4.0 mL of a saturated aqueous solution) and separated. The aqueous layer was washed with DCM (2 x 5 mL) then the combined organic phases were dried over anhydrous $MgSO_4$, filtered, and concentrated *in vacuo*. The crude residue was purified using flash column chromatography (90:9:0.8:0.2 DCM:MeOH:H_2O:NH_3; R_f 0.07) to give an off-white semisolid (R_f 0.14, 39.1 mg, 168 μmol, 56%).

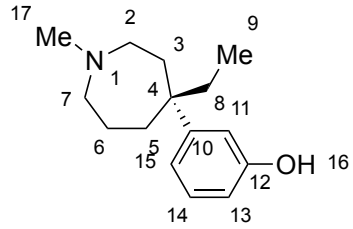

69

^{1}H NMR (400 MHz, $CDCl_3$) δ 7.33 (s (br.), 1H, H-16), 7.11 (dd, *J* = 8.0, 7.9 Hz, 1H, H-14), 6.72 (ddd, *J* = 8.0, 1.9, 0.9 Hz, 1H, H-15), 6.67 (dd, *J* = 2.3, 1.9 Hz, 1H, H-11), 6.60 (ddd, *J* = 7.9, 2.3, 0.9 Hz, 1H, H-13), 2.77 – 2.66 (m, 2H, H-2, H-7), 2.62 – 2.51 (m, 2H, H-2, H-7), 2.34 (s, 3H, H-17), 2.25 (dd, *J* = 15.6, 8.4 Hz, 1H, H-3), 2.16 (ddd, *J* = 14.8, 9.6, 1.4 Hz, 1H, H-5), 1.90 (dd, *J* = 15.5, 8.9 Hz, 1H, H-3), 1.83 – 1.60 (m, 3H, H-5, H-6), 1.56 (apparent qd, *J* = 7.4, 3.1 Hz, 2H, H-8), 0.54 (t, *J* = 7.4 Hz, 3H, H-9); **^{13}C{^{1}H} NMR** (101 MHz, $CDCl_3$) δ 157.1 (C-12), 149.4 (C-10), 129.2 (C-14), 118.1 (C-15), 114.6 (C-11), 113.1 (C-13), 60.1 (C-7), 53.0 (C-2), 46.3 (C-17), 44.3 (C-4), 38.1 (C-5), 37.7 (C-8), 36.4 (C-3), 23.0 (C-6), 8.7 (C-9); **FTIR** (neat) ν_{max} /cm^{-1} 3190 (br.), 3151, 3055, 2960, 2933, 2876, 2857, 2804, 1583, 1451; **HRMS** (ESI) *m/z* calc'd for $C_{15}H_{24}NO$ $[M+H]^+$: 234.1852, found: 234.1854; **$[\alpha]_D^{25}$** -14.2° (*c*. 1.0, $CHCl_3$)

3.6.7 References

1 N. D. Zelinsky and M. W. Gawerdowskaja, *Ber. Dtsch. Chem. Ges.*, 1927, **60**, 713–715.
2 Y. Gao, J. Liu, Z. Li, T. Guo, S. Xu, H. Zhu, F. Wei, S. Chen, H. Gebru and K. Guo, *J. Org. Chem.*, 2018, **83**, 2040–2049.
3 Y. Zhou, J. Dong, F. Zhang and Y. Gong, *J. Org. Chem.*, 2011, **76**, 588–600.
4 J. Frelek, L. Huang, F. Kerek, G. Snatzke and W. J. Szczepek, *Liebigs Ann.* , 1991, **1991**, 89–91.
5 J. K. Augustine, R. Kumar, A. Bombrun and A. B. Mandal, *Tetrahedron Lett.*, 2011, **52**, 1074–1077.
6 W. Borsche and K. Thiele, *Ber. Dtsch. Chem. Ges.*, 1923, **56**, 2012–2015.
7 J. H. Glans and G. R. Hatfield, *J. Label. Compd. Radiopharm.*, 1989, **27**, 1341–1343.
8 X. Mo, T. D. R. Morgan, H. T. Ang and D. G. Hall, *J. Am. Chem. Soc.*, 2018, **140**, 5264–5271.
9 R. E. Lyle and H. J. Troscianiec, *J. Org. Chem.*, 1955, **20**, 1757–1760.
10 Y. Chen, D. Cantillo and C. O. Kappe, *European J. Org. Chem.*, 2019, **2019**, 2163–2171.
11 H. Hu, X. Cai, Z. Xu, X. Yan and S. Zhao, *Molecules*, 2018, **23**, 1–9.
12 D. L. Gamble, W. P. Hems and B. Ridge, *J. Chem. Soc. Perkin 1*, 2001, 248–260.
13 K. Suzuki, T. Watanabe and S. I. Murahashi, *J. Org. Chem.*, 2013, **78**, 2301–2310.
14 B. A. Trofimov, E. Y. Schmidt, N. V. Zorina, E. Y. Senotrusova, N. I. Protsuk, I. A. Ushakov, A. I. Mikhaleva, R. Méallet-Renault and G. Clavier, *Tetrahedron Lett.*, 2008, **49**, 4362–4365.
15 Z. F. Xu, T. Zhang and W. Hong, *Tetrahedron*, 2019, **75**, 3113–3117.
16 T. Ohwada, N. Yamagata and K. Shudo, *J. Am. Chem. Soc.*, 1991, **113**, 1364–1373.
17 H. Grund and V. Jäger, *Liebigs Ann.* , 1980, **1980**, 80–100.
18 D. C. Miller, J. M. Ganley, A. J. Musacchio, T. C. Sherwood, W. R. Ewing and R. R. Knowles, *J. Am. Chem. Soc.*, 2019, **141**, 16590–16594.
19 J. Zhang and S. Chang, *J. Am. Chem. Soc.*, 2020, **142**, 12585–12590.
20 K. Maruoka, T. Miyazaki, M. Ando, Y. Matsumura, S. Sakane, K. Hattori and H. Yamamoto, *J. Am. Chem. Soc.*, 1983, **105**, 2831–2843.
21 I. Sorribes, J. R. Cabrero-Antonino, C. Vicent, K. Junge and M. Beller, *J. Am. Chem. Soc.*, 2015, **137**, 13580–13587.
22 G. Barker, P. O'Brien and K. R. Campos, *Org. Lett.*, 2010, **12**, 4176–4179.
23 M. Movassaghi and M. D. Hill, *J. Am. Chem. Soc.*, 2006, **128**, 14254–14255.
24 S. Kehrli, D. Martin, D. Rix, M. Mauduit and A. Alexakis, *Chem. - A Eur. J.*, 2010, **16**, 9890–9904.
25 J. C. Holder, A. N. Marziale, M. Gatti, B. Mao and B. M. Stoltz, *Chem. - A Eur. J.*, 2013, **19**, 74–77.
26 E. L. Stoll, T. Tongue, K. G. Andrews, D. Valette, D. J. Hirst and R. M. Denton, *Chem. Sci.*, 2020, **11**, 9494–9500.
27 C. Meng, P. Liu, N. T. Tung, X. Han and F. Li, *J. Org. Chem.*, 2020, **85**, 5815–5824.
28 J. Scragg, PhD thesis, University of Nottingham, 2015.
29 S. Cheng, W. Zheng, P. Gong, Q. Zhou, Q. Xie, L. Yu, P. Zhang, L. Chen, J. Li, J. Chen, H. Chen and H. Chen, *Bioorganic Med. Chem.*, 2015, **23**, 3110–3118.
30 G. Bradley, J. F. Cavalla, T. Edington, R. Shepherd, A. White, B. J. Bushell, J. R. Johnson and G. Weston, *Eur. J. Med. Chem.*, 1980, **15**, 375–385.